



Universitat de Lleida

Identification of novel signaling pathways for cardiomyocyte differentiation and growth

Junmei Ye

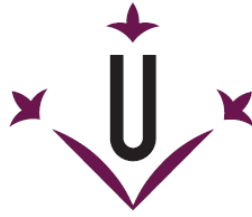
Dipòsit Legal: L.287-2013

<http://hdl.handle.net/10803/110543>

ADVERTIMENT. L'accés als continguts d'aquesta tesi doctoral i la seva utilització ha de respectar els drets de la persona autora. Pot ser utilitzada per a consulta o estudi personal, així com en activitats o materials d'investigació i docència en els termes establerts a l'art. 32 del Text Refós de la Llei de Propietat Intel·lectual (RDL 1/1996). Per altres utilitzacions es requereix l'autorització prèvia i expressa de la persona autora. En qualsevol cas, en la utilització dels seus continguts caldrà indicar de forma clara el nom i cognoms de la persona autora i el títol de la tesi doctoral. No s'autoritza la seva reproducció o altres formes d'explotació efectuades amb finalitats de lucre ni la seva comunicació pública des d'un lloc aliè al servei TDX. Tampoc s'autoritza la presentació del seu contingut en una finestra o marc aliè a TDX (framing). Aquesta reserva de drets afecta tant als continguts de la tesi com als seus resums i índexs.

ADVERTENCIA. El acceso a los contenidos de esta tesis doctoral y su utilización debe respetar los derechos de la persona autora. Puede ser utilizada para consulta o estudio personal, así como en actividades o materiales de investigación y docencia en los términos establecidos en el art. 32 del Texto Refundido de la Ley de Propiedad Intelectual (RDL 1/1996). Para otros usos se requiere la autorización previa y expresa de la persona autora. En cualquier caso, en la utilización de sus contenidos se deberá indicar de forma clara el nombre y apellidos de la persona autora y el título de la tesis doctoral. No se autoriza su reproducción u otras formas de explotación efectuadas con fines lucrativos ni su comunicación pública desde un sitio ajeno al servicio TDR. Tampoco se autoriza la presentación de su contenido en una ventana o marco ajeno a TDR (framing). Esta reserva de derechos afecta tanto al contenido de la tesis como a sus resúmenes e índices.

WARNING. Access to the contents of this doctoral thesis and its use must respect the rights of the author. It can be used for reference or private study, as well as research and learning activities or materials in the terms established by the 32nd article of the Spanish Consolidated Copyright Act (RDL 1/1996). Express and previous authorization of the author is required for any other uses. In any case, when using its content, full name of the author and title of the thesis must be clearly indicated. Reproduction or other forms of for profit use or public communication from outside TDX service is not allowed. Presentation of its content in a window or frame external to TDX (framing) is not authorized either. These rights affect both the content of the thesis and its abstracts and indexes.



Universitat de Lleida

Departament de Ciències Mèdiques Bàsiques

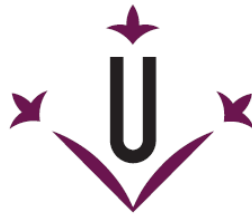
**Identification of novel signaling pathways for
cardiomyocyte differentiation and growth**

Junmei Ye

Thesis supervisor:

Daniel Sanchis Morales

Lleida, October 2012



Universitat de Lleida

Daniel Sanchis Morales, Doctor en Ciències Biològiques, investigador Ramon y Cajal al Departament de Ciències Mèdiques Bàsiques de la Universitat de Lleida i director de la present tesi,

Faig constar que,

La llicenciada en Bioquímica per Wuhan University (Xina) i Màster en Medicina per Wuhan University (Xina), **Junmei Ye**, ha realitzat sota la meua direcció i supervisió dins del grup de Aenyalització Cel·lular i Apoptosi del Departament de Ciències Mèdiques Bàsiques, el treball experimental titulat “**Identification of novel signaling pathways for cardiomyocyte differentiation and growth**”.

El treball reuneix les condicions adients per tal de poder ser defensat davant del Tribunal de Tesi corresponent i, si s'escau, obtenir le grau de **Doctor** per la Universitat de Lleida.

I perquè així consti i als effects oportuns signo el present document a

Lleida, 1 de octubre de 2012

Dr. Daniel Sanchis Morales

To my dear family
献给我亲爱的父母和丈夫

Acknowledgements

Acknowledgements

How time flies, it seems yesterday that I first came here. I have been in Spain, in Lleida for nearly four years. Although four years is not so long compared with one's life, for me, these four years is such an important period in my life.

First I will express my sincere appreciation to Dr. Daniel Sanchis Morales, my supervisor, a very nice director of my research and the thesis. From the time that I applied for the fellowship of UdL in China, he is always giving many help. Thanks to Dani for his patience, for his advice to my research and for his efficient training on my ability. Thanks for his help and encouragement during my participation to the publication of Nature. Thanks to Marta Llovera. She is always very kind to offer me any help whenever I have problems and explains with patience.

Thanks to Joan X. Comella, who always gives us good suggestions and helps with our work.

Thanks to AGAUR, University of Lleida and IRB Lleida for the financial support during my doctoral studies.

I would like to thank all the members in the cardiovascular group –Maria Cardona, Nati Blasco, Jisheng, Marta C., Cristina and Maya. Thanks to Jisheng, who offered me many help with the most patience in those first days I arrived in Spain. And thanks to Maria Cardona, she is a very nice work companion, and she also gives me many help. Thanks to her for helping me to call the police station, explaining the documents for me, and helping me to look for the flats.

During my whole doctoral studies in the lab, I have been working with kind and friendly doctoral students and co-workers of IRB Lleida and ARNAU: Thanks to Judit, Carles, José, Mario and Eloi for their kind help during my study; Thanks to Xavi for offering protein samples and antibody; Thanks to Milica, Anna Macià, Núria E, Noelia, Laura, Cristina M, Andree, Mireia, Myriam, Marta, Petya, Annabel, Gemma, Berta, Esmeralda, Anaïs, Monica, Dolors, Viki, thank you all for offering any help whenever I need.

Acknowledgements

Thanks to Cristina G, Azahar, Carme and Isu for their technical help during my research, and thanks to Jessica for the help in manipulating the rats in the animal house.

Thanks to Arindam, Upasana, Charu and Deepshikha for the warm invitation to their houses for the delicious Indian food.

Thanks to Ana Velasco, who helped my husband and me a lot when we first came here and had problems in the police station. I appreciate very much for your help, although you were so busy with your work those days.

Thanks to Ana Novell for practicing Spanish with me weekly, and we have been continuing for three years! This experience is undoubtedly a deep impression of my Spanish living.

Finally, I would like to thank my family. Thanks to my parents for their support when I am in Spain. Especially, I would like to thank my excellent and patient husband, Haijing, who came to Spain with me and made his greatest effort to support my study during these years. I appreciate very much for his comfort when I am depressed with unexpected results, and also his encourage which helps me go forward. Now we are making our dreams true little by little and I believe that there is a wonderful future waiting for us!

¡Muchas gracias a todos!

衷心地谢谢大家！

Junmei Ye

Index

Abbreviations	17
Abstracts	21
Introduction	35
1 Basic concepts of heart development and growth	37
1.1 Architecture and function of the heart	37
1.2 Cardiac morphogenesis	37
1.3 Proliferation and differentiation of cardiomyocytes in postnatal period	39
1.4 Main signaling pathways during heart development: a scheme	41
1.5 Role of apoptosis during heart development	43
1.5.1 Caspases and apoptosis during heart development	45
1.5.2 Non-apoptotic role of caspases in heart development	47
1.6 Cardiac metabolism, hypertrophy and failure	48
1.6.1 Function of mitochondria	53
1.6.1.1 Mitochondria in heart function and failure	53
1.6.1.2 The role of mitochondria during cardiomyocyte death	55
1.6.1.2.1 EndoG: A mitochondrial nuclease in the heart	57
1.6.2 Signaling for cardiac hypertrophy	58
1.6.2.1 G proteins	62
1.6.2.2 Calcineurin	65
1.6.2.3 Protein translation during hypertrophy	67
2 Signaling regulation of gene expression in the heart: relevant aspects for this work	68
2.1 Myocyte enhancer factor 2 (MEF2)	68
2.1.1 MEF2 family: structure and regulation	69
2.1.2 MEF2 isoforms and their function in the heart	74
2.1.3 The cooperation of MEF2 and microRNA (miRNA) in cardiomyocyte development	78
2.2 Histone deacetylases (HDACs)	80
2.2.1 Function of HDACs	81
2.2.2 Control of gene expression by HDACs	81

2.2.3 Control of cardiovascular growth and function by HDACs	82
2.2.4 Control of cell death by HDACs	86
2.3 Polypyrimidine tract binding protein (PTB)	87
2.3.1 Function of PTB	88
2.3.2 Control of apoptotic signaling by PTB	90
Hypothesis and objectives	93
Material and methods	97
1 Cell culture	99
1.1 Cell culture dishes coating	99
1.2 Maintaining of HEK293T cells	99
1.3 Primary cardiomyocytes maintenance	100
1.4 Cell recovery and cryopreservation	101
1.5 Polyethylenimine (PEI) transfection	102
1.6 Cell transduction	104
1.7 Immunofluorescence (IF)	104
2 Molecular biology	106
2.1 General technique for gene cloning	106
2.2 Principle of RNAi action	107
2.3 Primers design for shRNA and subcloning procedures	109
2.4 Subcloning of shRNA in pLVTHM vector	110
2.5 Lentivirus production	110
3 Reverse transcription and polymerase chain reaction (RT-PCR)	111
3.1 RNA extraction	111
3.2 Reverse transcription (RT)	111
3.3 Conventional PCR	112
3.4 Real time PCR	113
3.5 Radioactive quantitative PCR	114
4 Biochemistry	114
4.1 Western-blot (WB)	114

Index

4.2 <i>In vitro</i> ³⁵ S-protein labeling and Immunoprecipitation	120
5 Statistics	121
Results	123
1 Endonuclease G is involved in cardiomyocyte growth and mitochondrial metabolism	125
2 Translation of MEF2 is induced by hypertrophic stimuli in cardiomyocytes through a Calcineurin-dependent pathway	135
3 A pathway involving HDAC5, cFLIP and caspases regulates PTB expression influencing Mef2 alternative splicing in the heart	155
Discussion	173
Conclusions	185
References	189
Annex	207

Abbreviations

Abbreviations

ADS	Buffered saline glucose solutions
ANF	Atrial Natriuretic Factor
AngII	Angiotensin II
ATP	Adenosine Triphosphate
BNIP3	Bcl2 nineteen kD interacting protein 3
CaM	Camodulin
Caspase	Cystein Aspartate Protease
Cn I	Calcineurin Inhibitor
DISC	Death Inducing Signaling Complex
DMEM	Dolbecco's modified Eagle medium
DNA	Desoxirribonucleic Acid
EndoG	Endonuclease G
ET-1	Endothelin-1
FADD	Fas Associated Death Domain
FLICE	FADD-like Interleukin-1 β -converting enzyme
FLIP	Fas-Associated Death Domain-like Interleukin-1- β -converting enzyme-inhibitory protein
GAPDH	Glyceraldehyde 3-Phosphate Dehydrogenase
HATs	Histone Acetyl Transferases
HDACs	Histone Deacetylases
IF	Immunofluorescence
IP	Isoproterenol
IRES	Internal Ribosome Entry Site
kb	kilobase
kDa	Kilo Dalton
KO	Knock Out
MAPK	Mitogen-Activated Protein Kinase

Abbreviations

MEF	Mouse Embryonic Fibroblast
MEF2	Myocyte Enhancer Factor 2
MOMP	Mitochondrial Outer Membrane Permeabilization
MPTP	Mitochondrial Permeability Transition Pore
NaB	Sodium Butyrate
NFATs	Nuclear Factors of Activated T Cells
NEAA	Non-essential Amino Acids
PBS	Phosphate Buffered Saline
PARP	Poly (ADP) Ribose Polymerase
PCD	Programmed Cell Death
PCR	Polymerase Chain Reaction
PE	Phenylephrine
PEI	Polyethilenimine
PFA	Paraformaldehyde
PTB	Polypyrimidine tract binding protein
PVDF	Ployvinylidene Fluoride
RISC	RNAi-Induced Silencing Complex
RNA	Ribonucleic Acid
ROS	Reactive Oxygen Species
RT	Room Temperature
Scr	Scrambled
SDS	Sodium Docecyl Sulfate
shRNA	Short Hairpin RNA
TBS-T	Tris Buffered Saline-Tween
UNR	Upstream of N-Ras
WB	Western Blot

Abstract

Left ventricular mass (LVM) is a highly heritable trait (Post W.S. et al., 1997) and an independent risk factor for all-cause mortality (Lorell B.H. and Carabello B.A., 2000). To date, genome-wide association studies (GWASs) have not identified the genetic factors underlying LVM variation (Vasan R.S. et al., 2009) and the regulatory mechanisms for blood pressure (BP)-independent cardiac hypertrophy remain poorly understood (McGavock J.M. et al., 2006; Wong C. and Marwick T.H., 2007). The group of Prof. Stuart Cook identified endonuclease G (EndoG), previously implicated in apoptosis (Li L.Y. et al., 2001) but not hypertrophy, as a gene located on a BP-independent LVM region of rat chromosome 3p and demonstrated that a loss-of-function mutation in EndoG is associated with increased LVM and impaired cardiac function. In collaboration with S Cook's group and based on this conclusion, we identified that inhibition of EndoG in cultured neonatal cardiomyocytes resulted in an increase in cell size, hypertrophic biomarkers and reactive oxygen species (ROS) in the absence of pro-hypertrophic stimulation. We also observed that, under electronic microscopy, EndoG deleted (*Endog*^{-/-}) mouse heart established no gross morphological changes of mitochondria but lipid-like droplets associated with mitochondria from *Endog*^{-/-} mice were more numerous and larger than those seen in control mice, which were proved to be steatosis according to Oil Red O staining and molecular studies. Therefore, our studies demonstrate a new role for EndoG in mitochondrial metabolism and cardiac growth.

To investigate the mechanisms involved in cardiac hypertrophy, we focused also on Myocyte Enhancer Factor-2 (MEF2) family, which has been proved to play an important role in proper cardiac development and function as well as cardiac hypertrophy and cardiomyopathy (Black B.L. and Olson E.N., 1998; Naya F.J. et al., 2002; Xu J. et al., 2006). MEF2 activity is enhanced by increasing its transcription and by MAPK-dependent phosphorylation, and is reduced by binding to class II Histone Deacetylases and by miR-1-mediated degradation of its transcript. In our research we show that MEF2 protein abundance is regulated at the translational level, determining myocyte size, during hypertrophy. MEF2 expression silencing through RNA interference required serum deprivation and protein abundance recovered to the basal level in the presence of phenylephrine despite low mRNA

expression. Hypertrophic agonist stimulation of neonatal ventricular cardiomyocytes increased Mef2 expression by enhancing its translation, without changing its transcription or blocking degradation of the protein. MEF2 abundance was increased by Calcineurin overexpression *in vivo* and was reduced by Calcineurin inhibition *in vitro*, without affecting Mef2 mRNA levels. Calcineurin activity influenced expression of Polypyrimidine Tract Binding Protein (PTB), contributing to MEF2 translation. Thus, our results show a previously unrecognized but relevant level of MEF2 activity regulation through the control of its translation that involves Calcineurin and PTB.

During heart development an exon known as exon β is progressively included in the MEF2 mRNA conferring stronger transcriptional activity to MEF2 (Yu Y. et al., 1992). Class II Histone Deacetylases (HDACs) are abundant in the heart and inhibit MEF2 transcriptional activity (Olson E.N., 2006). In the absence of stress signals, class II HDACs interact with MEF2 to attenuate cardiac growth (Berry J.M. et al., 2008). Polypyrimidine Tract Binding Protein (PTB) inhibits exon inclusion during mRNA maturation and induces Internal Ribosome Entry Site (IRES) - dependent translation of many genes (Spellman R. et al., 2005). Our previous results showed that PTB induced translation of apoptotic genes in cardiomyocytes and was abundant in the embryonic heart whereas its expression reduced during development by postranscriptional mechanisms (Zhang J. et al., 2009). Further investigation showed a transient divergence between abundances of PTB protein and its transcript and also simultaneous reduction of HDACs expression. Therefore, we were interested in investigating a possible link between HDAC control of cardiac differentiation, PTB abundance and the expression of MEF2. Our results showed HDAC5-deficient mice had reduced cardiac PTB protein abundance and HDAC inhibition caused caspase-dependent cleavage of PTB protein abundance and a reduction in endogenous expression of cFLIP in myocytes. Cardiac PTB expression was abnormally high in mice with cardiac-specific executioner caspase deficient and cFLIP overexpression prevented PTB cleavage *in vitro*. Initial cleavage triggered further fragmentation of PTB and fragments accumulated in the presence of proteasome inhibitors. Experimental modification of the above process *in vivo*

and *in vitro* resulted in coherent changes in the splicing of MEF2's exon β , which codes for a peptide conferring stronger transcriptional activity of MEF2. These results establish a pathway connecting HDAC, cFLIP and caspases regulating the progressive disappearance of PTB, which enables the expression of the adult variants of Mef2 during heart development.

La masa ventricular izquierda (LVM) es un rasgo altamente heredable (Post W.S. et al., 1997) y un factor de riesgo independiente para la mortalidad por cualquier causa (Lorell B.H. and Carabello B.A., 2000). Hasta la fecha, ningún estudio de asociación del genoma (GWAS) ha identificado los factores genéticos que controlan la variación en la LVM (Vasan R.S. et al., 2009) y los mecanismos de regulación de la hipertrofia cardíaca independiente de la presión arterial (PA) siguen siendo poco conocidos (McGavock J.M. et al., 2006; Wong C. and Marwick T.H., 2007). El grupo del Profesor Stuart Cook identificó Endonucleasa G (Endo G), previamente implicada en la apoptosis (Li L.Y. et al., 2001) pero no en la hipertrofia, como un gen localizado en una región LVM independiente de la PA del cromosoma 3p de rata, y demostró que una pérdida de función de EndoG se asocia con un aumento de la LVM y con un deterioro de la función cardíaca. En colaboración con el grupo de S. Cook y en base a esta conclusión, hemos identificado que la inhibición de EndoG en cardiomiocitos neonatales en cultivo resulta en un aumento del tamaño celular y un aumento de los biomarcadores hipertróficos y especies reactivas del oxígeno (ROS) en ausencia de estimulación pro-hipertrófica. También se observó que, mediante microscopía electrónica, los corazones de ratón sin EndoG (EndoG^{-/-}) no presentan grandes cambios morfológicos en las mitocondrias pero, en cambio, las gotas de lípidos asociadas a las mitocondrias de los ratones EndoG^{-/-} son más numerosas y de mayor tamaño que las observadas en los ratones control; por medio de estudios moleculares y tinción con Oil Red O hemos determinado que se trata de esteatosis. Por lo tanto, nuestros estudios refuerzan aún más el vínculo entre la disfunción mitocondrial, ROS y las enfermedades cardíacas y demuestra una nueva función de EndoG en crecimiento cardíaco.

Con el fin de encontrar los mecanismos implicados en la hipertrofia cardíaca nos hemos centrado también en la familia de los Myocyte Enhancer Factor-2 (MEF2), que se ha demostrado que tienen un papel importante en el correcto desarrollo y función cardíaca, así como en la hipertrofia cardíaca y la cardiomiopatía (Black B.L. and Olson E.N., 1998; Naya F.J. et al., 2002; Xu J. et al., 2006). La actividad de MEF2 es potenciada por un incremento en su transcripción y por la fosforilación dependiente de MAPK, por el contrario, su actividad se reduce mediante su unión a las Histona Deacetylases de clase II (HDAC) y por la

degradación de su transcrito mediada por miR-1. Nosotros mostramos que la abundancia proteica de MEF2 está regulada a nivel traduccional, determinando el tamaño de los miocitos, durante la hipertrofia. La disminución de la expresión proteica de MEF2 la conseguimos mediante su silenciamiento con RNA de interferencia, que en presencia de Phenylephrine recupera sus niveles basales. La estimulación agonista hipertrófica de los cardiomiocitos ventriculares neonatales aumenta la expresión de MEF2 gracias a una mejora en su traducción, sin cambiar su transcripción ni bloquear la degradación de la proteína. La abundancia de MEF2 se incrementa mediante la sobreexpresión de Calcineurina *in Vivo* y se reduce por la inhibición de la Calcineurina *in Vitro*, sin afectar los niveles de mRNA de MEF2. La actividad de la Calcineurina influye en la expresión de la Polypyrimidin Tract Binding Protein (PTB), contribuyendo en la traducción de MEF2. Por lo tanto, nuestros resultados muestran el proceso de regulación de la actividad de MEF2 mediante el control de su traducción, que involucra la Calcineurina y PTB, un proceso hasta ahora desconocido.

Durante el desarrollo cardíaco, un exón conocido como Exón β es progresivamente incluido en el mRNA de MEF2 proporcionándole una mayor actividad transcripcional (Yu Y. et al., 1992). Las HDAC de clase II son abundantes en el corazón e inhiben la actividad transcripcional de MEF2 (Olson EN, 2006). En ausencia de señales de estrés, las HDAC de clase II interactúan con MEF2 con el fin de atenuar el crecimiento cardíaco (Berry J.M. et al., 2008). PTB inhibe la inclusión del exón durante la maduración del mRNA e induce la traducción IRES de muchos genes (Spellman R. et al., 2005). Resultados previos de nuestro grupo demuestran que PTB induce la traducción de genes apoptóticos en los cardiomiocitos y que es abundante en el corazón embrionario mientras que su expresión se reduce durante el desarrollo por mecanismos posttranscripcionales (Zhang J. et al., 2009). Posteriormente hemos mostrado una divergencia transitoria entre la abundancia de la proteína de PTB y su transcripción y también que simultáneamente tiene lugar una reducción de la expresión de las HDACs. Esto incrementó nuestro interés en encontrar una posible relación entre el control de las HDACs durante la diferenciación cardíaca, la abundancia de PTB y la expresión de MEF2. Nuestros resultados muestran que ratones deficientes en HDAC5 tienen menos proteína PTB cardíaca y que la inhibición de HDAC causa el corte dependiente de caspasa de la proteína

PTB cardíaca y una reducción de la expresión endógena de cFLIP en los miocitos. La expresión cardíaca de PTB es anormalmente elevada en ratones deficientes en caspasa ejecutora en el corazón y la sobreexpresión de cFLIP impide el corte de PTB *in Vitro*. El corte inicial inicia una mayor fragmentación de PTB y los fragmentos se acumulan en presencia de inhibidores del proteasoma. Modificaciones en el procedimiento anterior *in Vitro* e *in Vivo* han resultado en cambios coherentes en el splicing del exón β de MEF2, que codifica por un péptido que confiere una mayor actividad transcripcional. Estos resultados establecen una vía de conexión entre HDAC, cFLIP y caspasas que regulan la progresiva desaparición de PTB, que permite la expresión de las variantes adultas de MEF2 durante el desarrollo cardíaco.

La massa ventricular esquerra (LVM) és un tret altament heretable (Post W.S. et al., 1997) i un factor de risc independent per a la mortalitat sigui quina sigui la causa (Lorell B.H. and Carabello B.A., 2000). Fins avui, cap estudi d'associació del genoma (GWAS) ha identificat els factors genètics que controlen la variació en la LVM (Vasan R.S. et al., 2009), i els mecanismes de regulació de la hipertròfia cardíaca independent de la pressió arterial (PA) segueixen sent poc coneguts (McGavock J.M. et al., 2006; Wong C. and Marwick T.H., 2007). El grup del Professor Stuart Cook va identificar l'Endonucleasa G (EndoG), prèviament implicada en l'apoptosi (Li L.Y. et al., 2001) però no en la hipertròfia, com a un gen localitzat en una regió LVM independent de la PA del cromosoma 3p de rata, i va demostrar que una pèrdua de funció d'EndoG s'associa amb un augment de la LVM i un deteriorament de la funció cardíaca. En col·laboració amb el grup de S. Cook i en base a aquesta conclusió, hem identificat que la inhibició d'EndoG en cardiomiòcits neonatals en cultiu resulta en un augment de la mida cel·lular, i un augment dels biomarcadors hipertròfics i espècies reactives d'oxigen (ROS) en absència d'estimulació pro-hipertròfica. També hem observat, mitjançant microscòpia electrònica, que els cors de ratolí sense EndoG (EndoG^{-/-}) no presenten grans canvis morfològics en els mitocondris però, en canvi, les gotes de lípids associades als mitocondris dels ratolins EndoG^{-/-} són més nombroses i de major grandària que les observades en els ratolins control; per mitjà d'estudis moleculars i tinció amb Oil Red O hem determinat que es tracta d'esteatosi. Per tant, els nostres estudis suporten encara més el vincle entre la disfunció mitocondrial, ROS i les malalties cardíques i demostren una nova funció d'EndoG en creixement cardíac.

Per tal de trobar els mecanismes implicats en la hipertròfia cardíaca ens hem centrat també en la família dels Myocyte Enhancer Factor-2 (MEF2), que s'ha demostrat que tenen un paper important en el correcte desenvolupament i funció cardíaca, així com també en la hipertròfia cardíaca i la cardiomiopatia (Black B.L. and Olson E.N., 1998; Naya F.J. et al., 2002; Xu J. et al., 2006). L'activitat de MEF2 és potenciada per un increment en la seva transcripció i per la fosforilació dependent de MAPK, per contra, la seva activitat es redueix mitjançant la unió a les Histona Deacetylases de tipus II (HDAC) i per la degradació del seu trànscrip mediada per miR-1. Nosaltres mostrem que l'abundància proteica de MEF2 està

regulada a nivell traduccional, determinant la grandària dels miòcits, durant la hipertròfia. La disminució de l'expressió proteica de MEF2 l'aconseguim mitjançant el seu silenciament amb RNA d'interferència, que en presència de Phenylephrine recupera els seus nivells basals. L'estimulació agonista hipertròfica dels cardiomiòcits ventriculars neonatals augmenta l'expressió de MEF2 gràcies a una millora de la seva traducció, sense canviar la seva transcripció ni bloquejar la degradació de la proteïna. L'abundància de MEF2 s'incrementa mitjançant la sobreexpressió de Calcineurina *in Vivo* i es redueix per la inhibició de la Calcineurina *in Vitro*, sense afectar els nivells de mRNA de MEF2. L'activitat de la Calcineurina influencia l'expressió de la Polypyrimidin Tract Binding Protein (PTB), contribuint en la traducció de MEF2. Per tant, els nostres resultats mostren el procés de regulació de l'activitat de MEF2 mitjançant el control de la seva traducció, que involucra la Calcineurina i PTB, un procés fins ara desconegut.

Durant el desenvolupament cardíac, un exó conegut com Exó β és progressivament inclòs en el mRNA de MEF2, proporcionant-li una major activitat transcripcional (Yu Y. et al., 1992). Les HDAC de tipus II són abundants en el cor i inhibeixen l'activitat transcripcional de MEF2 (Olson E.N., 2006). En absència de senyals d'estrès, les HDACs de tipus II interaccionen amb MEF2 per tal d'atenuar el creixement cardíac (Berry J.M. et al., 2008). PTB inhibeix la inclusió de l'exó durant la maduració del mRNA i indueix la traducció IRES de molts gens (Spellman R. et al., 2005). Resultats previs del nostre grup demostren que PTB indueix la traducció de gens apoptòtics en els cardiomiòcits i que és abundant en el cor embrionari mentre que la seva expressió es redueix durant el desenvolupament per mecanismes posttranscripcionals (Zhang J. et al., 2009). Més endavant hem mostrat una divergència transitòria entre l'abundància de la proteïna de PTB i la seva transcripció i també que simultàniament té lloc una reducció de l'expressió de HDACs. Això va fer créixer el nostre interès en trobar una possible relació entre el control de les HDAC durant la diferenciació cardíaca, l'abundància de PTB i l'expressió de MEF2. Els nostres resultats mostren que els ratolins deficients en HDAC5 tenen menys proteïna PTB cardíaca i que la inhibició de HDAC causa el tall depenent de caspasa de la proteïna PTB cardíaca i una reducció de l'expressió endògena de cFLIP en els miòcits. L'expressió cardíaca de PTB és

anormalment elevada en ratolins deficients en caspasa executora en el cor i la sobreexpressió de cFLIP impedeix el tall de PTB *in Vitro*. El tall inicial desencadena una major fragmentació de PTB i els fragments s'acumulen en presència d'inhibidors del proteasoma. Modificacions en el procediment anterior *in Vitro* i *in Vivo* han resultat en canvis coherents en l'splicing de l'exó β de MEF2, que codifica per un pèptid que confereix una major activitat transcripcional. Aquests resultats estableixen una via de connexió entre HDAC, cFLIP i caspases que regulen la progressiva desaparició de PTB, que permet l'expressió de les variants adultes de MEF2 durant el desenvolupament cardíac.

左心室质量 (LVM) 具有高度遗传性 (Post W.S. et al., 1997), 也是各种原因的死亡率中一个独立的危险因素 (Lorell B.H. and Carabello B.A., 2000)。迄今为止, 全基因组关联研究 (GWASs) 尚未确定遗传因素相关的 LVM 变化 (Vasan, R.S. et al., 2009), 且血压 (BP) 不相关的心肌肥厚的调控机制目前仍然知之甚少 (McGavock J.M. et al., 2006; Wong C. and Marwick T.H., 2007)。核酸内切酶 G (EndoG) 过去一直被认为与凋亡相关 (Li L.Y. et al., 2001), 而非细胞肥大。Stuart Cook 教授的研究小组确定 EndoG 位于大鼠染色体 3p 上与血压不相关的 LVM 区域, 并证实 EndoG 的缺失与 LVM 的增加和心功能受损有关。作为 S. Cook 教授课题组的合作伙伴并基于上述结论, 我们发现在培养的原代乳鼠心肌细胞中通过抑制 EndoG 的表达, 即使在没有致肥大刺激的情况下, 也可导致细胞体积增大, 肥厚性生物标志物和活性氧 (ROS) 的数量增加。我们还通过电子显微镜观察到, EndoG 敲除 (Endog^{-/-}) 小鼠心脏线粒体无明显的形态学改变, 但与线粒体相关的脂质小滴的数量和体积都明显高于对照组, 油红染色和分子生物学研究结果表明是脂肪变性。因此, 我们的研究进一步证实 EndoG 在心肌发育及线粒体代谢过程中一个新的作用。

为进一步探讨心肌肥厚的机制, 我们主要研究对心脏发育及其功能发挥重要作用, 且对心肌肥厚和多种心肌病有重要作用的肌细胞增强因 2 (MEF2) 的家族 (Black B.L. and Olson E.N., 1998; Naya F.J. et al., 2002; Xu J. et al., 2006)。MEF2 活性通过增加其转录和蛋白激酶依赖性磷酸化得到增强, 并通过与 II 类组蛋白去乙酰化酶结合或 miR-1 介导的转录降解而减弱。我们的研究表明, MEF2 蛋白表达主要在翻译水平进行调节, 这个过程决定了在心肌肥大过程中心肌细胞的大小。为了减少 MEF2 的蛋白的表达, 通过 RNA 干扰, 在肾上腺素存在的情况下, 其表达量又恢复到基线水平。肥大刺激可在翻译水平导致新生大鼠心肌细胞肥大, 而非通过增加其转录或抑制蛋白的降解。动物体内钙调磷酸酶过表达可引起 MEF2 表达量增高, 体外实验抑制钙调神经磷酸酶则引起 MEF2 表达下降, 这些都没有影响 Mef2 mRNA 的表达。钙调神经磷酸酶的活性也影响多聚嘧啶通道蛋白 (PTB) 的表达, 从而促进 MEF2 的翻译。因此, 我们的研究表明 MEF2 的活性是在钙调磷酸酶和 PTB 调控下, 在翻译水平进行调节。

心脏发育过程中一个外显子 β 在 MEF2 mRNA 中含量递增并能赋予 MEF2 更强的转录活性 (Yu Y. et al., 1992)。心脏组织中 II 型组蛋白去乙酰化酶 (HDACs) 含量丰富

并能抑制 MEF2 转录活性 (Olson E.N., 2006)。在无应激的情况下, II 型 HDACs 与 MEF2 相互作用并延缓心脏发育 (Berry J.M. et al., 2008)。多聚嘧啶通道结合蛋白 (PTB) 在 mRNA 成熟过程中的抑制外显子表达并诱导内部核糖体进入位点 (IRES) - 依赖的多种基因的翻译 (Spellman R. et al., 2005)。我们过去的研究表明, PTB 可诱导心肌细胞凋亡相关基因的翻译, 其自身在胚胎心肌中含量丰富, 但随着个体的发育通过转录后机制的调节表达逐渐减少 (Zhang J. et al., 2009)进一步的研究表明在机体发育过程中 PTB 蛋白水平及其转录水平的变化并不一致, 同时伴随 HDACs 表达下降。因此, 我们对 HDAC 调控下的心肌分化、PTB 表达以及 MEF2 之间的联系有着浓厚兴趣。我们的研究表明 HDAC5 基因敲除小鼠心脏 PTB 蛋白表达降低, HDAC 抑制后所引起的 caspase 依赖的 PTB 蛋白丰度减少, 并导致内源性 cFLIP 在心肌细胞中的表达减少。Caspase 敲除后的小鼠心脏 PTB 的表达异常增高, 体外实验证实心肌细胞中 cFLIP 过表达可抑制 PTB 断裂。Caspase 依赖的 PTB 断裂可引发其进一步蛋白酶依赖的断裂, 且这个过程可被蛋白酶抑制剂所阻断。这些结果建立了一个连接 HDAC, cFLIP 和 caspase 调节 PTB 的通路, 并通过这个途径影响 PTB 对 Mef2 外显子 β 的调节。

Introduction

1 Basic concepts of heart development and growth

1.1 Architecture and function of the heart

The heart is the organ that helps supply blood and oxygen to all parts of the body. It is divided by a partition or septum into two halves, and the halves are in turn divided into four chambers, they are left atria, right atria, left ventricle and right ventricle. The two ventricles are thick-walled chambers that pump blood out of the heart. The heart is situated within the chest cavity and surrounded by a fluid filled sac called the pericardium, which is an involuntary striated muscle tissue found only in this organ. This amazing muscle produces electrical impulses that cause the heart to contract, pumping blood throughout the body. The heart and the circulatory system together form the cardiovascular system.

The heart acts as a double pump. The right atrium receives deoxygenated blood from systemic veins (via superior and inferior vena cavae) and pumps it, via the right ventricle, into the lungs (pulmonary circulation) so that carbon dioxide can be dropped off and oxygen picked up (gas exchange). This happens through the passive process of diffusion. The left atrium receives oxygenated blood from the pulmonary veins and from the left atrium the blood moves to the left ventricle which pumps it out to the body (via the aorta). Starting in the right atrium, the blood flows through the tricuspid valve to the right ventricle and is pumped out of the pulmonary semilunar valve and travels through the pulmonary artery to the lungs. From there, blood flows back through the pulmonary vein to the left atrium. It then travels through the mitral valve to the left ventricle, from where it is pumped through the aortic semilunar valve to the aorta and to the rest of the body. The (relatively) deoxygenated blood finally returns to the heart through the inferior vena cava and superior vena cava, and enters the right atrium where the process begins.

1.2 Cardiac morphogenesis

Mammalian cardiogenesis requires the generation of a highly diversified set of both muscle and nonmuscle cell types, including atrial and ventricular cardiomyocytes; conduction

system and pacemaker cells; and smooth muscle, endothelial, valvular, and endocardial cells. The formation of these various cardiovascular cell lineages in distinct heart and vascular compartments has its basis in the existence of a closely related set of multipotent progenitors in the early embryonic heart field, which can be divided into the primary (first) heart field (FHF) and secondary heart field (SHF) lineages (Fig. 1) (Chien K.R. et al., 2008).

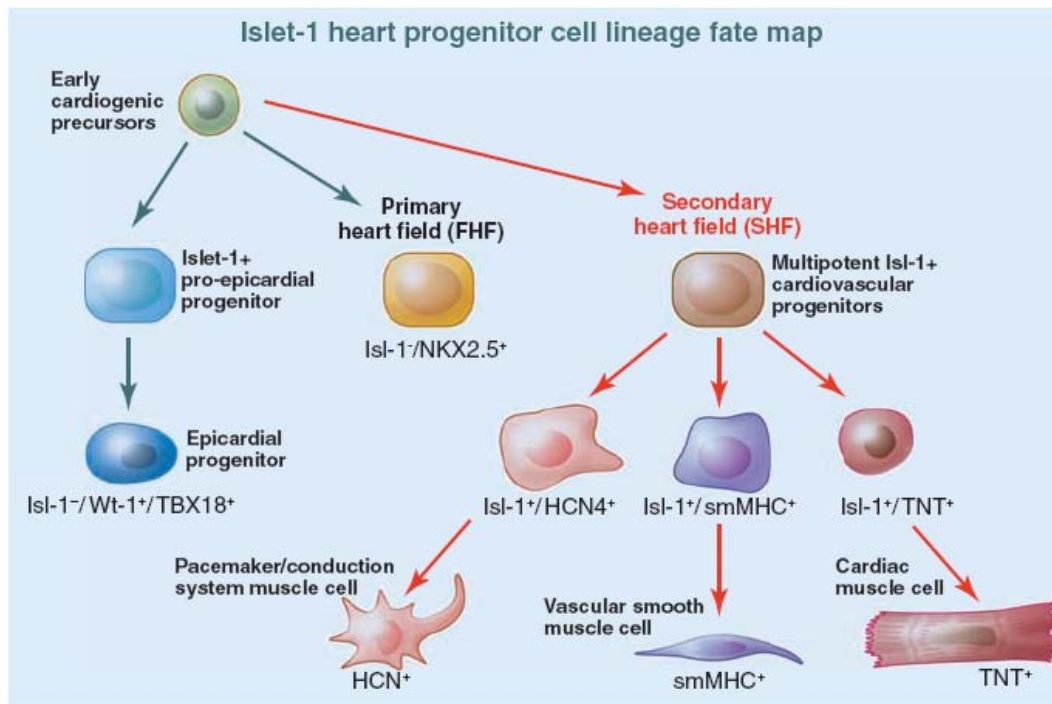


Fig. 1 Multipotent heart progenitors in the *Isl1* lineage. Early mesoderm-derived cardiac precursors give rise to progenitors in the first and second heart fields (FHF and SHF, respectively). The LIM-homeodomain transcription factor *Isl1* marks a multipotent cardiovascular progenitor lineages (Chien K.R. et al., 2008).

As the heart tube forms, SHF cells migrate into the midline and position themselves dorsal to the heart tube in the pharyngeal mesoderm (Fig. 2). Upon rightward looping of the heart tube, SHF cells cross the pharyngeal mesoderm into the anterior and posterior portions, populating a large portion of the outflow tract, future right ventricle, and atrial. Precursors of the left ventricle are sparsely populated by the SHF and appear to largely be derived from the FHF. Once within the heart, FHF and SHF cells appear to proliferate in response to endocardial-derived signals, such as neuregulin, and epicardial signals dependent on retinoic acid, although these mechanisms remain poorly understood (Olson E.N., 2004).

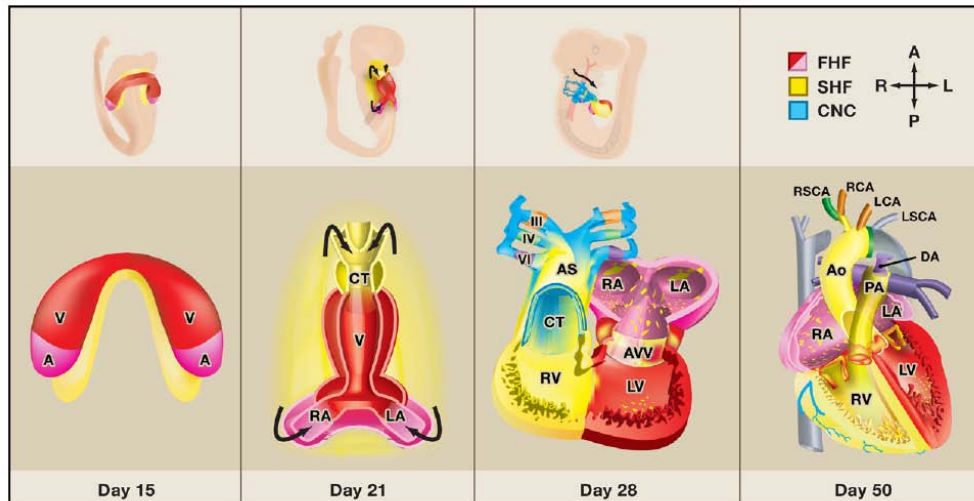


Fig. 2 Mammalian heart development. Oblique views of whole embryos and frontal views of cardiac precursors during human cardiac development are shown. (First panel) First heart field (FHF) cells form a crescent shape in the anterior embryo with second heart field (SHF) cells medial and anterior to the FHF. (Second panel) SHF cells lie dorsal to the straight heart tube and begin to migrate (arrows) into the anterior and posterior ends of the tube to form the right ventricle (RV), conotruncus (CT), and part of the atria (A). (Third panel) Following rightward looping of the heart tube, cardiac neural crest (CNC) cells also migrate (arrow) into the outflow tract from the neural folds to septate the outflow tract and pattern the bilaterally symmetric aortic arch arteries (III, IV, and VI). (Fourth panel) Septation of the ventricles, atria, and atrioventricular valves (AVV) results in the four-chambered heart. V, ventricle; LV, left ventricle; LA, left atrium; RA, right atrium; AS, aortic sac; Ao, aorta; PA, pulmonary artery; RSCA, right subclavian artery; LSCA, left subclavian artery; RCA, right carotid artery; LCA, left carotid artery; DA, ductus arteriosus (Srivastava D., 2006).

1.3 Proliferation and differentiation of cardiomyocytes in postnatal period

Most of heart is made up of contractile muscle cell, as known as cardiomyocytes. Cardiomyocytes constitute approximately 75% of the total volume of the myocardium (Brilla C.G. et al., 1991; Zak R., 1973). Cardiomyocytes occupy most normal myocardial tissue volume, but they are the minority (only 30%) in terms of cell numbers.

Proliferation and differentiation are two different aspects of cell growth. Soon after birth, cardiac myocytes lose their ability to proliferate and the continued increase in heart mass is produced by the enlargement of individual preexisting cardiac myocytes.

The ability of cardiac myocytes to proliferate during the early postnatal period is influenced by nutritional, hemodynamic and humoral factors (Penney D.G., et al., 1990). Enhanced nutrition due to smaller litter size and increased hemodynamic load may promote

myocyte proliferation (Hollenberg M. et al., 1976; Rakusan K. and Korecky B., 1985; Bai S.L. et al., 1990). There is also research suggesting that differentiation and cessation of myocyte proliferation are preprogrammed, and a rapid “trigger” mechanism may control cardiac growth during early postnatal development and that a sequence of master switch genes may regulate this rapid transition (Li F.Q. et al., 1996).

The switch from myocyte hyperplasia to hypertrophy occurs during the early postnatal period. The exact temporal sequence when cardiac myocytes cease dividing and become terminally differentiated is not certain, although it is currently believed that the transition takes place gradually over a 1-2-week period. Almost all myocytes are mononucleated and cell volume remained relatively constant during the first 3 days of age. Increases in cell volume and binucleation of myocytes are first detected at day 4. Myocyte volume increases 2.5-fold from day 3 to day 12. The percentage of binucleated myocytes begins to increase at day 4 and proceeded at a high rate, reaching the adult level of approximately 90% at day 12. Myocyte number increases 68% during the first 3 days and remains constant thereafter (Fig. 3) (Leu M. et al., 2001).

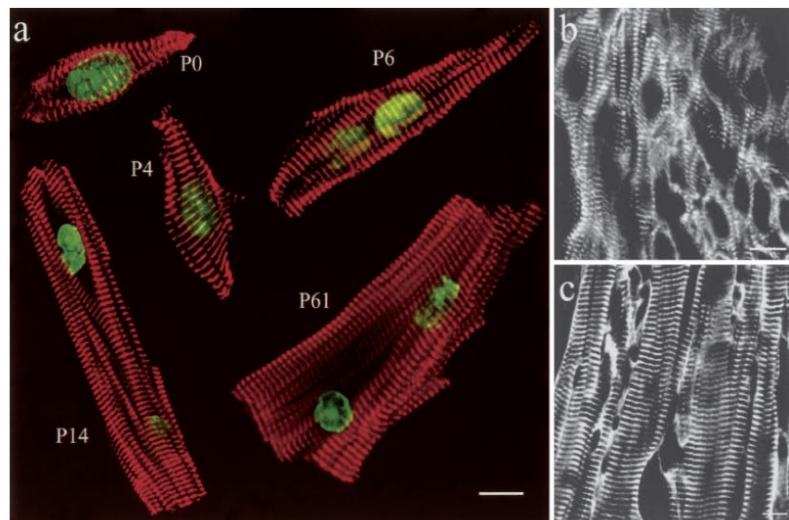


Fig. 3 Fixed freshly isolated mouse cardiomyocytes of different ages (P0, P4, P6, P14, P61) labeled with an anti-myomesin antibody (in red) and Pico Green (in green) as a nuclear stain. **(a)** Myomesin is located in the M-band. During the postnatal phase a morphological change from small spindle-shaped cells (P0, P4) to large rod-shaped cells occurs. Additionally from P6 onwards most of the cardiomyocytes contain two nuclei. Cryosections from newborn **(b)** and adult **(c)** heart stained with anti-myomesin antibodies, demonstrating similar shape differences as seen in the freshly isolated cardiomyocytes. Bar 10 μm . (Leu M. et al., 2001).

When the percentage of binucleated myocytes begins to increase, DNA synthesis of cardiac myocytes may prepare for nuclear division without cytokinesis rather than actual cell division which produces two daughter cells. Ventricular myocytes lose the ability to undergo cytokinesis before final withdrawal from the cell cycle, resulting in the formation of binucleated myocytes (Li F. et al., 1996).

The research also indicated that the increase in heart mass was caused solely by myocyte proliferation with cell volume remaining constant during the first 3 days of age. Continued heart growth was accomplished only by myocyte hypertrophy after day 4. Although embryonic and neonatal cardiac myocytes continued to divide while expressing muscle-specific genes, further differentiation of cardiac myocytes seemed to be incompatible with proliferation (Fig. 4) (Li F. et al., 1996).

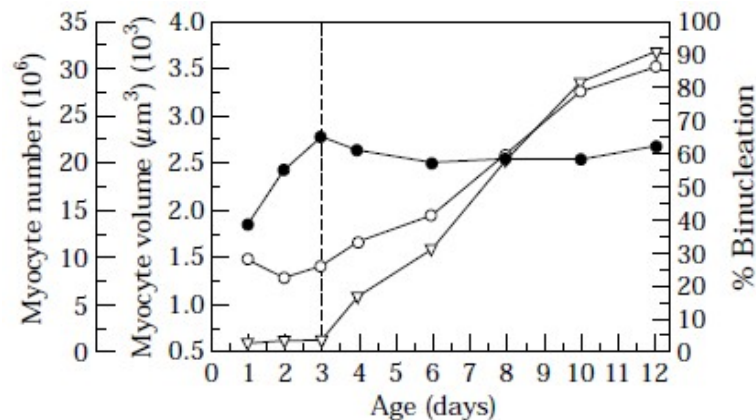


Fig. 4 Changes in myocyte number per heart, myocyte volume (\circ) and percent nucleation (Δ) in contractile cells enzymatically isolated from the hearts of neonatal rats at 1, 2, 3, 4, 6, 8, 10, and 12 days of age. Myocyte number (\bullet) reaches a peak at 3 days of age, remaining unchanged thereafter. At this time point (3-4 days of age) myocyte volume progressively increases while the percentage of myocytes that are binucleated also increases indicating the cessation of myocyte cellular hyperplasia, continuation of nuclear division, and the induction of myocyte hypertrophic enlargement. Each point represents the average value from at least ten hearts (Li F. et al., 1996).

1.4 Main signaling pathways during heart development: a scheme

Expansion of the number of ancestral cardiac regulatory genes and modification of the timing and pattern of their expression, as well as their regulatory interactions with each other and with other developmental control genes, is undoubtedly a major driving force for

building cardiac complexity during evolution. Cardiac genes are typically controlled by combinations of cis-regulatory elements that operate in distinct regions of the heart (Schwartz R.J. et al., 1999). Studies have also demonstrated histone acetylation/deacetylation to be a nodal point for the control of cardiac growth and gene expression in response to acute and chronic stress stimuli (Blacks J. and Olson E.N., 2006). Gene-targeting studies in the mouse have provided the most striking evidence of the importance of class II HDACs as signal-repressive suppressors of postnatal cardiac growth, which associate directly or indirectly with and repress the transcriptional activities of SRF, GATA factors, NFAT, and myocardin, each of which have been shown to be involved in cardiac hypertrophy (Fig. 5) (Blacks J. and Olson E.N., 2006).

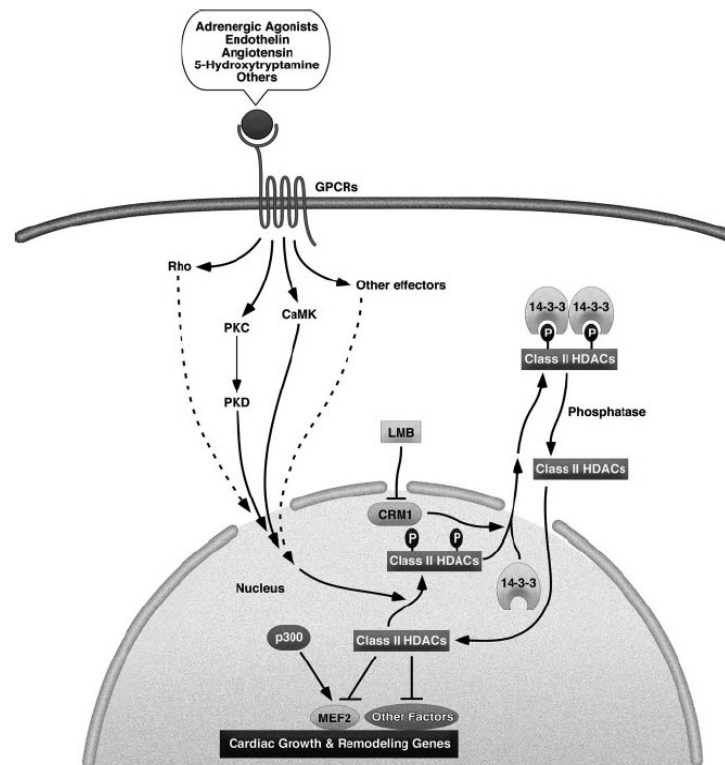


Fig. 5 Kinase signaling to class II HDACs. Diverse agonists act through G-protein-coupled receptors to activate the PKC-PKD axis, CaMK, Rho, and other effectors leading to phosphorylation of class II HDACs. Phospho-HDACs dissociate from MEF2, bind 14-3-3, and are exported to the cytoplasm through a CRM1-dependent mechanism. CRM1 is inhibited by leptomycin B (LMB). Release of MEF2 from class II HDACs allows p300 to dock on MEF2 and stimulate genes involved in cardiac growth and remodeling. Dephosphorylation of class II HDACs in the cytoplasm enables reentry into the nucleus (Blacks J. and Olson E.N., 2006).

1.5 Role of apoptosis during heart development

Programmed cell death (PCD) is a controlled process to eliminate used-up, damaged, or misplaced cells during the embryonic development and in the tissue homeostasis of multicellular organisms (Jacobson M.D., 1997). Apoptosis, the most abundant form of PCD, is a morphologically defined process characterized by cell shrinkage, plasma membrane blebbing, nuclear condensation and fragmentation, the formation of membrane enclosed apoptotic bodies and their selective uptake by phagocytes without provoking inflammatory responses (Kerr J.F. et al., 1972).

The interactions between the various pro- and anti-apoptotic molecules are complex. The many apoptotic stimuli converge into one of two major pathways (extrinsic or intrinsic). The intrinsic pathway of apoptosis is mediated by various stimuli that cause the release of cytochrome c from mitochondria into the cytoplasm, which will bind to the adaptor protein Apaf-1. This structure binds a protease, the initiator Caspase-9, which gets activated, forming the apoptosome complex. Intracellular stimuli include oxidative stress, DNA damage, and protein misfolding. The apoptotic pathway can also be initiated via exogenous stimuli through activation of death receptors. These receptors belong to the TNF receptor family and characteristically bear a death domain (DD) in their intracellular tail. Extracellular stimuli include deficiencies in survival/trophic factors/nutrients, radiation, and other chemical (e.g. drugs) and physical stresses. Both pathways converge on a common downstream pathway involving executioner caspase activation, broad protein cleavage and cell dismantle, which mediates the final morphological and biochemical alterations that are characteristic of apoptosis (Fig. 6) (Kang P.M. and Izumo S., 2003).

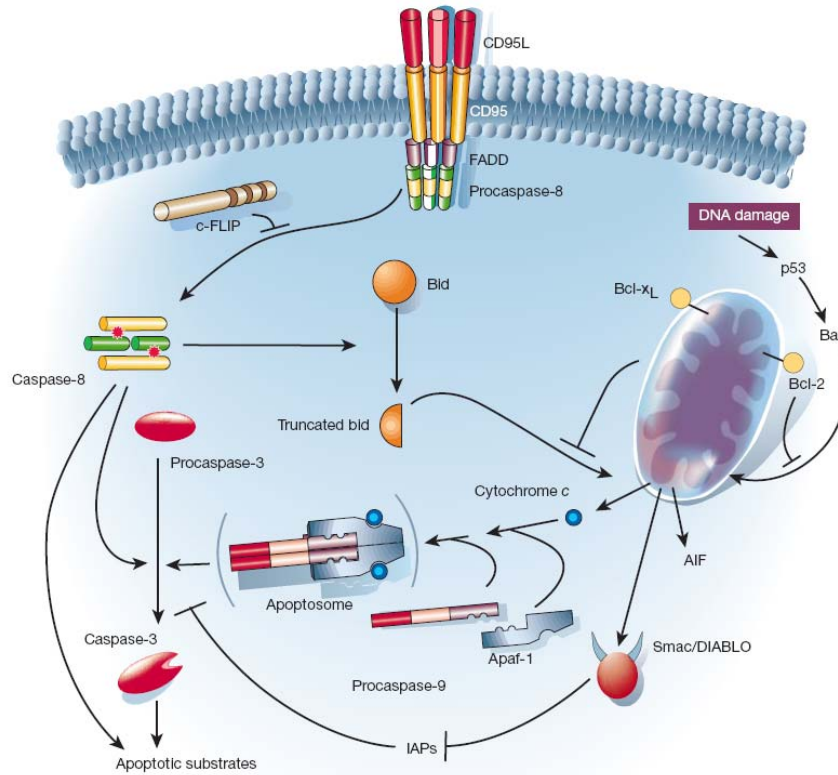


Fig. 6 Two major apoptotic pathways in mammalian cells. In the external triggering of apoptosis, the membrane receptors are activated by extracellular ligands and mediators that allow to trimerize the receptors. In the intracellular side the death receptors are activated and start the downstream activation of caspase-8. In the mitochondrial internal apoptotic response. Bcl-2 family of proteins plays a key role in apoptosis. Bcl is an anti-apoptotic protein that is released after activation of the mitochondrial cytochrome C and AIF. The final product is the formation of the apoptosome (Hengartner M.O., 2000).

Morphogenesis and developmental remodeling of cardiovascular tissues involve coordinated regulation of cell proliferation and apoptosis. The prevalence of apoptosis has been well documented during heart development. During cardiac valve formation, cardiac cushions form as localized expansions of an extracellular matrix, known as the cardiac jelly, at the sites of atrioventricular and ventriculoarterial connections. Endothelial cells invade the cushions and transform into a mesenchymal cell type, and the cushions are sculpted to form the fine inflow (mitral, tricuspid) and outflow (aortic and pulmonary) valves and portions of the atrial and ventricular septa. It would appear that this occurs in part by apoptosis

(Eisenberg L.M. et al., 1995; Huang J.X. et al., 1995). It has also been proved in one study with chick embryo that the embryonic outflow tract (OFT), in contrast to the growth of the atrial and ventricular compartments, shortened at specific stages of rodent, human, and avian development and showed a coincidence with OFT cardiomyocyte apoptosis, the prevalence of which was stage-dependent and reached a peak of nearly 50% at embryonic day 6 (Hamburger V. and Hamilton H.L., 1992; Fisher S.A. et al., 2000).

Moreover, apoptosis has been proposed to play a relevant role in cardiomyocyte death in response to a myriad of stimuli including hypoxia (Tanaka M. et al., 1994), especially followed by reoxygenation, (Kang P.M. et al., 2000) acidosis, (Webster K.A. et al., 1999) oxidative stress (von Harsdorf R. et al., 1999), serum deprivation (Fujio Y. et al., 1997), glucose deprivation and metabolic inhibition (Bialik S. et al., 1999), β 1-adrenergic agonists (Shizukuda Y. et al., 1998), stretch (Cheng W. et al., 1995), angiotensin II (Kajstura J. et al., 1997), tumor necrosis factor- α (Krown K.A. et al., 1996), Fas ligand (Lee P. et al., 2003) and anthracyclines (Wang L. et al., 1998). While several lines of evidence show that canonic apoptosis is not involved in differentiated myocardium cell death (Ohno M. et al., 1998; Knaapen M.W. et al., 2001), including previous work of our group (Sanchis D. et al., 2003; Bahi N. et al., 2008; Zhang J. et al., 2009).

1.5.1 Caspases and apoptosis during heart development

Caspases (cysteiny l aspartate proteinases) belong to a family of highly conserved aspartate-specific cysteine proteases that are expressed as inactive zymogens in most animal cells. When activated, these enzymes cleave their protein substrates on the carboxy-terminal side of an aspartate residue (Fig. 7) (Regula K.M. and Kirshenbaum L.A., 2005).

The death receptor pathway (the extrinsic pathway), involved in the activation of caspase-8 and -10, is initiated when death receptors are stimulated. An alternative pathway of activation of upstream caspases (the intrinsic pathway), involved in the activation of caspase-9, relies on the release of cytochrome c and other mitochondrial proteins in the cytoplasm (Cain K. et al., 2002), and this release is controlled by proteins of the Bcl-2 family.

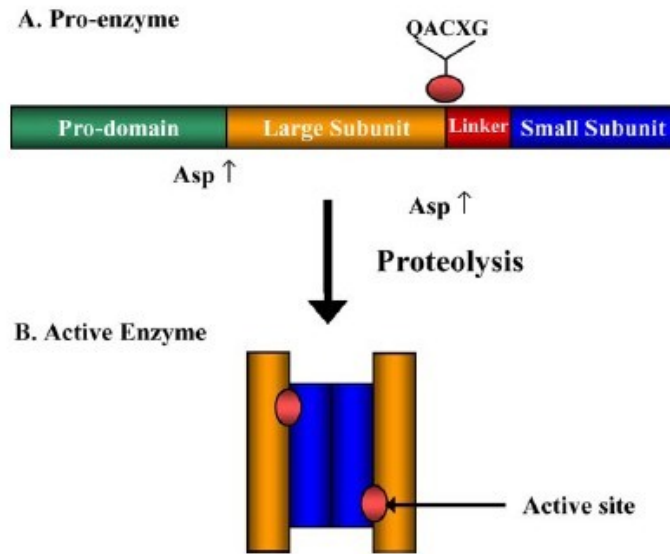


Fig. 7 Schematic representation of caspase structure. Caspases are cysteine proteases. They are produced in cells as inactive precursors containing common structural elements: a pro-domain, large and small subunits and linker region. The active site cysteine is harbored within a conserved QACXG motif in the large subunit. Proteolysis is required to activate the pro-enzyme and occurs at aspartate residues, which reside between the pro-domain and the large subunit and within the linker. The active caspase is a tetramer consisting of two large/small subunit heterodimers each with an active site (Regula K.M. and Kirshenbaum L.A., 2005).

Once caspases 3, 6, and 7, which are proteolytic enzymes, are activated, they cleave a variety of proteins or death substrates. During early apoptosis, caspase-3 cleaves Poly (ADP-ribose) Polymerase (PARP), which decreases its DNA repair activity and leads to apoptotic cell death (Lopez-Nebolina F. et al., 2005). Activation of caspases does not result in the wholesale degradation of cellular proteins. Rather, caspases selectively cleave a restricted set of target proteins, usually at one or a few positions in the primary sequence. This nuclease cuts the genomic DNA between nucleosomes, to generate DNA fragments with lengths corresponding to multiple integers of approximately 180 base pairs. The presence of this DNA ladder has been used extensively as a marker for apoptotic cell death. DNA ladder nuclease (known as caspase-activated DNase, or CAD) pre-exists in living cells as an inactive complex with an inhibitory subunit, dubbed ICAD. Activation of CAD occurs by means of caspase-3-mediated cleavage of the inhibitory subunit, resulting in the release and activation of the catalytic subunit (Hengartner M.O., 2000).

1.5.2 Non-apoptotic role of caspases in heart development

The non-apoptotic functions of caspases involve both proteolysis exerted by their catalytic domains and non-proteolytic functions exerted by their catalytic prodomains. The non-apoptotic function of caspases shows that they may become activated independently of - or without- including an appropriate cascade, thus leading to the cleavage of a specific subset of substrates to avoid the dismantling of the cell. These substrates include members of diverse protein families such as cytokines, kinases, transcription factors and polymerases (Lahm A. et al., 2007).

Although caspase-3 and -7 are traditionally known as downstream effector caspases (Thornberry N.A. and Lazebnik Y., 1998), recent data from mice deficient in these caspases suggest that these downstream caspases may in fact serve to amplify Bax translocation to mitochondria as well as cytochrome c release during apoptosis. Whereas mice deficient in either caspase-3 or caspase-7 were viable, mice that lacked both caspases were present at normal Mendelian numbers through embryonic day 20 (E20), but had defects in heart development and died immediately after birth (Lakhani S. et al., 2006), suggesting a relevant function of these caspases in the growth and/or differentiation of the myocardium.

Histologic examination of caspase-3 and -7 DKO hearts revealed dilation of the atria (Fig. 8A and B) and disorganization and noncompaction of the ventricular musculature (Fig. 8C through F). Thus, caspases-3 and -7 together are important for proper cardiac development, and noncompaction may occur because they act downstream of death receptor signaling. However, the precise mechanisms regulated by caspases during heart development are unknown (Lakhani S. et al., 2006).

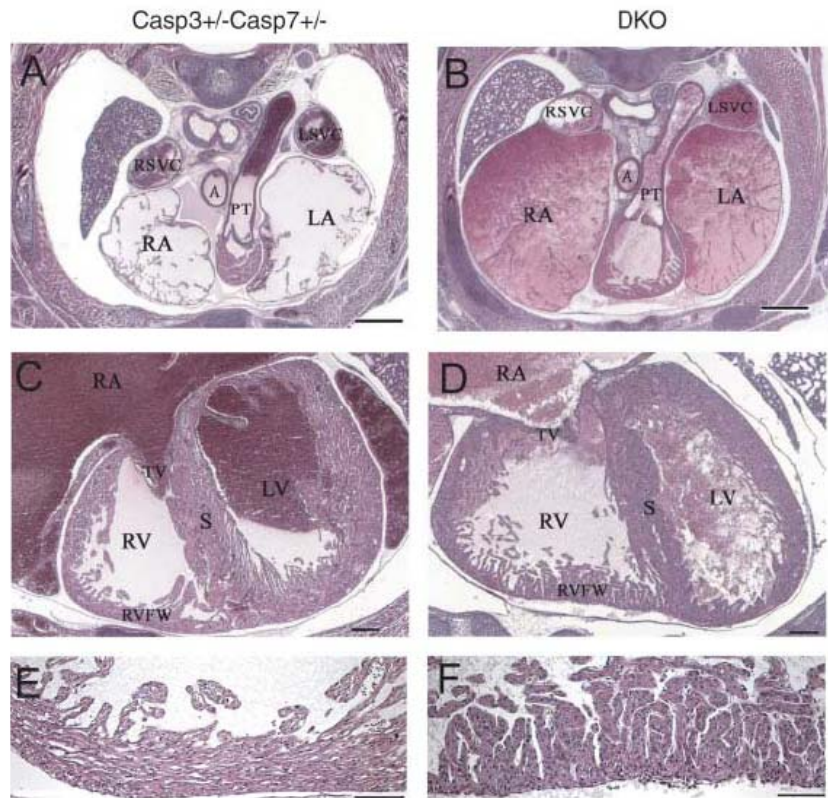


Fig. 8 (A to F) Defective cardiac development in DKO embryos. Hematoxylin-and-eosin staining of transverse sections of caspase 3^{+/-}/caspase 7^{+/-} and DKO E20 embryo hearts. Higher magnification of the right ventricular free wall (E and F). Scale bars: (A and B), 500 mm; (C and D), 200 mm; and (E and F), 100 mm. Abbreviations: A, aorta; PT, pulmonary trunk; RA, right atrium; LA, left atrium; RSV, right superior vena cava; LSV, left superior vena cava; LV, left ventricle; RV, right ventricle; S, septum; TV, tricuspid valve; RVFW, right ventricular free wall (Lakhani S. et al., 2006).

1.6 Cardiac metabolism, hypertrophy and failure

The heart is an “omnivore” organ, capable of metabolising a range of substrates, including fatty acids, glucose, ketone bodies, lactate and amino acids, to fulfill a continuous demand for ATP (Taegtmeyer H. et al., 2004). Under normal physiological conditions, 90% of the ATP is produced via mitochondrial oxidative phosphorylation, with the remainder from substrate level phosphorylation (Neely J.R. et al., 1972). The heart will normally switch its metabolic preference amongst substrates depending on their availability and the physiological conditions.

In contrast to most other tissues that rely on glucose oxidation for energy, cardiomyocytes depend primarily on the mitochondrial oxidation of fatty acids for fuel, deriving up to 60% or more of the cell's energy budget from this source, especially the long chain fatty acids, which provide 60-70% of ATP to power contraction (Bing R.J. et al., 1954; van der Vusse G.J. et al., 1992). Fatty acid oxidation is completely dependent on oxygen, which is critically important in the context of the extremely high ATP demands of the cardiomyocyte (Czubryt M.P. and Olson E.N., 2004).

During short-term exertion or ischemia, when oxygen supply may be severely limited, glycolysis can become more important than oxidation for meeting the cell's energy requirements, because glucose oxidation has a lower oxygen requirement. However, anaerobic glycolysis provides only two molecules of ATP per glucose molecule, since glucose is metabolized to lactate instead of to acetyl-CoA. Glucose uptake into the cardiomyocyte occurs by facilitated transport regulated by sarcolemmal glucose transporters, the GLUTs. Intracellular glucose is rapidly phosphorylated by hexokinase (HK) to glucose-6-phosphate, which serves as a central point in metabolism, capable of entering a number of pathways including glycolysis and glycogenesis, plus the pentose phosphate and hexosamine biosynthetic pathways. Pyruvate is the end product of glycolysis, which, depending on oxygen availability, can either enter the mitochondria for oxidation or be reduced to lactate in the cytosol. Mitochondrial pyruvate dehydrogenase (PDH) is responsible for the oxidative decarboxylation of pyruvate to acetyl CoA for entry into the Krebs cycle, and is a key regulated enzyme complex in glucose metabolism (Randle P.J. et al., 1963). A switch to glucose as a preferred substrate, with a concomitant reduction in fatty acid oxidation, also occurs during cardiac hypertrophy and failure. The energy-producing machinery of the heart thus is highly tuned to meet the specific and significant demands of individual myocytes. Stresses acting on these processes that may affect the efficiency of energy production may, therefore, have serious consequences for the heart as a whole (Czubryt M.P. and Olson E.N., 2004).

Recent studies indicate that energy metabolism in the heart changes during pathologic hypertrophy. It has been well documented that during cardiac hypertrophy and failure, the

contribution to energy production by glycolysis is augmented significantly while energy production by fatty acid oxidation significantly decreases as glucose becomes the favored fuel (Czubryt M.P. and Olson E.N., 2004). The mechanism by which this switch in substrate utilization occurs may involve regulation of transcription and mobilization of the major glucose transporters in the heart, GLUT1 and GLUT4 (Young L.H. et al., 1999). In response to increased energy demand by the heart -- for example, during ischemia -- there is increased recruitment of both transporters to the sarcolemmal membrane, although the response is greater for GLUT4 (Young L.H. et al., 1997). In cardiac hypertrophy, GLUT1 levels rise, while GLUT4 expression is reduced, which may account for the insulin-dependent increase in glucose uptake noted in hypertrophy (Czubryt M.P. and Olson E.N., 2004)? Ultimately, loss of energy stores, either due to decreased synthesis or increased consumption of high-energy compounds like ATP, may be the critical factor in the shift from compensated to decompensated hypertrophy. Some studies (Liu J. et al., 2001; de las Fuentes L. et al., 2003) reveal that energy metabolism changes significantly in the hypertrophied heart but also suggest that the changes that occur during physiological vs. pathological hypertrophy are different. These studies also suggest that defects in ATP generation or usage, resulting in decreased energy stores, actually may underlie pathologic hypertrophic scenarios in general, regardless of the exact cause (Czubryt M.P. and Olson E.N., 2004).

Another possibility for how altered energy metabolism leads to cardiac hypertrophy involves generation of reactive oxygen species (ROS). ROS may arise from numerous sources within cardiomyocytes as well as within other cell types found in the heart. Normal oxidative metabolism produces ROS due to leakage out of the electron transport chain. However, it is unclear what sources may produce sufficient quantities of ROS to affect cardiac metabolism in otherwise-healthy tissue. One theory suggests that some ROS are generated during normal fatty acid oxidation. As fatty acid oxidation increases to meet increased workload, ROS are generated in greater numbers. If the workload elevation is chronic, over time, the antioxidant defenses of the cell are neutralized and ROS builds to toxic levels. Another possibility is that increased workload over time may increase necrosis of cardiomyocytes. As cells die, monocytes and macrophages move into the myocardium, both of which produce high levels

of ROS during respiratory bursts (Czubryt M.P. et al., 1996; Czubryt M.P. and Olson E.N., 2004). Exactly how ROS cause hypertrophy is unclear but numerous studies have implicated ROS production in the hypertrophic process (Jerkic M. et al., 2011; Maejima Y. et al., 2011; Wu R. et al., 2012). It is reported in a recent research that mitochondrial ROS (mtROS) plays a critical role in the development of Angiotensin II (Ang II) induced cardiac hypertrophy. In the research it is proved that during Ang II-induced cardiac hypertrophy, the amplification of mtROS will cause a decline of mitochondrial membrane potential and increases cardiac mitochondrial protein oxidative damage and mtDNA deletions (Dai D.F. et al., 2011).

Since MEF2 transactivate expression of numerous hypertrophic marker genes, it may play a much wider role in cardiac metabolism, including regulation of fatty acid oxidation in the heart and maintenance of mitochondrial function. It has been reported that deletion of MEF2A in mice results in derangement of mitochondrial structure, significant loss of mitochondria accompanied by reduced cytochrome c oxidase activity, cardiac dilation and activation of a fetal gene program reminiscent of that activated in heart failure (Naya F.J. et al, 2002). So when the heart undergoes a sustained increase in workload, many changes occur in the milieu of the cardiomyocyte, including ATP depletion and increased calcium levels (Fralix T.A. et al., 1991). A model can be envisioned in which MEF2 and PGC-1 α co-ordinately regulate the heart's response to increased workload (Fig. 9). The decrease in ATP levels and rise in intracellular calcium concentration activates the two major pathways of this model by activating AMPK and CaMK, which results in stimulation of MEF2 transactivation and increased synthesis of PGC-1 α (Czubryt M.P. and Olson E.N., 2004).

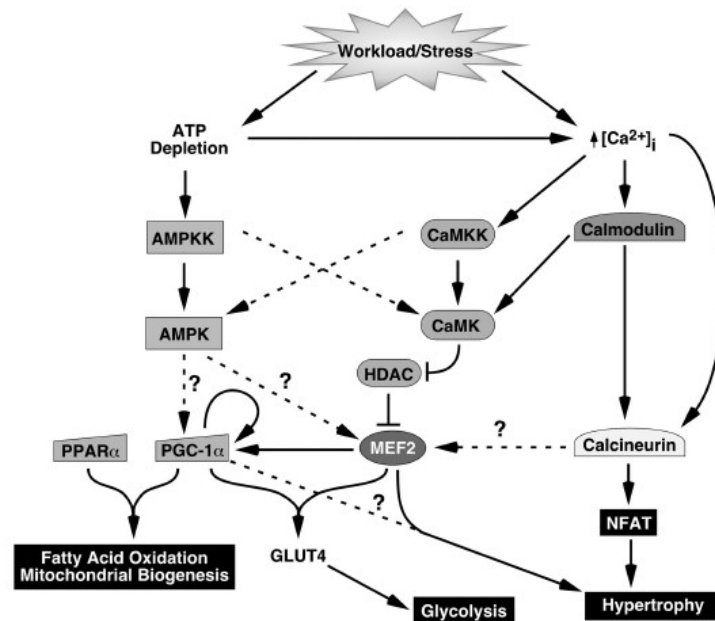


Fig. 9 Myocyte enhancer factor 2 (MEF2) participates in transducing adenosine triphosphate (ATP) and calcium signals to mediate hypertrophic gene expression. In response to increased workload or stress (e.g., inefficient coupling of excitation and contraction, inefficient contraction due to genetic defect), ATP levels fall and intracellular calcium concentration rises. The rise in intracellular calcium may be exacerbated when ATP levels are low due to reduced activity of calcium pumps in the sarcolemma or sarcoplasmic reticulum, resulting in reduced calcium sequestration during relaxation. Increased adenosine monophosphate (AMP): ATP ratio activates AMP-activated protein kinase (AMPK) kinase, or AMPK directly, while at the same time, increased calcium concentration activates calcium/calmodulin-dependent protein kinase (CaMK) kinase and calmodulin, which, in turn, activate CaM kinases. Activated CaMKs activate MEF2-regulated transcription by phosphorylating histone deacetylases (HDACs), which repress MEF2 transactivation, resulting in HDAC release from MEF2 and export of HDACs from the nucleus by 14-3-3. Activated AMPK increases transcription of peroxisome proliferator-activated receptor (PPAR) gamma coactivator-1 α (PGC-1 α) and MEF2A and MEF2D via an unknown mechanism. PGC-1 α also coactivates its own expression, ostensibly mediated by MEF2. PGC-1 α and PPAR γ cooperate to drive expression of fatty acid oxidation enzymes and promote mitochondrial biogenesis. PGC-1 α and MEF2 cooperate to drive expression of GLUT4, thereby increasing glycolysis and/or glucose oxidation by augmenting glucose import, and may participate in driving expression of genes involved in hypertrophy such as contractile proteins. Increased intracellular calcium concentration and activation of calmodulin also activate the protein phosphatase calcineurin, which dephosphorylates and activates the nuclear factor of activated T cell (NFAT) transcription factor family that is involved in driving the hypertrophic program. Calcineurin may activate MEF2 directly but the mechanism of this process has not been elucidated. Numerous other signaling pathways are expected to interact with components of this model -- for example, the phosphatidylinositol 3-kinase/glycogen synthase kinase-3 β (PI-3K/GSK-3 β) pathway -- since GSK-3 β regulates NFAT transcriptional activity (Czubryt M.P. and Olson E.N., 2004).

1.6.1 Function of mitochondria

A mitochondrion (plural mitochondria) is a membrane-enclosed organelle found in most eukaryotic cells (Henze K. and Martin W., 2003). These organelles range from 0.5 to 10 μm in diameter. Mitochondria are sometimes described as “cellular power plants” because they generate most of the cell’s supply of adenosine triphosphate (ATP), used as a source of chemical energy (Campbell N.A. et al., 2006). In addition to supplying cellular energy, mitochondria are involved in a range of other processes, such as signaling, cellular differentiation, cell death, as well as the control of the cell cycle and cell growth (McBride H.M. et al., 2006). Mitochondria have been implicated in several human diseases, including mitochondrial disorders (Gardner A. and Boles R.G., 2005) and cardiac dysfunction (Lesnefsky E.J., et al. 2001) and may play a role in the aging process.

Mitochondria are composed of compartments that carry out specialized functions. These compartments or regions include the outer membrane, the inter membrane space, the inner membrane, and the cristae and matrix. Mitochondrial proteins vary depending on the tissue and the species. In humans, 615 distinct types of proteins have been identified from cardiac mitochondria (Taylor S.W. et al., 2003), whereas in murine (rats), 940 proteins encoded by distinct genes have been reported. The mitochondrial proteome is thought to be dynamically regulated (Zhang J. et al., 2008). Although most of a cell’s DNA is contained in the cell nucleus, the mitochondrion has its own independent genome. Furthermore, mitochondrial DNA shows substantial similarity to bacterial genomes (Andersson S.G. et al., 2003).

1.6.1.1 Mitochondria in heart function and failure

Cardiac muscle cells depend on mitochondria to provide energy, even subtle perturbations in mitochondria content or function can result in cardiac dysfunction. Indeed, cardiomyopathies are frequently associated with mitochondria DNA mutations and mitochondrial diseases. Many cardiac diseases result from primary or secondary mitochondrial defects. For example, both dilated and hypertrophic cardiomyopathies have been associated with point mutations in mitochondrial DNA coding for tRNAs and metabolic

genes such as cytochrome b and cytochrome c oxidase. In some instances, defects in mitochondria are secondary to other phenomena, yet still evoke cardiac hypertrophy (Czubryt M.P. and Olson E.N., 2004).

The targeted inactivation of nuclear-encoded mitochondrial genes has demonstrated the importance of mitochondrial function in the pathophysiology of cardiac disease. Mice with mutations in the genes encoding the mitochondrial transcription factor A (mtTFA) and manganese superoxide dismutase (MnSOD) develop dilated cardiomyopathy in the early postnatal period, whereas a knockout of the adenine nucleotide translocator (ANT) results in hypertrophic cardiomyopathy (Wang J. et al., 1999; Li Y. et al., 1995; Graham B.H. et al., 1997). In transgenic mice, overexpression of the peroxisome proliferator-activated receptor- γ coactivator (PGC-1) in the heart results in dilated cardiomyopathy with excess mitochondria and alterations in mitochondrial respiratory activity (Lehman J.J. et al., 2000).

Recent studies have demonstrated a correlation between deficits in mitochondrial function and cardiac arrhythmias or sudden death. It has also been proved that the mitochondrial respiratory deficiency in Mef2a mutant hearts could contribute to ventricular dysfunction and/or electrophysiological disturbances resulting in a higher incidence of sudden death (Naya F.J. et al., 2002). It has been shown in one study that a substantial reduction in the number of mitochondria in hearts of Mef2a^{-/-} mutants, and quantification of mitochondrial content by analysis of electron micrographs indicated there were 57% fewer mitochondria in the right ventricle of viable adult mutants compared with wild-type controls. The mitochondrial DNA copy number per nuclear genome was reduced three fold in Mef2a null hearts, consistent with the deficiency of mitochondria observed at the ultrastructural level (Naya F.J. et al., 2002). In addition, oxidative stress generated in mitochondria has been shown to govern hypertrophy by increasing mitochondrial ROS which will activate MAP kinases and lead to cardiac hypertrophy (Dai D.F. et al., 2011). All of these results indicate that MEF2A is important for the function of mitochondria and its metabolism in the heart.

1.6.1.2 The role of mitochondria during cardiomyocyte death

Mitochondria play a very important role in transmitting and amplifying death signaling to the intrinsic even extrinsic pathway apoptosis. The most critical mitochondrial events during apoptosis are the structural and functional remodeling of this organelle and subsequent release of apoptogenic proteins to the cytosol. These proteins include cytochrome c, Smac/DIABLO (second mitochondria-derived activator of Caspase/direct IAP-binding protein with low pI), Omi/HtrA2 (high temperature requirement protein A2), AIF (Apoptosis Inducing Factor) and EndoG (Endonuclease G) (Fig.10) (Mani C. et al., 2004).

However, the implication of the mitochondria-dependent intrinsic apoptotic pathway leading to caspase activation has been questioned recently by several evidences. One research has proved that Bnip3 induces caspase-independent mitochondrial permeabilization during cardiac ischemia, involving a role of mitochondrial damage unrelated to caspases yet involving Bcl-2-related proteins (Kubasiak L.A. et al., 2002). The results from our group suggested that mitochondrial damage is an important event leading to cardiomyocyte death without downstream activation of caspases (Sanchis D. et al., 2003) and EndoG-linked Bnip3-mediated mitochondrial dysfunction and DNA degradation during ischemia in cardiomyocytes assembled a protein network unrelated to caspases in postmitotic cells (Zhang J. et al., 2011). It is also stated that in cardiomyocytes, mitochondrial permeability transition (MPT) is implied in cell death in a caspase-independent and Bcl-2-independent manner during ischemia and reperfusion (Baines C.P. et al., 2005). Finally, the antiapoptotic protein ARC (Apoptotic Repressor with CARD domain) that has been shown to safeguard the heart and to block caspase activation in cell lines can also protect from caspase-independent death, suggesting that ARC dependent protection could be caspase-independent in post-mitotic cardiomyocytes (Kung G. et al., 2011). Therefore, the role of mitochondria has been taken into account and canonical apoptosis is discarded to play a major role in heart disease.

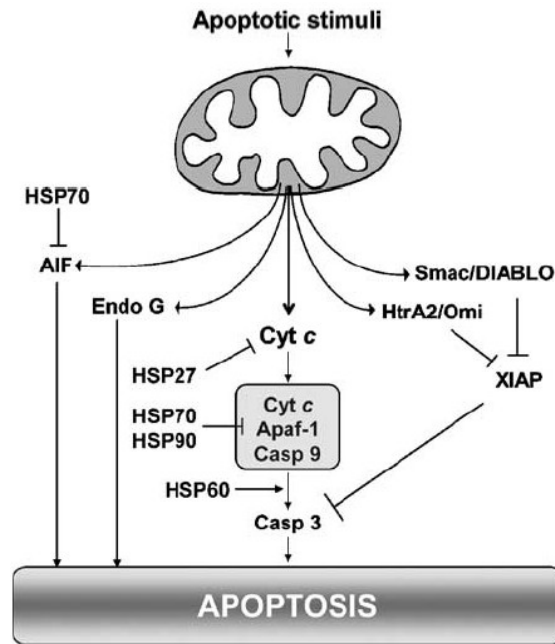


Fig. 10 Mitochondrial release of proapoptotic molecules. Soluble molecules from the IMS include Cyt c which, once in the cytosol, is able to interact with Apaf-1 to generate the apoptosome, a molecular platform for caspase-9 activation. The catalytic maturation of caspase-9 activates the caspase cascade and, ultimately, favors the acquisition of the apoptotic morphology of cell death. These events are controlled by several HSPs at different levels along the apoptotic cascade, and by the X-linked inhibitor of apoptosis protein (XIAP), that negatively regulates caspase-3 and -9. Smac/DIABLO and HtrA2/Omi neutralize XIAP. AIF and EndoG translocate to the nucleus where they trigger DNA fragmentation and chromatin condensation in a caspase-independent fashion. Casp, caspase (Garrido C. et al., 2006).

The mitochondria events involve opening of a pore in the inner mitochondrial membrane (IMM) referred to as the mitochondrial permeability transition pore (MPTP) a multiprotein megachannel connecting the mitochondrial matrix with the cytosol that is normally closed. The MPTP is known to be regulated by cyclophilin D, a peptidyl-prolyl *cis-trans* isomerase located in the mitochondrial matrix. The cellular consequences of MPTP opening are profound. There is loss of $\Delta\psi_m$, the electrical potential across the IMM that is needed to drive ADP→ATP production. Moreover, MPTP opening results in marked mitochondrial swelling and potentially outright rupture of the OMM (Kitsis R.N. and Molkenin J.D., 2010; Rodríguez-Sinovas A. et al., 2007).

Ca^{2+} is a second messenger in numerous signaling pathways and regulates many processes including muscle contraction and cardiac rhythm. Models of cardiomyocyte death secondary to transient ischemia have proved that various strategies will interfere with Ca^{2+} overload-induced cardiomyocyte hypercontracture. (Inserre J. et al., 2009). Researches have shown that mitochondria isolated from ischemically preconditioned or postconditioned myocardium exhibit a reduced susceptibility to induction of MPTP by supraphysiological Ca^{2+} concentrations or ROS. To date, the cause-effect relationship between MPTP opening and cell death has remained elusive. It seems possible that MPTP opening contributes to myocardial cell death in reperfusion or MPTP could cause cell death by initiating apoptosis (Rodríguez-Sinovas A. et al., 2007).

1.6.1.2.1 EndoG: A mitochondrial nuclease in the heart

Apoptosis is a physiological process critical for normal mammalian development and tissue homeostasis. Biochemical and genetic studies have identified at least two endonucleases important for mammalian DNA fragmentation during apoptosis, the DNA fragmentation factor DFF and Endonuclease G (EndoG). EndoG, a well-conserved nuclease, is a homodimer that is thought to be involved in mitochondrial DNA replication with important roles in recombination and repair. EndoG is localized in the mitochondria, and then translocates to the nucleus during apoptosis with cell death stimuli such as truncated Bid (tBid), tumor-necrosis factor- α (TNF- α) and UV irradiation (David K.K. et al., 2006).

Until now there are three labs that have produced EndoG knock out mice. One of them, Zhang and his colleagues reported that mice with $\text{EndoG}^{-/-}$, the embryos lost normal morphology and died between embryonic days 2.5 and 3.5, which demonstrated that EndoG was required for early embryogenesis (Zhang J. et al., 2003). Whereas the EndoG null mice generated by other labs were available and developed to adulthood without obvious abnormalities and undergo normal apoptosis to a variety of apoptotic stimuli (Irvine R.A. et al., 2005; David K.K. et al., 2006). They explained the reason for this disparity was that the other group inadvertently deleted half of a gene immediately adjacent to the EndoG gene in addition to the EndoG gene.

Our previous research by Bahi and coworkers has demonstrated that the release of EndoG together with cytochrome c and AIF from mitochondria to cytosol in rat postnatal differentiated cardiomyocytes was induced by experimental ischemia (Bahi N. et al., 2006). By using short-hairpin based RNA (shRNA) interference of EndoG, we demonstrated the essential role of EndoG in the ischemia-induced caspase-independent DNA degradation/processing in differentiated neonatal cardiomyocytes (Bahi N. et al., 2006). We also proved that endogenous Bnip3 induced EndoG release and caspase independent EndoG-dependent DNA fragmentation, supporting that EndoG executes DNA damage triggered by Bnip3, which provides that EndoG and Bnip3 are expressed abundantly in the differentiated myocardium compared to the embryo, in contrast to the caspase-dependent machinery, and EndoG was the link between Bnip3-mediated mitochondrial dysfunction and DNA degradation during ischemia in cardiomyocytes, assembling a protein network unrelated to caspases in postmitotic cells (Zhang J. et al., 2011).

Despite its role in DNA degradation during ischemia, EndoG is highly expressed in the adult heart. This is surprising because we previously showed that myocytes repressed the expression of other apoptotic proteins during differentiation (Zhang J. et al., 2007). The sustained expression of EndoG in the myocardium suggests an important function of this protein in the biology of the adult heart that remains to be elucidated.

1.6.2 Signaling for cardiac hypertrophy

Myocardial hypertrophy is a response of cardiac muscle to altered conditions of haemodynamic overload caused by a large number of physiological and pathological conditions. The heart modifies its shape as well as its volume in response to a need for altered force production (Selvetell G. et al., 2004).

Cardiac hypertrophy -- that is, enlargement of the heart resulting from increased myocyte size -- is observed in many forms of human heart disease. Traditionally, it has been widely believed that hypertrophy occurred as an adaptive response to normalize increased wall stress due to disease. Recently, however, it is observed that while hypertrophy initially appears

to improve the function of the heart following insult, over time, it frequently leads to a decompensated state, characterized by fibrosis and chamber dilation, sustained hypertrophy, in response to hormonal, genetic, and mechanical stimuli can finally lead to heart failure. Hypertrophy also occurs during fetal development, immediately after birth, and in trained athletes; however, it does not lead to decompensation in these states. Some biochemical pathways determine a maladaptive cardiac hypertrophy that rapidly leads to reduction of cardiac contractility and heart failure (Fig. 11) (Czubryt M.P. and Olson E.N., 2004).

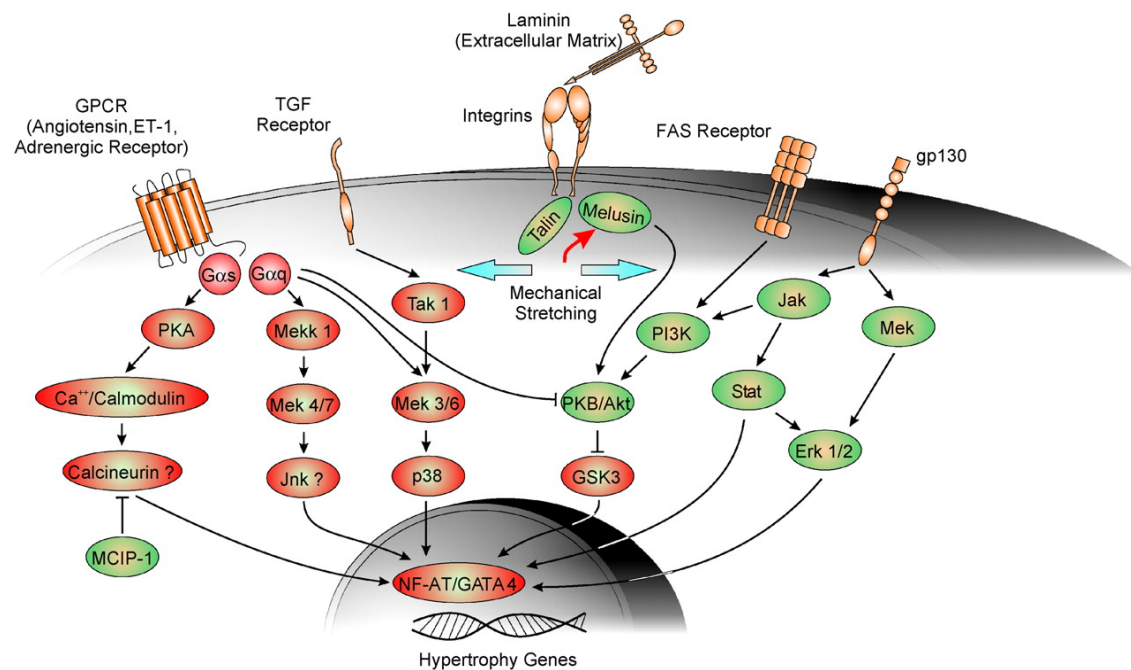


Fig. 11 Adaptive and maladaptive intracellular signaling molecules activated during cardiac hypertrophic remodeling. The green signaling molecules, when activated, exert a protective role in the progression towards heart failure, on the contrary, the activation of the red molecules favors the transition towards heart failure (Selvetella G. et al., 2004).

Because the adult myocardial cell is terminally differentiated and has lost the ability to proliferate, cardiac growth during the hypertrophic process results primarily from an increase in protein content per individual myocardial cell, with little or no change in muscle cell number (Chien K.R., et al., 1991). Hypertrophic stimulation of the adult heart is associated

with activation of a number of intracellular signaling pathways, including mitogen-activated protein kinase (MAPK), calcineurin, protein kinase C, calmodulin-dependent protein kinase, insulin-like growth factor 1 pathway constituents, and altered intracellular Ca^{2+} handling. Consistent with the activation of these discrete intracellular signaling pathways, MEF2 factors can be activated by Ca^{2+} , calcineurin, p38 MAPK, big MAPK-1 (BMK1), and calmodulin-dependent protein kinase (Xu J. et al., 2006).

Pathologic hypertrophy essentially can be divided into two subcategories. The early stage of pathologic cardiac hypertrophy is termed “compensation” because, in response to a stress, the heart walls thicken in an attempt to compensate for the increased stress. This enlargement is due to increased cardiomyocyte size as well as to increased deposition of collagens and other extracellular matrix components in a process called fibrosis, which may account for a significant proportion of the size increase. By increasing cardiac wall volume, fibrosis helps alleviate transmural stress. However, stiffness of the cardiac muscle increases and compliance decreases as fibrosis progresses (Jalil J.E. et al., 1989). Compensated cardiac hypertrophy frequently devolves into the latter stage of hypertrophy-- decompensation. As mentioned before, significant cardiac fibrosis typically precedes decompensation and likely plays a causative role. As collagen fibrils are deposited in the cardiac interstitium, cardiac function becomes progressively impaired. Eventually, the heart is unable to pump enough blood to meet the body’s demands and patients go into overt cardiac failure (Fig. 12) (Czubryt M.P. and Olson E.N., 2004).

Introduction

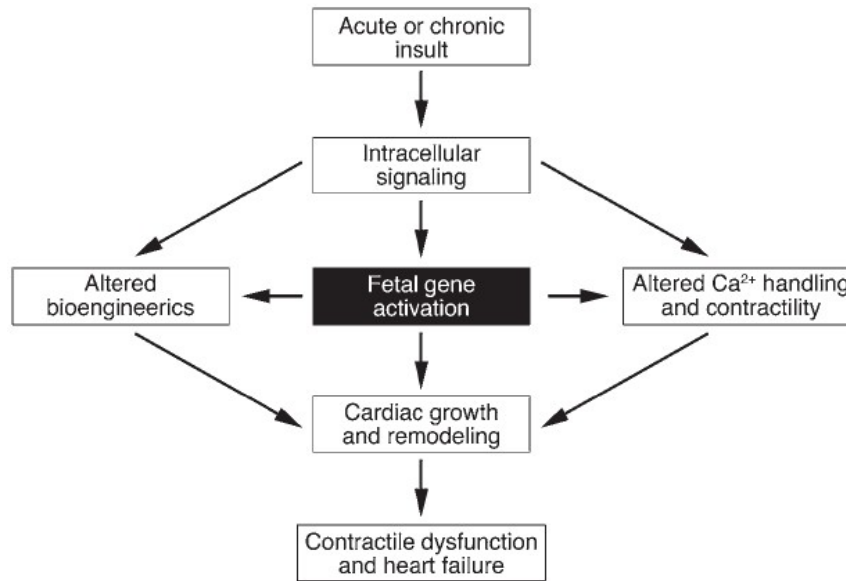


Fig. 12 Abnormalities associated with cardiac remodeling during pathological hypertrophy and heart failure (McKinsey T.A. and Olson E.N., 2005).

Diverse and distinct hormonal stimuli have been documented to activate several features of the hypertrophic response, including several autocrine and paracrine factors (Fig. 13). Increased protein synthesis is a key feature of cardiac hypertrophy and likely underlies the increased cell and organ size observed under this condition (Proud C.G., 2004). Of the known noncontractile protein genes that are up-regulated during ventricular hypertrophy, the reactivation of atrial natriuretic factor (ANF) expression may be one of the most well-characterized.

During embryonic development, the ANF gene is expressed in both the atrium and the ventricle. Shortly after birth, the expression of ANF is down-regulated in the ventricle, and the atrium is the primary site of ANF synthesis within the mature myocardium. The induction of ANF gene expression is a highly conserved and cardinal feature of ventricular hypertrophy, as it can be found in a wide variety of species (mouse, rat, hamster, humans) in response to a wide variety of stimuli such as hormonal, pressure and volume overload, hypertension, genetic, etc. (Chien K.R. et al, 1991).

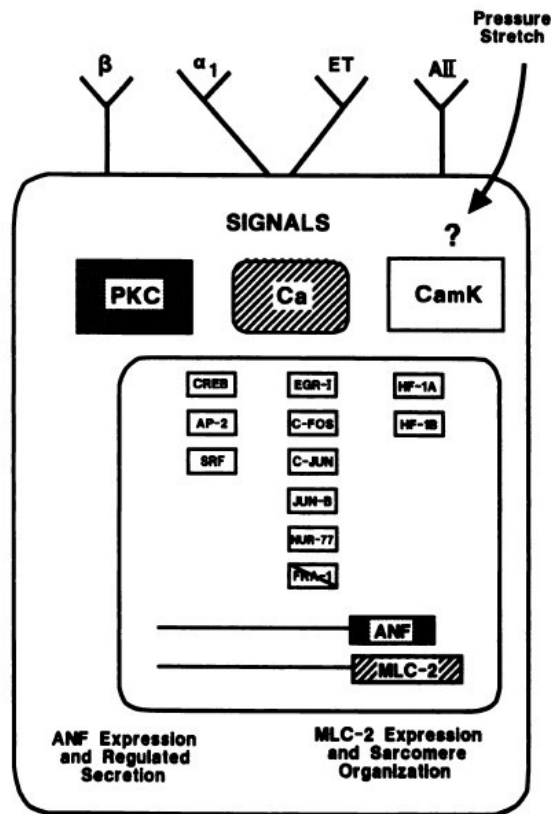


Fig. 13 Candidate signaling mechanisms that may activate growth and hypertrophy of myocardial cell. Hypertrophic response is caused by several receptors: α -adrenergic receptor (α), β -adrenergic receptor (β), endothelin-1 receptor (ET) and angiotensin II receptor (AII), which will activate the PKC, Ca^{2+} or CamK pathways to induce cardiac hypertrophy (Chien K.R., et al., 1991).

1.6.2.1 G proteins

Accumulating evidence suggests that cardiac responses to a number of circulating or locally released humoral factors contribute to adaptive responses after hemodynamic stress or myocardial injury. Heterotrimeric GTP-binding proteins transduce stimulatory or inhibitory signals from agonist-occupied seven-transmembrane-spanning-domain receptors of the rhodopsin superfamily. Within the cardiovascular system, three functional classes of G protein-coupled receptors are of primary importance owing to their acute hemodynamic and chronic myotrophic effects. The functional classes of cardiovascular receptors correspond to

the three major classes of G proteins. Thus, β -adrenergic receptors (β AR), which couple primarily to $G_{\alpha s}$, mediate acute enhancement of heart rate and myocardial contractility in response to epinephrine and norepinephrine stimulation. The second class of myocardial receptors is the cholinergic receptors, typically coupled to $G_{\alpha i}$, which are activated by acetylcholine. The third class of receptors, coupled primarily to $G_{\alpha q}$, includes angiotensin II, endothelin, and α -adrenergic (α AR) receptors (Molkentin J.D. and Dorn II G.W., 2001). Each of these structurally diverse hypertrophic agonists stimulates a membrane receptor that activates PLC via the Gq class of GTP-binding proteins, which suggests that Gq and PLC could be hypertrophy-signaling effectors (McDonough P.M. et al., 1987; Shubeita H.E. et al., 1990; Brown J.H. et al., 1992; Sadoshima J-I. et al., 1993; Clerk A. et al., 1997; Adams J.W. et al., 1998;).

In particular, hormones such as angiotensin II, endothelin-1, norepinephrine (phenylephrine) and prostaglandin $F_{2\alpha}$ which bind to and activate cardiomyocyte membrane receptors coupled to the Gq class of GTP binding proteins have been implicated in the development and ultimate decompensation of cardiac hypertrophy. Using variations of neonatal rat ventricular myocytes culture model, hypertrophic effects of phenylephrine, angiotensin II, endothelin, and prostaglandin $F_{2\alpha}$ (PG $F_{2\alpha}$) have all been demonstrated (Sadoshima J. and Izumo S., 1993; Adams J.W. et al., 1996). A critically important feature of these structurally diverse hypertrophic factors is that, they each stimulate a seven transmembrane-spanning or heptahelical receptor that activates phospholipase C via the Gq class of GTP binding proteins (Fig. 14).

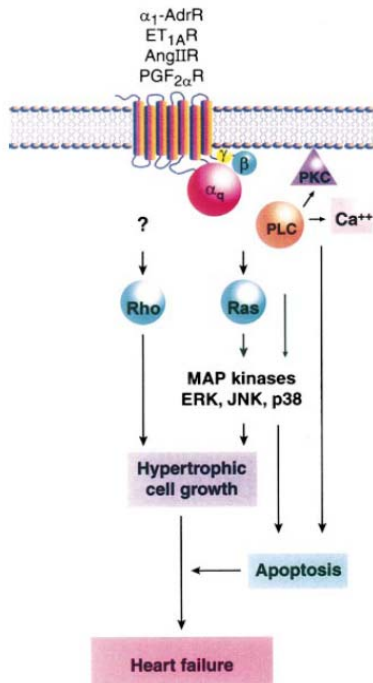


Fig. 14 Schematic of Gq-coupled receptor, Gq, and small G protein involvement in hypertrophy and failure (Dorn II G.W. and Brown J.H., 1999).

A recent study shows that endothelin-1 (ET-1) stimulates $InsP_3$ -induced Ca^{2+} release (IICR) from perinuclear $InsP_3$ Rs, causing an elevation in nuclear Ca^{2+} . Ca^{2+} has a fundamental role in the biology of cardiac myocytes -- stimulating their contraction during every heartbeat as well as the transcription of genes involved in cardiac hypertrophy (Fig. 15). Indeed, studies also show that IICR could activate the CaMK, causing export of an exogenously expressed GFP-HDAC and induction of a synthetic myocyte enhancer factor (MEF2) reporter in cardiac myocytes (Higazi D.R. et al., 2009).

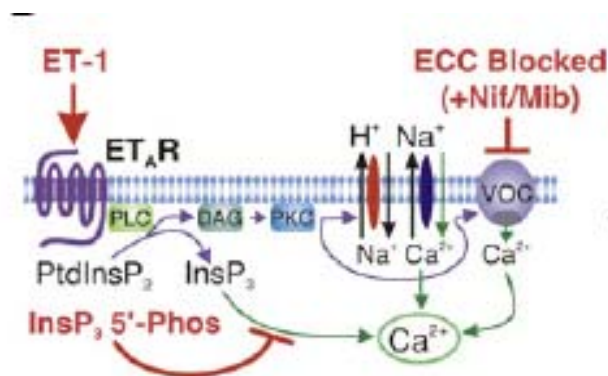


Fig. 15 Schematic of the Ca^{2+} pathways activated by ET-1 in cardiac myocytes and interventions imposed to inhibit ECC (+Nif/Mib indicates nifedipine and mibefradil application) and IICR ($InsP_3$ 50-Phos). VOC is an abbreviation of voltage-operated channel (Higazi D.R. et al., 2009).

1.6.2.2 Calcineurin

Calcineurin, a Ca^{2+} /calmodulin (CaM)-activated phosphatase, has been implicated as a molecular decoder of sustained Ca^{2+} signals evoked in muscle cells in response to frequent nerve-mediated depolarizations and as an integral signaling intermediate in pathways that promote muscle fibre hypertrophy and expression of a slower contractile protein phenotype. It is postulated that nerve-mediated increases in muscle intracellular Ca^{2+} activate calcineurin and CaM-sensitive kinases which in turn trigger the action of nuclear factor of activated T cells c1 (NFATc1) and myocyte enhancer factor 2 (MEF2) proteins (Chin E.R. et al., 1998; Olson E.N. and Williams R.S., 2000; Wu H. et al., 2000). It is thought that these proteins bind cooperatively with other transcription factors such as GATA-2 to activate the transcription of slow fibre-specific or growth-regulatory genes. Recent progress in this field has clearly shown that calcineurin is critically implicated in cardiac hypertrophy. When calcineurin is activated, it dephosphorylates transcription factors called nuclear factors of activated T cells (NFATs), which in turn promote nuclear translocation of NFAT (Molkentin J.D. et al., 1998). The NFAT transcription factors then cooperate with nuclear transcription factors such as GATA-4 and stimulate the transcriptional activation of various genes that are involved in cardiac hypertrophy (Olson E.N. and Molkentin J.D., 1999).

Indeed, recent work has shown that increased Ca^{2+} entry through L-type Ca^{2+} channels can activate the transcription factor myocyte enhancer factor 2 (MEF2), leading to up-regulation of Arc and spine elimination (Flavell S.W. et al., 2006). It has been proved that calcineurin-mediated dephosphorylation of NFATc1, MEF2A and MEF2D to be nerve activity-dependent and to occur in all muscle types. Dephosphorylation of these transcription factors by calcineurin appeared to be positively correlated with muscle usage under normal weightbearing conditions. It is also reported that calcineurin-MEF2 signaling was initiated in all muscle fibre types in response to increased nerve-mediated activity (Fig. 16) (Dunn S.E. et al., 2001; Sakuma K. and Yamaguchi A., 2010). These results suggest that the regulation of calcineurin on MEF2 plays an important role during cardiac hypertrophy.

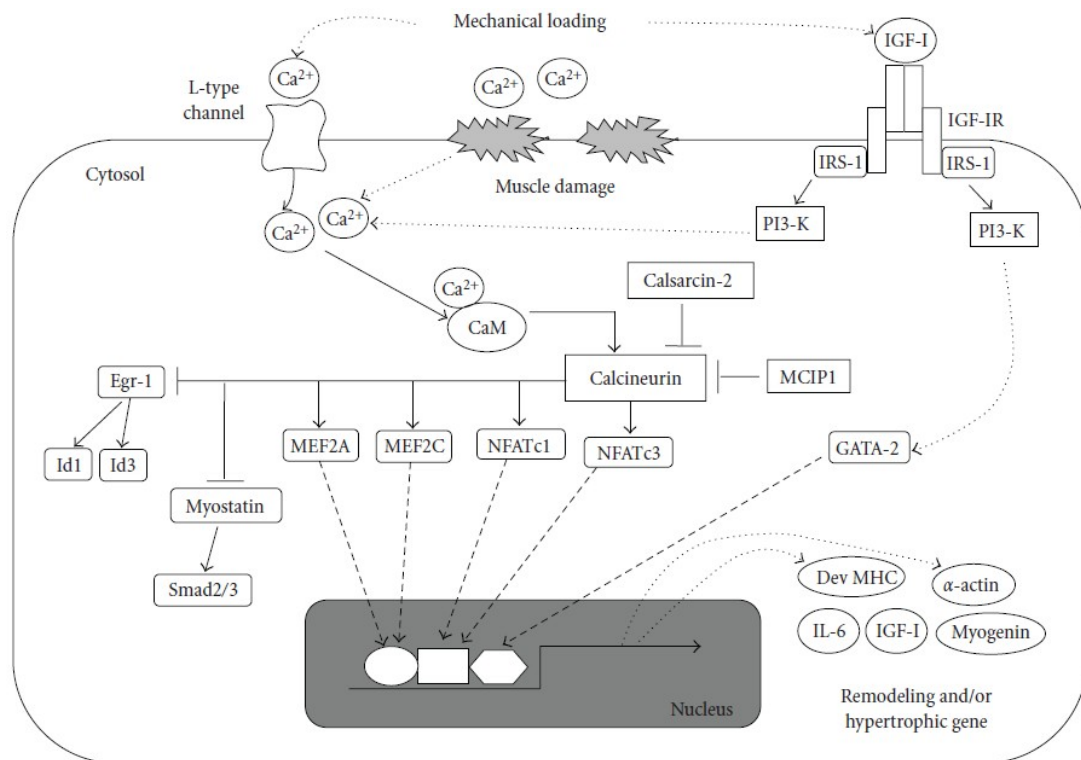


Fig. 16 Schematic diagram of calcineurin signaling to regulate hypertrophy and regeneration of skeletal muscle. Mechanical loading of skeletal muscle increase intracellular Ca^{2+} levels via the influx (L-type Ca^{2+} channel) of Ca^{2+} from the extracellular space and its efflux from the sarcoplasmic reticulum. The damage of muscle fiber membrane after treatment with myotoxin also elicits an increase in intracellular Ca^{2+} levels via the influx of Ca^{2+} from the extracellular space. Binding of the Ca^{2+} /CaM complex to the calcineurin regulatory subunit led to its activation. Activated calcineurin dephosphorylates NFATc1, NFATc3, MEF2C, and MEF2A resulting in their translocation from the cytoplasm to the nucleus. These transcription factors induce the expression of hypertrophic and/or remodeling genes such as Dev MHC, α -actin, IGF-I, myogenin, and IL-6. In addition, activated calcineurin inhibits the functional role of Egr-1 and myostatin. Mechanical overloading upregulates gene expression of IGF-I. IGF-I modulates calcineurin signaling via increasing intracellular Ca^{2+} levels and activating GATA-2. MCIP1 and calsarcin-2 are potent inhibitors of calcineurin signaling. MEF2A: Myocyte enhancer factor 2A; NFATc1: nuclear factor of activated T cells c1; MCIP1: Modulatory calcineurin-interacting protein 1; IRS-1: Insulin receptor substrate-1; PI3-K: Phosphatidylinositol 3-kinase; CaM: Calmodulin; Dev MHC: Developmental myosin heavy chain; IL-6: Interleukin-6. (Sakuma K. and Yamaguchi A., 2010)

1.6.2.3 Protein translation during hypertrophy

Hypertrophic growth of myocytes is accompanied by increases in both protein synthesis and proteolysis rates; however, the more rapid rate of protein synthesis relative to protein breakdown results in a net increase in protein accumulation and myocyte mass. Increases in cellular protein synthetic rates can, theoretically, have three sources of origin that are not mutually exclusive: (i) a general augmentation of transcription; (ii) an increase in post-transcriptional rates; (iii) accelerated translation rates. Numerous studies have shown that changes in the rate of transcription and post-transcriptional modification can account for the qualitative changes in expression of specific genes during hypertrophic growth (Ojamaa K. et al., 1994; Boheler K. et al., 1992).

Moreover, the availability of mRNA is not generally limiting for increases in overall cell protein synthesis during growth, suggesting that global protein synthesis rates are regulated at the level of mRNA translation. There are two general mechanisms that lead to accelerate rates to translation: (i) an increased efficiency of translation; or (ii) an increase in the capacity for protein synthesis (Fig. 17) (Hannan R.D. et al., 2003). Increased rates of protein synthesis in cardiac myocytes have been shown to correlate with an increase of activity of translation initiation factors and with a concomitant rise in the rate of translation initiation (Nagatomo Y. et al., 1999; Tuxworth Jr W.J. et al., 1999; Makhoouf A.A. et al., 2001).

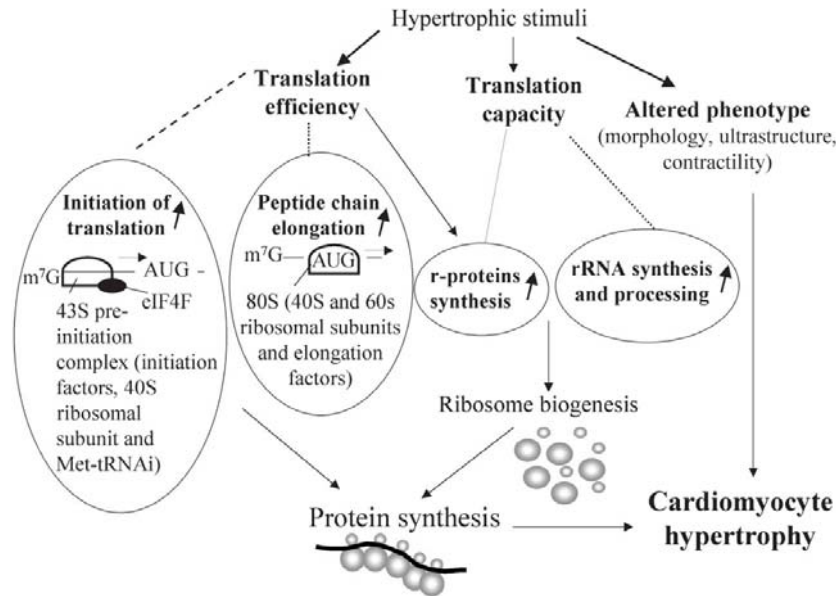


Fig. 17 Hypertrophic growth of cardiomyocytes is accompanied by various phenotypic changes. However, the primary cause of hypertrophic growth results from increased rates of protein synthesis. The regulation of protein synthesis rates in eukaryotes is controlled at the level of translation efficiency (i.e. the efficiency of translation of existing ribosomes) and of translation capacity (i.e. the amount of ribosomes actively translating mRNAs). Increases in both translation efficiency and capacity appear to be necessary for the rise in protein synthesis rates during the hypertrophic growth of cardiomyocytes. An increase of the translation initiation is rate limiting for the rise in translation efficiency and is stimulated acutely during the first phase of hypertrophic growth. An increase of translation capacity is subsequent to increases of translation efficiency and is necessary to face the demand for a sustained high protein level. AUG, initiation codon; m⁷G, 7-methylguanosine; eIF4F, eukaryotic initiation factor 4F (Hannan R.D. et al., 2003).

2 Signaling regulating gene expression in the heart: relevant aspects for this work

2.1 Myocyte enhance factor 2 (MEF2)

The formation of specialized cell types and their integration into different tissues and organs during development requires the interpretation of extracellular signals by components of the transcriptional apparatus and through the subsequent activation of cascades of regulatory and structural genes by combinations of widely expressed and cell type-restricted transcription factors. The myocyte enhancer factor 2 (MEF2) family has been shown to play a pivotal role in morphogenesis and myogenesis of skeletal, cardiac, and smooth muscle cells (Black B.L. and Olson E.N., 1998).

2.1.1 MEF2 family: structure and regulation

The myocyte enhancer factor 2 (MEF2) proteins belong to the evolutionarily ancient MADS (named for MCM1, which regulates mating type-specific genes in yeast; Agamous and Deficiens, which have a homeotic function in plants; and Serum Response Factor (SRF), which mediates serum-inducible transcription) family of transcription factors (Shore P. and Sharrocks A.D., 1995). The MADS-box is a 57-amino acid motif located at the extreme N terminus of the MEF2 factors (Fig. 18). This motif serves as a minimal DNA-binding domain, which requires an adjacent 29-amino acid extension, referred to as the MEF2 domain, for high-affinity DNA binding and dimerization (Molkentin J.D. et al., 1996). In addition to its role in DNA binding, the MADS-box mediates dimerization of MADS-box proteins, and the MEF2 domain is important for interactions with accessory factors (Black B.L. and Olson E.N., 1998).

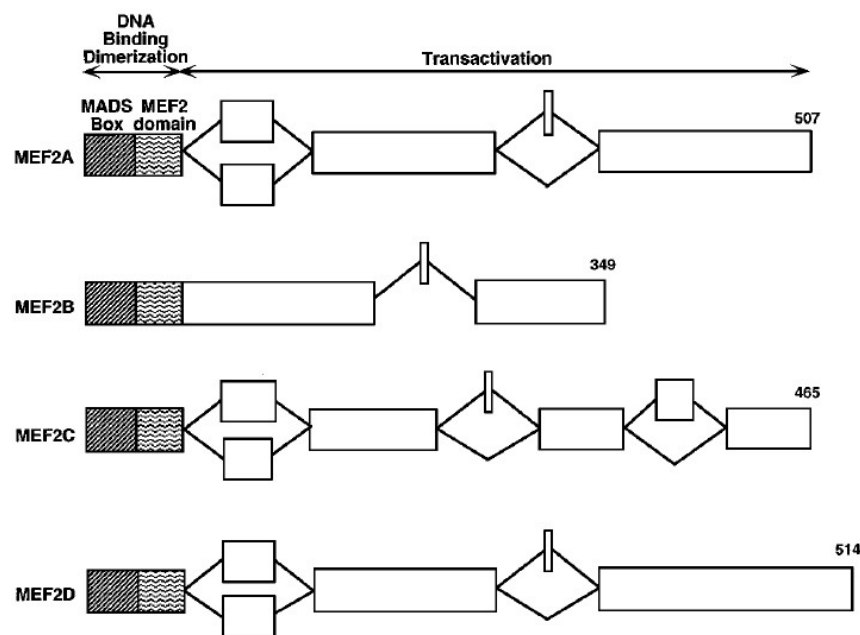


Fig. 18 Schematic diagrams of MEF2 factors. Structures of the four vertebrate MEF2 gene products are shown. Alternative exons within the C-terminal activation domains are indicated, along with the number of amino acids in the longer form of each protein (Black B.L. and Olson E.N., 1998).

MEF2 acts as a lynchpin in the transcriptional circuits that control cell differentiation and organogenesis. The spectrum of genes activated by MEF2 in different cell types depends on extracellular signaling and on co-factor interactions that modulate MEF2 activity (Potthoff M.J. and Olson E.N., 2007). As referred above, the N-terminus of MEF2 factors contain a highly conserved MADS-box and an immediately adjacent motif termed the MEF2 domain (Fig. 19), which together mediate dimerization, DNA binding, and co-factor interactions (Black B.L. and Olson E.N., 1998). The MADS-box and MEF2 domain are necessary and sufficient for DNA binding, but they lack transcriptional activity on their own. The C-terminal regions of MEF2 proteins, which function as transcriptional activation domains, are subject to complex patterns of alternative splicing with certain exons being present ubiquitously and others being muscle- or neural-specific (Fig. 19) (Martin J.F. et al., 1994).

	MADS	MEF2	
Yeast MEF2	61%	11%	7%
<i>Drosophila</i> MEF2	90%	68%	14%
<i>C. elegans</i> MEF-2	95%	84%	7%
hMEF2A	100%	100%	100%
hMEF2B	91%	68%	6%
hMEF2C	98%	87%	11%
hMEF2D	95%	82%	16%

DNA binding, dimerization, co-factor recruitment
Transcriptional activation

Fig. 19 Sequence conservation of MEF2. The percentage amino acid identity within the MADS, MEF2 and transcriptional activation domains of different MEF2 proteins from various organisms relative to human (h) MEF2A. N-termini are to the left (Potthoff M.J. and Olson E.N., 2007).

Although MEF2 is a transcriptional activator, similar to other MADS-box proteins, it relies on the recruitment of, and cooperation with, other transcriptional factors to activate diverse programs of gene expression, for example, the skeletal muscle bHLH proteins. In addition, complex transcriptional, translational and post-translational mechanisms govern the functions of MEF2 (Black B.L. and Olson E.N., 1998; Potthoff M.J. and Olson E.N., 2007).

Cardiac muscle cells in both the right and left ventricles rely on the same set of transcription factors for activation of the gene program for cardiomyocyte differentiation and the expression of contractile protein genes, but the upstream inputs into this regulatory network differ in cells derived from the primary and secondary heart fields (Fig. 20A). The evolutionary addition of the secondary heart field requires a signaling mechanism to activate the core cardiac transcriptional network. The *Isl1* transcription factor, which is expressed specifically in the secondary heart field, directly activates the *Mef2c* gene in this population of cardiac precursor cells (Fig. 20B) (Dodou E. et al., 2004).

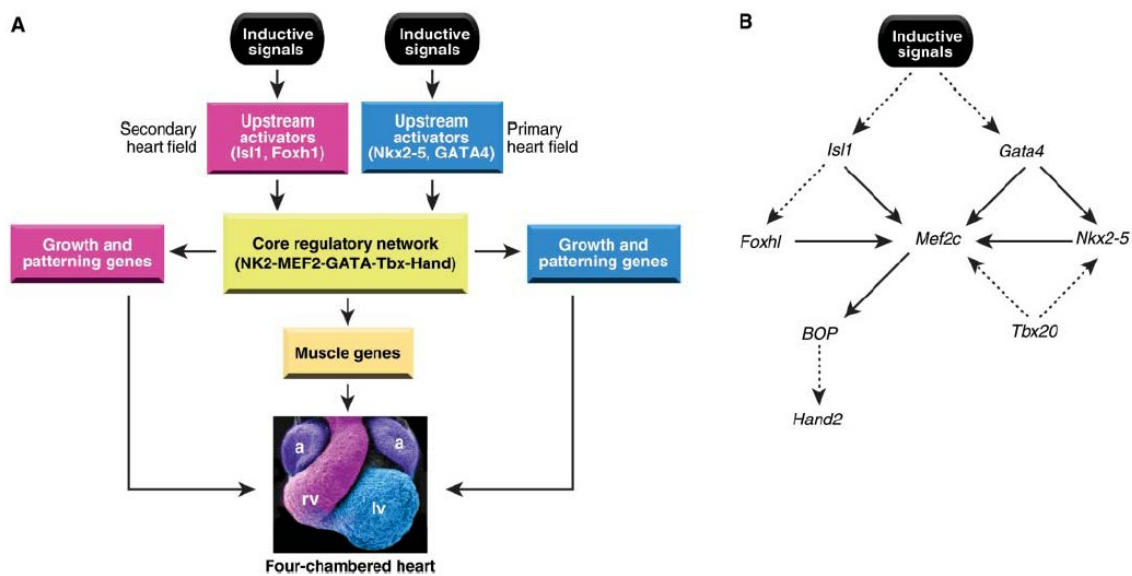


Fig. 20 Schematic of transcriptional networks in mammalian heart development. Inductive signals activate a set of upstream regulatory genes, encoding transcription factors, in the primary and secondary heart fields. The products of these genes activate the genes in the core cardiac network (NK2-MEF2-GATA-Tbx-Hand). Some components of the network, such as *Nkx2-5*, are also activated in the primary heart field in response to inductive signals. The core network genes cross- and autoregulate their expression and serve as the central regulatory network for the activation of muscle-specific genes and genes that control the growth and patterning of derivatives of the primary and secondary heart fields. The primary heart field gives rise to the left ventricle (lv) and portions of the atria (a), whereas the secondary heart field gives rise to the right ventricle (rv), portions of the atria, and the outflow tract. A scanning electron micrograph of a mouse heart at embryonic day 14.5 is shown at the bottom. Derivatives of primary and secondary heart fields are shown in blue and pink, respectively. The atria, which are derived from the primary and secondary heart fields, are shown in purple. (Bucks J. and Olson E.N., 2006). Regulatory interactions among cardiac transcription factors in the secondary heart field. Solid lines indicate direct transcriptional connections, and dotted lines indicate connections not yet shown to be direct (Olson E.N., 2006).

In vertebrates, there are four MEF2 genes, referred to as MEF2A, -B, -C and -D that are located on different chromosomes and display distinct, but overlapping, temporal and spatial expression patterns in embryonic and adult tissues, with highest expression in striated muscles and brain (Edmondson D.G. et al., 1994). The four isoforms share homology in an NH₂-terminal MADS-box and an adjacent motif known as the MEF2 domain and bind an A-T-rich DNA sequence associated with muscle-specific genes. In the mouse, MEF2C are co-expressed in the precardiogenic mesoderm beginning at embryonic day 7.75 (E7.75), MEF2A and MEF2D are expressed about 12 hours later and throughout the developing heart (Lin Q. et al., 1997). After birth, MEF2A, MEF2B and MEF2D transcripts are expressed ubiquitously. MEF2C transcripts are restricted to skeletal muscle, brain and spleen (Molkentin J.D. et al., 1996).

The expression of MEF2 proteins in many cell types, including neurons, chondrocytes and muscle (cardiac, skeletal, and smooth), occurs concomitantly with the activation of their differentiation programs, and the balance between the transcription-activating functions of MEF2 and the repressive function of class IIa histone deacetylases (HDACs) dictates the development of the tissues. MEF2 factors have also been implicated in transcriptional activation in response to T cell receptor activation which is mediated by a calcium-dependent signaling pathway that is sensitive to cyclosporin A (CsA), which inhibits the calcium-calmodulin-dependent protein phosphatase, calcineurin. It has been proved that calcineurin signaling enhances MEF2 signaling by inducing a cofactor at post transcriptional modification of MEF2 that potentiates transcriptional activity (Fig.21) (Black B.L. and Olson E.N., 1998; Lu J. et al., 2000; Youn H.D. and Liu J.O., 2000; Chang S. et al., 2004; Arnold M.A. et al., 2007; Verzi M.P. et al., 2007;).

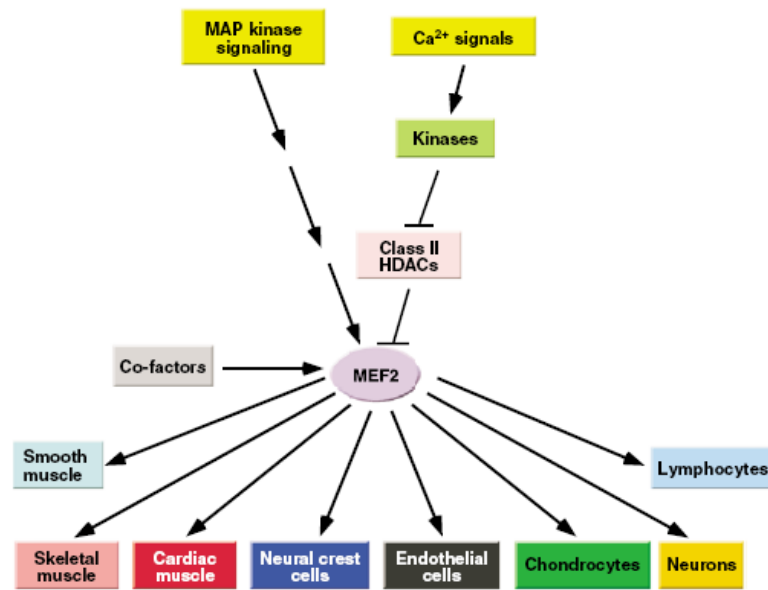


Fig. 21 MEF2 as a central regulator of differentiation and signal responsiveness. MAP kinase signaling activates MEF2. Calcium dependent signals also activate MEF2 by stimulating calcium-dependent kinases that phosphorylate class II HDACs, thereby promoting their dissociation from MEF2 and derepressing MEF2 target genes. MEF2 recruits numerous co-factors to drive the differentiation of the various cell types shown. Although MAPK and HDAC signaling pathways have been implicated in the modulation of numerous MEF2-dependent developmental programs, these signaling pathways have not yet been shown to operate in all the cell types under MEF2 control (Potthoff M.J. and Olson E.N., 2007).

MEF2 plays central roles in the transmission of extracellular signals to the genome and in the activation of the genetic programs that control cell differentiation, proliferation, morphogenesis, survival and apoptosis of a wide range of cell types (Potthoff M.J. and Olson E.N., 2007). Biochemical and genetic studies in vertebrate and invertebrate organisms have shown that MEF2 factors regulate myogenesis through combinatorial interactions with other transcription factors. MEF2 factors are evolutionarily conserved and appear to function at the core of an ancient regulatory network for muscle formation (Black B.L. and Olson E.N., 1998). Also in the face of biomechanical stress, the heart develops compensatory hypertrophy, which links to pathological changes in cardiomyocyte gene expression. MEF2 is a major target of Ca/CaM signaling which leads to hypertrophy (Ikeda S. et al., 2009).

MEF2 activity has been shown to be regulated at several levels. Mef2 transcription is regulated during embryonic development (Edmondson D.G. et al., 1994) and recent findings

show that MEF2A can regulate its own transcription (Ramachandran B. et al., 2008). Posttranslational modifications allow rapid increase of MEF2-dependent transcription by growth and stress signals. MAPK-dependent phosphorylation enhances MEF2 transcriptional activity (Molkentin J.D. et al., 1996; Ornatsky O.I. et al., 1999; Zhao M. et al., 1999 ; Lu J. et al., 2000). Transcription of MEF2-dependent genes is also stimulated by Calcium/Calmodulin signaling through activation of the Calcineurin phosphatase (Stewart A.A. et al., 1982). Calcineurin directly dephosphorylates different residues of MEF2, enhancing its activity (Wu H. et al., 2000; Wu H. et al., 2001) and also dephosphorylates cytosolic nuclear factor of activated T cells (NFAT), triggering its nuclear import (Molkentin J.D. et al., 1998) and potentiating MEF2 activity (Chin E.R. et al., 1998). MEF2 activity has also been shown to be enhanced by interaction with myocardin (Creemers E.E. et al., 2006). On the opposite, MEF2 transcriptional activity is blocked by its binding to ClassII Histone Deacetylases--HDAC4 and 5 (Miska E.A. et al., 1999; Lu J. et al., 2000). This inhibitory mechanism can be reverted by CaMK-dependent phosphorylation of ClassII HDACs, which triggers their nuclear export, freeing MEF2-dependent transcription (McKinsey T.A. et al., 2005).

2.1.2 MEF2 isoforms and their function in the heart

MEF2 regulates the expression of numerous cardiac structural and contractile proteins. MEF2A and MEF2D are the primary MEF2 factors expressed in the adult heart. Some research findings reveal specific roles for MEF2A in maintaining appropriate mitochondrial content and cyto-architectural integrity in the post-natal heart and show that other MEF2 isoforms cannot support these activities. It is reported that mice deficient in MEF2A display an increased incidence of mortality beginning at postnatal day (P) 2, with most MEF2A^{-/-} pups dying between P5 and P10 (Fig.22a). Most of the mice exhibit pronounced dilation of the right ventricle (Fig.22b), myofibrillar fragmentation, mitochondrial disorganization and activation of a fetal cardiac gene program. The few MEF2A^{-/-} mice that survived to adulthood also showed a deficiency of cardiac mitochondria and susceptibility to sudden death (Naya F.J. et al., 2002).

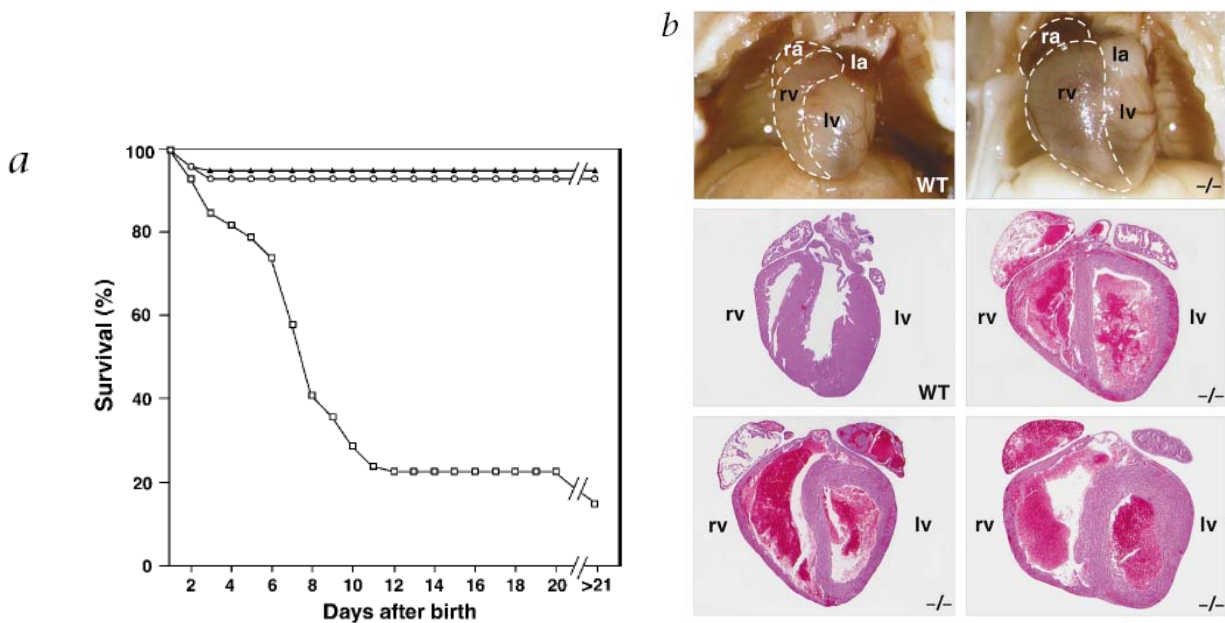


Fig. 22 Sudden death and cardiac abnormalities in *Mef2a*^{-/-} mice. **(a)** Survival curves of offspring from *Mef2a*^{+/-} intercrosses in the mixed C57/Bl6 background. Numbers of mice of each genotype were as follows: wild type, 120 (▲); *Mef2a*^{+/-}, 203 (○); *Mef2a*^{-/-}, 104 (□). Sudden death was also observed in 13% of adult (>P21) viable *Mef2a*^{-/-} mice. **(b)** Gross and histological sections of hearts from wild-type and *Mef2a*^{-/-} neonatal mice that died suddenly. Hearts from mutants were dilated without evidence of hypertrophy. la, left atrium; lv, left ventricle; ra, right atrium; rv, right ventricle. Magnification, ×50 (Naya F.J. et al., 2002).

In a research of transgenic mice with MEF2A overexpression, it is observed that mice with 4.2-fold more MEF2A protein expression in the heart died between 2 and 4 weeks of age with significant elevation in heart weight; at 3 weeks of age the mice showed impairment in ventricular performance and a severe reduction in fractional shortening and dramatic dilation of the left ventricles, together with increased expression of hypertrophy-associated genes such as atrial natriuretic factor (ANF) and skeletal α -actin. The mice with 3.5-fold more MEF2A expression showed no lethality but had ventricular chamber dilation at 2 and 3 months old, these mice also showed 91% increase in the heart weight compared with 33% in the wild-type when subjected to transverse aortic constriction (TAC). Histological assessment demonstrated greater cardiac enlargement and ventricular wall dilation in these mice compared with wild-type control, indicating a role for MEF2A in regulating cardiac hypertrophy / cardiomyopathy (Xu J. et al., 2006). These results demonstrate that MEF2A is a key regulator in the control of heart formation and development.

MEF2B gene expression is an early marker for the cardiac muscle lineage. It maps to the central region of mouse chromosome 8 and is unlinked to other Mef2 genes. It has been reported that human MEF2B, unlike MEF2A, C and D which showed similar DNA binding and transcriptional activation properties, was unable to bind the MEF2 consensus sequence unless the C terminus is deleted, this had led to the conclusion that MEF2B may have a function different from that of the other MEF2 factors and that its C terminus interferes with DNA binding of the N-terminal MADS and MEF2 domains (Yu Y.T. et al., 1992). But Olson E.N. and his colleagues proved that MEF2B, like the other MEF2 factors, was expressed in myogenic lineages during embryogenesis and acted as a potent transactivator through the MEF2 binding site. The basis for these different results is unclear (Molkentin J.D. et al., 1996).

Of the four vertebrate MEF2 genes, MEF2C is required for activation of a subset of cardiac contractile protein genes, as well as for the development of cardiac structures derived from the secondary heart field, which are unique to amniotes (Lin Q. et al., 1997). Thus, it appears that during evolution, this ancient myogenic regulator acquires new functions in regulating the formation of cardiac structures that occur only in more advanced hearts. Additional functions of vertebrate MEF2 genes are likely to be masked by redundancies (Olson E.N., 2006). Members of the GATA family of zincfinger transcription factors directly regulate numerous cardiac contractile protein genes, as well as upstream regulatory genes such as Nkx2-5, Mef2, and Hand (Sorrentino R.P. et al., 2005). The murine MEF2C gene is expressed in heart precursor cells before formation of the linear heart tube. The studies of MEF2C^{-/-} mice showed that in contrast to normal embryos, in which the heart tube initiated rightward looping to form the right ventricular chamber beginning at about day 8.5 (E8.5), the heart tubes of MEF2C^{-/-} embryos did not loop and the anterior heart field failed to form. The embryos appeared normal until about E9, when they began to show retarded growth, pericardial effusion, poorly developed trabeculae and extremely narrow ventricular chamber, and died during early embryonic development with arrested heart tube morphogenesis, which indicates that MEF2C is a nodal point in the development of the anterior heart field that gives rise to the outflow tract and right ventricle of the heart (Lin Q. et al., 1997). MEF2B was

coexpressed with MEF2C throughout the early stages of cardiogenesis, and was up-regulated in MEF2C^{-/-}, consistent with the possibility that it may partially substitute for MEF2C. Cardiac development occurs normally in MEF2B-null mice also suggests that MEF2C shares functions with MEF2B (Lin Q. et al., 1997).

Cardiac-specific overexpression of the repressive MEF2C-enrailed fusion protein under the control of the Nkx2-5 enhancer (~E7.5) is sufficient to inhibit cardiomyocyte differentiation *in vitro* and *in vivo* (Fig. 23) (Karamboulas C. et al., 2006). All the results suggest that MEF2C is important for the anterior heart field during early development, and can partially be compensated by MEF2B when it is deficient.

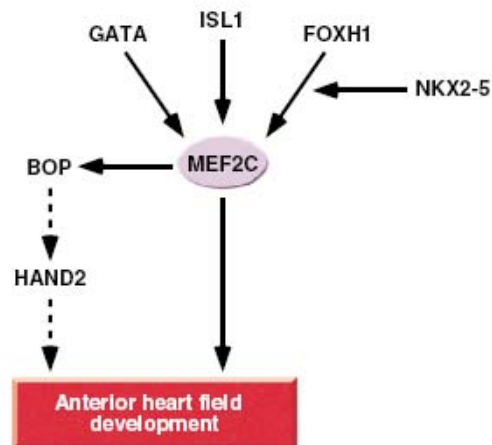


Fig. 23 Control of anterior heart field development by MEF2C. MEF2C expression in the anterior heart field is controlled by GATA4, ISL1 and FOXH1, together with NKX2-5. MEF2C directly activates the expression of BOP, which is required for expression of HAND2, an essential regulator of anterior heart field development. Solid lines indicate direct regulatory interactions and dotted lines indicate regulatory interactions for which the underlying mechanism has not yet been defined (Potthof M.J. and Olson E.N., 2007).

MEF2D is a critical component of the signaling pathways through which pressure overload and adrenergic signaling drive cardiac remodeling and fetal gene activation. A recent research shows that mice lacking MEF2D are viable, but display an impaired response to demonstrate that MEF2D plays a key role in mediating stress-dependent gene expression in the adult heart (Kim Y. et al., 2008).

In several studies which mice with MEF2 loss-of-function mutation were generated, such as MEF2A-null mice exhibited perinatal lethality from an array of cardiovascular defects, and MEF2C-null mice died around E9.5 from cardiac looping defects. By contrast, MEF2D-null mice appeared normal. The viability of MEF2D-null mice contrasts with the early embryonic lethality of MEF2C-null mice and perinatal lethality of MEF2A-null mice, pointing to distinct functions for each MEF2 isoforms at different stages of heart development (Naya F.J. et al., 2002).

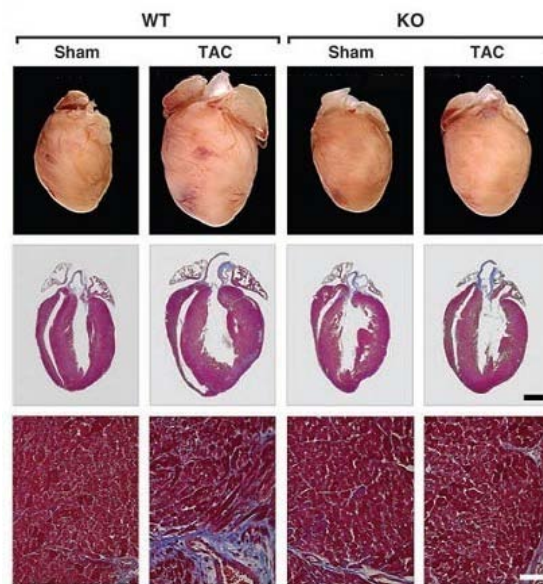


Fig. 24 Blunted hypertrophy of *Mef2d* mutant mice following TAC. Hearts from WT and *Mef2d* mutant mice subjected to either a sham operation or pressure overload (TAC) are shown at the top. Histological sections stained with Masson's trichrome are shown on the bottom. Masson's trichrome staining of WT and *Mef2d* mutant hearts indicates lack of fibrosis in *Mef2d*^{-/-} hearts in response to pressure overload by TAC. Scale bars: 1 mm (middle panel); 40 mm (bottom panel) (Kim Y. et al., 2008).

2.1.3 The cooperation of MEF2 and microRNAs (miRNAs) in cardiomyocyte development

MicroRNAs (miRNAs, miRs) are a class of endogenous noncoding small RNAs, which are around 22 nt long and modulate gene expression by targeting mRNAs for postranscriptional repression. The very first miRNA genes *lin-4* and *let-7* were identified more than a decade ago. Since then, additional genetic studies have been performed on *Caenorhabditis elegans* and *Drosophila melanogaster* to support the view that miRNAs

have crucial role in animal development (Johnstone R.J. and Hobert O., 2003). Recent studies indicate that miRNAs participate in many essential biological processes, including cell proliferation, differentiation and apoptosis. miRNAs are also associated with important diseases such as cancer and cardiovascular disease (Malizia A.P. and Wang D., 2011).

Recently, it is found that serum response factor (SRF) and MEF2 regulate the expression of two clusters of muscle-specific miRNA genes: miR-1-1/miR133a-2 and miR1-2/miR133a-1. On the other hand, miR-208, another myomiR specifically expressed in the cardiomyocytes, is involved in the regulation of the myosin heavy chain (MHC) isoform switch during development and in pathophysiological conditions. Emerging evidence also demonstrates that a complex network of myomiRs' postranscriptional-regulated gene expression coordinates the overall cardiomyocyte development and function (Malizia A.P. and Wang D., 2011).

A subset of miRNAs, miR-1, miR-133, miR-206, and miR-208 are either specifically or highly expressed in cardiac and skeletal muscle and are called myomiRs (Malizia A.P. and Wang D., 2011) (Fig. 25). It is also proved that MEF2 can activate transcription of the bicistronic miR-1/miR-133 transcript via an intragenic muscle-specific enhancer, which provides cooperative temporospatial regulation of miRNA expression (Liu N. et al., 2007). SRF enhances the expression of these miRNAs in ventricular and atrial myocytes (Niu Z. et al., 2007), whereas MEF2 binds to the intronic enhancer of these miRNA genes to activate their expression in ventricular myocytes (Malizia A.P. and Wang D., 2011).

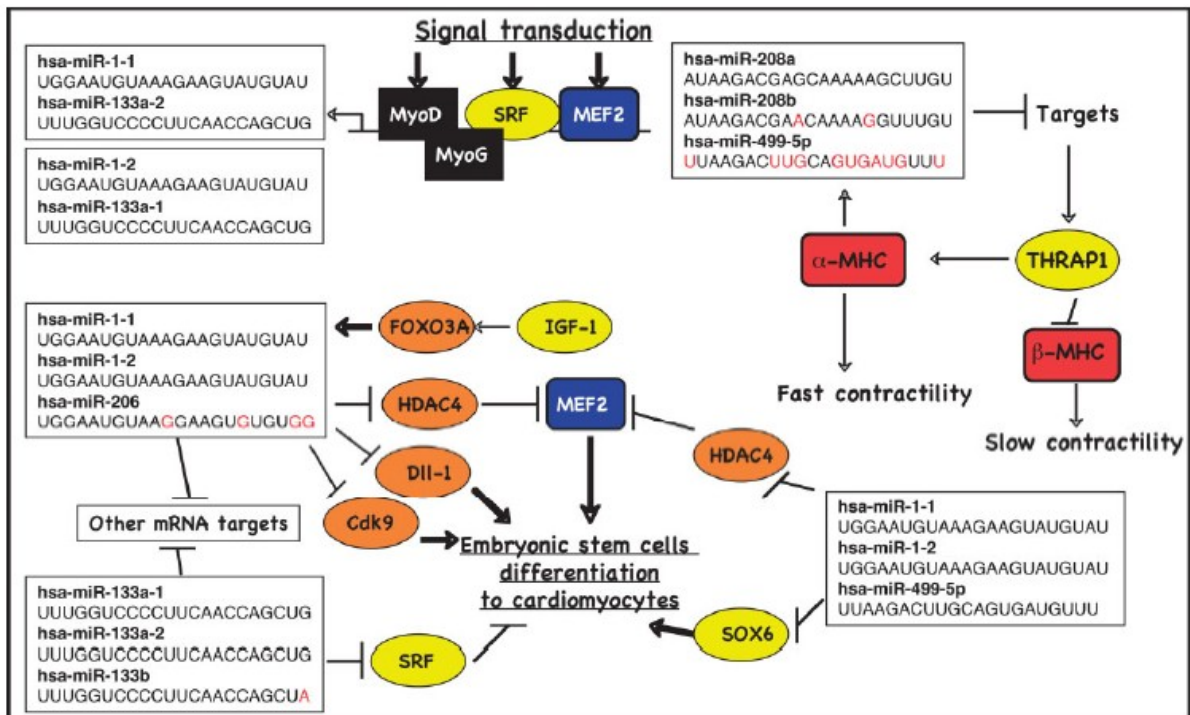


Fig. 25 Regulating circuit that involves transcription regulators, myomiRs, and their targets (Malizia A.P. and Wang D., 2011).

2.2 Histone deacetylases (HDACs)

Histone acetyl transferases (HATs) and histone deacetylases (HDACs) loosen or compact chromatin structure, respectively, and play an important role in global gene expression (Kuo and Allis, 1998; Grozinger and Schreiber, 2002). In general, HDACs repress transcription and are involved in cell-cycle regulation, cell proliferation and differentiation (Cress W.D. and Seto E., 2000). During hypertrophic cardiac remodeling, a complex network of signaling cascades is activated. Recent studies point to HDACs as integrators of these divergent stress-response pathways. Among the best-characterized examples are class II HDACs, in the absence of stress signals, these enzymes interact with MEF2 to attenuate cardiac growth (Berry J.M. et al., 2008).

2.2.1 Function of HDACs

Histone acetylation is a dynamic process controlled by the antagonistic actions of two large families of enzymes -- the histone acetyltransferases (HATs) and the histone deacetylases (HDACs). The balance between the actions of these enzymes serves as a key regulatory mechanism for gene expression and governs numerous developmental processes and disease states (Haberland M. et al., 2009).

Histone acetylation modulates transcription in multiple ways. Acetylation of ϵ -amino groups of lysine residues within histone tails neutralizes their positive charge, thereby relaxing chromatin structure. This interferes with the generation of higher-order chromatin structures, and increasing the accessibility of transcription factors to their target genes. Acetylated histones also serve as binding sites for bromodomain proteins, which often act as transcriptional activators. Conversely, histone deacetylation favors transcriptional repression by allowing for chromatin compaction. Direct acetylation and deacetylation of transcription factors have also been shown to have positive and negative consequences on gene transcription, respectively (Kouzarides T., 2000).

The recent creation of knockout mice lacking HDAC genes has revealed highly specific functions for individual HDAC isoforms during development and adulthood. These mutant mice are a powerful tool for defining the functions of HDACs *in vivo* and for identifying the molecular targets of HDAC inhibitors in disease (Haberland M. et al., 2009).

2.2.2 Control of gene expression by HDACs

HDACs lack intrinsic DNA-binding activity and are recruited to target genes via their direct association with transcriptional activators and repressors, as well as their incorporation into large multiprotein transcriptional complexes. Thus, the specificity of HDACs for regulation of distinct gene programs depends on cell identity and the spectrum of available partner proteins in a cell, in addition to the signaling milieu of the cell. Although diminished histone acetylation at promoter regions generally correlates with gene silencing, consistent with the well-established functions of HDACs as transcriptional repressors, there is also evidence that HDACs can activate some genes (Grunstein M., 1997).

HDACs have also been linked to transcriptional activation of a subset of genes in higher eukaryotes, but in settings in which HDAC inhibition leads to down-regulation of specific genes, it is difficult to rule out possible secondary effects that result in transcriptional repression. It should be noted, however, that deletion or inhibition of HDACs often results in the up-regulation or down-regulation of approximately equivalent percentages of genes (Glaser K.B. et al., 2003).

It has also become clear in recent years that HDACs can act on numerous cellular substrates in addition to histones, and that acetylation might rival phosphorylation in its importance. In this regard, class IIa deacetylases possess only minimal HDAC activity against acetylated histones, despite extensive evolutionary conservation of their deacetylases domain, pointing to the possible importance of other types of cellular substrates for their actions (Lahm A. et al., 2007).

2.2.3 Control of cardiovascular growth and function by HDACs

Mammalian HDACs can be classified into multiple classes based on their structure and homology to three *Saccharomyces cerevisiae* HDACs (Verdin E. et al., 2003). Class I HDACs (HDACs 1, 2, and 3) are expressed ubiquitously and comprise simply a catalytic domain. The class II HDACs (HDACs 4, 5, 7, and 9) are expressed at the highest levels in the heart, brain, and skeletal muscle and contain a C-terminal catalytic domain and an N-terminal extension that mediates interactions with other transcriptional repressors and activators (Fig. 26).





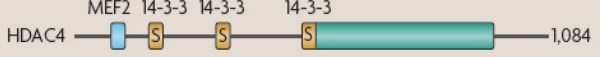






	Protein domains	Time of lethality	Phenotype
Class I	HDAC1  482	E10.5	Proliferation defects
	HDAC2  488	P1	Cardiac malformation
	HDAC3  428	E9.5	Gastrulation defects
	HDAC8  377	P1	Craniofacial defects
Class IIa	HDAC4  1,084	P7–P14	Chondrocyte differentiation defect in growth plate
	HDAC5  1,122	Viable	Exacerbated cardiac hypertrophy after stress
	HDAC7  912	E11	Endothelial dysfunction
	HDAC9  1,069	Viable	Exacerbated cardiac hypertrophy after stress
Class IIb	HDAC6  1,215	Viable	Increased tubulin acetylation
	HDAC10  669	ND	–
Class IV	HDAC11  347	ND	–

Fig. 26 The histone deacetylase (HDAC) superfamily, showing protein domains, loss-of-function phenotypes in mice and time point of lethality of the knockouts. Green rectangles indicate the conserved HDAC domain; numbers following the HDAC domain indicate the number of amino acids. Myocyte enhancer factor 2 (MEF2)-binding sites are marked by a blue square, and binding sites for the 14-3-3 chaperone protein are also shown. E, embryonic day; ND, not determined; P, days postnatal; S, serine phosphorylation sites; ZnF, zinc finger (Haberland M. et al., 2009).

The transcriptional activity of MEF2 is tightly governed by its interaction with HATs (Sartorelli V. et al., 1997) and HDACs (Zhou X. et al., 2001), which stimulate and suppress transcription, respectively, through their effects on histone acetylation and chromatin configurations. Consistent with the notion that class II HDACs suppress pathological cardiac growth, at least in part by modulating MEF2 activity, mice lacking either HDAC5 or HDAC9 display enhanced hypertrophy and superactivation of MEF2 in response to cardiac stress signals (Zhang, C.L. et al., 2002). Mice lacking both HDAC5 and HDAC9, but not mice lacking one of them, are prone to embryonic and early postnatal death from a spectrum of cardiac abnormalities, including ventricular septal defects and thin-walled myocardium. These findings reveal redundant roles for HDACs 5 and 9 as counterregulators of a specific subset of hypertrophic signaling pathways in the adult heart as well as in normal cardiac growth and development during embryogenesis (Fig. 27) (Zhang, C.L. et al., 2002). Given the interaction between class IIa HDACs and MEF2, and the central role of MEF2 in the control

of cardiomyocyte differentiation, the developmental cardiac defects in these double mutant mice probably result from superactivation of MEF2. This would be expected to lead to precocious differentiation and cell-cycle withdrawal of cardiomyocytes, causing hypocellularity of the myocardium (Mckinsey T.A. et al., 2002).

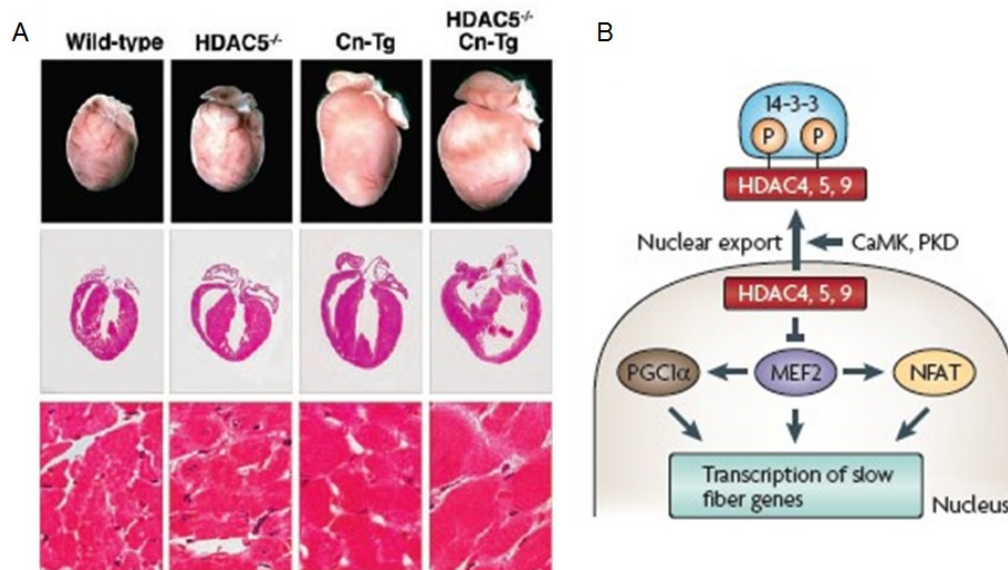


Fig. 27 Control of pathological cardiac hypertrophy by class IIa histone deacetylases (HDACs). **(A)** HDAC5 mutant mice were bred with mice harboring the MHC-calceinurin transgene (Cn-Tg). Hearts from 1-month-old mice of the indicated genotypes were isolated (top images), sectioned, and stained with hematoxylin and eosin (bottom images). **(B)** Schematic of the repressive influence of class IIa HDACs on myocyte enhancer factor 2 (MEF2), which acts together with PGC-1 α (peroxisome proliferator-activated receptor gamma, coactivator 1 alpha) and NFAT (nuclear factor of activated T-cells) to promote the formation of slow myofibres. Signaling by calcium/calmodulin-dependent protein kinase (CaMK) and protein kinase D (PKD) induces the phosphorylation of class IIa HDACs, which creates docking sites for the 14-3-3 chaperone protein, resulting in nuclear export with consequent activation of slow myofibre genes (Chang S. et al., 2004; Haberland M. et al., 2009).

The adult heart typically responds to stress by a pathological growth response that ultimately leads to loss of cardiac function. MEF2 is sufficient and necessary to drive the pathological cardiac hypertrophy and heart failure that takes place in response to injury. These stimuli typically activate the calcineurin and CamK–PKD pathways, which in turn lead to

phosphorylation of class IIa HDACs, promoting their nuclear export. Deletion of class IIa HDACs eliminates the counter-regulatory mechanism that restrains cardiac growth and sensitizes MEF2 and perhaps other transcription factors so that they become activated by stress-dependent intracellular signals (Fig. 28) (Liu N. and Olson E.N., 2006).

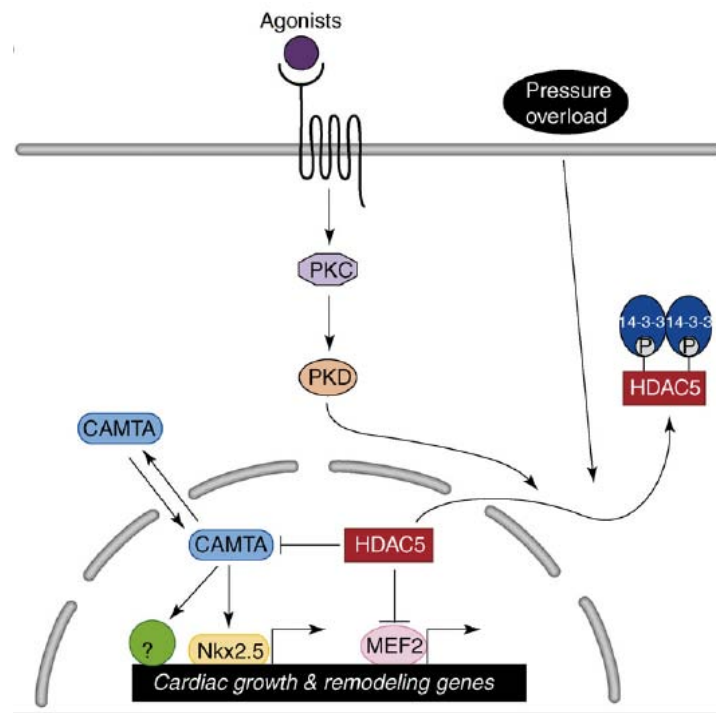


Fig. 28 Activation of PKC/PKD signaling or pressure overload leads to phosphorylation of HDAC5, which creates docking sites for 14-3-3 proteins and their nuclear export, releasing MEF2 from repression (Liu N. and Olson E.N., 2006).

Several protein kinases, including calmodulin-dependent protein kinases (CaMKs) (McKinsey T.A. et al., 2004), protein kinase D (PKD) (Berdeaux R. et al., 2007) and salt-inducible kinase (Vega R.B. et al., 2004), that phosphorylate HDAC5, leading to its export from the nucleus as mentioned above. The cAMP/protein kinase A (PKA) signaling pathway also regulates a variety of cellular functions and numerous important biological processes. Many of the effects of cAMP/PKA are mediated via changes in gene transcription. A large body of research has defined the cAMP-response element binding (CREB) protein as PKA substrates that mediate an increase in gene expression in response to cAMP (Gonzalez G.A.

and Montminy M.R., 1989). Recently a research has proved that PKA signaling specifically and negatively regulates the nuclear export of HDAC5 and also significantly inhibits PE-stimulated MEF2 transcriptional activity (Fig. 29), which suggests that cAMP/PKA dependent phosphorylation and nuclear accumulation of HDAC5 negatively regulate MEF2 transcriptional activity (Ha C.H. et al., 2010).

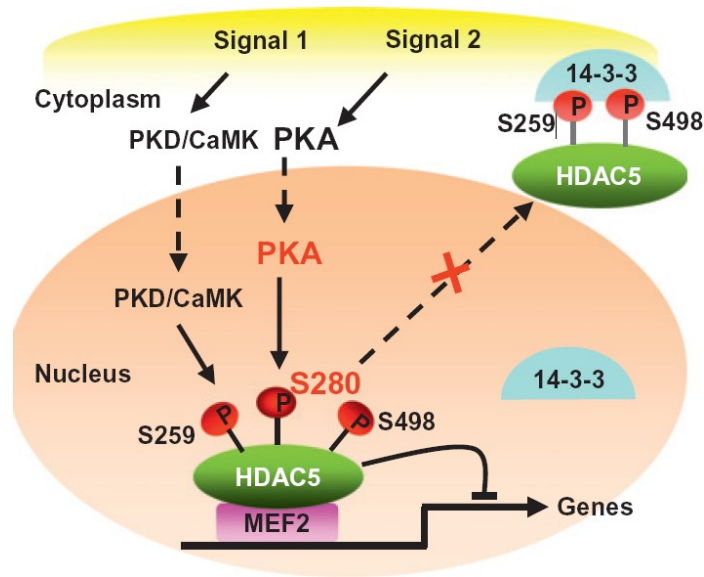


Fig.29 Scheme of PKA-dependent regulation of HDAC5 subcellular localization and gene transcription (Ha C.H. et al., 2010).

2.2.4 Control of cell death and differentiation by HDACs

Virtually all HDAC inhibitors currently in clinical development show some degree of preclinical activity against malignant cells proliferating in culture and also tumors growing in animal models; this antitumor activity may be characterized as either inducing cytostasis (cell cycle arrest), differentiation, or cell death. The later effect can be induced by activation of a programme leading to cell death by a highly regulated signal pathway known as apoptosis. By up-regulating apoptotic proteins, such as Fas/Fas ligand, Bcl2, Bak, Bax, Bim and so on, as well as Caspase 3, cysteine protease involved in apoptosis (Sawa H. et al., 2001), HDAC inhibitors are able to increase differentiation and apoptosis in cancer cells. The pretreatment

or co-administration of HDAC inhibitors with a wide range of agents has been shown repeatedly to additively or synergistically enhance apoptosis of cancer cells in culture as well as antitumor efficacy *in vivo* (Mitsiades C.S. et al., 2004). However, the mechanism modulating HDAC inhibitor-induced apoptosis are not clearly defined.

2.3 Polypyrimidine-tract-binding protein (PTB)

Polypyrimidine Tract Binding Protein (PTB), also referred to as hnRNP I [heterogeneous nuclear RNP (ribonucleoprotein) I], is a protein related to mRNA splicing regulation and the control of IRES-dependent translation (Sawicka K. et al., 2008). PTB binds to intron pyrimidine-rich elements and mediates tissue specific negative regulation of exons splicing in several mammalian genes. Structurally, PTB is a 57 kDa protein composed of four RRM domains (RNA recognition motifs) (Fig. 30) with interdomain linker regions and an N-terminal extension containing both nuclear localization and export signals. Each of the isoforms has four RRMs, as well as an N-terminal nuclear localization signal. Although each RRM has its own slightly different consensus RNA-binding sequence, all bind a short pyrimidine-rich sequence with a preference for sequences contained within a longer pyrimidine tract and containing cytosines (Oh Y.L. et al., 1998). RRM2, as well as the flanking sequence, has been demonstrated to be necessary for PTB oligomerization. RRM3 has been shown to be required for RNA binding. RRM4 appears to be required for function but not for RNA binding and thus may bind to an unknown corepressor (Wagner E.J. and Garcia-Blanco M.A., 2001).

PTB exists in two major alternatively spliced isoforms, termed PTB1 and PTB4, which arise from skipping or inclusion, respectively, of exon 9, which encodes a 26-amino acid insert. A minor isoform, PTB2, is produced by inclusion of exon 9 using an internal 3'-splice site, giving a 19-amino acid insert. In addition mammals have two other paralogues, nPTB and ROD1, which show a more restricted expression in neurons and haematopoietic cells respectively. A fourth paralogue, smPTB, is expressed at high levels in smooth muscle cells of rats and mice, but is restricted to rodents (Sharp G. et al., 1991).

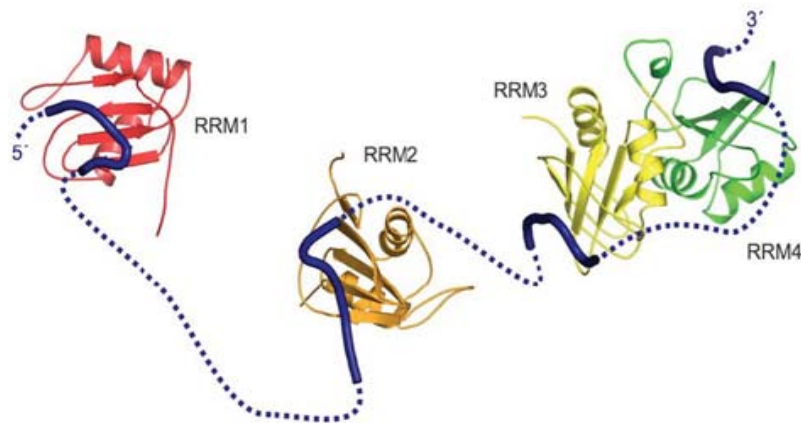


Fig. 30 Structural model of PTB and its interaction with RNA. The structure and spatial arrangement of the four RRM domains of the PTB protein are shown. The conformation of the RNA oligomer bound to each RRM domain is indicated by a solid blue line. The broken line indicates possible connectivity between these bound motifs and illustrates how RNA loops and structural rearrangement of an RNA strand could be achieved. (Sawicka K. et al., 2008)

PTB shuttles rapidly between the nucleus and cytoplasm (Knoch K.P. et al., 2004). The translocation of this protein to the cytoplasm occurs under conditions of cell stress including viral infection, apoptosis (Back S.H. et al., 2002) and exposure of cells to genotoxic agents (Dobbyn H.C. et al., 2008). Although PTB harbors an N-terminal nuclear localization signal peptide (NLS) (Back S.H. et al., 2002), previous results of our group show that other mechanisms are involved in the nuclear shuttling of PTB, because overexpressed PTB lacking the NLS is still sent to the nucleus in cardiomyocytes (Zhang J. et al., 2009).

2.3.1 Function of PTB

PTB is an RNA-interacting factor and is best known for a role in the control of alternative splicing of many transcripts including those coding for sarcomeric proteins (Mulligan G.J. et al, 1992). In alternative splicing regulation, PTB binds to splicing silencer elements within the pre-mRNA (Fig. 31) and has been shown to be responsible for repression (i.e. exclusion) of many tissue-specific exons in vertebrates including its own mRNA. PTB can repress different classes of alternative exons, namely cassette exons (Fig. 31a, d), mutually exclusive exons (Fig. 31b) and alternative 3' terminal exons (Fig. 31c) (Auweter S.D. and Allain F.H.-T., 2008). More recent global profiling of PTB targets in HeLa cells confirms that it represses

many muscle specific exons in genes encoding cytoskeletal proteins and regulators (Llorian M. et al., 2010). Biochemical analyses have further revealed that PTB could alter the recognition of splicing signals that are far away from its binding sites, indicating an extended competition between the splicing machinery and the PTB-induced splicing silencing complexes (Spellman R. and Smith C.W., 2006; Coutinho-Mansfield G.C. et al., 2007).

In addition to repressing the inclusion of exons in the mature mRNA, PTB has also been shown to positively regulate the inclusion of an alternative exon in the calcitonin (CT/ CGRP, calcitonin/calcitonin gene-related peptide) gene (Sawicka K. et al., 2008). This suggests an important function of PTB in the control of RNA splicing during heart development.

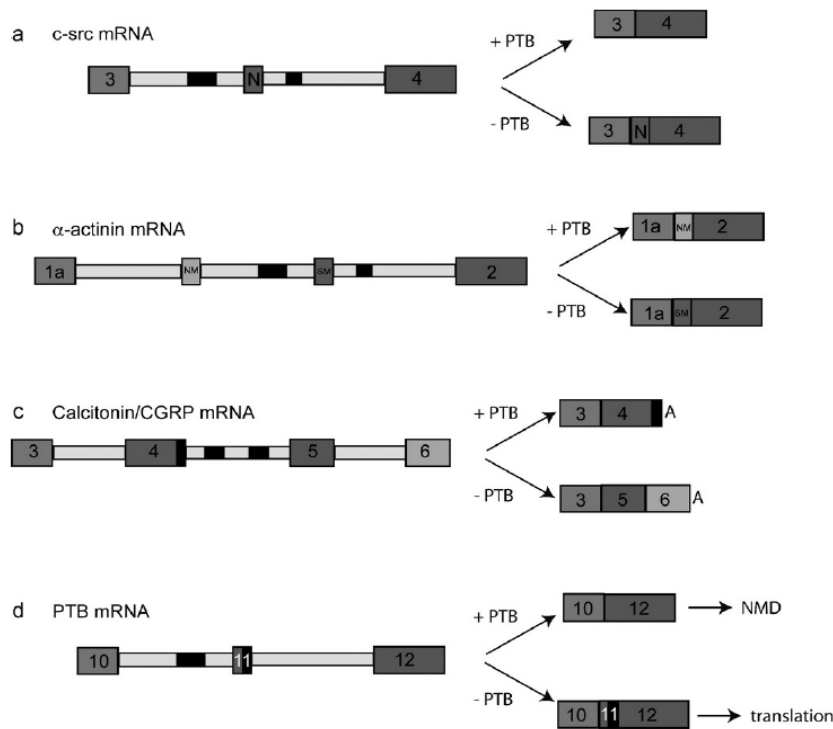


Fig. 31 Polypyrimidine tract binding protein (PTB) is a ubiquitous regulator of alternative splicing that influences different types of alternative-splicing events **(a)** PTB represses the N1 “cassette-exon” in the c-src pre-mRNA. **(b)** PTB represses the “mutually exclusive” SM exon of the α -actinin mRNA **(c)** PTB regulates the choice of the 3'-terminal exon of the calcitonin/CGRP mRNA. **(d)** PTB autoregulates its own splicing and its mRNA level by repressing the inclusion of its own exon 11. Skipping of exon11 of PTB mRNA leads to non-sense-mediated decay (NMD). Black boxes indicate the location of pyrimidine tracts bound by PTB. Intronic sequences are shown in yellow, while colored boxes indicate exonic sequences. Arrows indicates splicing in the presence (+) or absence (-) of PTB (Auweter S.D. and Allain F.H. 2008).

The second most studied function of PTB is its role in internal ribosomal entry site (IRES)-mediated translation initiation of both cellular and viral mRNAs. IRESs are large RNA structures present in the 5'-untranslated regions (UTR) of some cellular mRNAs and of many viral mRNAs. IRESs help recruiting the translation machinery to initiate translation. This recruitment often requires cellular factors binding the IRES (initiation of translation accessory factors, ITAFs) for efficient translation initiation. PTB is one of the most frequent encountered ITAFs (Auweter S.D. and Allain F.H.-T., 2008). Several footprinting studies have mapped PTB binding sites on different IRESs and identified several pyrimidine stretches embedded in stem loops and single-stranded regions (Song Y. et al., 2005). Reports have also shown that interactions between PTB and cellular or viral IRESs are essential for the IRESs to attain their correct functional conformation. Therefore in its interaction with IRES RNAs, PTB acts as an RNA chaperone (Auweter S.D. and Allain F.H.-T., 2008).

In addition to its role in splicing and translation regulation, PTB is implicated in 3'-end processing, localization and stability (Cote C.A. et al., 1999; Tillmar L. and Welsh N., 2002; Le Sommer C. et al., 2005) of various cellular mRNAs. In these systems, PTB acts through pyrimidine-tract binding sites within 5' and/or 3' UTRs. Recent genome wide investigations have identified the association of PTB with a distinct subset of cellular mRNAs that encode proteins implicated in cellular transport, vesicle trafficking and apoptosis, suggesting more regulatory functions for PTB in the cell (Bushell M. et al., 2006; Gama-Carvalho M. et al., 2006; Auweter S.D. and Allain F.H.-T., 2008).

2.3.2 Control of apoptotic signaling by PTB

PTB domains are protein modules that usually interact with the cytoplasmic tail of a wide variety of growth factor receptors. In so doing, they mediate the transduction of extracellular information to specific downstream targets within the cell that ultimately determine the fate of a number of important biological processes such as cell growth and differentiation, cell cycle regulation and apoptosis (Farooq A. and Zhou M. 2004). Normally PTBs reside in the nucleus; upon induction of apoptosis, PTBs are evenly redistributed between the cytoplasm and the nucleus. The cleavage of PTBs occurs in cells following the addition of a variety of

apoptosis-inducing agents and it has been proved that caspase-3 is responsible for the cleavage (Sung H.B. et al., 2002). Three caspase-3 target sites were identified in PTBs by experiments in both *in vitro* and *in vivo* systems (Back S.H. et al., 2002).

Reports have shown that interactions between PTB (or the neuronal nPTB) and cellular or viral IRESs are essential for the IRESs to attain their correct functional conformation. Hence, in its interaction with IRES RNAs, PTB acts as an RNA chaperone. More recently, PTB was also found associated with the 3'UTR of the ATP synthase b-subunit, where it helps enhancing translation in a cap-independent manner. Also there are two well-characterised examples of PTB affecting IRES-mediated initiation of proteins that have roles in the apoptotic process: both the Apaf-1 and BAG-1 IRESs require PTB for function (Spriggs K.A. et al., 2005; Reyes R. and Izquierdo J.M., 2007). Moreover, previous results of our group suggested that PTB was involved in IRES-dependent translation of apoptotic proteins in differentiating cardiomyocytes (Zhang J. et al, 2009).

Hypothesis and Objectives

1 Background and Hypothesis

Our previous studies showed that the genes controlling caspase-dependent cell death are expressed in the embryonic heart, but are later silenced and cardiomyocyte death is regulated by caspase-independent mechanisms after postnatal development (Bahi N. et al. 2008, Zhang J. et al., 2009). On the contrary, we observed that the pro-death gene EndoG is abundantly expressed in the differentiated myocardium and works as an important executor of caspase-independent DNA cleavage in differentiated cardiomyocytes and during cardiac ischemia (Bahi N. et al. 2008; Zhang J., 2011). Our recent research found that PTB regulates apoptotic gene expression including caspases in postnatal cardiomyocytes (Zhang J. et al., 2009) and controls splicing of some Mef2 genes. Here, I present three different lines of research focused on the regulation of gene expression during cardiomyocyte growth and differentiation.

1) We found sustained expression of EndoG in the adult heart. Despite its DNA-degradating role during ischemia, **sustained expression of EndoG in the differentiated myocardium suggested to us a relevant function of this gene in heart physiology.** EndoG was identified by Prof. Stuart Cook's group as a gene located on a blood pressure-independent left ventricular mass region of rat chromosome 3p. We wanted to investigate, in collaboration with this group, the potential role of EndoG in the regulation of cardiomyocyte growth and mitochondrial function.

2) While studying the mechanism involved in cardiac growth, we focused on the myocyte enhancer factor 2 (MEF2) family. It has been proved that mice lacking MEF2A suffer perinatal death and heart hypertrophy (Naya F.J. et al., 2002). It is also proved that calcineurin-MEF2 signaling is activated in all muscle fibre types in response to increased nerve-mediated activity (Sakuma K. and Yamaguchi A., 2010). We had preliminary results showing that Mef2's mRNA and protein abundance were not co-ordinately regulated during hypertrophy. Thus, **we suspected that MEF2 expression is regulated at the translational level during hypertrophy** and we wanted to investigate this fact.

3) Mef2's exon β codes for a peptide conferring stronger transcriptional activity to MEF2 (Yu Y.T. et al., 1992). Exon β is included in Mef2 in the adult heart (Yu Y.T. et al., 1992). PTB inhibits exon inclusion during mRNA maturation and induced IRES-dependent translation of many genes (Spellman R. et al., 2005). Class II HDACs are abundant in the developing heart and inhibit MEF2 transcriptional activity (Olson E.N., 2006). Our hypothesis was that **Mef2 mRNA splicing is regulated by PTB, probably involving HDAC activity** and we wanted to assess this possibility and also identify the involved signaling pathways.

2 Objectives

- 1) To check the role of EndoG in mitochondrial physiology and cardiac growth.
- 2) To investigate the signaling influencing MEF2 protein abundance unrelated to mRNA regulation during agonist-induced cardiomyocyte growth.
- 3) To identify the mechanisms controlling PTB expression and Mef2 splicing during heart development.

Materials and Methods

1 Cell culture

Cells were cultured in a CO₂ incubator under a humid atmosphere at 37°C, supplied with 5% CO₂. Cell culture media, supplements were from GIBCO Invitrogen: Dulbecco's modified Eagle's medium (DMEM) with L-glutamine, DMEM low glucose (1g/L), bovine serum (#10270-106), heat inactivated at 56°C for 30 minutes and HS-horse serum (#26050-088). L-Glutamine 200mM (#25030-024), NEAA (non essential amino acids) (#11140-035), sodium pyruvate 100mM (#11360-039), HEPES 1M (#15630-056), Trypsin (#25200-056) and penicillin-streptomycin antibiotics (P/S) (#15140-122) were bought as commercial sterile solutions 100× from Invitrogen.

1.1 Cell culture dishes coating

Collagenase: Type 2 collagenase from rat tail (Worthington, #40C11785) at a final concentration of 10u/μl diluted in ADS 1× (described in part 1.3).

Gelatin: (Type A gelatine from swine skin, SIGMA, #G9539) used at 0.1% for HEK 293T cells and 0.2% for cardiomyocytes as final concentration diluted in miliQ. Cardiomyocytes culture dishes were covered with a minimum volume of the solution, about 1ml for p35 and left in the laminar flow hood/cabinet for at least 1h. We aspirated the gelatine before seeding the cells.

1.2 Maintaining of HEK 293T cells

This is a cell line with an epithelial morphology, obtained from human embryonic kidney cells grown in tissue culture. We used it because of its capacity to overexpress cell line of choice for the packing and production of lentiviral particles. The growing medium is DMEM, supplemented with 20U/ml of penicillin, 20μg/ml of streptomycin, 10mM sodium pyruvate and 10% heat-inactivated FBS.

To perform the culture of this cell line, as this cell line does not attach to the plate so tightly that it is not necessary to use trypsin to make the cells detach. Then we transferred the

cell suspension to a sterile falcon. We centrifuged for 4 minutes at 800rpm, aspirated the medium, and suspended the cell pellet in fresh complete medium. We seeded the cells in new monolayers at a 1/20 dilution.

1.3 Primary cardiomyocytes maintenance

Medium for cardiomyocytes and ADS (1×, dilute with MiliQ water, from stocking solution of 10×) (Table 1) should be pre-warmed to 37°C. Treating cardiomyocytes with cold solutions will impair their functionality.

Table 1. Composition of cardiac medium and ADS

Cardiac Medium	Volume	ADS (10×)	Volume
DMEM	150ml	NaCl	6.8g
M199	50ml	Na₂HPO₄·2H₂O	120mg
FBS	10ml	KCl	400mg
Horse serum	20ml	MgSO₄·7H₂O	197mg
L-glutamine	2ml	Glucose	1g
P/S	1%	Hepes	4.8g
		add H₂O	To 100ml (PH 7.4)

We sacrificed 2~3 days old rats and excised hearts from all pups, and tore the excised hearts in a plate containing ADS 1 × on ice. Then we squeezed these hearts gently with forceps to expel the blood from the lumen and transferred the hearts into fresh ice-cold ADS 1×. Then we cut the ventricles and moved the ventricles to a new plate with ADS 1× and minced tissue as small as possible with a ophthalmic scissors. Next we transferred 4 minced neonatal hearts into pre-warmed digestion buffer (15μl type II collagenase + 950μl ADS 1×) in an 1.5ml eppendorf tube and incubated with shaking at the speed of 1100rpm for 15 minutes at the temperature of 37°C. Then we transferred the supernatant of every 5 eppendorfs to a 15ml falcon with 10ml neutralization medium (500ml DMEM with 10% heat-inactivated FBS) and centrifuged at 800rpm for 4min at room temperature (RT), then we aspirated the supernatant and suspended the cell pellet with cardiac medium (table 1) and put the suspension in a falcon in the hood.

For the eppendorfs containing the hearts, we added new pre-warmed digestion buffer and repeated the digestion procedure 2 more times. After centrifuging, we suspended all the cells in pre-warmed cardiac medium and collected the cells from the 3 times in a 50ml falcon. Then we resuspended the cells in enough cardiac medium (10ml per 10 hearts) and plated the cell suspension in uncoated 10cm dishes, and incubated for 45min at the condition of 37°C/5% CO₂. After the first 45min we transferred the cell suspension carefully from the plates directly to new 10cm dishes and incubated for another 45min. During the incubation time, fibroblasts would spread and get attached to the plate whereas cardiomyocytes, which need longer time to get attached, remained unattached. At the same time, we prepared plates of p35 or M4 coated with 0.2% gelatin. After the second incubation, we collected and counted the cells with trypan blue stain (#15250-061, GIBCO Invitrogen) to determine cell density. It is expected that a yield of around 1×10^6 cardiomyocytes per heart could be maintained.

Before seeding cardiomyocytes, we added mytomycinC (SIGMA ALDRICH) to the cell suspension at the concentration of 1:100 to inhibit the proliferation of cardiac fibroblasts. Then we seeded cardiomyocytes to the plates: M4 at the density of 75,000 cells/well; p35 at the density of 1×10^6 cells/plate; P60 at the density of 2.5×10^6 cells/plate. Finally we put the plates in the primary cell incubator for no less than 3 hours, then we changed the medium and continued with following treatments (MytomycinC can inhibit the growth of fibroblasts while it is harmful to cardiomyocytes for long period incubation).

1.4 Cell recovery and cryopreservation

Cell recovery: First we prepared 37°C water bath and pre-warmed complete culture medium to 37°C. Then we removed cells from liquid nitrogen and placed it into the water bath pot, and gently shook to ensure that cells could dissolve completely in 3min. (Note points: for too long a time will affect the dissolution of the vitality of cells, resulting in many dead cells). Then we moved the completely dissolved cells into sterile cabinet, transferred the dissolved cell suspension in a 15ml falcon containing standard medium 10ml and mixed gently, then centrifuged the tube at the speed of 800rpm for 4min. We discarded the

supernatant, added 2-3ml warm standard medium with gently blowing to ensure complete resuspension. Then we put all the cell suspension into a P100 plate with 10ml culture medium and incubated at 37°C, 5% CO₂. The next day we changed the medium to ensure the removal of dead cells.

Cryopreservation of cells: Then we got the logarithmic growth phase cells and washed the monolayer with PBS once and digested with 3ml trypsin (0.25%) and added 7ml medium to neutralize the trypsin and transferred the suspension to a 50 ml falcon and centrifuged for 4 min at the speed of 800rpm. Afterwards we suspended the cell pellet with cryopreservation medium (FBS containing 10% DMSO) and adjusted the cells at the density of 5×10^6 to 1×10^7 . We aliquoted the cell suspension to 1ml each tube and marked clearly. The tubes were kept at -80°C for 48h and then were stored into liquid nitrogen containers.

1.5 Polyethylenimine (PEI) transfection:

PEI preparation (polyethylenimine, SIGMA ALDRICH, cat. 40872-7):

- MW of PEI is 25000
- PEI has 580 free-Nitrogens/mol
- Use sterile miliQ water in the whole process

STEPS:

1) Prepare stock 20% PEI (C₂H₅N, 1N per monomer): this stock is 8mM PEI and 4.5M in Nitrogen equivalents.

4500mM/8mM=562.5 monomers of PEI in our solution 8mM PEI, because one monomer have 1N.

2) Dilute this stock to 200mM of Nitrogen equivalents. Move it to pH=5.6, 1ml mother stock (step 1) in 21.5ml miliQ water

3) Dilute to 5.47mM of Nitrogen equivalents (aprox. 10μM PEI) to get the final transfection reactive [4ml stock 200mM Nitrogen (step 2) in 142.26mM miliQ].

Day 1: The day before transfection, we coated p100 plates with 0.1% gelatine for at least 20min before seeding, and then we seeded each p100 plate with 3,500,000 cells.

Day 2: On the day of transfection, 1 or 2h before start, we changed medium to 8ml medium without serum or antibiotics. 40µg DNA is needed for transfection (Table 2), 5µl PEI per 1µg of DNA is needed. So we add 200µl PEI per plate and 4 times more salt than PEI [800µl NaCl (SIGMA ALDRICH), 150mM].

Table 2. Plasmids used for transfection

Vector lentiviral (RNAi or overexpression)	20µg
Packaging system (psPAX2)	13µg
Envelop plasmid (pM2G)	7µg

First we diluted the 40µg of DNA in 970~990ul of 150mM sterile NaCl, vortexed a few seconds to make drops go down. Then we diluted 200ul PEI in 800µl of 150mM sterile NaCl, vortexed and spin. Next we added the PEI dilution to the DNA (not the contrary) and vortexed 1min and let the mix in the hood for 10min at RT. Then we added the mix to each p100 plate gently and put the plates in the incubator. After 3h we changed the medium to complete HEK293T medium (500ml DMEM+10% FBS+1ml Penicillin-Streptomycin, 10ml per plate of p100).

Day3: Dilute to 5.47mM of Nitrogen equivalents (aprox. 10µM PEI) to get the final transfection reactive (4ml to stock 200mM Nitrogen (Step 2) in 142.26ml miliQ).

Day 4: We seeded an M24 with 293T (30,000 cell/well) and kept it in the incubator, in order to check the efficiency of lentivirus the next day.

Day 5: We collected the supernatant of each p100 at 48h (60h) in a 50ml falcon and centrifuged at the speed of 2500rpm for 5min, collected the supernatant carefully and filtered directly into an exclusion molecular column using 4.5µm filters, and centrifuged at the speed

of 50,000g for 3h at 4°C. Then in the biosafety cabinet we resuspended the pellet with 1% sterile BSA (for each pellet from the supernatant of one p100 we suspended with 1% BSA 30µl) and stored the lentivirus solution at -80°C or transfected the cardiomyocytes directly (15~20µl lentivirus suspension to each p35 plate).

The biological titer of viruses was expressed as the number of transducing units per µl (TU/ml) and was calculated by transducing HEK293T cells at two dilutions: 1µl and 0.1µl of concentrated virus. After 48h of incubation, the percentages of GFP-positive cells were counted and viruses with the efficiency of 5×10^8 - 1×10^9 TU/ml can be used for the following experiments.

1.6 Cell transduction

In experiments with gene overexpression or knock-down, we used lentiviral transduction. For that purpose, in the dishes seeded with cardiomyocytes at the density of 1,000,000 cells/plate, 15-20µl of the concentrated virus solution was added to the culture medium (Pay attention that all the procedure is performed in the BioAII). The medium was changed the next day (within 24h) and the efficiency of the transduction was continuously monitored under the fluorescence microscope. Usually different lentivirus should be kept for different period in order to achieve the optimum transduction effect. The percentage of GFP-positive cells was detected to be between 90-99%.

1.7 Immunofluorescence (IF)

Immunofluorescence is performed on cardiomyocytes growing on M4 plates, for the acquisition of confocal images on the Olympus FluoView™ FV 500 confocal laser scanning microscope.

Cell culture: Cells were seeded at low density, since it is important to acquire images of isolated cells. Therefore 75,000 cells/well were seeded for confocal microscope image acquisition.

Fixation: Once cell treatment finished, cells were fixed for 30min in 4% paraformaldehyde (PFA, SIGMA) diluted with PBS. Then cells were washed three times with PBS, 3 min/ time.

Permeabilization and blocking: We prepared blocking solution (BS) shown in Table 3, and we covered the wells with BS (0.5 μ l per well of M4) and incubated with mild shaking for 1h at RT.

Table 3. Composition of blocking solution

Components:	volume:	Percentage:
Horse serum	0.6ml	2.0%
Triton	30 μ l	0.1%
BSA	0.6g	2.0%
	V=30ml (in PBS 1 \times)	

Antibodies: Antibodies were diluted in blocking solution: α -actinin was used at 1:2000 dilution (see Table 7 for detail). Primary antibody was incubated for 2h at RT with mild shaking. After the incubation with primary antibody, we aspirated the solution and the wells were washed three times with BS (10min/time) and then incubated with the appropriate secondary antibody at a 1:500 dilution (see Table 8 for detail) for 1h at RT with mild shaking. From this step it is necessary to protect the plates from light by covering them with foil paper. After the secondary antibody incubation, we washed the plates with BS 3 times (5min/time) and then incubated with Hoeschst 33342 (SIGMA ALDRICH, #B2883) at the dilution of 1:2000 from stock for 30min at RT with mild shaking.

Mounting: Before mounting a final fast wash step with PBS 3 times was performed, in order to avoid salt crystals formation. Coverslips were mounted on slides with Vetashield (Roche, #H1000) (Take care that no air bubbles remained captured). Then we covered the plates with foil paper and store it at 4°C. We observe the plates after 24h when the backgroundd reduces.

Notes:

*Samples should be protected from light after adding the secondary antibody.

*PFA 8% preparation: Prewarm 70ml miliQ water at microwave and put it on a heater/magnetic mixer in the hood. Then measure the temperature with a thermometer to 60-70°C (before adding PFA). When temperature is fixed, add 8g PFA and a magnetic mixer and let it mix well (It is dissolved when the liquid is transparent, it is necessary to add 4-6 drops NaOH 10M to help it dissolve). We let the solution at RT in the hood to cool down. Then we add 10ml PBS 10× and fill up to 100ml with miliQ, adjust pH to 7 or 7.5 with HCl. Finally we filter the liquid and aliquot and keep the aliquots at -20°C.

2. Molecular biology

2.1 General technique for gene cloning

We extracted Plasmid DNA from E.coli using Qiagen plasmid kit (Qiagen, Hilden, Germany) or Nucleo bond ® AX (Macherey-Nagel) Kit following manufacturer's instructions. The concentration of plasmid DNA was quantified in a Micro Volume UV-visible Recording Spectrophotometer (NanoDrop, Thermo Scientific). Plasmid and insert were both digested with correspondent enzymes, except for the cloning of shRNA into pSUPER plasmid. Then the purified insert and vector were quantified with NanoDrop, and the ligation reaction was set-up with a molar ratio 1:3 vector and insert respectively. We added the T4 ligase (TaKaRa), the reaction was incubated at 16°C water bath overnight. Ligation was transformed into the E.coli DH5α, using the heat-shock transformation protocol. We checked the correct insert by PCR, using primers annealing close to the insert region, thus the size of the amplicons obtained allowed us to distinguish between empty vector and a vector which contains the insert, or check by enzymes that we used for the plasmid construction, then run in an agarose gel and check whether there are corresponding bands of both the vector and the insert.

Heat-shock protocol: We thaw one tube of CaCl₂ competent cells on ice. Then we put the entire ligation mix into the competent cell suspension, flicked the tube gently to mix and

incubated it on ice for 30min. Heat-shocked the cells at 42°C for 25~45sec and immediately put the tube in ice for 2min. Then we added 800µl pre-warmed LB (or SOC) medium to the tube and incubated it at 37°C with the agitation of around 200rpm for 1 hour. After that we spread 200~800µl cell suspension onto pre-warmed LB plates (with appropriate selection of antibiotics, i.e. ampicillin) and incubated the plate overnight at 37°C (within 16h). The next day we checked whether there were colonies.

2.2 Principle of RNAi action

RNA interference (RNAi) is an RNA-dependent gene silencing process that is controlled by the RNA-induced silencing complex (RISC) and is initiated by short double-stranded RNA molecules in a cell's cytoplasm, where they interact with the catalytic RISC component argonaute. It is popularized by groups working with *caenorhabditis elegans*, when double-stranded RNAs, injected into a worm's gonad, blocked the expression of endogenous genes in a sequence specific manner. Introduced RNA fragments induce the degradation of a specific messenger RNA by binding to a particular homologue RNA sequence (Fire A. et al., 1998). RNAi can regulate endogenous gene expression. It also has a role in antiviral defence, in which viral double-strand RNAs are targeted for destruction by the RNAi machinery. When long dsRNAs enter cells, they are recognized and cleaved by Dicer, which is a member of the RNase III family of dsRNA-specific nucleases. This cleavage creates short dsRNAs, characterized by long 3' overhangs, called small interfering (si) RNAs. siRNAs can form a ribonucleoprotein complex called RISC (RNAi silencing complex). RISC mediates the unwinding of the siRNA duplex, so that a single stranded siRNA, coupled to RISC, then binds to a target mRNA in a sequence-specific manner, which mediates target mRNA cleavage by the "Slicer" Argonaute proteins (Fig. 32).

The cleaved mRNA can be recognized by the cell as being abnormal and then it is destroyed by nucleases, preventing its translation. This mechanism of specific mRNA destruction results in silencing of gene expression.

The RNA interference technology serves as a revolutionary tool for studying gene function, biological pathways, and the physiology of disease. In the present work we have used the strategy to introduce shRNA (small hairpin RNA) by lentiviral vectors in to neonatal cardiomyocytes to silence the expression of specific endogenous genes.

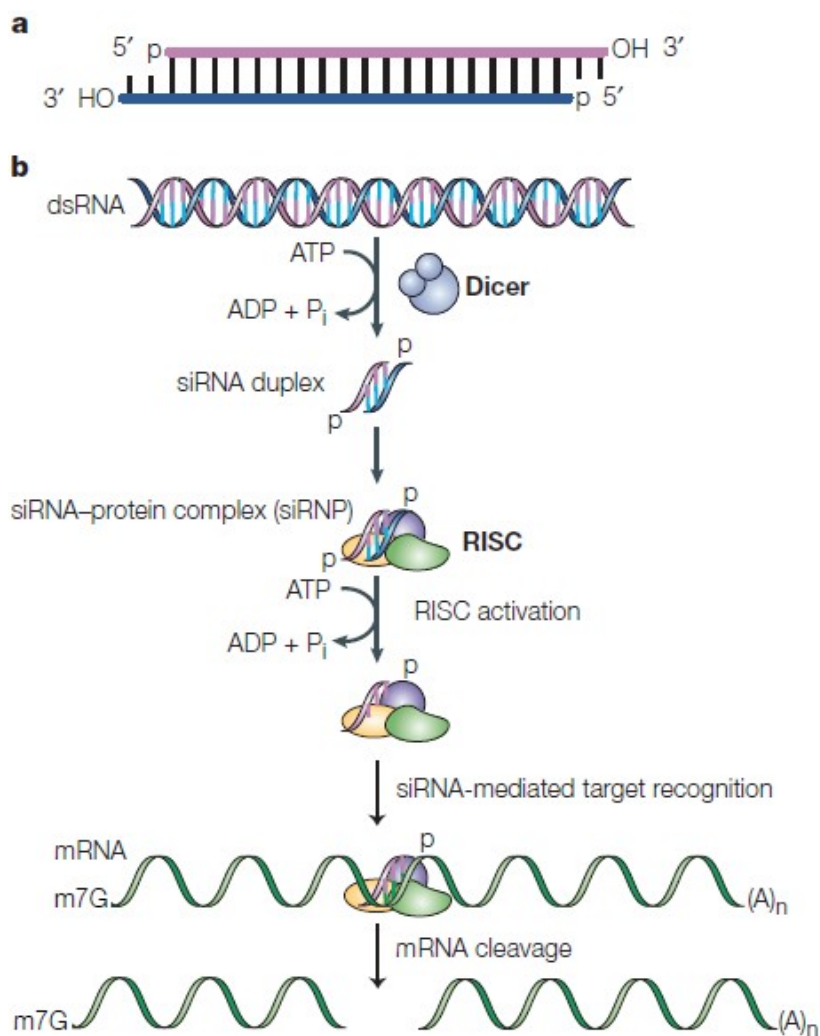


Fig. 32 The RNA interference pathway. **(a)** Short interfering (si) RNAs. Molecular hallmarks of an siRNA include 5' phosphorylated ends, a 19-nucleotide (nt) duplexed region and 2-nt unpaired and unphosphorylated 3' ends that are characteristic of Rnase III cleavage products. **(b)** The siRNA pathway. Long double-stranded (ds)RNA is cleaved by the Rnase III family member, Dicer, into siRNAs in an ATP-dependent reaction. These siRNAs are then incorporated into the RNA inducing silencing complex (RISC). Although the uptake of siRNAs by RISC is independent of ATP, the unwinding of the siRNA duplex requires ATP. Once unwound, the single-stranded antisense strand guides RISC to messenger RNA that has a complementary sequence, which results in the endonucleolytic cleavage of the target mRNA. (Dykxhoorn D.M. et al., 2003).

2.3 Primers design for shRNA and subcloning procedures

The pSUPER retro.puro vector (Oligo Engine) leads to efficient and specific reduction of the expression levels of the target gene. It is a mammalian expression vector, which directs the synthesis of shRNA transcripts. The subcloning strategy is based on choosing a sequence into the target gene, which is 19 nucleotide-long.

Thus, we designed several primer pairs against the target gene. Selected sequences are presented on table 4.

Primers were ordered from Invitrogen and upon arrival, lyophilized primers were dissolved in sterile miliQ water at the final concentration of 3mg/ml.

Primer annealing is done in 50mM Hepes pH 7.4, 100mM NaCl buffer, using 1µl of each primer stock (3mg/ml) to a final volume of 50µl (primer final concentration 60µg/m). The protocol for primer annealing consists of progressively reducing the temperature from 90°C to 10°C and increasing time intervals.

Temperature	90°C	70°C	60°C	50°C	37°C	10°C
Time	4min	10min	20min	30min	45min	60min

Annealed primers have protuberant ends compatible with restriction sites for ClaI and EcoRI, ready to be introduced directly into digested pSUPER vector.

Table 4. shRNA primer sequences

Gene	Oligonucleotides sequences (5'→3')
PTB	gatccccGCACAGTCCTGAAGATCATttcaagagaATGATCTTCAGGACTGTGCttttta
	agcttaaaaaGCACAGTCCTGAAGATCATtctcttgaaATGATCTTCAGGACTGTGCggg
EndoG	gatccccGGAACAACCTTGAGAAGTAttcaagagaTACTTCTCAAGGTTGTTCCttttta
	agcttaaaaaGGAACAACCTTGAGAAGTAttctcttgaaTACTTCTCAAGGTTGTTCCggg
Scrambled	gatccccGAATGCTAAGATGTCTAATttcaagagaATTAGACATCTTAGCATTCttttta
	agcttaaaaaGAATGCTAAGATGTCTAATtctcttgaaATTAGACATCTTAGCATTCggg

2.4 Subcloning of shRNA into pLVTHM vector

Enzymes: Enzymes from Roche: EcoRI, ClaI and HindIII. Enzymes from New England Biolabs: BglII. Enzymes from TaKaRa: T4 DNA ligase. Supra ThermTM DNA Polymerase was from GeneCraft. Taqman Reverse Transcriptase from Applied Biosystems and PfuUltra High-Fidelity DNA Polymerase from Stratagene.

Plasmids: The plasmids used in this work are: pSUPER.retro.puro (OligoEngine), pLVTHM viral vector was kindly donated by Dr. Trono.

Bacteria: We used two different E.coli strains DH5 α for plasmid constructs and E.coli One shot Stbl3TM (Invitrogen) for lentiviral constructs. Competent bacteria is transformed using the heat-shock protocol or following provider's instructions. Frozen aliquots of transformed bacteria were stored at -80°C in 20% glycerol.

The pLVTHM plasmid is the lentiviral vector we are going to use for the transduction of specific shRNAi into mammalian cells. Therefore, the pSUPER plasmid is used as a shuttle vector for our shRNA constructions. The promoter fragment H1 of pLVTHM is replaced by the "H1-shRNA" pSUPER fragment, using the restriction sites for EcoRI and ClaI. In this way, we obtained shRNA constructions into the lentiviral vector and proceeded with the employment of the RNA interference technique to silence the expression of target genes in cardiomyocytes.

2.5 Lentivirus production

Dr Trono and colleagues have developed three generations of vectors for lentiviral production. Naldini and colleagues described lentivirus production protocols in 1996. Plasmids used for lentivirus production that belong to the second generation are the following:

1) Vectors pEIGW and pLVTHM are used for over-expression or inhibition of the gene expression respectively. The vector itself is the only genetic material transferred to the target cells, as they have lost the transcriptional capacity of the viral long terminal repeat (LTR). The vector sequence includes the transgene cassette flanked by cis-acting elements, required for its encapsidation, reverse transcription and integration into the genome.

2) pCDNA3 vector codifies for viral packaging proteins. psPAX2 contains a very compounds, such as: TAT protein, DNA polymerase and Reverse Transcriptase. The CAG promoter includes the CMV enhancer, the chicken β -actin promoter and intron.

3) pM2G vector codifies for a viral envelope protein from Vesicular Stomatitis Virus (VSV) and triggers the transduction of a wide range of tissues and cell lines.

We used HEK293T cells as packaging cell line for lentivirus production. Cells were seeded at a density of 3.5×10^6 in P100 cell culture dishes, coated with 0.1% of gelatine before seeding. Each cell culture dish was transfected following the step described in the section of 1.5.

The transfection was performed according to the PEI transfection protocol (see part 1.5). The efficiency of transfection was checked after 72h on the fluorescence microscope. To obtain a high transduction efficiency, lentiviruses were finally suspended in 1% BSA diluted in PBS and stored at -80°C to preserve their transduction capacity and we should avoid re-freezing the aliquots, which will decrease the efficiency of the lentivirus.

3 Reverse Transcription and Polymerase Chain Reaction (RT-PCR)

3.1 RNA extraction

For RT-PCR, total RNA was isolated from cardiomyocytes and animal tissues using Rneasy Mini Kit (QIAGEN) following the manufacturer's protocol.

3.2 Reverse Transcription (RT)

The preparation of RT mix: We added H_2O $5\mu\text{l}$, buffer $10 \times$ $4\mu\text{l}$, dNTPs $8\mu\text{l}$, MgCl_2 $9\mu\text{l}$, random Hexamers $2\mu\text{l}$, Rnase Inhibitor RNAsin $1\mu\text{l}$, enzRT $1\mu\text{l}$, RNA $10\mu\text{l}$ (contains $1\mu\text{g}$ of RNA) to the final volume of $40\mu\text{l}$.

Process:

Prepare the Mix (except RNA)

RNA: first keep in 90°C for 2min, then put the tube in ice immediately.

Add all the mix in the tubes

RT :

25 °C	42 °C	95 °C	4 °C
10min	60min	5min	∞

We store the RT products at -20°C, or go on with PCR.

3.3 Conventional PCR

The preparation of PCR mix: We added each tube cDNA 5µl, forward primer 1µl, reverse primer 1µl (Table 5), dNTPs 1µl, buffer 10× 4µl, MgCl₂ 1.25µl, enz Taq 0.2µl, H₂O 26.55µl to the final volume of 40µl.

PCR reaction:

94 °C	94 °C	55 °C	72 °C	72 °C	4 °C
5min	30sec	30sec	30sec	10min	∞
27 to 35 cycles					

Electrophoresis: Aliquots were taken at different PCR cycles as required, and migrated in 3% agarose gel mixed with 1% SYBR Safe dye (Invitrogen). Loading was checked by amplification of unr.

Table 5. Primers for RT-PCR

Target gene	Forward (5'-3')	Reverse (5'-3')
MEF2A Rn	GGAATGAACAGTCGGAAACC	CAAGCTTGGAGTTGTCACAG
MEF2A Mm	GGAATGAACAGTCGGAAACC	GAGGCAAGCTCGGAGTTGTC
MEF2A RnMm with exonβ	GGCAAAGTCATGCCTACAAAGTC	TTGGGCATTCAACTCCAATTC
MEF2A RnMm without exonβ	CCAAATGGAGCTGGAAATAG	TTATCCTTTGGGCATTAAGTGG
MEF2C Rn	CCAAATCTCCTCCCCCTATG	CCAATGACTGGGCCGACTG
MEF2D Rn	AGGGAGGCAAAGGGTTAATG	AGTGGGCATGGAGGAGAAG
MEF2D RnMm with exonβ	GGTTAATGCATCATTGACTGAG	AGTGGGCATGGAGGAGAAG
MEF2D RnMm without exonβ	GGTAATGCAACATTTGAACAATG	AGTGGGCATGGAGGAGAAG
PTB1/4 Rn	ACAACGACAAGAGCCGAGAC	GGCTCCATGGACATTAGGAA
EndoG Rn	GACTTCCACGAGGACGATTC	AAGCTGCGGCTGTACTTCTC
UNR RnMm	ATCATCTGACCGGAGGACTG	TGAACGTTCCCTTCCCATC

Rn: Rattus novegicus; Mm: mouse novegicus; Scr: scrambled sequence

3.4 Real Time PCR

Real time PCR was performed in a iCycler iQ PCR detection system and iQ v.3 and iQ v.5 software (BioRad), using the Taq Man Gene Expression Master Mix (Cat.N. 4369016) and the Gene Expression Assays to amplify mouse and rat Mef2a, Mef2d, nppa, acta 1 respectively, with simultaneous amplification of Gapdh as loading control (Applied Biosystems). Quantitative Real Time PCR was performed by Servei de Proteomica i Genomica of Lleida University, using specific genes and primer assays (Table 6).

Table 6. TaqMan Assays for real-time PCR

Name of Gene	Catalogue number
Mef2a	Rn01478096_ml
Mef2d	Rn01455530_gl
Nppa	Rn00561661_ml
Acta1	Rn01641150_ml
Flip	Rn00589205_ml
Ptb (mouse)	Mm00943334_ml
Ptb (rat)	Rn00821112_ml
Gapdh	Rn01775763_gl

3.5 Radioactive quantitative PCR

Reverse transcript reactions were carried out using 1µg of total RNA, oligo dT and Superscript II (Invitrogen) following manufacturer's instructions. PCR reactions were carried out with 10pmol of forward primer (Table 5) and 4pmol of ³²P-labeled reverse primer and 1U/µl of Taq polymerase, under the following conditions: 94°C for 30s, 55°C for 30s and 72°C for 30s, 25 or 30 cycles. 1/20 of the PCR was separated on 8% urea gel, PCR band ratios were determined using Molecular Dynamics PhosphorImager and shown as fraction of the total. Radioactive quantitative PCR was performed by Miriam Llorian in Cambridge.

4 Biochemistry

4.1 Western-blot (WB)

Cell lysis: Cell monolayer was washed twice with ice-cold PBS and lysed in sodium dodecyl sulfate (SDS) lysis buffer (2% SDS and 125mM Tris-HCl pH6.8) for western blot analysis. When immunoprecipitation experiment was performed, cells were lysed in another lysis buffer (10% 100mM Tris pH7.4, 1% SDS).

Protein quantification with the method of Lowry: We quantified the protein concentration of cell lysates according to the BioRad protein assay kit (BioRad, #500-0113, #500-0114, #500-0115). Quantification of proteins in samples before migrating SDS-PAGE gels is necessary and important for the subsequent interpretation of results. If the different samples of the same experiment for the immunodetection of proteins are not equally loaded, no conclusions can be made as we do not know whether the differences are due only to the loading or due to the effects of different treatments.

We used Lowry to determine the concentration of protein in a sample. The reagents are from Bio-Rad. We added BSA for standard curve and samples in the wells of a 96-well plate, in duplicate. Mix the reagents A and S (in proportion 50:1), and the mixture was added to the wells with samples, then we added reagent B. Afterwards we let the mixture react for 10 minutes at RT and then the plate was read at an absorbency of 620nm. The standard curve was done by using different concentrations of BSA and it was used to standardize the results. The values of absorbency of the samples were interpolated to the line pattern to determine the protein concentration.

Note that this method is incompatible with the presence of detergent (such as DTT) in the sample, so if our extraction buffer DTT is in need for proper protection of the extracted protein (e.g. cytosolic extracts) while the sample is extracted without DTT, quantify immediately and quickly add DTT to protect the extract from possible degradation.

SDS-Polyacrylamide Gel Electrophoresis (SDS-PAGE): The proteins of the sample were separated using gel electrophoresis. We used polyacrylamide gels and loading buffer with sodium dodecyl sulfate (SDS). SDS-polyacrylamide gels were prepared according to the size of the target proteins. For proteins with molecular weight ranging from 20 to 100kDa such as PTB (62kDa), MEF2A (54kDa), MEF2D (56kDa), etc. we used 10% polyacrylamide gels. Resolving gel was prepared in 375 μ M Tris-HCl buffer pH8.8, 0.1% SDS and finally we added 0.08% ammonium persulfate (PSA) and 1 μ l/ml TEMED. Stacking gels were of 4 or 5% polyacrylamide in 125 μ M Tris-HCl buffer pH6.8, 0.1% SDS, 0.067% PSA and 1.7 μ l/ml TEMED. Electrophoresis running buffer contained 1.44% glycine, 0.1% SDS and

25mM Tris. We loaded the samples, assuring that all wells have the same volume, adding loading buffer 1× into empty wells, and one lane was reserved for a bench marker, a commercially available mixture of proteins having defined molecular weights, typically stained so as to be visible, coloured bands. Electrophoresis was run at constant current, 20mA per gel of 1mm thickness and 8cm wide, during the time required until the front bromophenol blue leaked out of the gel.

Transfer: We used a Hoefer semi-dry system to transfer the resolved proteins from the gel to a polyvinylidene difluoride (PVDF) membrane. We cut Blotting paper sheets (GE, #80-6211-29) and the PVDF membrane (Immuobilon-P, Milipore) at the exact size of the gel. We hydrated the PVDF membrane with methanol for 20 min and then we washed it with water, after that we submerge the membrane, blotting paper and gel (separately) in transfer buffer (48mM Tris, 0.0375% SDS, 39mM glycine, 20% methanol). Before transferring, we placed 2 pieces of wet filter paper on the node (+), then the membrane and the gel and then another 2 pieces of filter paper. To remove all the air bubbles that could have formed between the layers we rolled a plastic tube on top of the transfer sandwich carefully. Finally we placed the cathode (-) over the “sandwich” and run at constant current of 0.8mA/cm² membrane surface for 1h.

The uniformity and overall effectiveness of transfer of protein from the gel to the membrane were checked by staining the gel and membrane with Coomassie Brilliant Blue and Ponceau S dyes respectively.

Notes:

* Gel staining with coomassie: the dye Coomassie brilliant blue R-250 (Fluka, Sigma) binds to almost all the proteins, both in denaturalized and not denaturalized, which can be used after electrophoresis. We use it to dye the gel once transfer finishes, marking proteins remnant of the polyacrylamide gels as loading controls of the western blot. We put the gel in the staining solution over night (0.1% coomassie brilliant blue R-250, 25% isopropanol, 10% acid acetic), leaving all the gel below the solution. Then we use another bleaching solution (10% isopropanol, 10% acid acetic) to decolor the gel, which will make the gel transparent with protein bands remaining blue.

* Membrane staining with Ponceau S: After the protein transfer, to verify whether the transfer is successful, the membrane can be stained with a solution of red dye (Ponceau S, in 5% acetic acid) for 5min at RT. Then the membrane is washed with TBS-T and the stained protein bands are reversible in red bands. After washing several times with TBS-T the color disappears and we can continue with the blocking step. Attention that the reversible coloration is not suitable for checking the loading control.

Blocking: Once the transfer finished, we washed the membrane with TBS-T (Tris-Buffered Saline-Tween 20, 20mM Tris pH7.6, 150mM NaCl, 0.1% Tween 20) and blocked the membrane with 5% non-fat dry milk (diluted in TBS-T) for 1h at RT with mild agitation.

Incubation with primary antibody: we diluted the primary antibody in TBS-T to the concentration referred in table 7. We usually performed the incubation of primary antibody overnight at 4°C with constant mild agitation. Some antibodies, such as α -actin, GAPDH, prohibitin which give very strong bands could be incubated for 1h at RT. We could re-utilize the primary antibody, by adding 2% of sodium azide to preserve from contamination and storing the diluted antibody at 4°C for up to 1-3 months.

Incubate with secondary antibody: After rinsing the membrane to remove unbound primary antibody with TBS-T for 3 times, we incubated it with the appropriate secondary antibody conjugated to horseradish peroxidase (HRP), which produces luminescence in proportion to the amount of protein. The secondary antibody was diluted in blocking solution and we incubated with gentle agitation for 1h at RT (Table 8).

Development: The secondary antibody was conjugated to peroxidase, therefore to detect its presence we used a commercial reagent, the EZ-ECL kit (Biological Industries) that associated the catalysis of hydrogen peroxide with the luminol oxidation, which leads to the emission of light (chemiluminescence). With antibodies that produce a faint signal with ECL, we developed with Super Signal® West Dura (Pierce) that has a stronger and prolonged

signal. Right after the ECL (enhanced chemiluminescence) reaction, we exposed membranes on photosensitive films Fuji super RX at several time intervals and we used the Kodak HC 110 developer and Kodak Tmax fixation solution for film development. The expected band was determined by comparing the stained bands of the bench marker loaded during electrophoresis, which shows the approximate size.

Removing of antibody complexes from the membrane (membrane stripping): If we want to incubate the membrane with a different primary antibody which is about the same size as the previous one, the first immunodetection can interfere with the result, therefore we must eliminate the antibody complexed by membrane stripping. We used two different stripping solutions: the first was 62.5mM Tris, pH 6.8, 2% SDS and 100mM β -mercaptoethanol for 10-30min at 60°C with constant mild shaking. Alternatively, we used a special commercial stripping solution-Restore™ Western Blot Stripping Buffer (Pierce) and we incubated the membrane at 37°C for 15-30min. The commercial stripping buffer, different from the previous one, is softer and requires re-block of the membrane 30-60min. After stripping, membrane was washed well with TBS-T and we initiate the second immunodetection process with milk blocking.

Table 7. Primary antibodies used in assays of Immunofluorescence or Western Blot

Antigen	Provider	Catalogue Number	Dilution	Incubation	Application
PTB (N-terminus)	Abcam	ab5642	1: 5000	O.N. 4 °C	WB
PTB (C-terminus)	ZYMED	324800	1:3500	O.N. 4 °C	WB
Caspase-3	Cell Signaling	9665	1: 5000	O.N. 4 °C	WB
Caspase-7	Enzo	ADI-AAM-127	1:1000	O.N. 4 °C	WB
MEF2A	Cell Signaling	9736	1: 2000	O.N. 4 °C	WB
MEF2C	Abcam	Ab64644	1: 5000	O.N. 4 °C	WB
MEF2D	Abcam	ab60717	1: 1000	O.N. 4 °C	WB
FLIP	Dave-2	ALX-804-127	1:1000	O.N. 4 °C	WB
HDAC1	Cell Signaling	2026	1: 2000	O.N. 4 °C	WB
HDAC2	Cell Signaling	2540	1: 2000	O.N. 4 °C	WB
HDAC5	Cell Signaling	2082	1: 2000	O.N. 4 °C	WB
EndoG	Sigma	E5654	1:3000	O.N. 4 °C	WB
FLAG	Sigma	F3165	1:4000	O.N. 4 °C	WB
eIF2S1	Abcam	Ab26197	1:2000	O.N. 4 °C	WB
eIF2S1 (phosphor-Ser51)	Abcam	Ab32157	1:2000	O.N. 4 °C	WB
eIF4EBP1	Abcam	Ab2606	1:2000	O.N. 4 °C	WB
Prohibitin	Neo Markers	292P501F	1: 5000	O.N. 4 °C	WB
α-actin	Sigma	A2172	1:100000	20min RT	WB
GAPDH	Abcam	Ab9483	1:10000	1h RT	WB
α-actinin	Sigma	A7811	1:500	1h RT	IF
MEF2A	Santa Cruze	H-300:sc-10794			IP

IF: immunofluorescence; WB: Western Blot; IP: Immunoprecipitation

Table 8. Secondary antibodies used in assays of Immunofluorescence or Western Blot

Antigen	Provider	Catalogue Number	Dilution	Incubation	Application
anti-mouse IgG HRP	SIGMA	A9046	1: 10000	1h RT	WB
anti-rabbit IgG HRP	SIGMA	A0545	1: 5000	1h RT	WB
anti-goat IgG HRP	SIGMA	A 9046	1: 20000	1h RT	WB
anti-rat IgG HRP	Jackson IR Lab	112-036-072	1: 10000	1h RT	WB
Mouse IgG AlexaFluor 594	Molec. Probes	A 11005	1: 500	1h RT	IF
Rabbit IgG AlexaFluor 594	Molec. Probes	A 11012	1: 500	1h RT	IF
Goat IgG AlexaFluor 594	Molec. Probes	A 11055	1: 500	1h RT	IF

IF: immunofluorescence; WB: Western Blot

4.2 *In vitro* ³⁵S-protein labeling and Immunoprecipitation

General reagents for preparing biochemical solutions: salts, detergents, sepharose beads were from SIGMA. The cocktail of protease inhibitors (EDTA free) was from Roche. We used NP-40 lysis buffer for cell lysis and Immunoprecipitation: Tris pH7.4 50mM, NaCl 150mM, EDTA 5mM, 1% Nonidet P-40, 0.1% sodium deoxycholate, and 1× cocktail of protease inhibitors.

Cardiomyocytes were cultured in standard medium with serum for 24 hours after seeding. After medium was discarded, cells were washed with PBS and cultured 24h in fresh medium without serum. Then standard medium was replaced by Methionine / Cysteine-free medium (GIBCO Cat. No. 21013-024) and 120μCi of ³⁵S labelled Cysteine and Methionine cocktail (EasyTag EXPRESS ³⁵S Protein Labeling Mix 74MBq (2mCi), Cat. No. NEG772002MC, Perkin Elmer). Duplicate plates were cultured in these conditions in the presence or absence

of 100 μ M Phenylephrine or 2 μ M proteasome inhibitor Lactacystin. Thirty six hours later, cells were rinsed with cold PBS and placed the dishes on ice. If we wanted to stop the procedure here, we removed completely the PBS and froze the cells at -80 °C. The whole Immunoprecipitation protocol was performed on ice. For cell lysis, we added lysis buffer (100 μ l/p60 cell culture dish), and recovered all the cells debris with a plastic scraper and collected them in a 1.5ml tube. Lysates were incubated on the orbital shaker for 20min to complete the lysis and then were centrifuged 15min at 13,000rpm to eliminate the insoluble cell debris and nuclei. We quantified the protein concentration of cell lysates according to the BioRad protein assay kit. We prepared the samples in order to maintain the same final volume and protein concentration.

We performed the Immunoprecipitation with a fixed amount of protein (100 μ g-500 μ g) adjusting to the same concentration for each sample and adding NP-40 lysis buffer to adjust the final protein concentration to 0.2-1 μ g/ μ l. Then certain amount of primary antibody was added to the tubes and incubated for 1-2h on the orbital shaker at 4°C. Afterwards, 40 μ l protein A-Sepharose beads suspension (50% of A-Sepharose) was added to the samples and incubated overnight. Then we washed three times with the washing buffer w/o protease inhibitors (50mM Tris pH7.4, 150mM NaCl, 5mM EDTA, 1% Nonidet P-40, 0.1% sodium deoxycholate and 0.1% SDS). To pellet the beads after each wash, we centrifuged at 6000rpm for 3min at 4°C. Finally, in the samples containing sepharose beads, we aspirated the residues of lysis buffer with an insulin syringe and then added 20 μ l loading buffer 2 \times . The samples were boiled for 3min, and we spined at 13,000g for 1min to collect the whole volume. Then SDS-PAGE was performed and after electrophoresis the gel was dried up and was exposed for different time intervals (2h and 16h) in a cassette at -80°C. 10 μ g total cell lysate of each sample was used as loading control.

5 Statistics

Results are presented as mean \pm SEM. Comparisons between values (e.g. control vs. agonist-treated) are made using a Student's t-test.

Results

Part 1. Endonuclease G is involved in cardiomyocyte growth and mitochondrial metabolism

Cardiac muscle cells depend on mitochondria to obtain energy. Endonuclease G (EndoG) is a nuclear DNA-coded mitochondrion-specific nuclease (Côté J. et al., 1993; Apostolov E.O. et al., 2007) that translocates to the nucleus during apoptosis and causes chromatin DNA degradation independently of caspases (Li L. et al., 2001). We were interested in EndoG because our previous studies showed that most caspase-dependent apoptotic proteins were repressed during heart differentiation while EndoG, on the contrary, was abundant in the adult heart in cardiomyocytes (Bahi N. et al., 2006; Zhang J. et al., 2009), suggesting that it has an important role in the biology of the heart.

1.1 Endonuclease G is abundant in the heart and increases progressively during heart development

It has been proved that Endonuclease G (EndoG), which is localized in the mitochondrial intermembrane space, influences mitochondrial DNA replication probably by recombination and repair (Côté J. and Ruiz-Carrillo A., 1993). The group of Prof. Stuart Cook identified that EndoG was a gene located on a region of rat chromosome 3p influencing blood pressure-independent left ventricular mass, indicating its possible important role in the heart. To characterize and identify the function of EndoG, first we performed immunoblotting across rat and mouse tissues and determined that EndoG was most highly expressed in the heart, localised to cardiomyocytes (Fig. 33A and B) and its expression increased during heart development (Fig. 33C).

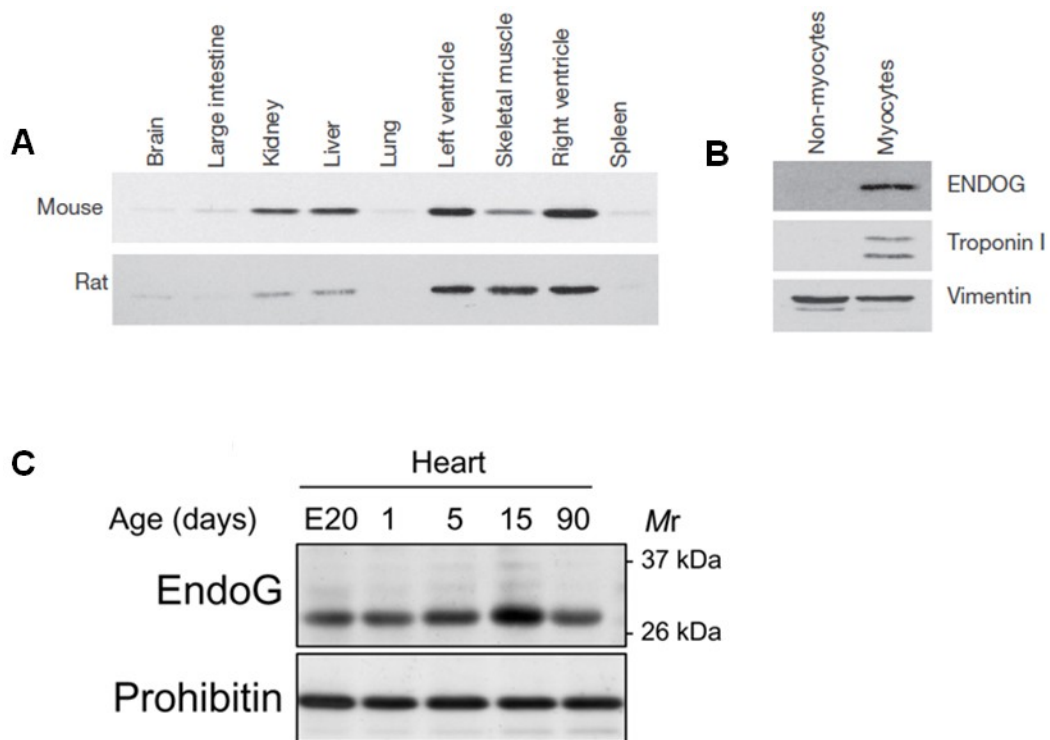


Fig. 33 EndoG expression in different tissues. **(A)** Immunoblot of EndoG expression in mouse and rat tissues (EndoG: ~30 kDa). **(B)** Immunoblot of EndoG expression in myocyte and non-myocyte populations isolated from neonatal rat heart (TroponinI, ~28kDa; Vimentin, ~57kDa). **(C)** Immunoblot of EndoG in rat heart ranging from the age of Embryonic day 20 (E20) to day 90 after birth. Results are from two independent samples.

1.2 EndoG contributes to the regulation of cardiac hypertrophy

EndoG is best known as a gene involved in DNA degradation during cell death; our previous data also suggested that during experimental ischemia EndoG was released together with cytochrome C and AIF from mitochondria to cytosol, inducing DNA degradation via caspase-independent mechanisms (Bahi N. et al., 2006). Moreover, we demonstrated that EndoG was the link between Bnip3-mediated mitochondrial dysfunction and DNA degradation during ischemia in cardiomyocytes (Zhang J. et al., 2011). However, until now there is no known effect of EndoG on other cardiac functions. The group of S. Cook observed reduced expression of EndoG transcript and lack of EndoG protein in rat with elevated cardiac mass and marked reduction in cardiac nuclease activity that was EndoG-dependent. We assessed the role of EndoG in cardiac cell growth *in vitro*. By using short hairpin RNA (shRNA) knockdown of EndoG (shEndog) (Fig. 34A) we checked the effect of EndoG loss-of-function in cardiomyocytes and observed increased cell size of shEndog cardiomyocytes compared to control in the absence of pro-hypertrophic stimuli (Fig. 34B); consistent with this result, we also found an increase in hypertrophic biomarkers atrial natriuretic factor (Anf) by real-time PCR (Fig. 34C). These results demonstrated that EndoG loss-of-function in cardiomyocytes would cause disproportionate cell growth, and suggested its important and direct role during cardiac hypertrophy.

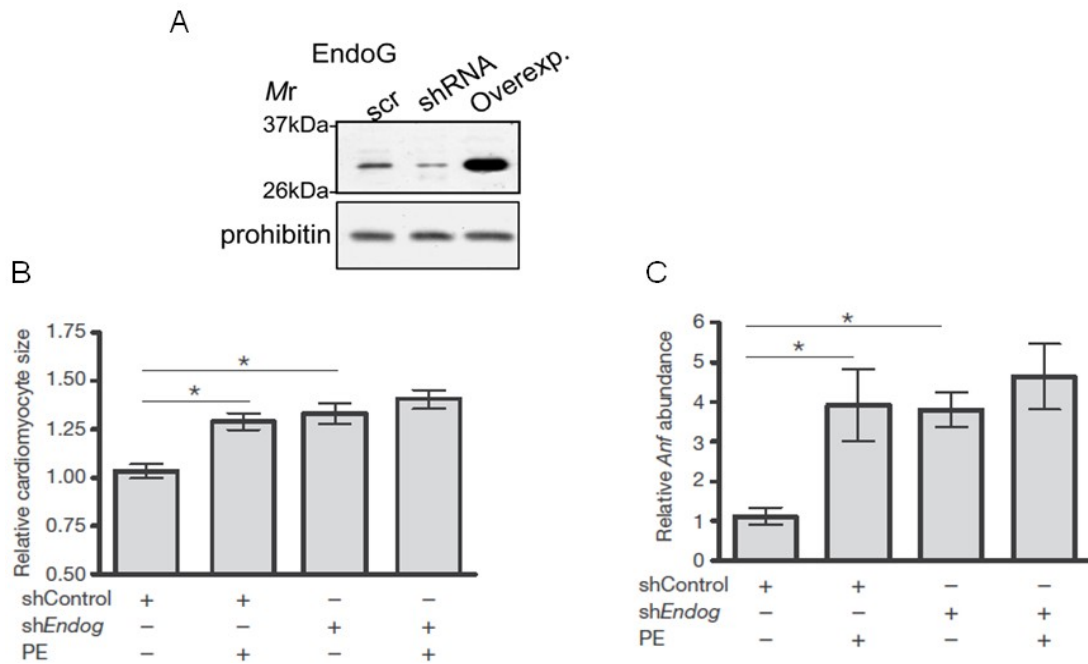


Fig. 34 EndoG regulates cardiac hypertrophy. **(A)** Immunoblot of EndoG expression in neonatal cardiomyocytes transfected with scrambles siRNA (scr), EndoG shRNA (shRNA) and EndoG overexpression (Overexp.) **(B)** Cardiomyocyte size ($n \geq 100$ cells) treated with shRNA against EndoG (shEndog) or control shRNA (shControl) in the presence or absence of the hypertrophic stimulant phenylephrine (PE, 100 μ M, 24h). **(C)** Real-time PCR of Anf in cardiomyocytes with the same treatment as B. Three independent experiments were performed with similar results. * $p < 0.05$.

1.3 EndoG is involved in the control of mitochondrial metabolism

Numerous studies have implicated reactive oxygen species (ROS) production in the hypertrophic process, and a recent study also proved that during angiotensin II (AngII) induced cardiac hypertrophy, the amplification of mtROS will cause a decline of mitochondrial membrane potential and increases cardiac mitochondrial protein oxidative damage and mtDNA deletions (Dai D.F. et al., 2011). S. Cook's group found that compared to controls, Endog^{-/-} mice had larger cardiomyocytes at baseline in the absence of stimulation. Following AngII stimulation of hypertrophy, which is largely ROS-dependent since it binds to angiotensin receptor-1 and stimulates NADPH oxidase to produce ROS (Mukhopadhyay P. et al., 2007), they observed an increase in cardiomyocyte size, hypertrophic biomarkers and LVM in Endog^{-/-} mice. We checked *in vitro* the production of reactive oxygen species (ROS) in shEndog cardiomyocytes using Dihydroethidium (DHE) by flow cytometry and the result

suggested increased ROS in shEndog cardiomyocytes compared to control (Fig. 35), which was in agreement with the results *in vivo* and indicated a direct effect of EndoG in the control of ROS production, since ROS products *in vivo* could be secondary to hypertrophy.

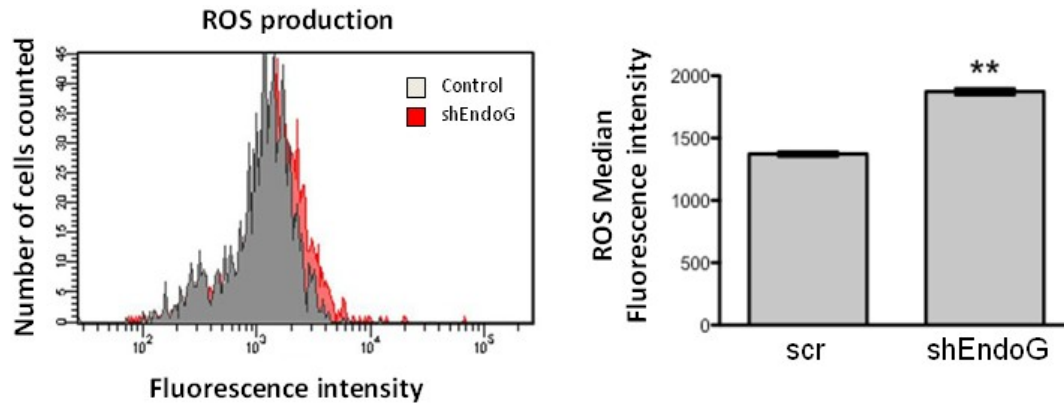


Fig. 35 EndoG regulates mitochondrial metabolism. Flow cytometry detection of ROS in cardiomyocytes of scrambled (scr) or shEndog (left panel) by DHE and fluorescence-based median fluorescence intensity (MFI) of ROS production in cardiomyocytes treated with shControl or shEndog (right panel). Error bars are s.e.m. from three independent experiments. ** $p < 0.01$.

It is known that energy production in cardiac muscle cells depends on mitochondrial respiration. There was increased ROS production in EndoG-deleted ($Endog^{-/-}$) mouse heart (proved by the group of Prof. Stuart Cook). Thus it would be interesting to check if there were also changes in the number and/or morphology of mitochondria in $Endog^{-/-}$ heart. By checking with electronic microscopy we found that lack of EndoG induced no gross morphological changes of mitochondria but we observed that vacuole-like items associated with mitochondria from $Endog^{-/-}$ mice were more numerous and larger than those seen in control mice (Fig. 36A and C). We suspected that these vacuole-like items could be lipid accumulation, therefore we stained heart tissue of $Endog^{-/-}$ mice with Oil Red O. We observed that $Endog^{-/-}$ mouse heart had obvious increase in the content of lipids (Fig. 36B); quantification of the lipids revealed marked elevation of triglyceride and phospholipid levels in these tissues which was manifested as cardiomyocyte steatosis (Fig. 36D). Combining all the results we are able to draw the conclusion that EndoG activity contributes to ROS production and its deficiency induces lipid accumulation.

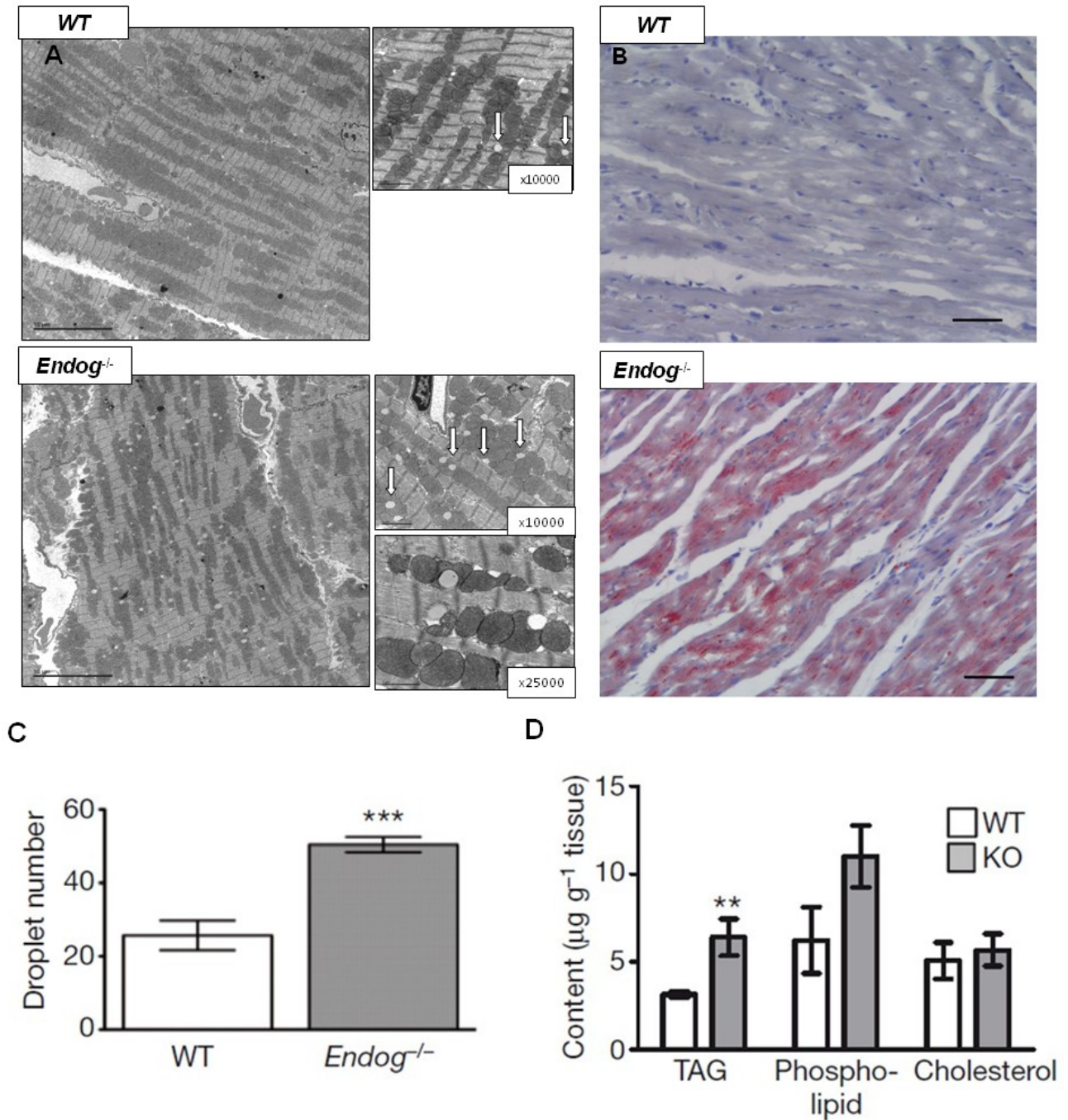


Fig. 36 EndoG influences cardiac lipid metabolism. **(A)** Transmission electron micrographs of left ventricular sections from WT (upper panel) and *Endog*^{-/-} mice (lower panel). **(B)** Oil red O staining of left ventricular sections from WT (upper panel) and *Endog*^{-/-} mice (lower panel). **(C)** Quantification of the number of mitochondrial-associated droplets in WT and *Endog*^{-/-} mice. **(D)** Quantification of cardiac triglyceride (TAG), phospholipid and cholesterol content in WT and *Endog*^{-/-} mice (n=5). Error bars are s.e.m. from three independent hearts per genotype. ** p<0.01; *** p<0.001.

Part 2. Translation of MEF2 is induced by hypertrophic stimuli in cardiomyocytes through a Calcineurin-dependent pathway

To continue our study on cardiac hypertrophy, we focused on myocyte enhancer factor 2 (MEF2), a family of transcriptional factors which has been proved to play key roles in embryonic morphogenesis and myocyte differentiation and stress-dependent gene expression (Naya F.J. et al., 2002; Xu J. et al., 2006). Our preliminary results showed that the mRNA and protein abundance of MEF2 were not regulated in parallel in hypertrophic cardiomyocytes and we were interested in identifying this fact that had not been described previously.

2.1 Abundance of MEF2A and MEF2D in the heart does not correlate with their transcript levels

Myocyte enhancer factor 2 (MEF2) family of transcription factors has been shown to play a pivotal role in morphogenesis and myogenesis of skeletal, cardiac, and smooth muscle cells (Black B.L. and Olson E.N., 1998). To characterize the expression of MEF2A and D in the heart, first the expression of both MEF2A and MEF2D were analyzed in the developing heart of rats ranging from embryo of 18 days (E18) to postnatal 60 days (P60) (Fig. 37A). Our results suggested that during heart development the expression of MEF2A increased (Fig. 37A), while in contrary, MEF2D decreased (Fig. 37A), and their protein abundance did not correlate with the transcriptional levels (Fig. 37B). These results suggested their different roles during heart development (Edmonson D.G. et al., 1994; Molkentin J.D. et al. 1996; Lin Q. et al., 1997) and also indicated that in the heart the expression of MEF2A and D protein and their RNA levels were not regulated in a similar way.

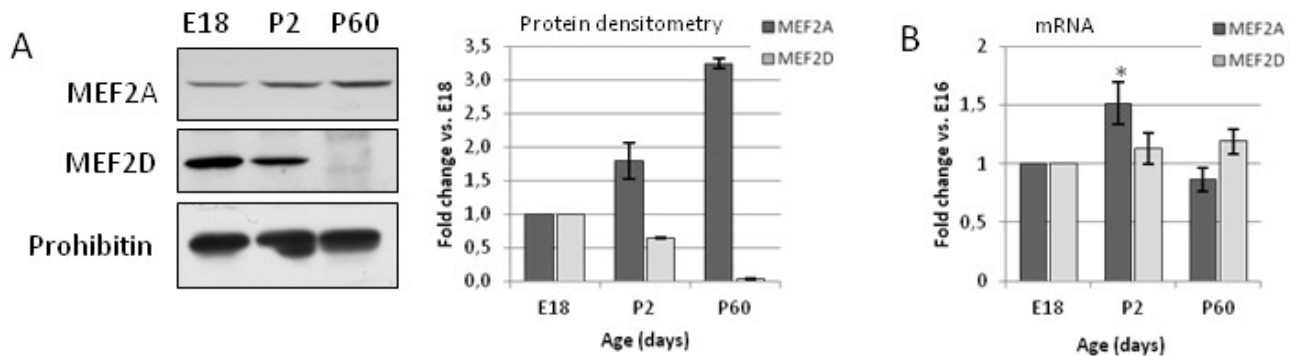


Fig.37 Expression of MEF2A and MEF2D in rat hearts at different ages. **(A)** Left panel: MEF2A and MEF2D protein expression was analyzed by Western Blot in heart samples of rats at embryonic day 18 (E18), postnatal day 2 (P2) and 2-month old adults (P60). Expression was analyzed in three independent set of samples. A representative image is shown. Right panel: Densitometry was performed using the Image J software and the bar graph shows means \pm SEM, n=3. **(B)** Mef2a and Mef2d transcript abundance in hearts of rats at the same ages as in A was analyzed by TaqMan quantitative PCR of reverse transcribed products from total RNA as described in the Methods section, n=3. * $p < 0.05$ vs E18.

2.2 Pro-hypertrophic agonists induce an increase in myocyte size that depends on increased MEF2 protein abundance without changes in its transcript.

MEF2A protein abundance was not reduced in neonatal ventricular cardiomyocyte cultures transduced with lentivirus carrying a small hairpin RNA (shRNA)-based RNA interference (RNAi) vector, in the presence of the standard serum concentrations (5% FCS and 10% HS) in the culture medium (Fig. 38A, inset). However, a reduction of 80% of Mef2a transcript abundance in RNAi-treated cells was detected by Real Time RT-PCR using validated genespecific assays. Because serum is pro-hypertrophic (Simpson P. et al., 1982) and could stimulate MEF2 expression, we deprived cells from serum after viral transduction. In these conditions, MEF2A protein abundance was reduced to almost undetectable amounts by shRNA-driven RNAi (Fig. 38A) coinciding with efficient gene silencing to 20% of the basal mRNA levels (Fig. 38B). Upon addition of Phenylephrine (PE), MEF2A protein abundance increased threefold in shRNA-treated cardiomyocytes (Fig. 38A) despite no changes in the RNAi-induced low mRNA level (Fig. 38B). The changes in MEF2A protein abundance by RNAi and PE treatment affected cell size, showing that MEF2A abundance determines cell size in neonatal myocytes (Fig. 38C), in addition to the well-known effects on cell growth due to MEF2A posttranslational modification (Potthoff M.J. et al., 2007). These results suggested strong posttranscriptional regulation of MEF2A expression in the presence of hypertrophic agonists, influencing cell size, which was different to the one controlled by miR-1 (Ikeda S. et al., 2009) in that the later has been shown to reduce Mef2 transcript levels.

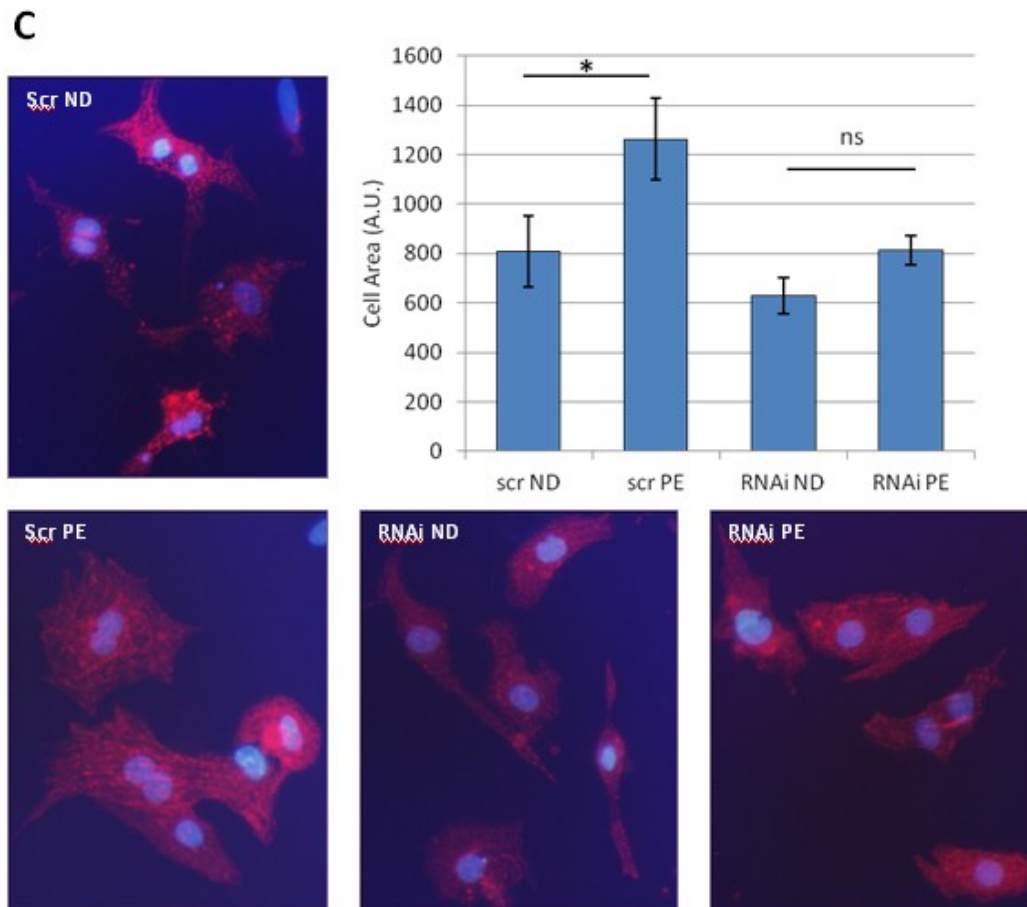
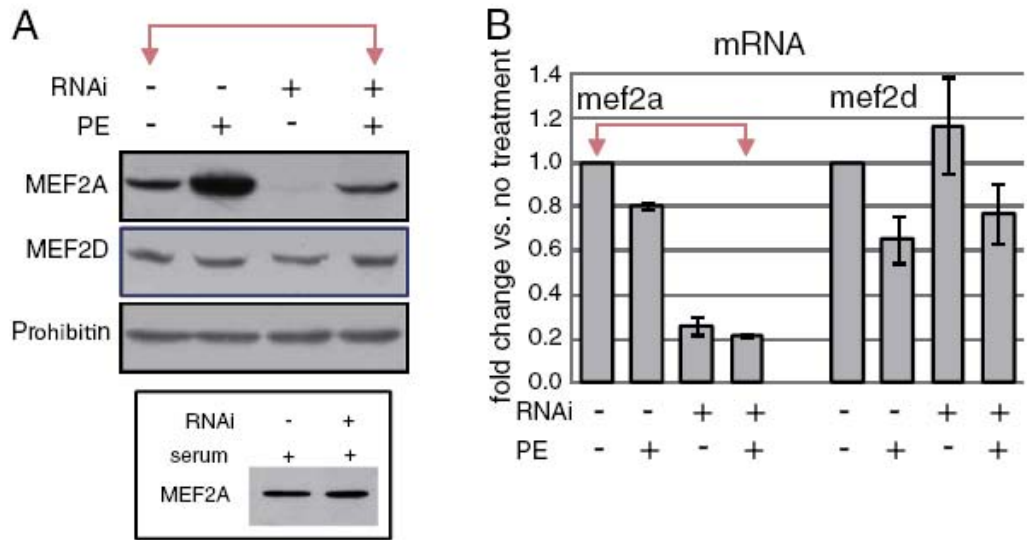


Fig.38 MEF2A protein abundance and function are unrelated to its transcript level during agonist stimulation in neonatal rat ventricular cardiomyocytes. **(A)** MEF2 protein expression was analyzed in serum-deprived cardiomyocytes transduced with a Mef2a-specific shRNA or a scrambled vector, in presence or absence of 100 μ M phenylephrine (PE) during 24 hours. Inset: Same treatments as in (A) but in the presence of serum (5% FCS, 10% HS) in the culture medium. Representative Western Blots are shown from n=5. **(B)** Mef2a and Mef2d mRNA abundance in the same cultures, measured by TaqMan quantitative PCR from total RNA extracts of cultures treated as in (A), n=5. Arrows highlight comparison between serum deprived myocytes and myocytes treated with PE and RNAi to point at the similar abundance of protein despite very different amounts of mRNA. **(C)** Cardiomyocyte areas were measured in cultures of neonatal cardiomyocytes treated as in A. Values (arbitrary units, A.U.) were calculated using Image J software, from 100 cells analyzed in two replicate wells from 4 independent experiments. The bar graph represents means of 4 independent experiments \pm SEM. * $p < 0.05$. ns: not significant. Representative fluorescence microscopy images of cardiomyocyte cultures are shown after staining for α -actinin (red) and nuclei (blue). Scr ND, scrambled no drug; Scr PE, scrambled phenylephrine (24h, 100 μ M); RNAi ND, MEF2a-specific RNA interference-driven silencing with no drug; RNAi PE, MEF2a-specific RNA interference-driven silencing plus phenylephrine (24h, 100 μ M).

Given the relevance of MEF2A and MEF2D in the postnatal heart response to stress (Naya F.J. et al., 2002; Kim Y. et al., 2008), we decided to investigate the mechanisms underlying the observed control of MEF2 abundance during agonist stimulation. Treatment of cardiomyocytes with different pro-hypertrophic drugs, in the absence of serum, induced a rapid increase of MEF2A protein abundance, detectable at 15h (data not shown) and steadily progressing at 24h and 48h, and a slower increase of MEF2D expression, detectable at 24h or 48h, depending on the stimulus (Fig. 39A). Mef2a and Mef2d transcript levels did not show any significant changes during these treatments, as analyzed by conventional RT-PCR (data not shown) and Real Time Quantitative PCR (Fig. 39B), while the hypertrophy markers atrial natriuretic precursor peptide (nppa) and skeletal α -actin (acta1) isoform were strongly induced as expected (Bishopric N.H. et al., 1987; Day M.L. et al., 1987). In addition to the well established pathways of posttranslational regulation (Potthoff M.J. et al., 2007), and the miR1-dependent pathway, which affects the transcript levels (Ikeda S. et al., 2009), our results suggested a previously undetected level in MEF2 regulation during cardiomyocyte growth.

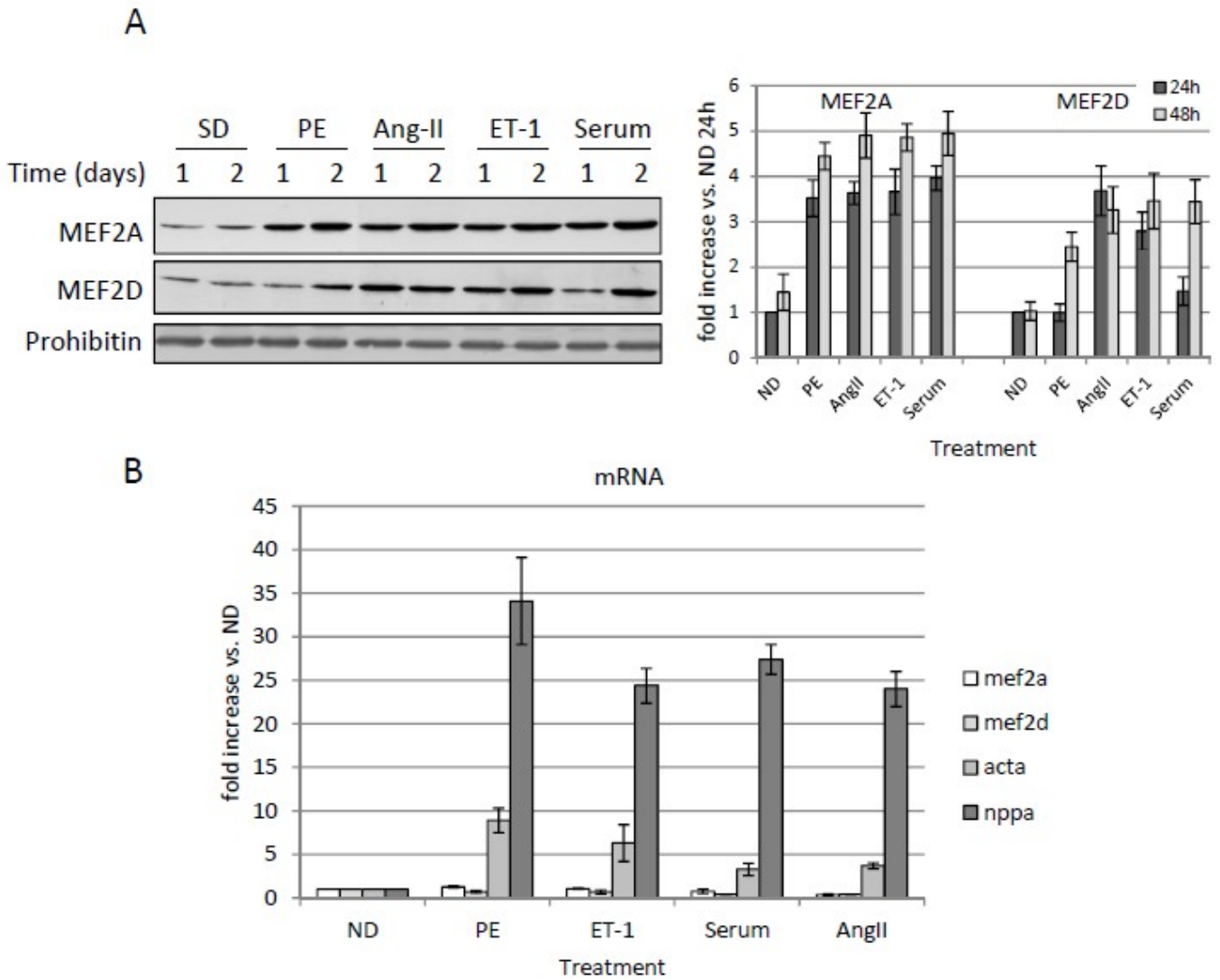


Fig.39 Pro-hypertrophic stimuli enhance MEF2 protein expression posttranscriptionally in primary cardiomyocytes. **(A)** MEF2 protein expression in serum-deprived cardiomyocytes treated during 1 or 2 days with different agonists: ND, no drug; PE, 100 μ M phenylephrine; Ang-II, 100mM Angiotensin II; ET1, 0.1 μ M Endothelin-1, or serum, 10% HS plus 5% FCS. Representative images are shown from 5 independent experiments. Densitometry of Western blot bands was performed with the Image J software. Bars are means of 5 independent experiments \pm SEM. **(B)** Mef2 mRNA abundance in cultures treated as in (A) was quantified by TaqMan quantitative PCR from total RNA extracts, n=5. Nppa (atrial natriuretic peptide precursor) and acta1 (alpha-actin) transcript abundance was also monitored to confirm induction of hypertrophic signaling. Bars are means of 5 independent experiments \pm SEM. No treatment induced statistically significant changes in Mef2 transcript abundance.

2.3 Agonist-induced increase of MEF2 protein abundance is due to its increased translation.

The role of transcription in the control of MEF2 expression in pro-hypertrophic culture medium was analyzed. Inhibition of transcription with Actinomycin D (ActD) induced a decrease of MEF2A and MEF2D protein abundance in cardiomyocytes treated with PE (Fig. 40A), correlating with an important decrease in the corresponding mRNA levels due to ActD (Fig. 40C). Addition of the translational inhibitor Cycloheximide (CHX) also rapidly hampered the increase of MEF2 levels observed during PE treatment (Fig. 40B) that did not correlate with changes in the respective mRNA levels (Fig. 40C), demonstrating the requirement of continuous translation and showing that MEF2 degradation was not arrested by PE treatment, otherwise CHX-treated cells would have kept high levels of MEF2. These results demonstrated a short life of MEF2 proteins compared, for example, with the mitochondrial protein prohibitin, used as loading control because of its steady expression both during cardiomyocyte differentiation and their response to stress (Zhang J. et al., 2007; Zhang J. et al., 2011). To directly assess induction of MEF2 by hypertrophic agonists, cardiomyocytes were deprived from serum to reach basal levels of MEF2 expression and then, the incorporation of ³⁵S-labeled aminoacids to MEF2 was analyzed in cultures treated with PE or the proteasome inhibitor Lactacystin. A twofold increase in ³⁵S-Cysteine and ³⁵S-Methionine incorporation to MEF2 was observed in serum and PE-treated myocytes compared to controls, but not in proteasome-treated cells, demonstrating that agonists were inducing *de novo* MEF2 translation (Fig. 40D). Inhibition of the proteasome only induced a small increase in newly synthesized protein.

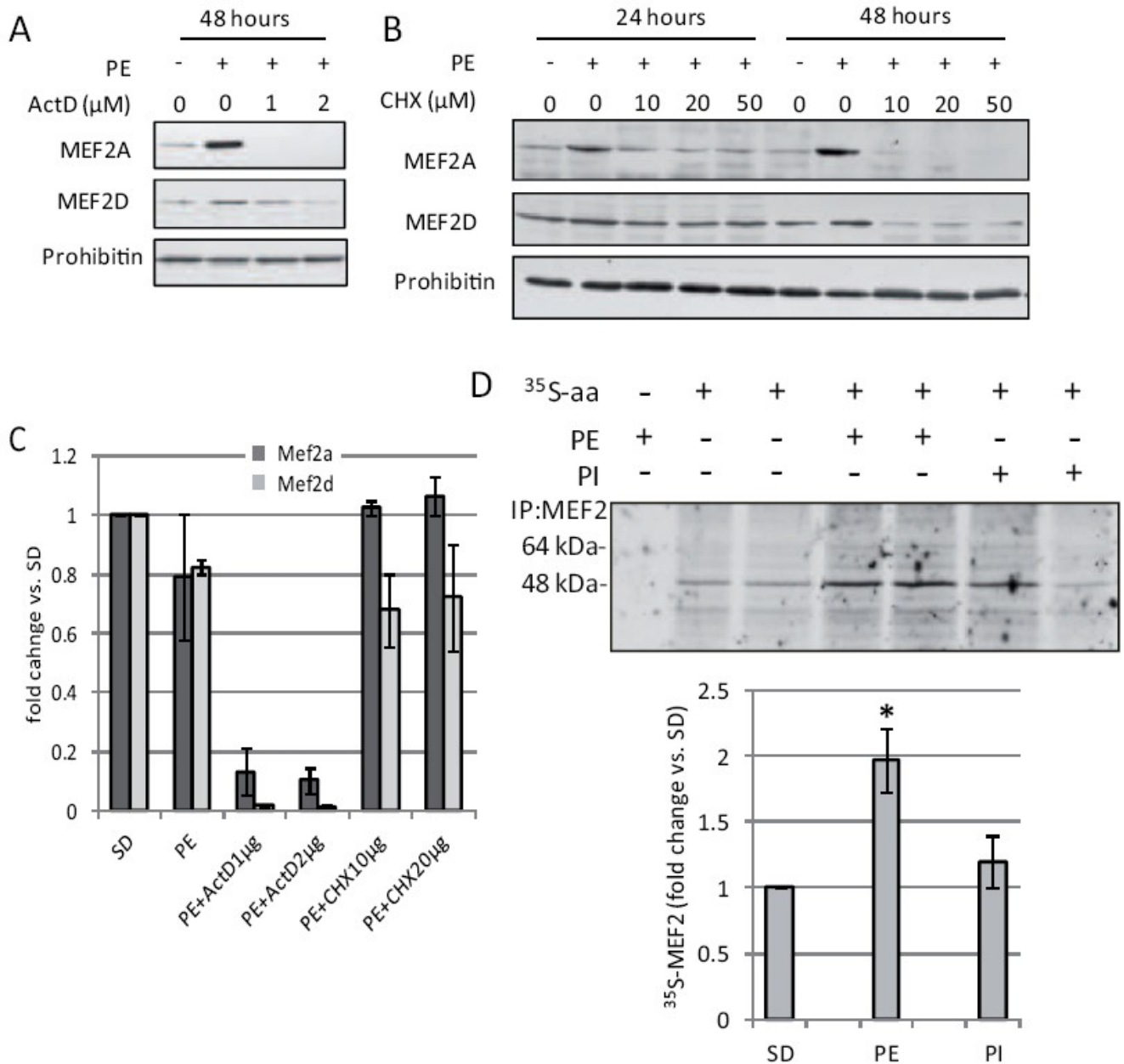
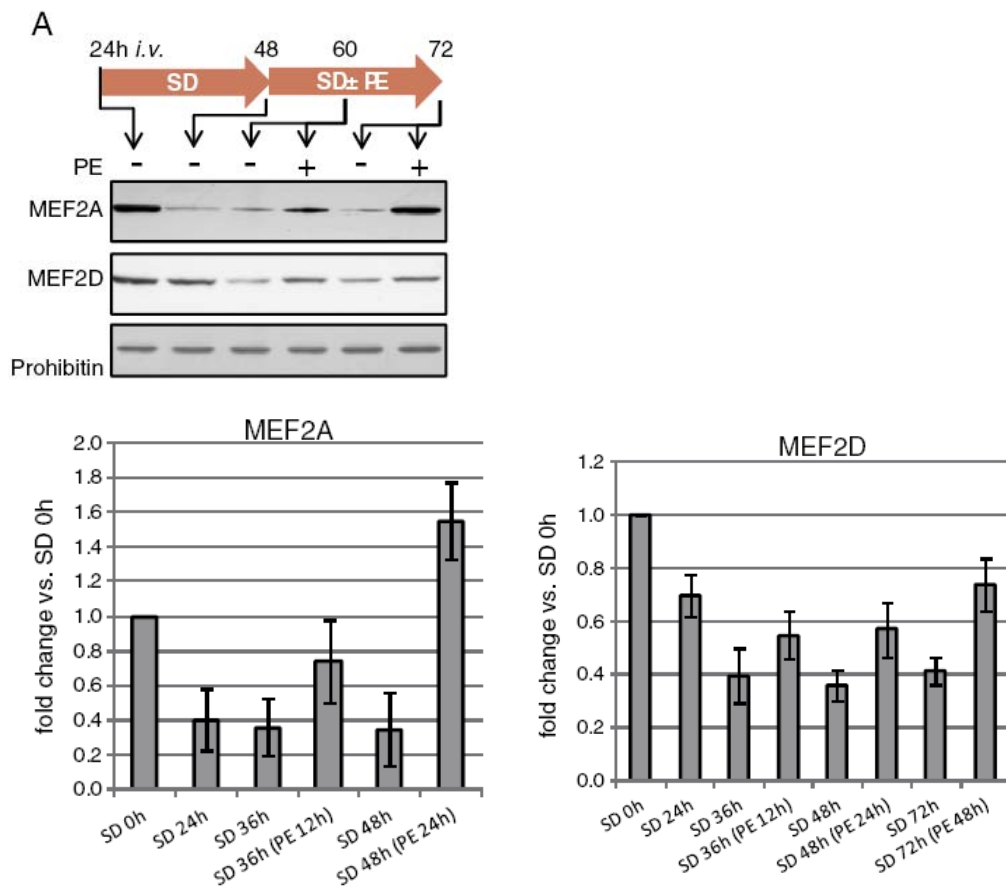


Fig. 40 MEF2A and MEF2D proteins have a short life requiring continuous translation sustained by agonist stimulation in cardiomyocytes. **(A)** MEF2 protein expression in cardiomyocytes treated with phenylephrine (PE) in the presence or absence of the transcription inhibitor Actinomycin D (ActD) or **(B)** in the presence or absence of the translational inhibitor cycloheximide (CHX). Representative Western blots are shown from 4 independent sets of samples. **(C)** Mef2 mRNA levels were measured by TaqMan quantitative PCR of retro-transcribed total RNA extracts from replicate cultures of cardiomyocytes used in **(A)** and **(B)**. Bars are means \pm SEM, $n=5$. **(D)** *De novo* MEF2 translation was assessed by analyzing 35 S-Cysteine and 35 S-Methionine incorporation into MEF2 during 24h in serum deprived cardiomyocytes treated with 100 μ M Phenylephrine (PE) or 2 μ M of the proteasome inhibitor Lactacystin (PI). Bars are means \pm SEM, $n=3$, * $p < 0.05$ vs. untreated, serum-deprived cells (SD).

Results

Comparison of MEF2 protein abundance in freshly isolated myocytes and serum deprived myocyte cultures treated or not with PE, showed a progressive loss of MEF2 in the absence of serum, in agreement with its short life suggested by the previous experiments, and an increase in MEF2 abundance upon PE addition starting from levels below the initial abundance (24h i.v.) (Fig. 41A), unrelated to changes in Mef2 transcript abundance (Fig. 41B). Then, the potential contribution of changes in protein degradation to increased MEF2 abundance was assessed by comparing MEF2 expression in cardiomyocytes treated with PE or with two different proteasome inhibitors (M132 and Lactacystin) after serum deprivation. Only PE induced a significant increase in MEF2 abundance (Fig. 41C). These results discarded an eventual reduction of MEF2 degradation contributing to the high abundance of MEF2 in agonist treated cells. Taken together, these data demonstrated a) that Mef2 transcripts and proteins are short lived, depending on continuous transcription and undergoing rapid proteasome-dependent degradation, respectively; b) that lack of serum neither decreased transcription nor protein degradation but reduced translation; and c) that PE addition in these conditions induced MEF2 expression through enhancing translation.



Results

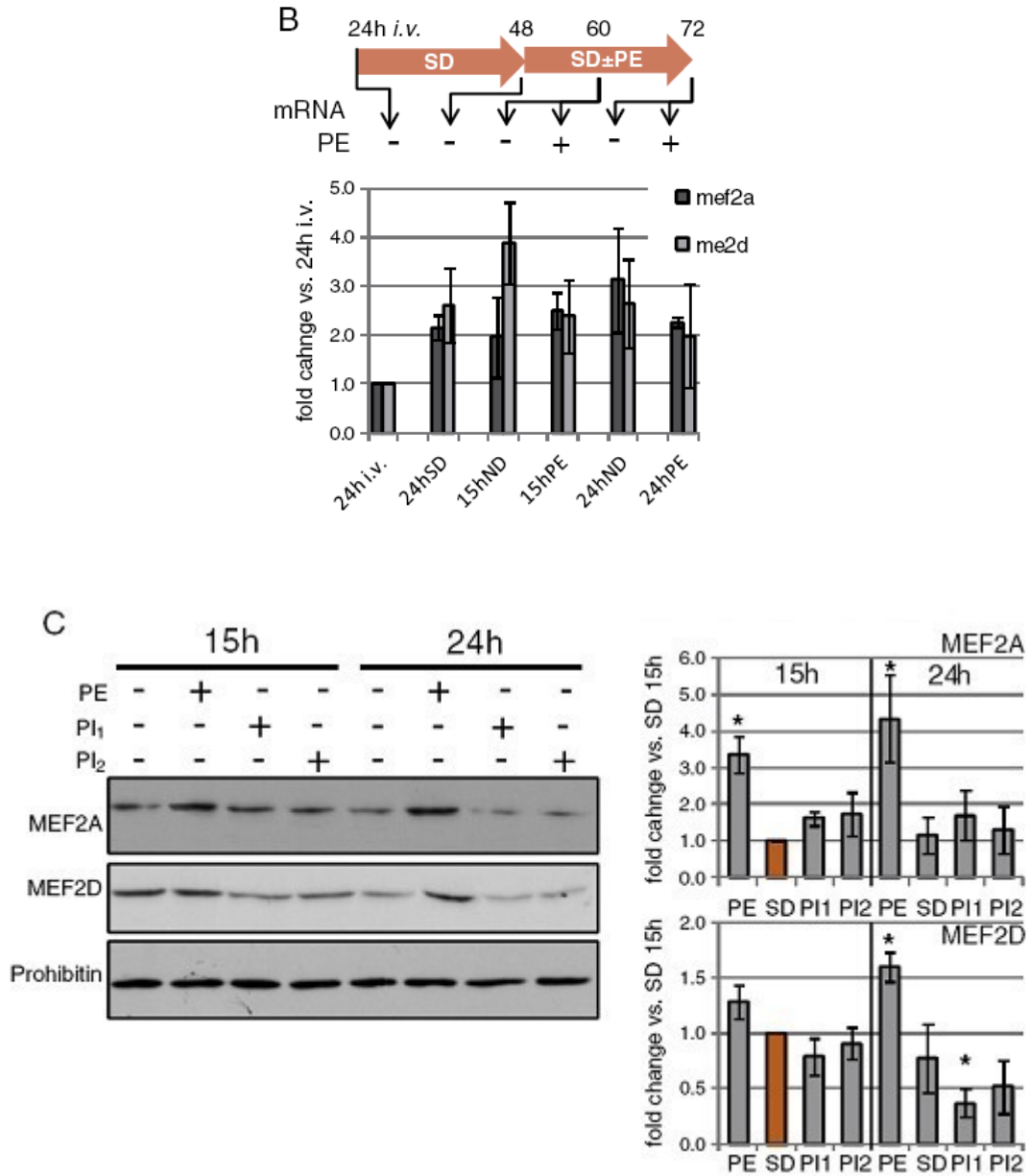


Fig. 41 Regulation of protein degradation does not contribute to sustain high levels of MEF2 during agonist stimulation in cardiomyocytes. **(A)** Time course of MEF2 protein expression during serum deprivation (SD) started 24 h after seeding (24h i.v. = 24 hours *in vitro*), and $\pm 100\mu\text{M}$ phenylephrine (PE) addition in cultured cardiomyocytes. Numbers above arrows are hours *in vitro* (after seeding). Bar graph shows the Western blot densitometric analysis of 4 independent experiments presented as means \pm SEM (hours in parenthesis is time in the presence of PE). **(B)** Mef2 transcript abundance was measured by TaqMan quantitative PCR of retro-transcribed total RNA extracts from replicate cultures as in A, bars are means \pm SEM, n=4. **(C)** Comparison of the time-related changes in MEF2 abundance in serum deprived cardiomyocytes (SD) and cardiomyocytes treated with Phenylephrine (100 μM , PE), or the proteasome inhibitors MG-132 (5 μM , PI1) or Lactacystin (2 μM , PI2). Bars are means \pm SEM, n=3. * p<0.05 vs. SD at 15h.

2.4 Calcineurin mediates the posttranscriptional enhancement of MEF2 expression in vivo and in vitro.

Calcium/Calmodulin-dependent phosphatase Calcineurin has been shown to be involved in MEF2 dephosphorylation (Wu H. et al., 2000; Wu H. et al., 2001) potentiating MEF2 activity and is activated during agonist stimulation (Taigen T. et al., 2000). We assessed MEF2 expression in the ventricles of adult mice overexpressing Calcineurin in the myocardium, which present hypertrophy (Molkentin J.D. et al., 1998) and observed that despite unchanged Mef2 transcript levels, MEF2A and MEF2D proteins were more abundant than in the heart of their wild type littermates (Fig. 42A and B). To discard that increased MEF2 abundance was indirectly induced by hemodynamic changes due to the hypertrophied heart in Calcineurin-transgenic mice, we treated cultured neonatal rat ventricular cardiomyocytes with the Calcineurin inhibitor CN585, which has been described recently to be specific for Calcineurin ($K_i=3.8 \mu\text{M}$) without affecting other Ser/Thr protein phosphatases or peptidyl prolyl cis/trans isomerases (Erdmann F. et al., 2010). A low dose of CN585 ($2\mu\text{M}$, far below its K_i) efficiently blunted the PE-dependent increase of MEF2 abundance (Fig. 42C), without affecting Mef2 transcript levels (Fig. 42D). This demonstrated a direct effect of Calcineurin signaling on Mef2 translation in myocytes in the absence of any hemodynamic input. These results show that Calcineurin is involved in agonist-induced translation of MEF2, adding a novel level of MEF2 activity regulation by this phosphatase.

The above results showed that hypertrophic agonist stimulation induced increased MEF2 translation, that this increase was dependent on Calcineurin activity in cultured myocytes and that Calcineurin overexpression *in vivo* also triggered higher MEF2 abundance. To gain insight about the mechanisms connecting Calcineurin and MEF2 translation, we checked phosphorylation of key regulators of Cap-dependent translation in cardiomyocytes stimulated with PE in the presence or absence of Calcineurin inhibitors and the Calcineurin

transgenic hearts. Initiation of Cap-dependent translation involves eukaryotic Initiation Factor-2 (eIF2), which mediates binding of tRNA^{met} to the 40S ribosome subunit (Siekierka J. et al., 1982) and phosphorylation of eIF4E-binding protein (4E-BP1) inducing its detachment mRNAs to the ribosome. The phosphorylation status of eIF2 and 4E-BP1 was different in PE-treated myocytes and Calcineurin transgenic hearts (Fig. 42A, C), both showing high levels of MEF2A (Fig. 42A, C). This suggested that Calcineurin-dependent control of phosphorylation of the cap-dependent translation complex was not determining MEF2 translation.

Results

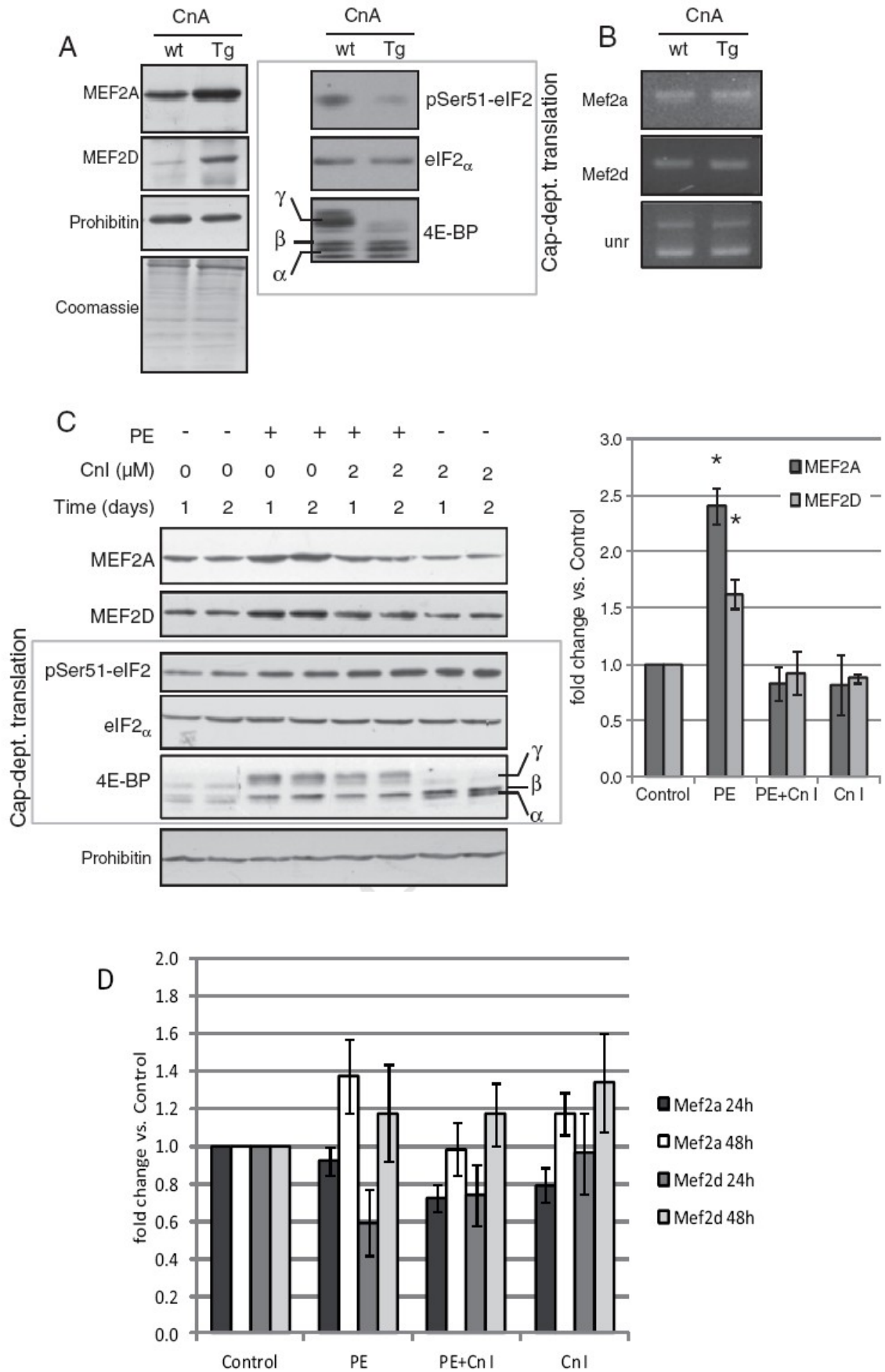


Fig. 42 Calcineurin mediates translation of MEF2 *in vivo* and *in vitro* during hypertrophy. **(A)** MEF2, eIF2 α , phosphoSer51-eIF2 and 4E-BP1 expression in total protein extracts of hearts of hypertrophied 5-months old Calcineurin A (CnA)-transgenic mice and wild type controls was analyzed by Western blot. A representative image is shown from the analysis of 4 independent hearts per genotype (wt: wild type; Tg: CnA-transgenic). **(B)** Representative image of an agarose gel showing RT-PCR reactions of Mef2 mRNA transcript expression in the same hearts. Amplification of a fragment of unr (upstream of n-ras) mRNA including two exons, which in addition detects two co-expressed unr isoforms is used as a well established loading control (Bahi N. et al., 2006; Zhang J. et al., 2007). **(C)** Effect of the addition of the Calcineurin Inhibitor VIII also known as CN585 (Cn I; Calbiochem, 207003, 2 μ M) in MEF2, eIF2 α , phosphoSer51-eIF2 and 4E-BP protein expression during phenylephrine (PE) treatment in cultured cardiomyocytes. Bar graph shows the Western blot densitometric analysis of 5 independent experiments presented as means \pm SEM. * $p < 0.05$ vs. control values. **(D)** Mef2 transcript abundance was measured by TaqMan quantitative PCR of retro-transcribed total RNA extracts from replicate cultures as in C and bars are means \pm SEM., α , β and γ indicate increasingly phosphorylation forms of 4E-BP1.

2.5 Calcineurin-mediated enhancement of MEF2A expression involves Polypyrimidine Tract Binding Protein.

Polypyrimidine Tract Binding Protein (PTB) is an RNA-interacting protein that contributes to cap-independent protein translation (Mitchell S.A. et al., 2001), in addition to be involved in RNA maturation. Our previous work identified PTB as a key regulator of apoptotic gene translation in differentiating cardiomyocytes (Zhang J. et al., 2009). We also showed that PTB expression decreases during heart development (Zhang J. et al., 2009). Calcineurin overexpression induced an important increase in PTB abundance in the adult heart (Fig. 43A), and agonist stimulation of cardiomyocytes *in vitro* also induced higher PTB expression (Fig. 43B). Interestingly, Calcineurin inhibition prevented PE triggered expression of PTB. Thus, PTB abundance correlated with MEF2 expression in PE-treated myocytes and in the Calcineurin-overexpression heart, suggesting a functional link. Lentiviral-driven PTB overexpression induced an increase of MEF2A protein abundance only in the presence of PE (Fig. 43C) without affecting its transcript (Fig. 43D), and lentiviral-driven silencing of Ptb expression hampered PE-induced MEF2A translation (Fig. 43E). Altogether, these results showed that Calcineurin-dependent regulation of MEF2 translation in the heart involved PTB.

Results

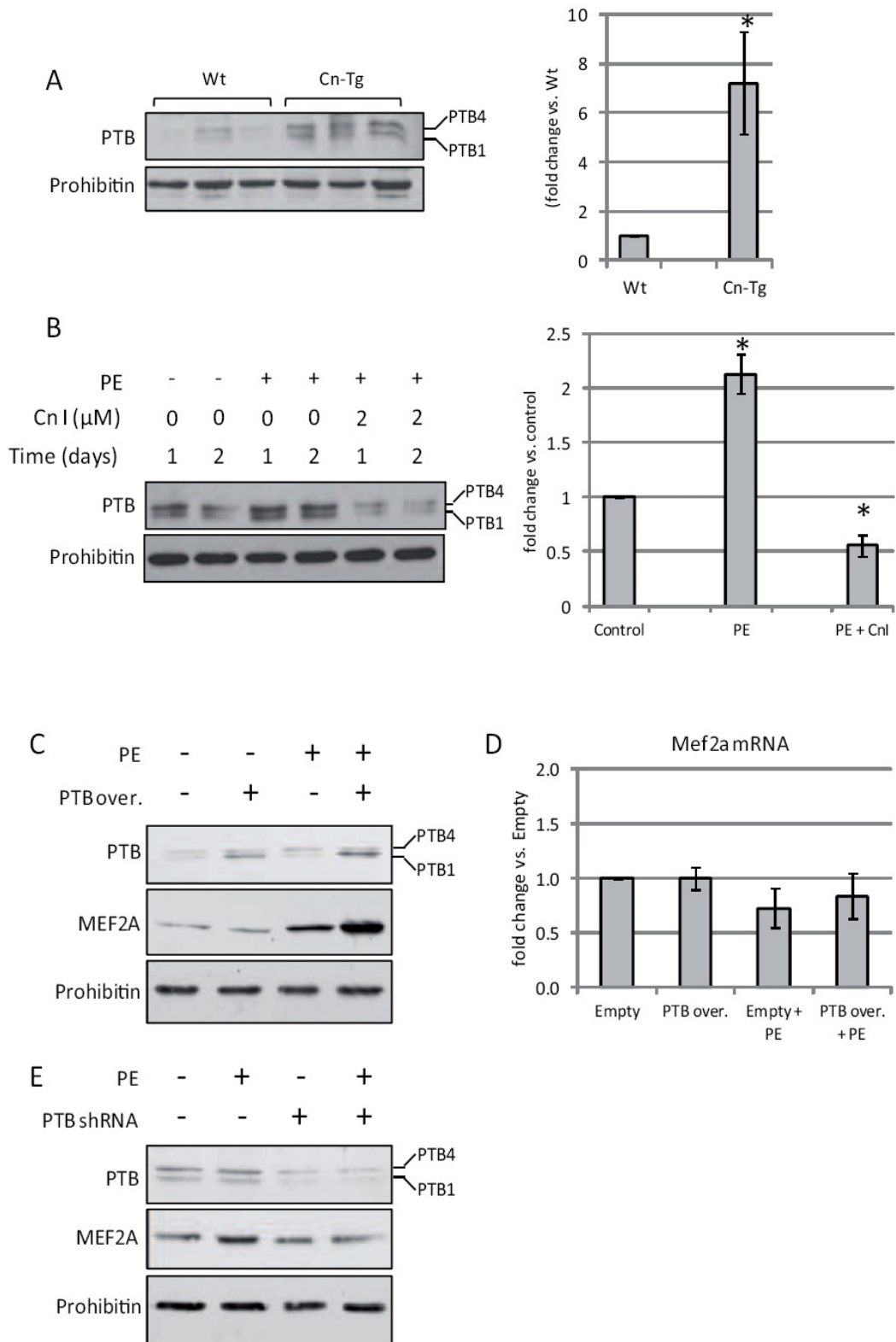


Fig. 43 Calcineurin-dependent control of PTB expression determines MEF2A protein abundance in cardiomyocytes. **(A)** PTB protein expression in total protein extracts of the hearts of hypertrophied 5-months-old Calcineurin (Cn-Tg) mice and wild type (Wt) controls were analyzed by Western blot. Right panel shows densitometric analysis of PTB expression in Cn-Tg hearts compared to paired wild type hearts in four independent sets of Western blots of 1 Wt heart and 1 Tg heart protein samples extracted, processed and analyzed together. * $p < 0.05$ vs. Wt. **(B)** PTB protein abundance in cultured cardiomyocytes during phenylephrine (100 μ M, PE) treatment for 1 or 2 days and effect of adding the Calcineurin Inhibitor VIII also known as CN585 (Cn I; Calbiochem, 207003). Right panel shows densitometric analysis of PTB expression in the same samples at 1 day of treatment. Bars are means \pm SEM, $n=3$. * $p < 0.05$ vs. Controls (cells cultured without neither serum nor PE). **(C)** PTB and MEF2A expression in cardiomyocytes transduced with lentiviruses carrying empty vector (empty) or a vector carrying the PTB1 human sequence (PTB over.) and treated or not with PE for the last 24h before protein extraction. $n=3$. **(D)** Quantitative RT-PCR analysis of MEF2A mRNA in cultures as in C. Bars are means \pm SEM, $n=3$. **(E)** PTB and MEF2A expression in cardiomyocytes transduced with lentiviruses containing a vector carrying a Ptb scrambled sequence or a vector carrying a sequence for Ptb expression silencing (shRNA) and treated or not with PE for the last 24h before protein extraction. $n=3$.

Part 3. A pathway involving HDAC5, cFLIP and caspases regulates Polypyrimidine Tract Binding Protein expression influencing Mef2 alternative splicing in the heart

Transcriptional activity of MEF2 is tightly governed by its interaction with Class II histone deacetylases (HDACs) (Zhou X. et al., 2001). In particular, HDAC4 and 5 bind MEF2 and inhibit its transcriptional activity (Lu J. et al., 2000). It is also reported that inclusion of exon β in Mef2 transcripts generates mRNAs coding for MEF2 variants bearing an acidic peptide in the transcription activation domain (Yu Y.T. et al, 1992) that enhances transcriptional activity of MEF2 (Zhu B. et al, 2005). Polypyrimidine Tract Binding Protein (PTB) is an RNA-interacting factor and is best known for a role in the control of alternative splicing of many transcripts including those coding for sarcomeric proteins (Mulligan G.J. et al, 1992). Our previous studies showed that PTB was involved in IRES-dependent translation of caspase-dependent apoptotic proteins in differentiating cardiomyocytes and its expression reduced during heart development (Zhang J. et al., 2009). We wanted to investigate whether there is a direct relationship between HDAC function, PTB expression and regulation of Mef2 splicing and to characterize the signaling pathway.

3.1 PTB expression is silenced perinatally during heart development through postranscriptional mechanisms blocked by HDAC5.

We examined the expression pattern of PTB in the developing rat heart. PTB protein levels reduced rapidly after birth (Fig. 44A), and by day 90, PTB was undetectable. On the other hand, our data showed no changes in the *Ptb* mRNA level during the perinatal period of development and in the adult it had decreased by only 40% in (Fig. 44B), suggesting postranscriptional regulation.

HDAC proteins are regulators of gene expression in many tissues and, in particular, they have an essential function during heart development (Chang S. et al., 2004; Montgomery R.L. et al., 2007). Mice deficient for Class II HDAC 5 and 9 or Class I HDAC 1 and 2 show propensity to lethal cardiac defects (Chang S. et al., 2004; Montgomery R.L. et al., 2007). Therefore, we measured the expression of HDAC proteins in the heart and observed that HDAC 1, 2 and 5 were abundant in the embryonic myocardium and their temporal expression pattern was similar to that of PTB (Fig. 44A). Consistent with a causal relationship between the decrease in expression of HDACs and PTB, we also observed lower amounts of PTB in the hearts of neonatal mice deficient for HDAC5 expression (Fig. 44C), although *Ptb* transcript levels were similar to wild type age-matched littermates (Fig. 44D). These results suggested that HDAC5 influences the post-transcriptional regulation of *Ptb in vivo*. However, given its molecular function as a histone deacetylase it is unlikely that it acts directly as a positive effector of PTB expression.

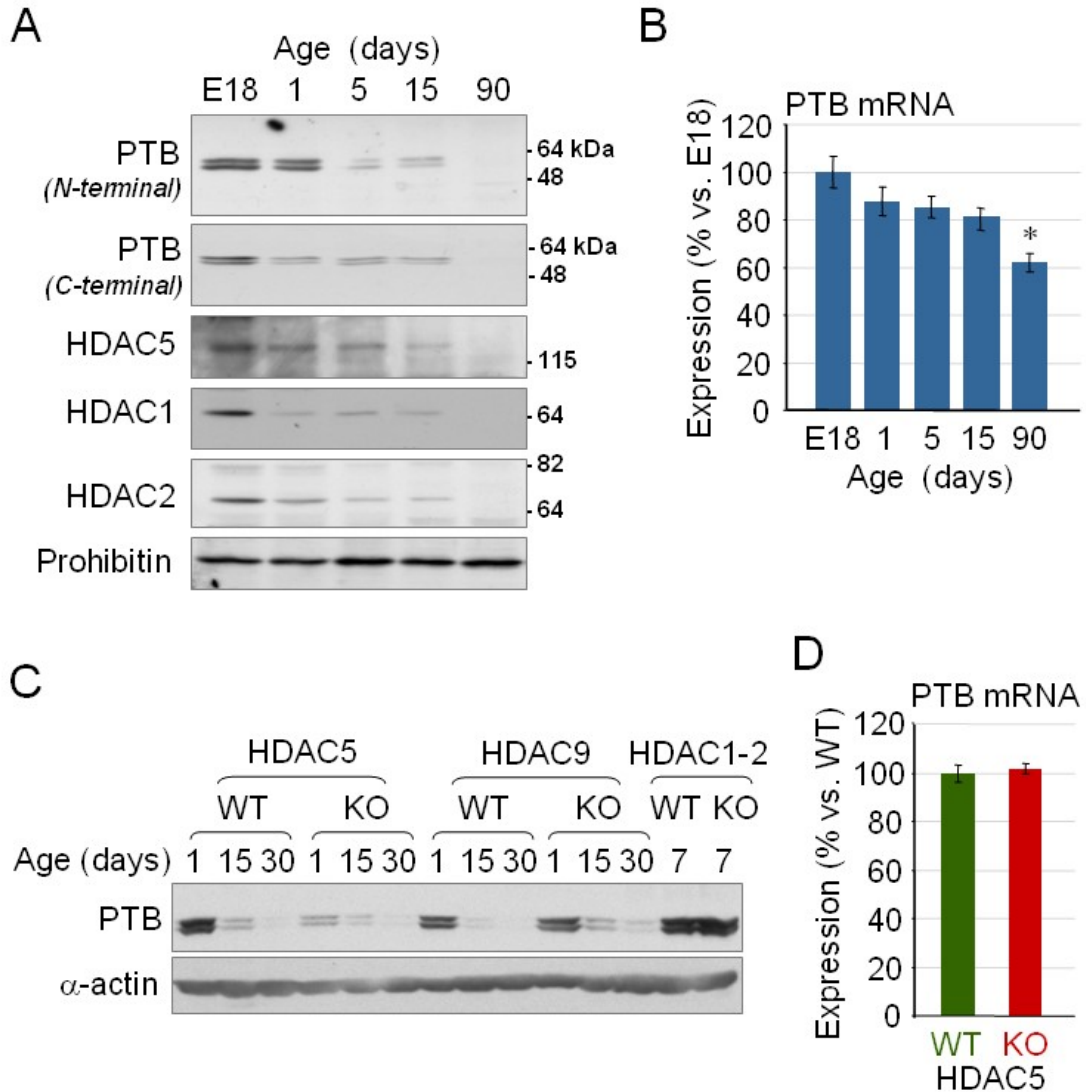


Fig. 44 PTB expression during cardiomyocyte differentiation is regulated postranscriptionally by HDAC5. **(A)** Expression of PTB and HDAC proteins in heart protein extracts from rats of different ages ranging from embryos (E18) to 3-month-old adults. PTB was analyzed with antibodies against the N-terminal region and C-terminal region. Two alternatively spliced variants of PTB were detected (lower band, PTB1 and upper band, PTB4 translated from a transcript including exon 9). **(B)** Ptb transcript abundance was quantified in quadruplicates by Real Time qRT-PCR in total RNA extracts of the same hearts as in A and referred to the value of the house keeping gene Gapdh amplified in the same reaction. Error bars are s.e.m. from three independent experiments. * $p < 0.05$ vs. embryo. **(C)** PTB abundance in protein extracts from hearts of wild type newborns, young and young adults and HDAC5-deficient and HDAC9-deficient littermates as well as wild type and HDAC1 and 2-double deficient neonates. Similar results were obtained with two independent set of samples. **(D)** Ptb total transcript abundance was quantified by Real Time PCR from retrotranscribed total mRNA from the hearts of 1-day-old neonatal wild type and HDAC5-deficient mice. Error bars: s.e.m. from 3 independent experiments.

3.2 HDAC sustains PTB expression in cardiomyocytes through inhibition of caspase-dependent PTB cleavage.

To further explore the relationship between HDAC activity and PTB expression, we investigated the effects of treating postnatal rat cardiomyocytes with the HDAC inhibitors, sodium-butyrate (NaB) or Trichostatin-A (TSA) (Fig. 45A, B). Both treatments led to a reduction of full length PTB protein abundance, with no effects upon Ptb mRNA levels (Fig. 45A, B). However, the reduction in full length PTB was accompanied by the appearance of faster migrating doublet (Fig. 45A, left panel) as detected with an antibody obtained against the C-terminal region of PTB. The size of the faster migrating PTB doublet (~40kDa) observed in cardiomyocytes treated with HDAC inhibitors is consistent with cleavage by caspases between the RRM1 and RRM2 domains of PTB (Back S.H. et al., 2002). This effect was not observed in HEK293 cells (Fig. 45A, right panel), which express high levels of Class I HDAC but lack detectable expression of HDAC5. Consistent with PTB cleavage by caspases in cardiomyocytes treated with HDAC inhibitors, the pan-caspase inhibitor z-VAD-fmk abolished appearance of the smaller PTB fragments, preserving the abundance of the full length form (Fig. 45A). Caspase-dependent PTB cleavage induced by HDAC inhibition was not associated with a significant increase in cell death (Fig. 45B). If caspases play a physiological role in PTB cleavage *in vivo*, caspase deficiency should lead to increased abundance of PTB in the developing heart. Consistent with this prediction, PTB was more abundant in the neonatal heart of cardiac-specific Caspase-3 and 7 deficient mice than in their wild type age-matched controls (Fig. 45C), while the abundance of the Ptb transcript was unchanged (Fig. 45D).

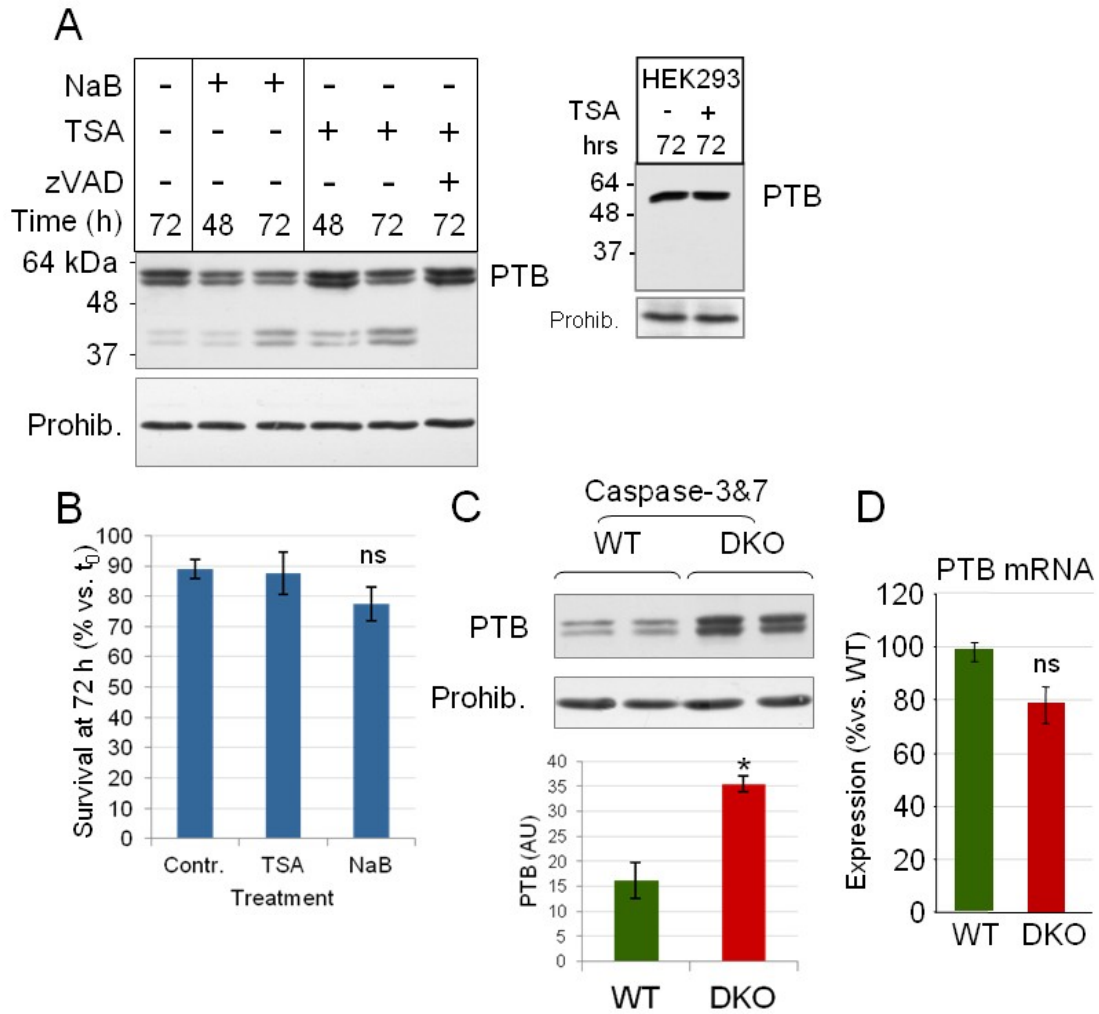


Fig. 45 HDAC inhibition induces caspase-dependent cleavage of PTB. **(A)** Rat neonatal ventricular cardiomyocytes were treated with HDAC inhibitors NaB (5mM) or TSA (100nM) for 48 or 72 hours in the presence or absence of the pan-caspase inhibitor z-VAD-fmk (50 μ M). PTB amounts were detected with an antibody against the C-terminal region. Small panel: Human Embryonic Kidney 293 cells were treated for 3 days with TSA and PTB was detected in total protein amounts with the same antibody. The experiments were repeated four times with comparable results. Prohib: prohibitin was used a loading control. **(B)** Cell survival was counted by the Trypan Blue exclusion assay in cardiomyocyte cultures treated for 3 days with either NaB or TSA at the doses reported above or cultured without drugs (Contr.). Values are expressed as percentage of cell survival versus control plates processed before addition of the drugs. Each experiment was made in triplicates. N=3, error bars are s.e.m. Ns: not significant changes vs. controls (paired Student's *t* test). **(C)** PTB abundance was analyzed in total protein extracts of hearts from young wild type (WT) and cardiac-specific Caspase-3 and 7 deficient mice (DKO). Lower panel: Western Blot densitometric analysis (AU: Arbitrary units). * $p < 0.05$ vs. WT. **(D)** Quantitative Real Time PCR of Ptb transcript in the same hearts as in C. N=3, Error bars: s.e.m. ns: not significant changes vs. WT (paired Student's *t* test).

The preceding data indicate that caspases are responsible for the reduction in PTB levels during cardiac development. However, it is not clear how the activity of caspases upon PTB is regulated. Given that disruption of cFLIP, a natural inhibitor of caspase activity, interferes with heart development (Yeh W.C. et al., 2000), we next aimed to assess the contribution of cFLIP to HDAC inhibitor-induced PTB cleavage *in vitro*. cFLIP mRNA (Fig. 46A) and protein (Fig. 46C) expression was reduced in cardiomyocytes treated with HDAC inhibitors and cFLIP-L overexpression or treatment with the Caspase-8 inhibitor z-IETD-fmk prevented HDAC inhibitor-induced PTB cleavage (Fig. 46B). cFLIP overexpression also prevented fragmentation of PTB into a smaller fragment of approximately 25 kDa (Fig. 46C). Taken together, our results demonstrated a role of the extrinsic pathway of apoptosis, unrelated to cell death and regulated by HDAC, in the control of PTB expression in the myocardium.

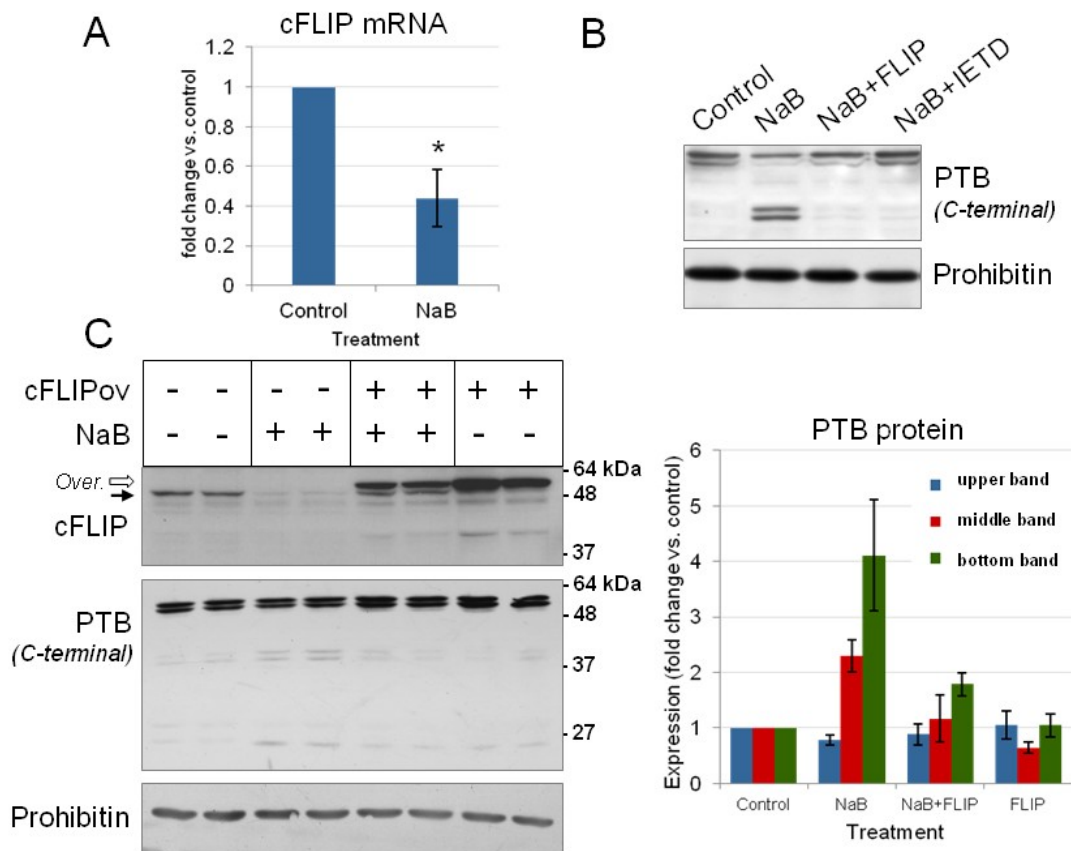


Fig. 46 HDACs block caspase-dependent cleavage of PTB in cardiomyocytes by supporting expression of the endogenous caspase inhibitor cFLIP. **(A)** Rat neonatal ventricular cardiomyocytes were treated with the HDAC inhibitor NaB (5mM) for 24h and cFLIP transcript abundance was analyzed by quantitative Real Time PCR of retro-transcribed total mRNA. N=3, Error bars: s.e.m. * $p < 0.05$ vs. control (paired Student's *t* test). **(B)** PTB protein abundance was assessed in protein extracts from rat primary neonatal cardiomyocyte cultures treated with HDAC inhibitors Na-But (5mM) during 24 hours or in cardiomyocytes transduced with empty viruses or viruses inducing cFLIP-L overexpression (FLIP) and treated or not with the HDAC inhibitor NB (5mM) during 24 h in the presence or absence of the Caspase-8 inhibitor z-IETD-fmk (20 μ M). **(C)** Cardiomyocytes were transduced with empty viruses or viruses inducing cFLIP-L overexpression and were treated or not with the HDAC inhibitor NaB (5mM) during the last 24 h. Expression of cFLIP (white arrow shows overexpressed FLAG-cFLIP and black arrow shows endogenous cFLIP) and PTB was analyzed in total protein extracts. The bar graph shows the densitometric analysis of PTB protein abundance from experiments shown in C. Error bars: s.e.m of n=4 experiments (upper band: full length PTB; middle band: ~40 kDa fragment; bottom band: ~25 kDa fragment).

3.3 Caspase-dependent cleavage of PTB triggers its proteasome-dependent degradation

Upon performing a time course of PTB degradation in cardiomyocytes treated with HDAC inhibitors, a small fragment of ~25kDa was observed at later time points (Fig. 47A). This suggested that the caspase-dependent fragments of PTB previously observed (Fig. 46) are being further processed. It has been reported that caspase-dependent fragmentation could trigger the proteasome-dependent degradation of the targeted protein (Demontis S. et al., 2006; Plesca D. et al., 2008). Therefore, we assessed if PTB was degraded by the proteasome. In the presence of the proteasome inhibitor Lactacystin we observed an accumulation of the smallest PTB fragments produced during Sodium Butyrate treatment (Fig. 47B), suggesting that PTB fragments generated by caspase activity were further degraded by the proteasome.

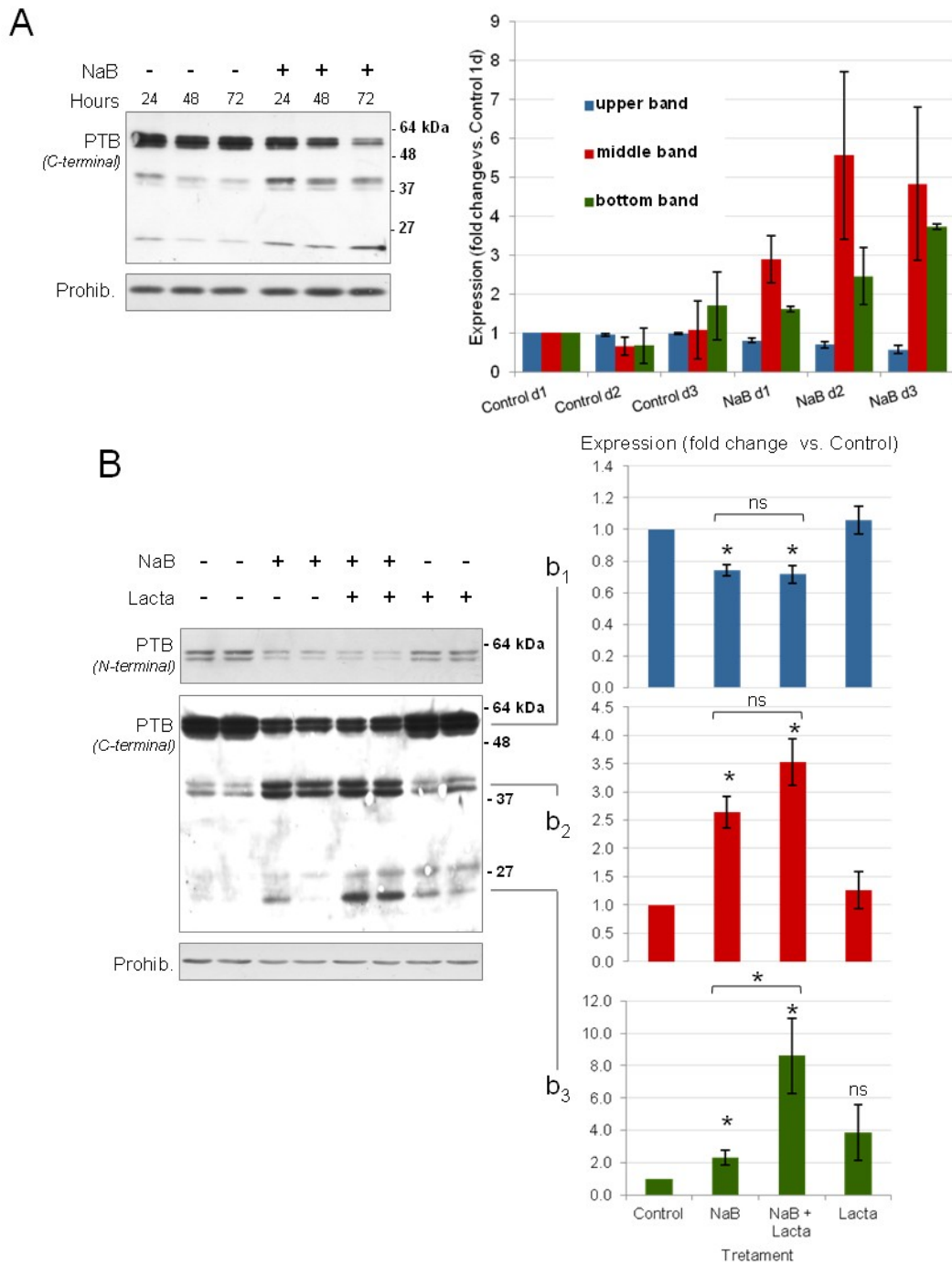


Fig. 47 Caspase-dependent cleavage of PTB triggers its proteasome-dependent degradation. **(A)** Time-course of PTB processing in rat neonatal cardiomyocytes treated with the HDAC inhibitor NaB (5mM). The bar graph shows the densitometric analysis of PTB protein abundance. Error bars: s.e.m of n=3 experiments (upper band: full length PTB; middle band: ~40 kDa fragment; bottom band: ~25 kDa fragment). **(B)** Effect of the addition of the proteasome inhibitor Lactacystin (2µM) on PTB processing during HDAC inhibitor NaB (5mM) treatment for 72 h. Right panels: Densitometric analysis of PTB protein abundance. b₁: full length PTB, b₂: ~40 kDa band, b₃: ~25 kDa band. Error bars: s.e.m of n=4 experiments made in duplicates. * p<0.05 vs. control. ns: not significant.

3.4 Abundance of PTB determines inclusion of exon β in Mef2 transcripts during cardiac muscle differentiation.

The reduction in PTB levels during cardiac development is likely to be responsible for numerous changes in alternative splicing (Llorian M. et al., 2010). We were interested in exploring the possibility that the MEF2 transcription factors may constitute important targets of regulation by altered PTB levels. MEF2 proteins are expressed abundantly in the developing heart, with MEF2A being most highly expressed at later stages of development (Fig. 48A). In muscle, brain and in differentiated C2C12 cells, Mef2 transcripts may contain an alternatively spliced exon (β) encoding a short glutamic acid-rich sequence (e.g. SEEEELEL in MEF2A) that gives rise to MEF2 proteins with stronger transcriptional activity (Yu Y.T. et al., 1992; Zhu B. et al., 2005; Fig. 48B and Fig. 52). Previous reports have shown that PTB can regulate different members of the Mef2 family in HeLa, C2C12 and N2A cells (Boutz P.L. et al., 2007; Llorian M. et al., 2010; Lin J.C. et al., 2011).

Our results showed that during heart development, exon β was progressively included in Mef2a and Mef2d transcripts at the same time as PTB protein levels decrease in the myocardium to form the transcript variants most abundant in the adult heart (the rat sequence has been deposited in GenBank with Acc. No. GU646868), while the most abundant Mef2c variant lacked this exon during the time scale of the experiment (Fig. 48B).

PTB regulates alternative splicing of genes relevant for muscular function (Pérez I. et al., 1997; Southby J. et al., 1999; Charlet-B N. et al., 2002; Naya F.J. et al., 2002) and we showed that its expression was reduced in the heart after birth (Zhang J. et al., 2009, Fig. 44A, Fig. 48A). Overexpression of either PTB1 or PTB4 in neonatal cardiomyocytes, which express low levels of these proteins, induced exon β skipping in Mef2a and Mef2d, but not in Mef2c (Fig. 48C). Moreover, deficiency of HDAC5, which induced premature reduction in PTB abundance, caused increased exon β inclusion in Mef2 (Fig. 48D), whereas cardiomyocyte-specific deficiency of executioner caspase 3 and 7, which induced abnormal abundance of PTB (Fig. 45C), caused reduced exon β inclusion in Mef2 (Fig. 48E).

We also assessed whether reducing PTB abundance in cells where PTB is abundant had the opposite effect on exon β inclusion. Simultaneous silencing in HeLa cells of endogenous PTB and neural PTB (nPTB) (Fig. 49A), which is known to compensate for PTB deficiency in these cells, induced a fourfold increase in exon β inclusion in the endogenous Mef2d transcript (Fig. 49A) and twofold increase in exon β inclusion in transcripts from a mouse Mef2d minigene construct simultaneously transfected with the PTB siRNA (Fig. 49A).

In order to test whether exon β inclusion can be mediated by direct interaction of PTB with the pre-mRNA, radiolabeled RNA probes for Mef2a and Mef2d fragments containing exon β and their respective flanking regions (200nt on each side) were prepared. UV-crosslinking experiments followed by immunoprecipitation with antibodies against PTB showed that PTB can bind to human Mef2a and Mef2d RNAs fragments containing exon β and their respective intronic flanking regions, suggesting that PTB might regulate Mef2 alternative splicing by binding to their RNAs.

Taken together, these results showed that PTB expression, controlled by HDAC and caspases, determined inclusion of exon β in Mef2a and Mef2d transcripts in differentiating myocytes.

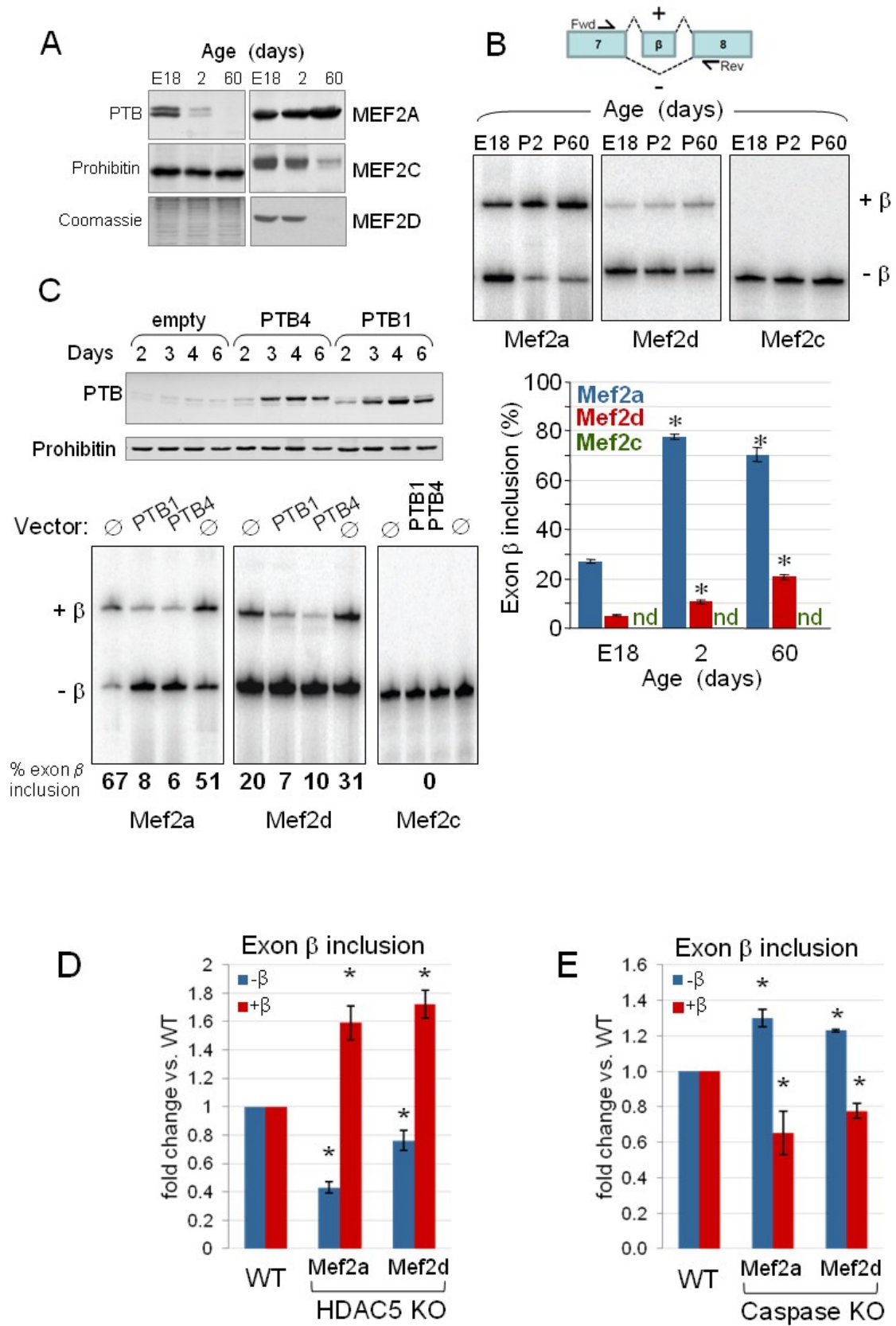


Fig. 48 PTB expression determines skipping of exon β in Mef2a and Mef2d transcripts in cardiomyocytes. **(A)** Expression of PTB and MEF2 (A, C and D) in cardiac protein extracts of rat embryos (E18), 2-day-old neonates and 2-month-old adults, with an antibody raised against the N-terminal region of PTB. Similar results were obtained in two analysis using independent samples. Prohibitin was used as loading control. **(B)** Mef2 alternative splicing event occurring during heart development (see more detailed explanation in Fig. 52). Exon β inclusion in Mef2a, Mef2c and Mef2d transcripts was analyzed by radioactive qRT-PCR with primers flanking the alternatively spliced exon in total mRNA samples from hearts of rat embryos (E18), 2-day-old neonates and 2-month-old adults. +/- β indicates inclusion or exclusion of exon β , respectively. Bar graph: Quantification of radioactive products obtained by qRT-PCR. Nd: not detected. Error bars are s.e.m. from three independent samples. * $p \leq 0.05$ vs. E18. **(C)** Effects of PTB overexpression in cardiomyocytes on Mef2 exon β splicing. Upper panels: Time-course of PTB1 and PTB4 overexpression in P4 cardiomyocytes. Neonatal cardiomyocytes were transduced with empty lentiviruses (\emptyset) or lentiviruses inducing overexpression of PTB, and PTB abundance was monitored by Western blot. Lower panels: Mef2 exon β splicing. Total RNA was extracted at day four post-transduction and exon β inclusion in Mef2a, Mef2c and Mef2d transcripts was analyzed by radioactive qRT-PCR. Two independent experiments were performed with similar results. **(D)** Analysis of exon β inclusion ($-\beta$, not included; $+\beta$, included) in Mef2 transcripts was assessed in total RNA extracts from hearts of 2-day-old wild type (WT) and HDAC5-deficient mice (HDAC5 KO) and is expressed as fold change compared to WT. **(E)** Analysis of exon β inclusion ($-\beta$, not included; $+\beta$, included) in Mef2 transcripts was assessed in total RNA extracts from hearts of 1-month-old wild type (WT) and cardiac-specific caspase 3 and 7-deficient mice (Caspase KO) and is expressed as fold change compared to WT. Error bars in D and E are s.e.m. of data from three hearts per genotype. * $p < 0.05$ vs. WT.

Results

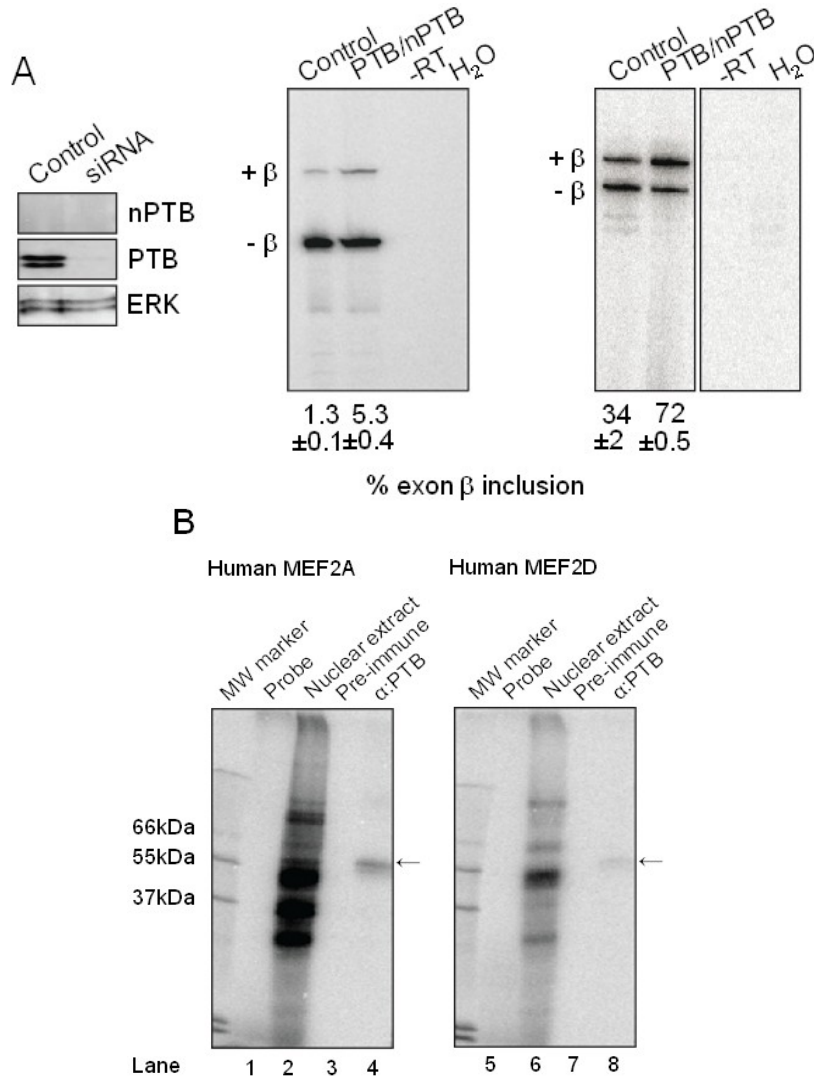


Fig. 49 PTB associates with Mef2A and Mef2D transcripts. **(A)** HeLa cells were transfected with siRNAs against PTB and nPTB or control siRNAs (upper panel). Effect of PTB knockdown on endogenous Mef2D exon β inclusion was assessed by RT-PCR (left panel). Amplicon size: 135 bp for inclusion and 114 bp for skipping. Mouse Mef2D minigene was cotransfected with siRNAs against PTB and nPTB or control siRNAs in HeLa cells. RT-PCR was then carried out with minigene specific primers (right panel). Amplicon size: 340 bp for inclusion and 319 for skipping. Percentage of exon β inclusion is shown at the bottom (mean \pm SD, n=3). Gels shown are representative of three independent transfections. **(B)** UV-crosslinking and immunoprecipitation of human Mef2A and Mef2D exon β containing RNAs, in HeLa nuclear extracts. Probes for the human MefA and Mef2D RNAs contain exon β and around 200nt of the flanking intronic sequence. Body-labeled RNA probes were incubated with buffer E (Lanes 1, 5) or 2ml of HeLa nuclear extract (lanes 2, 6). After UV-crosslinking samples were immunoprecipitated with pre-immune serum (lanes 3, 7) or anti-PTB antibody (lanes 4, 8). Molecular markers are shown to the left and the position of the PTB crosslinked doublet is shown as an arrow to the right of the gel. Gels shown are representative of three independent experiments.

3.6 Identification of the binding site of PTB to Mef2 during transcriptional modification

Trying to identify the binding site of PTB with pre-mRNA of Mef2a and Mef2d, we designed and constructed a plasmid containing mouse genomic Mef2a which includes exon β with 500bp flanking sequence of introns (Fig. 50). And we used Mef2c, in which there is no change of exon β regulated by PTB, as negative control. Therefore we designed and constructed a plasmid containing exon β of Mef2c with 500bp flanking sequence of introns from mouse genomic DNA (Fig. 51). Both sequences were inserted into plasmid vector pcDNA3 digested with HindIII and EcoRI.

MEF2A

LOCUS NT_039428 81978 bp DNA linear CON 19-OCT-2010 DEFINITION Mus musculus strain C57BL/6J chromosome 7 genomic contig, MGSCv37

Mef2a

ggatccTGGCCACTGGGAAAATAAAACACACAGCAGTTTTCTAACAATAGAGTCTGGTAGTAGACAGGC
 ATGTATACAAACTGTCTGGCCAGATGGGGTAGCTATGCAGGGATTAAATGTATATGTGCACAGTGTAA
 ACTTGAAGTGTCTCAGAAGCAATGCTGTGTGTAGGAGAGACCCATGTAAGAGGAGGTGGGATTAAGGG
 ACAGGATGGGGCTTTAAATCATTGGCTAGAGAATTTAAAAGAAATTTCCTTTATTTTGAAAAAGCAACT
 ATAATGTAGAGGCAAGTACTATATGCATCGTTTTGATATGTATAGAACCCTCTGTAAAGTTGCAAACAGCT
 ACTAGAATCCAAATGCCATGTTTTCTAAAAGAAAGATCTTGTGCAAGTTCCAACAGTCTTAGTTAACT
 CTCTTATCCCTCTTATGTGCTGAGTACAGTTCGGAGGAAGAGGAATTGGAGTTGGTGAGTGTGGTTTCCT
 GCTTGAACAGAGTTGAAAAATATATAAATAGTACTAATTTTAAATGTTCTTATTTAACCTTTGTTC
 CTTTGTACAAAGATATTTTTCTATTTGTTTTCCACTATCCAAACATTTTTTAATCAAGAAATCCACCT
 ACTGGCACTACTGATCCTAGTTATGTTTATGTTTATTGCTGTATATATTGGTCCCTTTTATTTGATGGG
 TAAAGGAGAAGACATATTGAAGTAACTTGTAAAAACAATAGCTATCCATGAACACAAGATACTTAAGCT
 TTTTTTGCTAAGGAAGTACACAAAATACCTTATGTGGCTTTCGAAATTAATAAGTGTTTTTAGAAAAT
 GACTTCACCCTCAGAGTCCCTGAGATCGTAACACAGAATCTTGTGTTATGTTTCTTTCTTTCAAAAAGA
 TTACATCATTTTTGGTGAGGTCACCTTTTTTCAGAGTTGATTATCTCATCCTGCATGAGGCAGTCGGAAC
CACAAGGGGGTTCCCTgatatc

Forward primer: BamHIMmMef2aFwd: ttggatccTGGCCACTGGGAAAATAAAAC

Reverse primer: Mef2agenomMmR2: aagatatcAGGGAACCCCTTGTG

Fragment cloned from BAC clone and Sequence verification shows correct.

The result of Mef2a reconstructed plasmid was sequenced using primers of T7F and SP6 and the results showed the insert sequence was correct.

Fig. 50 Sequence of genomic Mef2a that was amplified and included into the pcDNA3 plasmid. Red sequences are the sites digested by HindIII and EcoRI enzymes, blue sequences are binding sites of primers. Yellow sequence is exon β .

MEF2C

>chromosome: NCBI37:13:83642433:83807284:1

Mef2c

aagcttACTCTCGTCATGTATGACTCCCTTTTCCTCTAGCAAGTAGGGTTTAAAGTAGATTCCCTATTATCTTTTTATCAAAGTATGGGGCACAACAGTAAACAGAGAGACAATGACCTGTGCTGCAAACAAGATAGACAGTCTTCAGGTTTGAGACAAGGAACACCTCACTAAGAGAAAACAAAGAAATGTCTTTGTAAAGGAGTTGCTTTTGGCATCCCGTGTGCCAAGCTGTTTAAACTGTTGCGTCTATCAGAAGATGCATCTCCTTTTGCTAGA AAGATTTTCACAGTTATAAATATTTACAGACACTAATTAATAAACTCCTTCCCTCCTTCCCCATGCTCTCAGTCTGAGGATGTGGATCTGCTGTTGTAAGTGGGAAGGACTCGTCCCTTGAAGGGCATGCTCGGGAA GATAACAGAACTACCTCAGTGAAAGGTGCTAGCTGTGATCAAACAGAAAGATTTTAAAACCTTACCTCAA TAAATGAGGGTACTGATTATGCTTAAACACCATTAATTTCTAGGATCATTGACAGCCTGTGGAAAGCAT AGCTGGTTTTTTGTAGGCCTTTTTCTCTGTCCCCACCTTTTACCTAAAGACCATGTTTTAAATATTAAG ACTGAACTTACTCTAAAATAGAAAACAAAAATGCATCTTTAGCTATTTAAATAGTAAGACACTTATTCT TTCAAATTTAAAATACCAGGATTTTGAGCGTAAGCATCCTTTACCTCCTGGCTATTAGGAGTTAAATA CTGGCATTAGCTACTTTGCCATCCTTTTGCAAGGAAGTCGAAGCAGAAGAAAGTGGTCATAGCGCCACC TGCTGGCCATAACATAgatatc

Foward primer: ttaagcttACTCTCGTCATGTATGACTCC

Reverse primer: aagatatcTATGTTATGGCCAGCAGGT

Fragment cloned from mouse genomic DNA

Fragment cloned from BAC clone and Sequence verification shows correct.

The result of Mef2c reconstructed plasmid was sequenced using primers of T7F and SP6 and the results showed the insert sequence was correct.

Fig. 51 Sequence of genomic Mef2c that was amplified and included into the pcDNA3 plasmid. Red sequences are the sites digested by HindIII and EcoRI enzymes, blue sequences are binding sites of primers. Yellow sequence is exon β .

Discussion

EndoG is a novel determinant of cardiac hypertrophy and mitochondrial function

Cardiac muscle cells depend on mitochondria to obtain energy and even subtle perturbations in mitochondria content or function can result in cardiac dysfunction (Huss J.M. and Kelly D.P., 2005). EndoG is a nuclear-encoded, mitochondrial-localized nuclease with a proposed but disputed function in apoptosis (Lehman J.J. et al., 2000; Miñana J.B. et al., 2002; Handschin C. et al., 2007; Monti J. et al., 2008). Initial investigations suggested that absence of EndoG caused neither essential effects on apoptosis nor obvious phenotype in EndoG null mice indicating its dispensable role in apoptosis and embryogenesis (Irvine R.A., 2005; David K.K., 2006). However, in these two studies researchers used the mouse embryonic fibroblasts (MEFs) and splenocytes of wild type and EndoG knockout genotypes in order to study its role in apoptosis, both of which are able to activate caspase-dependent cell death. Thus these approaches were insufficient to prove whether EndoG is important during cell death, because it was described that EndoG served as an alternative pathway of DNA fragmentation in a caspase-independent manner when researchers compared DNA fragmentation in MEFs with and without the existence of caspases (Li L. et al., 2001). Hence it is more accurate to investigate the role of EndoG during cell death in cell models lacking caspases. Moreover, in agreement with this point of view, a recent research of our group also proved that EndoG translocated from mitochondria to cytosol upon cell death stimuli and caused caspase-independent DNA degradation in cardiomyocytes, which expressed low levels of apoptotic genes (Zhang J. et al., 2011).

So far no known effect of EndoG on cardiac mass or function has been reported. First, we observed that EndoG was highly expressed in the heart of the adult rat and mouse, localised to cardiomyocytes and co-localised with mitochondria. Stuart Cook's group identified that EndoG was a gene located in a region of rat chromosome 3p controlling blood pressure-independent left ventricular mass (LVM), and loss-of-function mutation in EndoG associated with increased LVM and impaired cardiac function. They also found that reduced expression of EndoG transcript and lack of EndoG protein in all rat strains with elevated cardiac mass and identified an SHR-specific frameshift-causing insertion in EndoG exon one that was

associated with increased heart weight and LVM, inferring its important role in cardiac mass and function. In parallel, we decided to measure the size of cardiomyocytes with EndoG RNA interference *in vitro* in order to determine if cardiac hypertrophy was direct consequence of EndoG absence or an adaptation of the EndoG knockout heart. By using shRNA knockdown of EndoG (shEndog) we found that in the absence of pro-hypertrophic stimuli, inhibition of EndoG in cultured neonatal cardiomyocytes resulted in an increase in cell size and hypertrophic biomarkers; we also observed increased reactive oxygen species (ROS), an additional pro-hypertrophic stimulus (Fuller T.F. et al., 2007), in shEndog cardiomyocytes. Our data showed that specific EndoG expression silencing directly induced cardiomyocyte hypertrophy *in vitro* that was associated with the activation of pro-hypertrophic pathways, thus demonstrating that the effects on cell size *in vivo* including increased cardiac mass are probably a direct effect due to the absence of EndoG and not an adaptation to EndoG knockout heart.

Until now, there are two groups who generated EndoG knockout mice that were alive until adulthood and both of them suggested that absence of EndoG did not induce obvious phenotypic abnormalities of different organs such as liver, brain, heart, lungs, stomach and small intestine (Irvine R.A. et al., 2005; David K.K. et al., 2006). However, in our opinion there are visible changes in histological images that they presented in their article, such as the liver (David K.K. et al., 2006) and in fact they did not investigate these organs at a biochemical or molecular level. The group of S. Cook examined the effects of EndoG loss-of-function *in vivo* in the EndoG deleted mouse (Endog^{-/-}) and observed that Endog^{-/-} mice had larger cardiomyocytes at baseline in the absence of stimulation compared to controls. Following stimulation of hypertrophy with angiotensin II, which was described to depend on ROS (Mukhopadhyay P. et al., 2007), there was an increase in cardiomyocyte size, hypertrophic biomarkers and LVM in Endog^{-/-} mice. We checked the heart tissue of Endog^{-/-} mice by electronic microscopy and observed that Endog^{-/-} mouse heart had no gross morphological changes of mitochondria but vacuole-like items associated with mitochondria from Endog^{-/-} mice were more numerous and larger than those seen in control mice, which were proved to be steatosis according to Oil Red O staining and lipid quantification. In

conclusion and combining all the results, our studies resolve some of the uncertainty as to the non-apoptotic function of EndoG showing that EndoG is required for the control of cardiomyocyte growth and mitochondrial metabolism.

Expression of MEF2A and D is increased during hypertrophy in vivo and in vitro through posttranscriptional mechanism under the regulation of Calcineurin A

Cardiac hypertrophy is observed in many forms of human heart disease, and MEF2A and MEF2D have been proved to play relevant roles in the regulation of morphogenesis and myogenesis of cardiac muscle cells and stress-dependent gene expression (Naya F.J. et al., 2002; Xu J. et al., 2006). Because of the early discovery that MEF2 activity is regulated by transcription during embryogenesis (Edmondson D.G. et al., 1994; Naya F.J. et al., 1999) and then by posttranslational modification (Molkentin J.D. et al., 1996) combined with association to enhancers such as NFAT (Chin E.R. et al., 1998) or inhibitors such as Class II HDACs (Lu J. et al., 1999; Miska E.A. et al., 1999), the vast majority of information available on MEF2 activity regulation focus on MEF2 transcription in the embryo (Molkentin J.D. and Olson E.N., 1996) and on its posttranslational regulation (McKinsey T.A. et al., 2002). This could lead to the impression that MEF2 abundance is not a relevant point of regulation during adaptation to stress in the postnatal heart and that relative MEF2 abundance influences only marginally cardiac growth. Reports simultaneously comparing expression of Mef2 both at the transcript and protein levels during agonist stimulation are scarce (Ikeda S. et al., 2009) and there was no such data available for cardiac development.

In our research, by comparing the response to the hypertrophic agonist phenylephrine of cardiomyocytes expressing different levels of MEF2A, we show that its abundance does influence agonist-induced growth of differentiated cardiomyocytes *in vitro*. These results are in agreement with the partial blockade of Calcineurin-induced hypertrophy *in vivo* by overexpression of a dominant negative Mef2a (van Oort R.J. et al., 2002) and with ventricular hypertrophy observed in Mef2a transgenic mice (Xu J. et al., 2006), but here we used a direct approach consistent in reducing the endogenous levels of Mef2a instead of adding a negative

competitor or enhancing its expression. In addition, our observation that Calcineurin-overexpressing mice express high levels of MEF2A and that Calcineurin inhibition *in vitro* blocks MEF2A expression during phenylephrine treatment establishes a link between Calcineurin and MEF2 expression that helps clarify the previous suggestion that MEF2 could function independently of Calcineurin-directed hypertrophy (Xu J. et al., 2006). Our results also show that MEF2A and MEF2D abundance increase during agonist stimulation by enhancing their translation and demonstrate that MEF2 proteins, not their transcripts, are more abundant in a model of hypertrophied heart *in vivo*. Given that our results also show, for the first time to our knowledge, that MEF2D expression decreases during aging, our data showing that MEF2D protein abundance is upregulated in the hypertrophied Calcineurin-overexpressing heart, contributes to the understanding of its essential role during stress-induced cardiac hypertrophy (Kim Y. et al., 2008).

Previous knowledge about posttranscriptional regulation of MEF2 abundance was limited to the autoinhibitory role of *Mef2a* transcript's 3'UTR (Black B.L. et al., 1997) and the miR-1-dependent *Mef2a* mRNA degradation (Ikeda S. et al., 2009). Ikeda and co-workers found that miR-1 binds to *Mef2a* 3'UTR and induces degradation of the transcript and that Calcium signaling induces reduction of miR-1 expression (Ikeda S. et al., 2009). Interestingly, these authors found increased MEF2A protein expression in the Calcineurin-overexpressing heart; the same *in vivo* model used by us, but suggested it was due to Calcium-dependent miR-1 downregulation (Ikeda S. et al., 2009). This would have lead to increased *Mef2a* mRNA levels. However, cardiac *Mef2a* mRNA levels, which should be higher in the transgenic heart if miR-1 played a relevant role in MEF2 regulation in this model, were not measured. Thus, our results showing that *Mef2a* and *Mef2d* transcripts are actually unaffected in the heart of Calcineurin transgenic mice are not in contradiction with Ikeda's group results, but rather complete them, opening the possibility that regulation of MEF2A protein abundance in the hypertrophied heart *in vivo* involves other mechanisms than miR-1-dependent signaling, including *Mef2* enhanced translation. Calcineurin has been shown to promote cap-dependent protein translation in pancreas (Sans M.D. and Williams J.A., 2004). However, our results suggested that cap-dependent translation is not involved in MEF2 translation in the

myocardium during hypertrophy because Calcineurin overexpression reduced the phosphorylation status of eIF2 and the abundance of the hyperphosphorylated form of 4E-BP1, yet induced MEF2 translation. Finally, our results demonstrate that PTB, which has been shown previously by many groups to be involved in cap-independent translation (Mitchell S.A. et al., 2001; Zhang J. et al., 2008) is a novel downstream target of Calcineurin activity and modulates MEF2A translation in cardiomyocytes.

In conclusion, our results a) support induction of translation as a previously unrecognized level modulating MEF2 activity; b) add information about the regulation of MEF2A, a master coordinator of gene expression during cell differentiation and organogenesis; c) contribute to understand the function of MEF2D, whose expression is shown here to decay during postnatal heart growth to almost undetectable levels, yet is known to be required for cardiac hypertrophy in the adult; and d) show a novel pathway, translation, by which Calcineurin signaling regulates MEF2 activity, involving the control of PTB expression.

HDAC5, cFLIP and caspases regulates Polypyrimidine Tract Binding Protein expression influencing Mef2 alternative splicing in the heart

Polypyrimidine Tract Binding Protein (PTB) is an RNA-interacting factor and is best known for a role in the control of alternative splicing of many transcripts including those coding for sarcomeric proteins (Mulligan G.J. et al, 1992). Though the importance of PTB in the regulation of relevant splicing events influencing the expression and function of many genes, including some coding for structural proteins relevant for muscle cells, is well established (Mulligan G.J. et al., 1992; Pérez I. et al., 1997; Southby J. et al., 1999; Charlet-B et al., 2002), the knowledge about the signaling pathways that control PTB expression in muscle cells is more limited, and is mainly derived from studies in the C2C12 myoblast cell line (Boutz P.L. et al., 2007; Lin J.C. and Tarn W.Y., 2011). In differentiating neurons expression of micro-RNA mir-124 down-regulates PTB expression leading to a series of neuronal specific alternative splicing events (Boutz P.L. et al., 2007; Makeyev E.V. et al.,

2007). In C2C12 cells, the protein RBM4 promotes skipping of PTB exon 11 and nPTB exon 10, leading to Nonsense Mediated mRNA Decay (NMD) and reduced PTB and nPTB levels (Makeyev E.V. et al., 2007). In addition, nPTB is targeted by miR-133 in C2C12 cells, allowing expression of PTB (Boutz P.L. et al 2007).

Here, we demonstrated a novel mechanism for the control of PTB expression in primary cardiomyocytes and in the rodent heart *in vivo*. Caspase-dependent cleavage of PTB is demonstrated *in vitro* in neonatal cardiomyocytes treated with HDAC inhibitors and is suggested to regulate PTB abundance in the heart *in vivo*, because cardiac-specific caspase-3 and 7 null mice express more PTB than wild type mice.

Caspases were previously shown to cleave PTB in cell lines treated with toxic drugs (Back S.H. et al., 2002), but here we show that this cleavage occurs as part of a normal developmental program. By reducing PTB abundance, caspase activity could contribute to the control of many PTB-dependent splicing events in the perinatal period of heart development. This could be involved in the deleterious effects caused by *in vivo* deletion of key regulators of the extrinsic apoptotic signaling, which obstruct heart development without affecting the rate of cardiac cell death (Yeh W.C. et al., 1998; Yeh W.C. et al., 2000). PTB cleavage induced by HDAC inhibitors in cardiomyocytes was blocked by overexpressing cFLIP-L or by adding a Caspase-8 inhibitor, in agreement with the contribution of the extrinsic pathway to PTB degradation. These results together with previous reports showing that Caspase-3 and caspase-9 regulate differentiation of C2C12 myoblasts to myotubes *in vitro* (Fernando P. et al., 2002; Murray T.V. et al., 2008) support a role of the caspase-dependent cell signaling during muscle differentiation (Bahi N. et al., 2006; Zhang J. et al., 2009). Although PTB cleavage induced by HDAC inhibition produced C-terminal fragments of ~40 kDa, we did not detect the presence of these fragments *in vivo* in correlation to the reduction of full length PTB in the developing heart. However, the increased abundance of PTB proteins in the cardiac-specific caspase-3 and 7 double knockout strongly support a role of caspases in the control of PTB expression *in vivo*. Our results also suggest that the initial cleavage of PTB by caspases triggers further PTB degradation by the proteasome. Caspase-dependent processing inducing further degradation of the target has been demonstrated for other proteins (Demontis S. et al.,

2006; Plesca D. et al., 2008). The regulated programs of alternative splicing in developing heart involve numerous factors in addition to PTB; bioinformatic analysis of exons that are co-regulated during cardiac development indicated enrichment of binding sites for CELF, MBNL and FOX proteins in addition to PTB (Kalsotra A. et al., 2008). Indeed, all of these proteins were also implicated in the computationally assembled muscle “splicing code” (Barash Y. et al., 2010. Also review: Llorian M. and Smith C.W., 2011). Curiously, while the preceding report demonstrated changes in the levels of CELF, MBNL and FOX proteins, no changes in levels of PTB expression were observed during post-natal heart development in mouse (Kalsotra A. et al., 2008). The reasons for this discrepancy between our observations and those of Kalsotra et al. (Kalsotra A. et al., 2008) are unclear. Nevertheless, we reproducibly observed a rapid decrease in PTB protein abundance in both mouse and rat hearts after birth, using two independent PTB-specific antibodies against two different regions of the protein, whose specificity has been previously confirmed (Zhang J. et al., 2009).

In addition, our findings expand the current knowledge about the relevance of PTB in the biology of striated muscle by showing its role in Mef2 alternative splicing in the developing heart. Thus, although it is known that PTB regulates splicing of many genes involved in muscle contraction, our data reveal that PTB is also involved in the splicing of the transcription factor Mef2a and Mef2d, which are important for the control of gene expression during cardiac muscle differentiation (Mulligan G.J. et al., 1992) and for the adaptation of the cardiac muscle to stress (Kim Y. et al., 2008).

MEF2 and HDAC are mutually regulated factors involved in the control of gene expression during heart development (Mc Kinsey T.A. et al., 2007; Potthoff M.J. et al., 2007). Deficiency in either MEF2A or MEF2C induces profound alterations in heart morphology, and MEF2D deficiency hampers the normal response of the heart to stress in the adult (Lin Q. et al., 1997; Naya F.J. et al., 2002; Kim Y. et al., 2008). Inclusion of exon β in Mef2 transcripts generates mRNAs coding for MEF2 variants bearing an acidic peptide in the transcription activation domain (Yu Y.T. et al., 1992; also Fig.52) that enhances transcriptional activity of MEF2 (Zhu B. et al., 2005). On the other hand, mice deficient for Class II HDAC5 and 9 or Class I HDAC1 and 2 show propensity to lethal cardiac defects (Chang S. et al., 2004; Montgomery R.L. et al., 2007). Class II HDACs directly bind to MEF2 and inhibit

MEF2-dependent gene transcription contributing to the regulation of muscle-specific gene expression (Lu J. et al., 2000). Given the essential role of MEF2 in heart development, it seems that adjusting MEF2 activity through regulation of exon β splicing can be relevant for the correct contribution of MEF2-dependent transcription, regulated by Class II HDAC, during heart organogenesis. Our results showed that exon β inclusion in Mef2a and Mef2d occurs progressively during heart development. We also observed an inverse relationship between exon β inclusion and PTB expression and show reduced PTB expression perinatally in the hearts of rats and mice. Furthermore, we show that PTB expression is sustained by HDAC5, thus linking HDAC5 with the regulation of MEF2A and MEF2D activity through the control of mRNA splicing. These results unveil an additional new pathway by which HDAC can influence MEF2 activity without direct interaction.

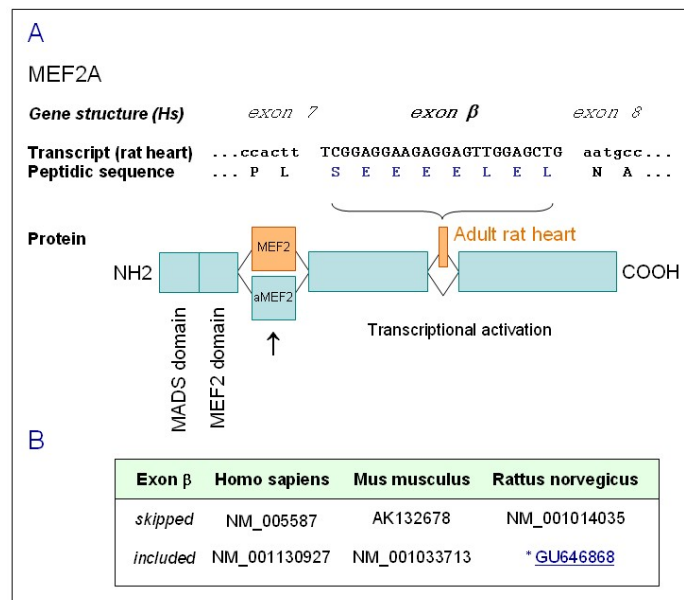


Fig. 52 Structure of the Mef2a gene, transcript and protein. **(A)** Mef2a human gene region around the alternatively spliced exon β , top row: gene structure (based on Yu et al., 1992); middle row: transcript sequence surrounding exon β in the rat Mef2a transcript obtained from adult cardiac ventricle retrotranscribed by random priming, PCR-amplified and sequenced using primers Forward: ggaatgaacagctcgaaacc, Reverse: gaggcaagcttggagttgctc. Location of the putative peptide in the protein sequence (from Olson E.N. et al Dev Biol 172: 2-14; 1995). Sequencing the region including the mutually exclusive exons coding for the peptides “MEF2” and “aMEF2” (\uparrow) with primers Forward: atgagaggaaccgacaggtg and Reverse: cgagtgaactccctgggtta showed that the most abundant Mef2a variant expressed in the rat heart includes “MEF2” exon (orange) and not “aMEF2”. **(B)** GenBank accession numbers of sequences for Mef2a transcript variants lacking (skipped) or containing (included) exon β .

* We have contributed the sequence of the rat (Rn) Mef2a isoform containing exon β expressed in the heart (GU646868).

The reason for exon β inclusion in the transcript of Mef2a and Mef2d but not in Mef2c in the heart is unknown but our results show that exon β inclusion in Mef2a and Mef2d is regulated by PTB. MEF2C is essential for the heart only during early development (Lin Q. et al., 1997), and our results show that PTB is abundant during that period. On the contrary, MEF2A plays a key role during the late phase of myocardial differentiation (Naya F.J. et al., 2002), precisely coinciding with the reduction of PTB expression and exon β inclusion, as we show here. Exon β inclusion in MEF2A seems correlated to its trans-activating activity (Yu Y.T. et al., 1992) suggesting that it could be essential for the correct function of MEF2A *in vivo*. Furthermore, we showed that a significant fraction of the transcript for MEF2D, which plays a relevant role in stress-induced gene expression in the adult (Kim Y. et al., 2008), includes exon β in a PTB-inhibitable manner progressively after birth. Interestingly, we have recently found increased expression of MEF2A and MEF2D in myocytes treated with hypertrophic agonists and the hypertrophied adult heart (Ye J. et al., 2012). It can be hypothesized that, in the heart, exon β inclusion is important to define the activity of MEF2A and MEF2D when they are essential, but not in MEF2C, and that this splicing event is regulated by different mechanisms depending on the gene, with PTB being a relevant regulator of exon β splicing in Mef2a and Mef2d transcripts.

In conclusion, our data show that abundance of PTB is dependent on HDAC5 through the regulation of its FLIP-inhibitable, caspase-dependent cleavage and that progressive reduction of PTB expression permits the inclusion of exon β in Mef2a and Mef2d mRNAs in the heart during cardiac muscle differentiation (Fig. 53). These findings contribute to the understanding of the role of caspases in myocyte differentiation, revealing the involvement of HDAC5 in its regulation and suggesting a previously unknown pathway for the control of MEF2 activity by HDAC without direct interaction, involving the splicing repressor PTB.

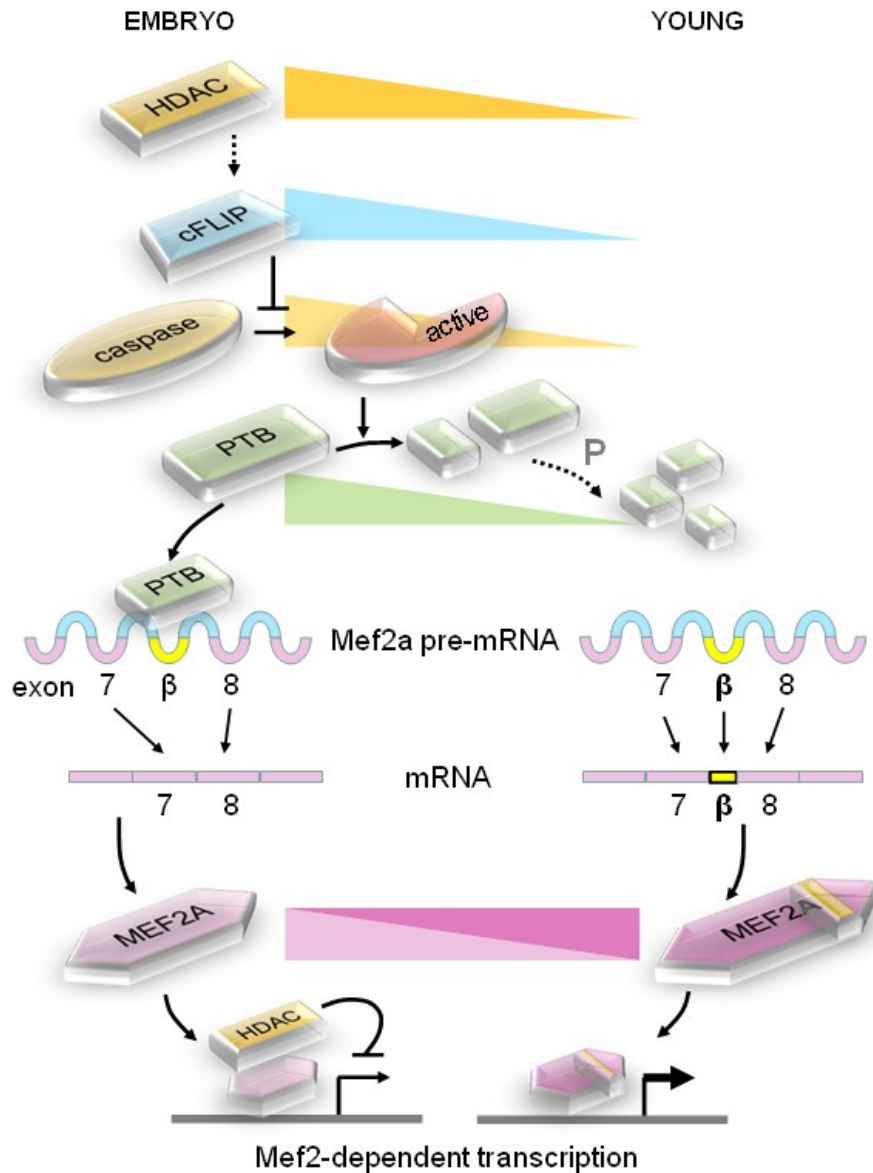


Fig. 53 Model of the regulation of Mef2 alternative splicing by HDAC and caspases through the control of PTB abundance during heart development. The expression of HDAC decreases during perinatal cardiomyocyte differentiation. In addition to regulate MEF2-dependent transcription by directly binding to this transcription factor, developmental downregulation of HDAC induce the reduction of cFLIP expression allowing caspases to cleave the splicing repressor PTB. Caspase-dependent PTB cleavage triggers its degradation by the proteasome. Low levels of PTB in the postnatal heart permits inclusion of exon β in the Mef2a and Mef2d transcripts, which code for variants with more robust transcriptional activity.

Conclusions

Conclusions

1. EndoG expression silencing in neonatal cardiomyocytes results in an increase of cell size and the expression of hypertrophic biomarkers in the absence of pro-hypertrophic stimuli.
2. EndoG null mice show increased ROS production and more lipid content in myocytes.
3. Hypertrophic agonist stimulation of neonatal cardiomyocytes increases Mef2 expression by enhancing its translation without affecting its transcription or blocking protein degradation.
4. Translation of MEF2 is induced by hypertrophic stimuli in cardiomyocytes through the regulation of Calcineurin-dependent pathway, which involves PTB.
5. PTB expression is reduced perinatally during heart development through posttranscriptional mechanisms blocked by HDAC5.
6. HDAC sustains PTB expression in the developing myocardium through inhibition of the FLIP-inhibitable caspase-dependent PTB cleavage.
7. Inclusion of exon β in Mef2a and Mef2d transcripts is repressed by PTB and increases during heart development.

References

References

- Adams JW, Migita DS, Yu MK, Young R, Hellickson MS, Castro-Vargas FE, et al. Prostaglandin F2 alpha stimulates hypertrophic growth of cultured neonatal rat ventricular myocytes. *J Biol Chem*. 1996 Jan 12;271(2):1179-86.
- Adams JW, Sah VP, Henderson SA, Brown JH. Tyrosine kinase and c-Jun NH2-terminal kinase mediate hypertrophic responses to prostaglandin F2alpha in cultured neonatal rat ventricular myocytes. *Circ. Res*. 1998, 83:167-78.
- Andersson SG, Karlberg O, Canbäck B, Kurland CG. "On the origin of mitochondria: a genomics perspective". *Philos. Trans. R. Soc. Lond., B, Biol. Sci*. 2003; 358 (1429): 165-77; discussion 177-9.
- Apostolov EO, Wang X, Shah SV, Basnakian AG. Role of EndoG in development and cell injury. *Cell Death Differ*. 2007 Nov;14(11):1971-4.
- Arnold MA, Kim Y, Czubyrt MP, Phan D, McAnally J, Qi X, et al. MEF2C transcription factor controls chondrocyte hypertrophy and bone development. *Dev Cell*. 2007;12(3): 377-89.
- Auweter SD, Allain FH. Structure-function relationships of the polypyrimidine tract binding protein. *Cell Mol Life Sci*. 2008;65(4):516-27.
- Back SH, Shin S, Jang SK. Polypyrimidine tract-binding proteins are cleaved by caspase-3 during apoptosis. *J Biol Chem*. 2002, 26;277(30):27200-9.
- Backs J, Olson EN. Control of cardiac growth by histone acetylation/deacetylation. *Circ Res*. 2006 Jan 6;98(1):15-24.
- Bahi N, Zhang J, Llovera M, Ballester M, Comella JX, Sanchis D. Switch from caspase-dependent to caspase-independent death during heart development: essential role of endonuclease G in ischemia-induced DNA processing of differentiated cardiomyocytes. *J Biol Chem* 2006;281(32): 22943-52.
- Bai SL, Campbell SE, Moore JA, Morales MC, Gerdes AM. Influence of age, growth, and sex on cardiac myocyte size and number in rats. *Anat Rec*. 1990 Feb; 226(2): 207-12.
- Baines CP, Kaiser RA, Purcell NH, Blair NS, Osinska H, Hambleton MA et al. Loss of cyclophilin D reveals a critical role for mitochondrial permeability transition in cell death. *Nature*. 2005;434(7033):658-62.
- Bamert A, Cristofanon S, Eckhardt I, Abhari BA, Kolodziej S, Häcker S et al. Histone deacetylase inhibitors sensitize glioblastoma cells to TRAIL-induced apoptosis by c-myc-mediated downregulation of cFLIP. *Oncogene*. 2012; doi: 10.1038/onc.2011.614.
- Barash Y, Calarco JA, Gao W, Pan Q, Wang X, Shai O, et al. Deciphering the splicing code. *Nature*. 2010;465:53-59.
- Berdeaux R, Goebel N, Banaszynski L, Takemori H, Wandless T, Shelton GD, Montminy M. SIK1 is a class II HDAC kinase that promotes survival of skeletal myocytes. *Nat Med* 2007;13:597-603.
- Berry JM, Cao DJ, Rothermel BA, Hill JA. Histone deacetylase inhibition in the treatment of heart disease. *Expert Opin Drug Saf*. 2008;7(1):53-67.
- Bialik S, Cryns VL, Drincic A, Miyata S, Wollowick AL, Srinivasan A, Kitsis RN. The mitochondrial apoptotic pathway is activated by serum and glucose deprivation in cardiac myocytes. *Circ Res*. 1999;85: 403-414.

References

- Bing RJ, Siegel A, Ungar I, Gilbert M. Metabolism of the human heart. II. Studies on fat, ketone and amino acid metabolism. *Am J Med* 1954;16:504-15.
- Bishopric NH, Simpson PC, Ordahl CP. Induction of the skeletal alpha-actin gene in alpha 1-adrenoceptor-mediated hypertrophy of rat cardiac myocytes. *J Clin Invest*, 1987; 80(4):1194-9.
- Black BL, Olson EN. Transcriptional control of muscle development by myocyte enhancer factor-2 (MEF2) proteins. *Annu Rev Cell Dev Biol*. 1998;14:167-96.
- Black BL, Lu J, Olson EN. The MEF2A 3' untranslated region functions as a cis-acting translational repressor. *Mol Cell Biol* 1997; 17(5):2756-63.
- Blacks J and Olson EN. Control of cardiac growth by histone acetylation/deacetylation. *Circ Res*. 2006; 98(1):15-24.
- Boatright KM, Renatus M, Scott FL, Sperandio S, Shin H, Pedersen IM, et al. A unified model for apical caspase activation. *Mol Cell*. 2003;11:529–541.
- Boheler K, Chassagne C, Martin X, Wisniewsky C, Schwartz K. Cardiac expressions of alpha- and beta-myosin heavy chains and sarcomeric alpha-actins are regulated through transcriptional mechanisms. Results from nuclear run-on assays in isolated rat cardiac nuclei. *J Biol Chem*. 1992; 267: 12 979-85.
- Boutz PL, Chawla G, Stoilov P, Black DL. MicroRNAs regulate the expression of the alternative splicing factor nPTB during muscle development. *Genes Dev*. 2007; 21(1):71-84.
- Boutz PL, Stoilov P, Li Q, Lin CH, Chawla G, Ostrow K, et al. A post-transcriptional regulatory switch in polypyrimidine tract-binding proteins reprograms alternative splicing in developing neurons. *Genes Dev*. 2007; 21:1636-1652.
- Black BL and Olson EN. Transcriptional control of muscle development by myocyte enhancer factor-2 (MEF2) proteins. *Annu Rev Cell Dev Biol*. 1998;14:167-96.
- Brilla CG, Janicki JS, Weber KT. Impaired diastolic function and coronary reserve in genetic hypertension. Role of interstitial fibrosis and medial thickening of intramyocardial coronary arteries. *Circ Res*. 1991;69(1):107-15.
- Brown JH, Martinson EA. Phosphoinositide- generated second messengers in cardiac signal transduction. *Trends Cardiovasc. Med*. 1992; 2:209–14.
- Brown GC, Borutaite V. Regulation of apoptosis by the redox state of cytochrome c. *Biochim Biophys Acta*. 2008;1777(7-8):877-81.
- Bulat N, Widmann C. Caspase substrates and neurodegenerative diseases. *Brain Res Bull*. 2009;80(4-5):251-67.
- Bushell M, Stoneley M, Kong YW, Hamilton TL, Spriggs KA, Dobbyn HC, et al. Polypyrimidine tract binding protein regulates IRES-mediated gene expression during apoptosis. *Mol. Cell* 2006;23, 401-412.
- Büttner S, Eisenberg T, Carmona-Gutierrez D, Ruli D, Knauer H, Ruckenstuhl C, et al. Endonuclease G regulates budding yeast life and death. *Mol. Cell* 2007;25, 233-246.
- Cain K, Bratton SB, Cohen GM. The Apaf-1 apoptosome: a large caspase-activating complex. *Biochimie*. 2002;84(2-3):203-14.
- Campbell NA, Williamson B, Heyden RJ. *Biology: Exploring Life*. Boston, Massachusetts: Pearson Prentice Hall. ISBN 0-13-250882-6.

References

- Chang HC, Liu LT, Hung WC. Involvement of histone deacetylation in ras-induced down-regulation of the metastasis suppressor RECK. *Cell Signal*. 2004; 16(6): 675-9.
- Chang S, McKinsey TA, Zhang CL, Richardson JA, Hill JA, Olson EN. Histone deacetylases 5 and 9 govern responsiveness of the heart to a subset of stress signals and play redundant roles in heart development. *Mol Cell Biol*. 2004;24(19):8467-76.
- Charlet-B N, Logan P, Singh G, Cooper TA. Dynamic antagonism between ETR-3 and PTB regulates cell type-specific alternative splicing. *Mol. Cell*. 2002; 9:649-658.
- Cheng W, Li B, Kajstura J, Li P, Wolin MS, Sonnenblick EH, et al. Stretch-induced programmed myocyte cell death. *J Clin Invest*. 1995; 96:2247-2259.
- Chien KR, Domian IJ, Parker KK. Cardiogenesis and the complex biology of regenerative cardiovascular medicine. *Science*. 2008;322(5907):1494-7.
- Chien KR, Knowlton KU, Zhu H, Chien S. Regulation of cardiac gene expression during myocardial growth and hypertrophy: molecular studies of an adaptive physiologic response. *FASEB J*. 1991;5(15):3037-46.
- Chin ER, Olson EN, Richardson JA, Yang Q, Humphries C, Shelton JM, et al. A calcineurin-dependent transcriptional pathway controls skeletal muscle fibre type. *GenesDev*. 1998; 12, 2499-2509.
- Chowdhury I, Tharakan B, Bhat GK. Caspase-an update. *Comp Biochem Physiol B Biochem Mol Biol*. 2008;151(1):10-27.
- Clerk A, Sugden PH. Regulation of phospholipases C and D in rat ventricular myocytes: stimulation by endothelin-1, bradykinin and phenylephrine. *J Mol Cell Cardiol*. 1997; 29:1593-604.
- Clerk A, Cole SM, Cullingford TE, Harrison JG, Jormakka M, Valks DM. Regulation of cardiac myocyte cell death. *Pharmacol Ther*. 2003;97(3):223-61.
- Coutinho-Mansfield GC, Xue Y, Zhang Y, Fu XD. TB/nPTB switch: a post-transcriptional mechanism for programming neuronal differentiation. *Genes Dev*. 2007;21(13):1573-7.
- Cote CA, Gautreau D, Denegre JM, Kress TL, Terry NA and Mowry KL. A Xenopus protein related to hnRNP I has a role in cytoplasmic RNA localization. *Mol Cell* 1999; 4, 431-437.
- Côté J, Ruiz-Carrillo A. Primers for mitochondrial DNA replication generated by endonuclease G. *Science*. 1993; 261(5122):765-9.
- Creemers EE, Sutherland LB, Oh J, Barbosa AC, Olson EN. Coactivation of MEF2 by the SAP domain proteins myocardin and MASTR. *Mol Cell*. 2006;23(1):83-96.
- Cress WD, Seto E. Histone deacetylases, transcriptional control, and cancer. *J Cell Physiol*. 2000;184(1):1-16.
- Cristopher GP. Ras, PI3-kinase and mTOR signaling in cardiac hypertrophy. *Cardiovascular Research*, 2004; 63:403-413
- Czubryt MP, Panagia V, Pierce GN. The roles of free radicals, peroxides and oxidized lipoproteins in second messenger system dysfunction. *EXS*. 1996;76:57-69.
- David KK, Sasaki M, Yu SW, Dawson TM, Dawson VL. EndoG is dispensable in embryogenesis and apoptosis. *Cell Death Differ*. 2006;13(7):1147-55.

References

- Dai DF, Hsieh EJ, Liu Y, Chen T, Beyer RP, Chin MT, Maccoss MJ, Rabinovitch PS. Mitochondrial proteome remodeling in pressure-overload induced heart failure: the role of mitochondrial oxidative stress. *Cardiovasc Res.* 2012; 93(1): 79-88.
- Day ML, Schwartz D, Wiegand RC, Stockman PT, Brunnert SR, Tolunay HE, et al. Ventricular atriopeptin. Unmasking of messenger RNA and peptide synthesis by hypertrophy or dexamethasone. *Hypertension* 1987;9(5):485-91.
- de las Fuentes L, Herrero P, Peterson LR, Kelly DP, Gropler RJ, Davila-Roman VG. Myocardial fatty acid metabolism: independent predictor of left ventricular mass in hypertensive heart disease. *Hypertension* 2003;41:83-87.
- Demontis S, Rigo C, Piccinin S, Mizzau M, Sonogo M, Fabris BC, and Maestro R. Twist is substrate for caspase cleavage and proteasome-mediated degradation. *Cell Death Differ.* 2006; 13:335-345.
- Dobbyn HC, Hill K, Hamilton TL, Spriggs KA, Pickering BM, Coldwell MJ, de Moor CH, Bushell M and Willis AE. Regulation of BAG-1 IRES-mediated translation following chemotoxic stress. *Oncogene* 2008;27, 1167- 1174
- Dodou E, Verzi MP, Anderson JP, Xu SM, Black BL. Mef2c is a direct transcriptional target of ISL1 and GATA factors in the anterior heart field during mouse embryonic development. *Development.* 2004;131(16):3931-42.
- Dorn GW and Brown JH. Gq signaling in cardiac adaptation and maladaptation. *Trends Cardiovasc Med.* 1999;9(1-2):26-34.
- Dufour CR, Wilson BJ, Huss JM, Kelly DP, Alaynick WA, Downes M, Evans RM, Blanchette M, Giguère V. Genome-wide orchestration of cardiac functions by the orphan nuclear receptors ERRalpha and gamma. *Cell Metab* 2007;5, 345-356,.
- Dunn SE, Simard AR, Bassel-Duby R, Williams RS, Michel RN. Nerve activity-dependent modulation of calcineurin signaling in adult fast and slow skeletal muscle fibers. *J Biol Chem.* 2001;276(48):45243-54.
- Dykxhoorn DM, Novina CD, Sharp PA. Killing the messenger: short RNAs that silence gene expression. *Nat Rev Mol Cell Biol.* 2003;4(6):457-67.
- Eisenberg LM, Markwald RR. Molecular regulation of atrioventricular valvuloseptal morphogenesis. *Circ Res.* 1995;77:1-6.
- Edmondson DG, Lyons GE, Martin JF, Olson EN. Mef2 gene expression marks the cardiac and skeletal muscle lineages during mouse embryogenesis. *Development.* 1994; 120(5):1251-63.
- Erdmann F, Weiwad M, Kilka S, Karanik M, Pätzelt M, Baumgrass R, et al. The novel calcineurin inhibitor CN585 has potent immunosuppressive properties in stimulated human T cells. *J Biol Chem* 2010; 285(3):1888-98.
- Farooq A, Zhou MM. Structure and regulation of MAPK phosphatases. *Cell Signal.* 2004 Jul;16(7):769-79.
- Fernando P, Kelly JF, Balazsi K, Slack RS, Megeney LA. Caspase 3 activity is required for skeletal muscle differentiation. *Proc. Natl. Acad. Sci. U. S. A.* 2002; 99: 11025-11030.
- Finck BN and Kelly DP. PGC-1 coactivators: inducible regulators of energy metabolism in health and disease. *J Clin Invest* 2006;116, 615-622.

References

- Fire A, Xu S, Montgomery MK, Kostas SA, Driver SE, Mello CC. Potent and specific genetic interference by double-stranded RNA in *Caenorhabditis elegans*. *Nature*. 1998; 391(6669):806-11.
- Fisher SA, Langille BL, Srivastava D. Apoptosis during cardiovascular development. *Circ Res*. 2000; 87(10):856-64.
- Flavell SW, Cowan CW, Kim TK, Greer PL, Lin Y, Paradis S, Griffith EC, Hu LS, Chen C, Greenberg ME. Activity-dependent regulation of MEF2 transcription factors suppresses excitatory synapse number. *Science* 2006;311:1008-1012.
- Foo RS, Mani K, Kitsis RN. Death begets failure in the heart. *J Clin Invest*. 2005; 115(3):565-71.
- Fralix TA, Heineman FW, Balaban RS. Effect of work on intracellular calcium of the intact heart. *Am J Physiol*. 1991;261(4 Suppl):54-9.
- Fujio Y, Kunisada K, Hirota H, Yamauchi-Takahara K, Kishimoto T. Signals through gp130 upregulate bcl-x gene expression via STAT1-binding cis-element in cardiac myocytes. *J Clin Invest*. 1997;99: 2898-2905.
- Fuller TF, Ghazalpour A, Aten JE, Drake TA, Lusis AJ, Horvath S. Weighted gene coexpression network analysis strategies applied to mouse weight. *Mamm Genome*. 2007; 18(6-7):463-72.
- Gama-Carvalho M, Barbosa-Morais NL, Brodsky AS, Silver PA and Carmo-Fonseca M. Genome-wide identification of functionally distinct subsets of cellular mRNAs associated with two nucleocytoplasmic-shuttling mammalian splicing factors. *Genome Biol*. 2006;7, R113.
- Gardner A, Boles RG. Is a “Mitochondrial Psychiatry” in the Future? A Review. *Curr. Psychiatry Review* 2005;1 (3): 255-271.
- Garrido C, Galluzzi L, Brunet M, Puig PE, Didelot C, Kroemer G. Mechanism of cytochrome c release from mitochondria. *Cell Death Differ*. 2006;13(9): 1423-33.
- Gil A, Sharp PA, Jamison SF, Garcia-Blanco MA. Characterization of cDNAs encoding the polypyrimidine tract-binding protein. *Genes Dev*. 1991 Jul;5(7): 1224-36.
- Gerald M. Cohen. Caspases: the executioners of apoptosis. *Biochem J*. 1997; 326 (Pt 1):1-16.
- Glaser KB, Li J, Staver MJ, Wei RQ, Albert DH, Davidsen SK. Role of class I and class II histone deacetylases in carcinoma cells using siRNA. *Biochem Biophys Res Commun*. 2003;310(2):529-36.
- Grozinger CM, Schreiber SL. Deacetylase enzymes: biological functions and the use of small-molecule inhibitors. *Chem Biol*. 2002;9(1):3-16.
- Golks A, Brenner D, Fritsch C, Krammer PH, Lavrik IN. c-FLIPR, a new regulator of death receptor-induced apoptosis. *J Biol Chem*. 2005;280(15): 14507-13.
- Gonzalez GA, Montminy MR. Cyclic AMP stimulates somatostatin gene transcription by phosphorylation of CREB at serine 133. *Cell* 1989;59:675-680.
- Graham BH, Waymire KG, Cottrell B, Trounce IA, et al. A mouse model for mitochondrial myopathy and cardiomyopathy resulting from a deficiency in the heart/muscle isoform of the adenine nucleotide translocator. *Nature Genet*. 1997;16, 226-234.
- Grunstein M. Histone acetylation in chromatin structure and transcription. *Nature*. 1997;389(6649):349-52.

References

- Ha CH, Kim JY, Zhao J, Wang W, Jhun BS, Wong C, Jin ZG. PKA phosphorylates histone deacetylase 5 and prevents its nuclear export, leading to the inhibition of gene transcription and cardiomyocyte hypertrophy. *Proc Natl Acad Sci USA* 2010; 107(35):15467-72.
- Haberland M, Johnson A, Mokalled MH, Montgomery RL, Olson EN. Genetic dissection of histone deacetylase requirement in tumor cells. *Proc Natl Acad Sci USA*. 2009; 106(19):7751-5.
- Hamburger V, Hamilton A. A series of normal stages in the development of the chick embryo. 1951. *Dev Dyn*. 1992;195(4):231-72.
- Handschin C, Choi CS, Chin S, Kim S, Kawamori D, Kurpad AJ, et al. Abnormal glucose homeostasis in skeletal muscle-specific PGC-1alpha knockout mice reveals skeletal muscle-pancreatic beta cell crosstalk. *J Clin Invest*. 2007;117(11):3463-74.
- Hannan RD, Jenkins A, Jenkins AK, Brandenburger Y. Cardiac hypertrophy: a matter of translation. *Clin Exp Pharmacol Physiol*. 2003; 30(8):517-27.
- Hannenhalli S, Putt ME, Gilmore JM, Wang J, Parmacek MS, Epstein JA. et al. transcriptional genomics associates FOX transcription factors with human heart failure. *Circulation* 2006; 114:1269-1276.
- Heinig M et al. A trans-acting locus regulates an anti-viral expression network and type 1 diabetes risk. *Nature* 2010;467, 460-464.
- Hengartner MO. The biochemistry of apoptosis. *Nature* 2000; 407 (6805): 770-6.
- Henze K, Martin W. Evolutionary biology: essence of mitochondria. *Nature* 2003;426 (6963): 127-8.
- Higazi DR, Fearnley CJ, Drawnel FM, Talasila A, Corps EM, Ritter O, McDonald F, Mikoshiba K, Bootman MD, Roderick HL. Endothelin-1-stimulated InsP3-induced Ca²⁺ release is a nexus for hypertrophic signaling in cardiac myocytes. *Mol Cell*. 2009; 33(4):472-82.
- Hollenberg M, Honbo N, Samorodin AJ. Effects of hypoxia on cardiac growth in neonatal rat. *Am J Physiol*. 1976;231(5 Pt. 1):1445-50.
- Huang JX, Potts JD, Vincent EB, Weeks DL, Runyan RB. Mechanisms of cell transformation in the embryonic heart. *Ann N Y Acad Sci*. 1995; 752:317-330.
- Huss JM and Kelly DP. Mitochondrial energy metabolism in heart failure: a question of balance. *J Clin Invest*. 2005; 115(3):547-55.
- Ikeda S, He A, Kong SW, Lu J, Bejar R, Bodyak N, et al. MicroRNA-1 negatively regulates expression of the hypertrophy-associated calmodulin and Mef2a genes. *Mol Cell Biol*. 2009; 29(8): 2193-204.
- Inserte J, Barrabés JA, Hernando V, Garcia-Dorado D. Orphan targets for reperfusion injury. *Cardiovasc Res*. 2009;83(2):169-78.
- Irvine RA, Adachi N, Shibata DK, Cassell GD, Yu K, Karanjawala ZE, Hsieh CL, Lieber MR. Generation and characterization of endonuclease G null mice. *Mol Cell Biol*. 2005; 25(1):294-302.
- Jacobson MD. Programmed cell death: a missing link is found. *Trends Cell Biol*. 1997; 7(12):467-9.
- Jalil JE, Doering CW, Janicki JS, Pick R, Shroff SG, Weber KT. Fibrillar collagen and

- myocardial stiffness in the intact hypertrophied rat left ventricle. *Circ Res* 1989; 64:1041-1050.
- Molkentin JD and Dorn II GW. Cytoplasmic signalling pathways that regulate cardiac hypertrophy. *Annu. Rev. Physiol.* 2001; 63:391-426.
- Jerkic M, Kabir MG, Davies A, Yu LX, McIntyre BA, Husain NW, et al. Pulmonary hypertension in adult Alk1 heterozygous mice due to oxidative stress. *Cardiovasc Res.* 2011;92(3):375-84.
- Johnstone RJ, Hobert O. A microRNA controlling left/right neuronal asymmetry in *Caenorhabditis elegans*. *Nature* 2003; 426: 845-845.
- Kajstura J, Cigola E, Malhotra A, Li P, Cheng W, Meggs LG, Anversa P. Angiotensin II induces apoptosis of adult ventricular myocytes *in vitro*. *J Mol Cell Cardiol.* 1997;29:859-870.
- Kalsotra A, Xiao X, Ward AJ, Castle JC, Johnson JM, Burge CB, and Cooper TA. A postnatal switch of CELF and MBNL proteins reprograms alternative splicing in the developing heart. *Proc. Natl. Acad. Sci. U. S. A.* 2008; 105:20333-20338.
- Kang PM, Haunstetter A, Aoki H, Usheva A, Izumo S. Morphological and molecular characterization of adult cardiomyocyte apoptosis during hypoxia and reoxygenation. *Circ Res.* 2000;87:118 -125.
- Kang PM, Izumo S. Apoptosis in heart: basic mechanisms and implications in cardiovascular diseases. *Trends Mol Med.* 2003; 9(4):177-82.
- Karamboulas C, Dakubo GD, Liu J, De Repentigny Y, Yutzey K, Wallace VA, Kothary R, Skerjanc IS. Disruption of MEF2 activity in cardiomyoblasts inhibits cardiomyogenesis. *J Cell Sci.* 2006;119(Pt 20):4315-21.
- Keppetipola N, Sharma S, Li Q, and Black DL. Neuronal regulation of pre-mRNA splicing by polypyrimidine tract binding proteins, PTBP1 and PTBP2. *Crit. Rev. Biochem. Mol. Biol.* 2012; 47:360-378.
- Kerr JF, Wyllie AH, Currie AR. Apoptosis: a basic biological phenomenon with wide-ranging implications in tissue kinetics. *Br J Cancer.* 1972; 26(4): 239-57.
- Kim Y, Phan D, van Rooij E, Wang DZ, McAnally J, Qi X, et al. The MEF2D transcription factor mediates stress-dependent cardiac remodeling in mice. *J Clin Invest.* 2008; 118(1): 124-32.
- Kitsis RN, Molkentin JD. Apoptotic cell death “Nixed” by an ER-mitochondrial necrotic pathway. *Proc Natl Acad Sci U S A.* 2010;107(20):9031-2.
- Knaapen MW, Davies MJ, De Bie M, Haven AJ, Martinet W, Kockx MM. Apoptotic versus autophagic cell death in heart failure. *Cardiovasc Res.* 2001; 51(2):304-12.
- Knoch KP, Meisterfeld R, Bergert H, Kolpe M, Altkruger A, Saeger HD and Solimena M. Regulation of PTB nucleocytoplasmic translocation and expression of secretory granule proteins in INS-1 cells. *Diabetologia* 2004; 47: A153.
- Kouzarides T. Acetylation: a regulatory modification to rival phosphorylation? *EMBO J.* 2000; 19(6):1176-9.
- Krown KA, Page MT, Nguyen C, Zechner D, Gutierrez V, Comstock KL, et al. Tumor necrosis factor alpha-induced apoptosis in cardiac myocytes. Involvement of the sphingolipid signaling cascade in cardiac cell death. *J Clin Invest.* 1996;98: 2854-2865.

References

- Krueger A, Schmitz I, Baumann S, Krammer PH, Kirchhoff S. Cellular FLICE-inhibitory protein splice variants inhibit different steps of caspase-8 activation at the CD95 death-inducing signaling complex. *J Biol Chem*. 2001; 276(23):20633-40.
- Kubasiak LA, Hernandez OM, Bishopric NH, Webster KA. Hypoxia and acidosis activate cardiac myocyte death through the Bcl-2 family protein BNIP3. *Proc Natl Acad Sci USA*. 2002; 99(20):12825-30.
- Kung G, Konstantinidis K, Kitsis RN. Programmed necrosis, not apoptosis, in the heart. *Circ Res*. 2011; 108(8):1017-36.
- Kuo MH, Allis CD. Roles of histone acetyltransferases and deacetylases in gene regulation. *Bioessays*. 1998; 20(8):615-26.
- Lahm A, Paolini C, Pallaoro M, Nardi MC, Jones P, Neddermann P, et al. Unraveling the hidden catalytic activity of vertebrate class IIa histone deacetylases. *Proc Natl Acad Sci USA*. 2007; 104(44): 17335-40.
- Lakhani SA, Masud A, Kuida K, Porter GA Jr, Booth CJ, Mehal WZ, et al. Caspases 3 and 7: key mediators of mitochondrial events of apoptosis. *Science*. 2006; 311(5762):847-51.
- Lamkanfi M, Festjens N, Declercq W, Vanden Berghe T, Vandenabeele P. Caspases in cell survival, proliferation and differentiation. *Cell death Differ*. 2007; 14(1):44-55.
- Lee P, Sata M, Lefer DJ, Factor SM, Walsh K, Kitsis RN. Fas pathway is a critical mediator of cardiac myocyte death and MI during ischemiareperfusion *in vivo*. *Am J Physiol Heart Circ Physiol*. 2003; 284: H456-H463.
- Lehman J, Barger PM, Kovacs A, Saffitz JE, Medeiros DM, Kelly DP. Peroxisome proliferator-activated γ coactivator-1 promotes cardiac mitochondrial biogenesis. *J. Clin. Invest*. 2000; 106 (7), 847-856.
- Lesnefsky EJ, Moghaddas S, Tandler B, Kerner J, Hoppel CL. Mitochondrial dysfunction in cardiac disease: ischemia--reperfusion, aging, and heart failure. *J Mol Cell Cardiol*. 2001;33(6):1065-89.
- Le Sommer C, Lesimple M, Mereau A, Menoret S, Allo MR and Hardy S. PTB regulates the processing of a 3'-terminal exon by repressing both splicing and polyadenylation. *Mol. Cell. Biol*. 2005; 25, 959-9607.
- Leu M, Ehler E, Perriard JC. Characterisation of postnatal growth of the murine heart. *Anat Embryol (Berl)*. 2001; 204(3):217-24.
- Li F, Wang X, Capasso JM, Gerdes AM. Rapid transition of cardiac myocytes from hyperplasia to hypertrophy during postnatal development. *J Mol Cell Cardiol*. 1996; 28(8):1737-46.
- Li LY, Luo X, Wang X. Endonuclease G is an apoptotic DNase when released from mitochondria. *Nature* 2001; 412, 95-99.
- Li Y, Huang TT, Carlson EJ, Melov S, Ursell PC, Olson JL, Noble LJ, Yoshimura MP, Berger C, Chan PH, Wallace DC, Epstein CJ. Dilated cardiomyopathy and neonatal lethality in mutant mice lacking manganese superoxide dismutase. *Nature Genet*. 1995; 11, 376-381.
- Lin Q, Schwarz J, Bucana C, Olson EN. Control of mouse cardiac morphogenesis and myogenesis by transcription factor MEF2C. *Science*. 1997; 276 (5317): 1404-7.

- Liu J, Wang C, Murakami Y, Gong G, Ishibashi Y, Prody C, Ochiai K, et al. Mitochondrial ATPase and high-energy phosphates in failing hearts. *Am J Physiol Heart Circ Physiol* 2001; 281:H1319–H1326.
- Liu N, Olson EN. Coactivator control of cardiovascular growth and remodeling. *Curr Opin Cell Biol*. 2006;18(6):715-22.
- Liu N, Williams AH, Kim Y, McAnally J, Bezprozvannaya S, Sutherland LB, Richardson JA, Bassel-Duby R, Olson EN. An intragenic MEF2-dependent enhancer directs muscle-specific expression of microRNAs 1 and 133. *Proc Natl Acad Sci USA* 2007; 104:20844-20849.
- Llorian M, Schwartz S, Clark TA, Hollander D, Tan LY, Spellman R, Dordon A, Schweitzer AC, de la Grange P, Ast G, Smith CW. Position-dependent alternative splicing activity revealed by global profiling of alternative splicing events regulated by PTB. *Nat Struct Mol Biol*. 2010;17(9):1114-23.
- Llorian M, and Smith CW. Decoding muscle alternative splicing. *Curr. Opin. Genet. Dev.* 2011; 21:380-37.
- Locksley RM, Killeen N, Lenardo MJ. The TNF and TNF receptor superfamilies: integrating mammalian biology. *Cell*. 2001;104(4):487-501.
- Lopez-Neblina F, Toledo AH, Toledo-Pereyra LH. Molecular biology of apoptosis in ischemia and reperfusion. *J Invest Surg*. 2005;18(6):335-50.
- Lorell, B. H. & Carabello, B. A. Left ventricular hypertrophy: pathogenesis, detection, and prognosis. *Circulation* 2000; 102, 470-479.
- Lu J, McKinsey TA, Zhang CL, Olson EN. Regulation of skeletal myogenesis by association of the MEF2 transcription factor with class II histone deacetylases. *Mol Cell*. 2000; 6(2):233-44.
- Lu J, McKinsey TA, Nicol RL, Olson EN. Signal-dependent activation of the MEF2 transcription factor by dissociation from histone deacetylases. *Proc Natl Acad Sci USA* 2000; 97(8):4070-5.
- Maejima Y, Kuroda J, Matsushima S, Ago T, Sadoshima J. Regulation of myocardial growth and death by NADPH oxidase. *J Mol Cell Cardiol*. 2011;50(3): 408-16.
- Makeyev EV, Zhang J, Carrasco MA, Maniatis T. The MicroRNA imR-124 promotes neuronal differentiation by triggering brain-specific alternative pre-mRNA splicing. *Mol. Cell*. 2007; 27(3):435-48.
- Makhlouf AA, Namboodiri AM, McDermott PJ. Transcriptional regulation of the rat eIF4E gene in cardiac muscle cells: The role of specific elements in the promoter region. *Gene* 2001; 267: 1-12.
- Malizia AP, Wang DZ. MicroRNAs in cardiomyocyte development. *Wiley Interdiscip Rev Syst Biol Med*. 2011; 3(2):183-90.
- Martin JF, Miano JM, Hustad CM, Copeland NG, Jenkins NA, Olson EN. A Mef2 gene that generates a muscle-specific isoform via alternative mRNA splicing. *Mol Cell Biol*. 1994; 14(3):1647-56.
- McBride HM, Neuspiel M, Wasiak S. Mitochondria: more than just a powerhouse. *Curr. Biol*. 2006; 16 (14): R551.

References

- McDonough PM, Brown JH, Glembotski CC. Phenylephrine and endothelin differentially stimulate cardiac PI hydrolysis and ANF expression. *Am. J. Physiol. Heart Circ. Physiol.* 1987; 264:H625–H30.
- McDermott-Roe C, Ye J, Ahmed R, Sun XM, Serafin A, Ware J, et al. Endonuclease G is a novel determinant of cardiac hypertrophy and mitochondrial function. *Nature.* 2011; 478(7367):114-8.
- McGavock JM, Victor RG, Unger RH, Szczepaniak LS. Adiposity of the heart, revisited. *Ann Intern Med* 2006; 144, 517-524.
- McKinsey TA, Olson EN. Toward transcriptional therapies for the failing heart: chemical screens to modulate genes. *J Clin Invest.* 2005;115(3):538-46.
- McKinsey TA, Zhang CL, Lu J, Olson EN. Signal-dependent nuclear export of a histone deacetylase regulates muscle differentiation. *Nature*;408: 106-111.
- McKinsey TA, Zhang CL, Olson EN. MEF2 : a calcium-dependent regulator of cell division, differentiation and death. *Trends Biochem Sci* 2002; 27(1):40-7.
- Czubryt MP and Olson EN. Balancing contractility and energy production: the role of myocyte enhancer factor 2 (MEF2) in cardiac hypertrophy. *Recent Prog Horm Res.* 2004; 59:105-24.
- Miñana JB, Gómez-Cambronero L, Lloret A, Pallardó FV, Del Olmo J, Escudero A, Rodrigo JM, Pellín A, et al. Mitochondrial oxidative stress and CD95 ligand: a dual mechanism for hepatocyte apoptosis in chronic alcoholism. *Hepatology.* 2002;35(5):1205-14.
- Miska EA, Karlsson C, Langley E, Nielsen SJ, Pines J, Kouzarides T. HDAC4 deacetylase associates with and represses the MEF2 transcription factor. *EMBO J.* 1999; 18(18):5099-107.
- Mitchell SA, Brown EC, Coldwell MJ, Jackson RJ, Willis AE. Protein factors requirements of the Apaf-1 internal ribosome entry segment: roles of polypyrimidine tract binding protein and upstream of N-ras. *Mol. Cell. Biol.* 2011; 21(10):3364-74.
- Mitsiades CS, Mitsiades NS, McMullan CJ, Poulaki V, Shringarpure R, Hideshima T, Akiyama M, Chauhan D, Munshi N, Gu X, Bailey C, Joseph M, Libermann TA, Richon VM, Marks PA, Anderson KC. Transcriptional signature of histone deacetylase inhibition in multiple myeloma: biological and clinical implications. *Proc Natl Acad Sci U S A.* 2004; 101(2):540-5.
- Molkentin JD, Firulli AB, Black BL, Martin JF, Hustad CM, Copeland N, Jenkins N, Lyons G, Olson EN. MEF2B is a potent transactivator expressed in early myogenic lineages. *Mol Cell Biol.* 1996; 16(7):3814-24.
- Molkentin JD, Olson EN. Combinatorial control of muscle development by basic helix-loop-helix and MADS-box transcription factors. *Proc Natl Acad Sci USA* 1996; 93(18):9366-73.
- Molkentin JD, Lu JR, Antos CL, Markham B, Richardson J, Robbins J, Grant SR, Olson EN. A calcineurin-dependent transcriptional pathway for cardiac hypertrophy. *Cell.* 1998; 93:215-228.
- Molkentin JD, Li L, Olson EN. Phosphorylation of the MADS-Box transcription factor MEF2C enhances its DNA binding activity. *J Biol Chem.* 1996; 271(29):17199-204.
- Montgomery RL, Hsieh J, Barbosa AC, Richardson JA, Olson EN. Histone deacetylases 1

References

- and 2 redundantly regulate cardiac morphogenesis, growth, and contractility. *Genes Dev.* 2007; 21:1790-1802.
- Monti J, Fischer J, Paskas S, Heinig M, Schulz H, Gösele C, et al. Soluble epoxide hydrolase is a susceptibility factor for heart failure in a rat model of human disease. *Nat Genet.* 2008 May;40(5):529-37.
- Mukhopadhyay P, tajesh M, Hasko G, Hawkins BJ, Madesh M, Pacher P. Simultaneous detection of apoptosis and mitochondrial superoxide production in live cells by flow cytometry and confocal microscopy. *Nat Protoc* 2007; 2:2295-2301.
- Mulligan GJ, Guo W, Wormsley S, Helfman DM. Polypyrimidine tract binding protein interacts with sequences involved in alternative splicing of beta-tropomyosin pre-mRNA. *J Biol Chem* 1992;267: 25480-25487.
- Murray TV, McMahon JM, Howley BA, Stanley A, Ritter T, Mohr A, Zwacka R, and Fearnhead HO. A non-apoptotic role for caspase-9 in muscle differentiation. *J. Cell Sci.* 2008; 121:3786-3793.
- Nagatomo Y, Carabello BA, Hamawaki M, Nemoto S, Matsuo T, McDermott PJ. Translational mechanisms accelerate the rate of protein synthesis during canine pressure-overload hypertrophy. *Am. J. Physiol.* 1999; 277: H2176-84.
- Naya FJ, Black BL, Wu H, Bassel-Duby R, Richardson JA, Hill JA, Olson EN. Mitochondrial deficiency and cardiac sudden death in mice lacking the MEF2A transcription factor. *Nat Med.* 2002; 8(11):1303-9.
- Naya FJ, Wu C, Richardson JA, Overbeek P, Olson EN. Transcriptional activity of MEF2 during mouse embryogenesis monitored with a MEF2-dependent transgene. *Development* 1999; 126(10):2054-52.
- Neely JR, Rovetto MJ, Oram JF. Myocardial utilization of carbohydrate and lipids. *Prog Cardiovasc Dis* 1972;15:289–329.
- Niu Z, Li A, Zhang SX, Schwartz RJ. Serum response factor micromanaging cardiogenesis. *Curr Opin Cell Biol* 2007; 19:618-627.
- Oh YL, Hahm B, Kim YK, Lee HK, Lee JW, Song O, et al. Determination of functional domains in polypyrimidine-tract-binding protein. *Biochem J.* 1998;331 (Pt 1): 169-75.
- Ohno M, Takemura G, Ohno A, Misao J, Hayakawa Y, Minatoguchi S, et al. "Apoptotic" myocytes in infarct area in rabbit hearts may be oncotic myocytes with DNA fragmentation: analysis by immunogold electron microscopy combined with in situ nick end-labeling. *Circulation.* 1998; 98(14):1422-30.
- Ojamaa K, Petrie J, Balkman C, Hong C, Klein I. Posttranscriptional modification of myosin heavy-chain gene expression in the hypertrophied rat myocardium. *Proc. Natl Acad. Sci. USA* 1994; 91: 3468-72.
- Olson EN. A decade of discoveries in cardiac biology. *Nat Med.* 2004; 10(5): 467-74.
- Olson EN. Gene regulatory networks in the evolution and development of the heart. *Science.* 2006; 313(5795):1922-7.
- Olson EN, Molkentin JD. Prevention of cardiac hypertrophy by calcineurin inhibition: hope or hype? *Circ Res.* 1999; 84:623-632.
- Olson EN and Williams RS. Remodeling muscles with calcineurin. *BioEssays* 2000; 22,510-519.
- Ornatsky OI, Cox DM, Tangirala P, Andreucci JJ, Quinn ZA, Wrana JL et al.,

References

- Post-translational control of the MEF2A transcriptional regulatory protein. *Nucleic Acids Res.* 1999; 27(13):2646-54.
- Penney DG, Robinson MC. Effects of verapamil and carbon monoxide on blood pressure and heart mass in the spontaneously hypertensive rat. *Eur J Pharmacol.* 1990; 182(1):29-36.
- Pérez I, Lin CH, McAfee JG, Patton JG. Mutation of PTB binding sites causes misregulation of alternative 3' splice site selection *in vivo*. *RNA.* 1997; 3:764-778.
- Petretto E, Sarwar R, Grieve I, Lu H, Kumaran MK, Muckett PJ, et al. Integrated genomic approaches implicate osteoglycin (Ogn) in the regulation of left ventricular mass. *Nat Genet* 2008; 40, 546-552.
- Plesca D, Mazumder S, Gama V, Matsuyama S, Almasan A. A C-terminal fragment of Cyclin E, generated by caspase-mediated cleavage, is degraded in the absence of a recognizable phosphodegron. *J. Biol. Chem* 2008; 283:30796-30803.
- Post WS, Larson MG, Myers RH, Galderisi M, Levy D. Heritability of left ventricular mass: the Framingham Heart Study. *Hypertension* 1997; 30, 1025-1028.
- Potthoff MJ, Olson EN. MEF2: a central regulator of diverse developmental programs. *Development.* 2007; 134(23):4131-40.
- Proud CG. The multifaceted role of mTOR in cellular stress responses. *DNA Repair (Amst).* 2004 Aug-Sep;3(8-9):927-34.
- Rakusan K, Korecky B. Regression of cardiomegaly induced in newborn rats. *Can J Cardiol.* 1985; 1(3):217-22.
- Ramachandran B, Yu G, Li S, Zhu B, Gulick T. Myocyte enhancer factor 2A is transcriptionally autoregulated. *J Biol Chem.* 2008; 283(16):10318-29.
- Randle PJ, Garland PB, Hales CN, Newsholme EA. The glucose fatty-acid cycle. Its role in insulin sensitivity and the metabolic disturbances of diabetes mellitus. *Lancet* 1963; 1:785-9.
- Regula KM, Kirshenbaum LA. Apoptosis of ventricular myocytes: a means to an end. *J Mol Cell Cardiol.* 2005; 38(1):3-13.
- Renatus M, Stennicke HR, Scott FL, Liddington RC, Salvesen GS. Dimer formation drives the activation of the cell death protease caspase 9. *Proc Natl Acad Sci U S A.* 2001; 98:14250-14255.
- Reyes R, Izquierdo JM. The RNA-binding protein PTB exerts translational control on 3'-untranslated region of the mRNA for the ATP synthase beta-subunit. *Biochem Biophys Res Commun.* 2007; 357(4):1107-12.
- Rodríguez-Sinovas A, Abdallah Y, Piper HM, Garcia-Dorado D. Reperfusion injury as a therapeutic challenge in patients with acute myocardial infarction. *Heart Fail Rev.* 2007; 12(3-4):207-16.
- Sadoshima J, Izumo S. Signal transduction pathways of angiotensin II--induced c-fos gene expression in cardiac myocytes *in vitro*. Roles of phospholipid-derived second messengers. *Circ Res.* 1993; 73(3):424-38.
- Sakamaki K, Inoue T, Asano M, Sudo K, Kazama H, Sakagami J et al. Ex vivo whole-embryo culture of caspase-8-deficient embryos normalize their aberrant phenotypes in the developing neural tube and heart. *Cell Death Differ.* 2002; 9(11):1196-206.
- Sakuma K, Yamaguchi A. The functional role of calcineurin in hypertrophy, regeneration, and

- disorders of skeletal muscle. *J Biomed Biotechnol.* 2010; 2010: 721219.
- Sanchis D, Mayorga M, Ballester M, Comella JX. Lack of Apaf-1 expression confers resistance to cytochrome c-driven apoptosis in cardiomyocytes. *Cell Death Differ.* 2003;10(9):977-86.
- Sans MD, Williams JA. Calcineurin is required for translational control of protein synthesis in rat pancreatic acini. *Am J Physiol Cell Physiol.* 2004; 287(2):C310-9.
- Sartorelli V, Huang J, Hamamori Y, Kedes L. Molecular mechanisms of myogenic coactivation by p300: direct interaction with the activation domain of MyoD and with the MADS box of MEF2C. *Mol Cell Biol.* 1997; 17(2):1010-26.
- Sawa H, Murakami H, Ohshima Y, Sugino T, Nakajyo T, Kisanuki T, et al. Histone deacetylase inhibitors such as sodium butyrate and trichostatin A induce apoptosis through an increase of the bcl-2-related protein Bad. *Brain Tumor Pathol.* 2001; 18(2):109-14.
- Sawicka K, Bushell M, Spriggs KA, Willis AE. Polypyrimidine-tract-binding protein: a multifunctional RNA-binding protein. *Biochem Soc Trans.* 2008; 36(Pt 4):641-7.
- Schwartz RJ, Olson EN. Building the heart piece by piece: modularity of cis-elements regulating Nkx2-5 transcription. *Development.* 1999;126(19):4187-92.
- Selvetella G, Hirsch E, Notte A, Tarone G, Lembo G. Adaptive and maladaptive hypertrophic pathways: points of convergence and divergence. *Cardiovasc Res.* 2004; 63(3):373-80.
- Shizukuda Y, Buttrick PM, Geenen DL, Borczuk AC, Kitsis RN, Sonnenblick EH. beta-adrenergic stimulation causes cardiocyte apoptosis: influence of tachycardia and hypertrophy. *Am J Physiol.* 1998;275:H961-H968.
- Shore P, Sharrocks AD. The MADS-box family of transcription factors. *Eur J Biochem.* 1995; 229(1):1-13.
- Shubeita HE, McDonough PM, Harris AN, Knowlton KU, Glembotwski CC, et al. Endothelin induction of inositol phospholipid hydrolysis, sarcomere assembly and cardiac gene expression in ventricular myocytes: a paracrine mechanism for myocardial cell hypertrophy. *J. Biol. Chem.* 1990;265:20555-62.
- Simpson P, McGrath A, Savion S. Myocyte hypertrophy in neonatal rat heart cultures and its regulation by serum and by catecholamines. *Circ Res* 1982; 51(6):787-801.
- Smith G, Wermuth UD, Young DJ, White JM. Proton transfer versus nontransfer in compounds of the diazo-dye precursor 4-(phenyldiazenyl) aniline (aniline yellow) with strong organic acids: the 5-sulfosalicylate and the dichroic benzenesulfonate salts, and the 1:2 adduct with 3,5-dinitrobenzoic acid. *Acta Crystallogr C.* 2009;65(Pt 10):0543-8.
- Song Y, Tzima E, Bassili G, Trusheim H, Linder M, Preissner KT, Niepmann M. Evidence for an RNA chaperone function of polypyrimidine tract-binding protein in picornavirus translation. *RNA* 2005; 11, 1809-1824.
- Sorrentino RP, Gajewski KM, Schulz RA. GATA factors in *Drosophila* heart and blood cell development. *Semin Cell Dev Biol.* 2005;16(1):107-16.
- Southby J, Gooding C, Smith CW. Polypyrimidine tract binding protein functions as a repressor to regulate alternative splicing of alpha-actinin mutually exclusive exons. *Mol. Cell. Biol.* 1999; 19:2699-2711.
- Spellman R, Smith CW. Novel modes of splicing repression by PTB. *Trends Biochem Sci.*

- 2006;31(2):73-6.
- Spriggs KA, Mitchell SA, Willis AE. Investigation of interactions of polypyrimidine tract-binding protein with artificial internal ribosome entry segments. *Biochem Soc Trans.* 2005;33(Pt 6):1483-6.
- Srivastava D. Making or breaking the heart: from lineage determination to morphogenesis. *Cell.* 2006;126(6):1037-48.
- Stennicke HR, Deveraux QL, Humke EW, Reed JC, Dixit VM, Salvesen GS. Caspase-9 can be activated without proteolytic processing. *J Biol Chem.* 1999; 274:8359-8362.
- Stewart AA, Ingebritsen TS, Manalan A, Klee CB, Cohen P. Discovery of a Ca²⁺- and calmodulin-dependent protein phosphatase: probable identity with calcineurin (CaM-BP80). *FEBS Lett.* 1982;137(1):80-4.
- Suzuki E, Guo K, Kolman M, Lu J, Bejar R, Bodyak N, et al. MicroRNA-1 negatively regulates expression of the hypertrophy-associated calmodulin and Mef2a genes. *Mol Cell Biol* 2009; 29(8):2193-204.
- Taegtmeyer H, Golfman L, Sharma S, Razeghi P, van Arsdall M. Linking gene expression to function: metabolic flexibility in the normal and diseased heart. *Ann NY Acad Sci* 2004;1015:202-13.
- Tanaka M, Ito H, Adachi S, Akimoto H, Nishikawa T, Kasajima T, et al. Hypoxia induces apoptosis with enhanced expression of Fas antigen messenger RNA in cultured neonatal rat cardiomyocytes. *Circ Res.* 1994;75: 426-433.
- Tatsumi T, Ahiraishi J, Keira N, Akashi K, Mano A, Yamanaka S, et al. Intracellular ATP is required for mitochondrial apoptotic pathways in isolated hypoxic rat cardiac myocytes. *Cardiovasc Res* 2003; 59:428-440.
- Taylor SW, Fahy E, Zhang B, Glenn GM, Warnock DE, Wiley S, et al. "Characterization of the human heart mitochondrial proteome". *Nat Biotechnol.* 2003;21(3):281-6.
- Thornberry NA, Lazebnik Y. Caspases: enemies within. *Science.* 1998; 281(5381):1312-6.
- Tillmar L and Welsh N. Hypoxia may increase rat insulin mRNA levels by promoting binding of the polypyrimidine tract-binding protein (PTB) to the pyrimidine-rich insulin mRNA 3'-untranslated region. *Mol. Med.* 2002;8:263-272.
- Tuxworth Jr WJ, Wada H, Ishibashi Y, McDermott PJ. Role of load in regulating eIF-4F complex formation in adult feline cardiocytes. *Am. J. Physiol.* 1999; 277: H1273-82.
- van den Heuvel AF, van Veldhuisen DJ, van der Wall EE, Blanksma PK, Siebelink HM, Vaalburg WM, et al. Regional myocardial blood flow reserve impairment and metabolic changes suggesting myocardial ischemia in patients with idiopathic dilated cardiomyopathy. *J Am Coll Cardiol* 2000; 35:19-28.
- van der Vusse GJ, Glatz JF, Stam HC, Reneman RS. Fatty acid homeostasis in the normoxic and ischemic heart. *Physiol Rev* 1992; 72:881-940.
- van Oort RJ, van Rooij E, Bourajjaj M, Schimmel J, Jansen MA, van der Nagel R, et al. MEF2 activates a genetic program promoting chamber dilation and contractile dysfunction in calcineurin-induced heart failure. *Circulation* 2006; 114(4):298-308.
- Varfolomeev EE, Schuchmann M, Luria V, Chiannilkulchai N, Beckmann JS, et al. Targeted disruption of the mouse Caspase 8 gene ablates cell death induction by the TNF receptors, Fas/Apo1, and DR3 and is lethal prenatally. *Immunity* 1998; 9(2):267-76.

References

- Vasan RS, Glazer NL, Felix JF, Lieb W, Wild PS, Felix SB et al. Genetic variants associated with cardiac structure and function: a meta-analysis and replication of genome-wide association data. *JAMA* 2009; 302(2):168-78.
- Vega RB, et al. Protein kinases C and D mediate agonist-dependent cardiac hypertrophy through nuclear export of histone deacetylase 5. *Mol Cell Biol* 2004;24: 8374-8385.
- Verdin E, Dequiedt F, Kasler HG. Class II histone deacetylases: versatile regulators. *Trends Genet.* 2003; 19(5):286-93.
- Verzi MP, Agarwal P, Brown C, McCulley DJ, Schwarz JJ, Black BL. The transcription factor MEF2C is required for craniofacial development. *Dev Cell.* 2007; 12(4):645-52.
- von Harsdorf R, Li PF, Dietz R. Signaling pathways in reactive oxygen species-induced cardiomyocyte apoptosis. *Circulation.* 1999;99:2934-2941.
- Wagner EJ, Garcia-Blanco MA. Polypyrimidine tract binding protein antagonizes exon definition. *Mol Cell Biol.* 2001; 21(10):3281-8.
- Wallace, D. Mitochondria defects in cardiomyopathy and neuromuscular disease. *Amer. Heart J.* 2000; 139(2 Pt 3):S70-85.
- Wang J, Wilhelmsson H, Graff C, Li H, Oldfors A, Rustin P et al. Dilated cardiomyopathy and atrioventricular conduction blocks induced by heart-specific inactivation of mitochondrial DNA gene expression. *Nature Genet.* 1999; 21(1):133-7.
- Wang L, Ma W, Markovich R, Chen JW, Wang PH. Regulation of cardiomyocyte apoptotic signaling by insulin-like growth factor I. *Circ Res.* 1998; 83: 516-522.
- Webster KA, Discher DJ, Kaiser S, Hernandez O, Sato B, Bishopric NH. Hypoxia-activated apoptosis of cardiac myocytes requires reoxygenation or a pH shift and is independent of p53. *J Clin Invest.* 1999; 104: 239-252.
- Wong C and Marwick TH. Obesity cardiomyopathy: pathogenesis and pathophysiology. *Nat Clin Pract Cardiovasc Med.* 2007; 4(8):436-43.
- Wu H, Naya FJ, McKinsey TA, Mercer B, Shelton JM, Chin ER, Simard AR, Michel RN, Bassel-Duby R, Olson EN, Williams RS. MEF2 responds to multiple calcium-regulated signals in the control of skeletal muscle fiber type. *EMBO J.* 2000; 19(9):1963-73.
- Wu H, Rothermel B, Kanatous S, Rosenberg P, Naya FJ, Shelton JM, Hutcheson KA, DiMaio JM, Olson EN, Bassel-Duby R, Williams RS. Activation of MEF2 by muscle activity is mediated through a calcineurin-dependent pathway. *EMBO J.* 2001; 20(22):6414-23.
- Wu R, Wyatt E, Chawla K, Tran M, Ghanefar M, Laakso M, et al. Hexokinase II knockdown results in exaggerated cardiac hypertrophy via increased ROS production. *EMBO Mol Med.* 2012 Apr 20. doi: 10.1002/emmm.201200240. Epub ahead of print
- Wu Z, Puiqserver P, Andersson U, Zhang C, Adelmant G, Mootha V, et al. Mechanisms controlling mitochondrial biogenesis and respiration through the thermogenic coactivator PGC-1. *Cell.* 1999; 98(1):115-24.
- Xu J, Gong NL, Bodi I, Aronow BJ, Backx PH, Molkenin JD. Myocyte enhancer factors 2A and 2C induce dilated cardiomyopathy in transgenic mice. *J Biol Chem.* 2006; 281(14):9152-62.
- Yeh WC, Itie A, Elia AJ, Ng M, Shu HB, et al. Requirement for Casper (c-FLIP) in regulation of death receptor-induced apoptosis and embryonic development. *Immunity* 2000; 12:633-642.

- Youn HD, Liu JO. Cabin1 represses MEF2-dependent Nur77 expression and T cell apoptosis by controlling association of histone deacetylases and acetylases with MEF2. *Immunity*. 2000; 13(1):85-94.
- Young LH, Renfu Y, Russell R, Hu X, Caplan M, Ren J, et al. Low-flow ischemia leads to translocation of canine heart GLUT-4 and GLUT-1 glucose transporters to the sarcolemma *in vivo*. *Circulation* 1997; 95: 415-422.
- Young LH, Russell RR 3rd, Yin R, Caplan MJ, Ren J, Bergeron R, et al. Regulation of myocardial glucose uptake and transport during ischemia and energetic stress. *Am J Cardiol* 1999; 83:25H-30H.
- Yu YT, Breitbart RE, Smoot LB, Lee Y, Mahdavi V, Nadal-Ginard B. Human myocyte-specific enhancer factor 2 comprises a group of tissue-restricted MADS box transcription factors. *Genes Dev*. 1992;6(9):1783-98.
- Zak R. Cell proliferation during cardiac growth. *Am J Cardiol*. 1973;31(2):211-9.
- Zhao M, New L, Kravchenko VV, Kato Y, Gram H, di Padova F, Olson EN, Ulevitch RJ, Han J. Regulation of the MEF2 family of transcription factors by p38. *Mol Cell Biol*. 1999; 19(1):21-30.
- Zhang CL, McKinsey TA, Chang S, Antos CL, Hill JA, Olson EN. Class II histone deacetylases act as signal-responsive repressors of cardiac hypertrophy. *Cell*. 2002; 110(4):479-88.
- Zhang J, Bahi N, Llovera M, Comella JX, Sanchis D. Polypyrimidine tract binding proteins (PTB) regulate the expression of apoptotic genes and susceptibility to caspase-dependent apoptosis in differentiating cardiomyocytes. *Cell Death Differ*. 2009; 16(11):1460-8.
- Zhang J, Bahi N, Zubiaga AM, Comella JX, Llovera M, Sanchis D. Developmental silencing and independency from E2F of apoptotic gene expression in postmitotic tissues. *FEBS Lett*. 2007; 581(30):5781-6.
- Zhang J, Dong M, Li L, Fan Y, Pathre P, Dong J, Lou D, Wells JM, Olivares-Villagómez D, Van Kaer L, Wang X, Xu M. Endonuclease G is required for early embryogenesis and normal apoptosis in mice. *Proc Natl Acad Sci USA*. 2003; 100(26):15782-7.
- Zhang J, Li X, Mueller M, Wang Y, Zong C, Deng N, et al. Systematic characterization of the murine mitochondrial proteome using functionally validated cardiac mitochondria. *Proteomics* 2008; 8 (8): 1564-1575.
- Zhang J, Liem DA, Mueller M, Wang Y, Zong C, Deng N, et al. Altered Proteome Biology of Cardiac Mitochondria Under Stress Conditions. *J. Proteome Res* 2008; 7(6):2204-14.
- Zhang J, Ye J, Altafaj A, Cardona M, Bahi N, Llovera M, Cañas X, Cook SA, Comella JX, Sanchis D. EndoG links Bnip3-induced mitochondrial damage and caspase-independent DNA fragmentation in ischemic cardiomyocytes. *PLoS One* 2010; 6(3):e17998.
- Zhou X, Marks PA, Rifkind RA, Richon VM. Cloning and characterization of a histone deacetylase, HDAC9. *Proc Natl Acad Sci USA*. 2001; 98(19): 10572-7.
- Zhu B, Ramachandran B, Gulick T Alternative premRNA splicing governs expression of conserved acidic transactivation domain in myocyte enhancer factor 2 factors in striated muscle and brain. *J Biol Chem* 2005; 280: 28749-28760.

Annex

Annex 1. Endonuclease G is a novel determinant of cardiac hypertrophy and mitochondrial function

LETTER

doi:10.1038/nature10490

Endonuclease G is a novel determinant of cardiac hypertrophy and mitochondrial function

Chris McDermott-Roe¹, Junmei Ye², Rizwan Ahmed¹, Xi-Ming Sun¹, Anna Serafin³, James Ware¹, Leonardo Bottolo¹, Phil Muckett¹, Xavier Cañas³, Jisheng Zhang², Glenn C. Rowe⁴, Rachel Buchan¹, Han Lu¹, Adam Braithwaite¹, Massimiliano Mancini⁵, David Hauton⁶, Ramon Martí⁷, Elena García-Arumi⁷, Norbert Hubner^{8,9}, Howard Jacob¹⁰, Tadao Serikawa¹¹, Vaclav Zidek¹², Frantisek Papousek¹², Frantisek Kolar¹², Maria Cardona², Marisol Ruiz-Meana¹³, David García-Dorado¹³, Joan X. Comella^{14,15}, Leanne E. Felkin¹⁶, Paul J. R. Barton^{16,17}, Zoltan Arany⁴, Michal Pravenec¹², Enrico Petretto^{1,18}, Daniel Sanchis² & Stuart A. Cook^{1,17}

Left ventricular mass (LVM) is a highly heritable trait¹ and an independent risk factor for all-cause mortality². So far, genome-wide association studies have not identified the genetic factors that underlie LVM variation³, and the regulatory mechanisms for blood-pressure-independent cardiac hypertrophy remain poorly understood^{4,5}. Unbiased systems genetics approaches in the rat^{6,7} now provide a powerful complementary tool to genome-wide association studies, and we applied integrative genomics to dissect a highly replicated, blood-pressure-independent LVM locus on rat chromosome 3p. Here we identified endonuclease G (*Endog*), which previously was implicated in apoptosis⁸ but not hypertrophy, as the gene at the locus, and we found a loss-of-function mutation in *Endog* that is associated with increased LVM and impaired cardiac function. Inhibition of *Endog* in cultured cardiomyocytes resulted in an increase in cell size and hypertrophic biomarkers in the absence of pro-hypertrophic stimulation. Genome-wide network analysis unexpectedly implicated *ENDOG* in fundamental mitochondrial processes that are unrelated to apoptosis. We showed direct regulation of *ENDOG* by *ERR-α* and *PGC1α* (which are master regulators of mitochondrial and cardiac function)^{9–11}, interaction of *ENDOG* with the mitochondrial genome and *ENDOG*-mediated regulation of mitochondrial mass. At baseline, the *Endog*-deleted mouse heart had depleted mitochondria, mitochondrial dysfunction and elevated levels of reactive oxygen species, which were associated with enlarged and steatotic cardiomyocytes. Our study has further established the link between mitochondrial dysfunction, reactive oxygen species and heart disease and has uncovered a role for *Endog* in maladaptive cardiac hypertrophy.

Increased LVM is a clinically important trait that independently predicts the risk of heart failure, sudden death and all-cause mortality². Although LVM is a heritable complex trait¹, large genome-wide association studies have not identified LVM-associated genes³. Blood-pressure-dependent regulation of LVM, which is perhaps surprisingly limited⁷, has been studied extensively in model systems and acts through well-characterized and overlapping signalling modules¹². By contrast, the pathways that underlie blood-pressure-independent cardiac

hypertrophy, which is commonly seen in obesity and type 2 diabetes and is associated with mitochondrial dysfunction and lipotoxicity^{4,5}, remain largely unknown. Here we took advantage of the recent step changes in integrative systems genetics approaches in the rat^{6,7} to dissect a blood-pressure-independent cardiac mass quantitative trait locus (QTL) and to identify the causative gene and underlying mechanism.

The rat is unique for the study of cardiac mass, with more than 75 QTLs identified for this trait (Rat Genome Database; <http://rgd.mcw.edu/>). Rat chromosome 3p (0–25 megabase pairs (Mbp)) contains a highly replicated and blood-pressure-independent QTL for cardiac mass, which has been mapped in crosses of the spontaneously hypertensive rat (SHR) or the SHR stroke prone (SHRSP) rat to Wistar Kyoto (WKY) or salt sensitive (SS) rats^{13,14}. To dissect this locus genetically, we generated an F₂ intercross of SHR and Brown Norway (BN) strains and further replicated the LVM QTL (logarithm of odds (LOD) = 4.2) (Fig. 1a). We confirmed the blood-pressure-independent QTL effect in a congenic strain (SHR.BN-(3L)) that had a lower LVM and smaller cardiomyocytes than the SHR strain (Fig. 1b, c), and we refined the QTL region (to chromosome 3, 6.4–11.2 Mbp) using a second congenic strain (SHR.BN-(3S)) (Supplementary Fig. 1). In the F₂ cross, in the SHR.BN-(3L) strain and in previous experimental crosses^{13,14}, the SHR allele at the locus was associated with increased cardiac mass, and this effect was blood pressure independent (Fig. 1a, b, d). Functional assessment *in vivo* revealed that the SHR.BN-(3L) strain had better cardiac performance at baseline and after stimulation, compared with the SHR strain (Supplementary Fig. 1). These data show that an SHR allele at the cardiac mass QTL on rat chromosome 3p increases LVM and adversely affects cardiac function.

We used the new genotypes generated in our F₂ cross and those from previous experiments^{13,14} to refine the QTL region, and we identified five distinct loci (spanning 750 kilobase pairs in total) that cosegregated with the haplotypes associated with LVM variation (Fig. 1e). *Endog*, which we had previously shown to be *cis* regulated in the heart ($P = 3 \times 10^{-6}$)⁷, was the only gene at these loci that was differentially regulated in a consistent direction in the SHR and SHRSP hearts compared with the WKY heart (Supplementary Table 1). *ENDOG* is a nuclear-encoded, mitochondria-localized nuclease with

¹Medical Research Council Clinical Sciences Centre, Faculty of Medicine, Imperial College London, Hammersmith Hospital, Du Cane Road, London W12 0NN, UK. ²Cell Signaling & Apoptosis Group, University Lleida, Biomedical Research Institute of Lleida (IRBLLEIDA), Avenida Rovira Roure 80, 251 98 Lleida, Spain. ³Platform of Applied Research on Laboratory Animal, Barcelona Science Park, Baldri Reixac 4, 08028 Barcelona, Spain. ⁴Cardiovascular Institute, Beth Israel Deaconess Medical Institute, CLS906, 3 Blackfan Circle, Boston, Massachusetts 02215, USA. ⁵Department of Radiological, Oncological and Anatomic-Pathological Sciences, University of Rome, 00161 Sapienza, Italy. ⁶School of Clinical and Experimental Medicine, College of Medical and Dental Sciences, University of Birmingham, Edgbaston, Birmingham B15 2TT, UK. ⁷Unitat de Patologia Mitochondrial i Neuromuscular CIBERER, Institut de Recerca Hospital Universitari Vall d'Hebron, Universitat Autònoma de Barcelona, 08035 Barcelona, Spain. ⁸Max-Deibrick Center for Molecular Medicine, Robert-Rössle-Strasse 10, 13125 Berlin, Germany. ⁹CC4, Campus Charité Mitte, Charité-Universitätsmedizin Berlin, Charitéplatz 1, 10117 Berlin, Germany. ¹⁰Department of Physiology, Medical College of Wisconsin, Milwaukee, Wisconsin 53226, USA. ¹¹Institute of Laboratory Animals, Graduate School of Medicine, Kyoto University, Yoshidakonoe-cho, Sakyo-ku, Kyoto 606-8501, Japan. ¹²Institute of Physiology, Academy of Sciences of the Czech Republic, Videnska 1083, 142 20 Prague 4, Czech Republic. ¹³Grup de Patologia Cardiovascular, Institut de Recerca Hospital Universitari Vall d'Hebron, Universitat Autònoma de Barcelona, Pg. Vall d'Hebron, 119, 08035 Barcelona, Spain. ¹⁴Cell Signaling & Apoptosis Group at OBERNED and Vall d'Hebron Institute of Research (VHIR), Pg. Vall d'Hebron, 119-129, 08035 Barcelona, Spain. ¹⁵Department of Biochemistry and Molecular Biology and the Institut de Neurociències at Universitat Autònoma de Barcelona, 08035 Barcelona, Spain. ¹⁶Heart Science Centre, National Heart and Lung Institute, Imperial College London, Harefield Hospital, Harefield, Middlesex UB9 6JH, UK. ¹⁷Cardiovascular Biomedical Research Unit, Royal Brompton and Harefield NHS Trust, Sydney Street, London SW3 6NP, UK. ¹⁸Department of Epidemiology and Biostatistics, Faculty of Medicine, Imperial College London, Praed Street, London W2 1PG, UK.

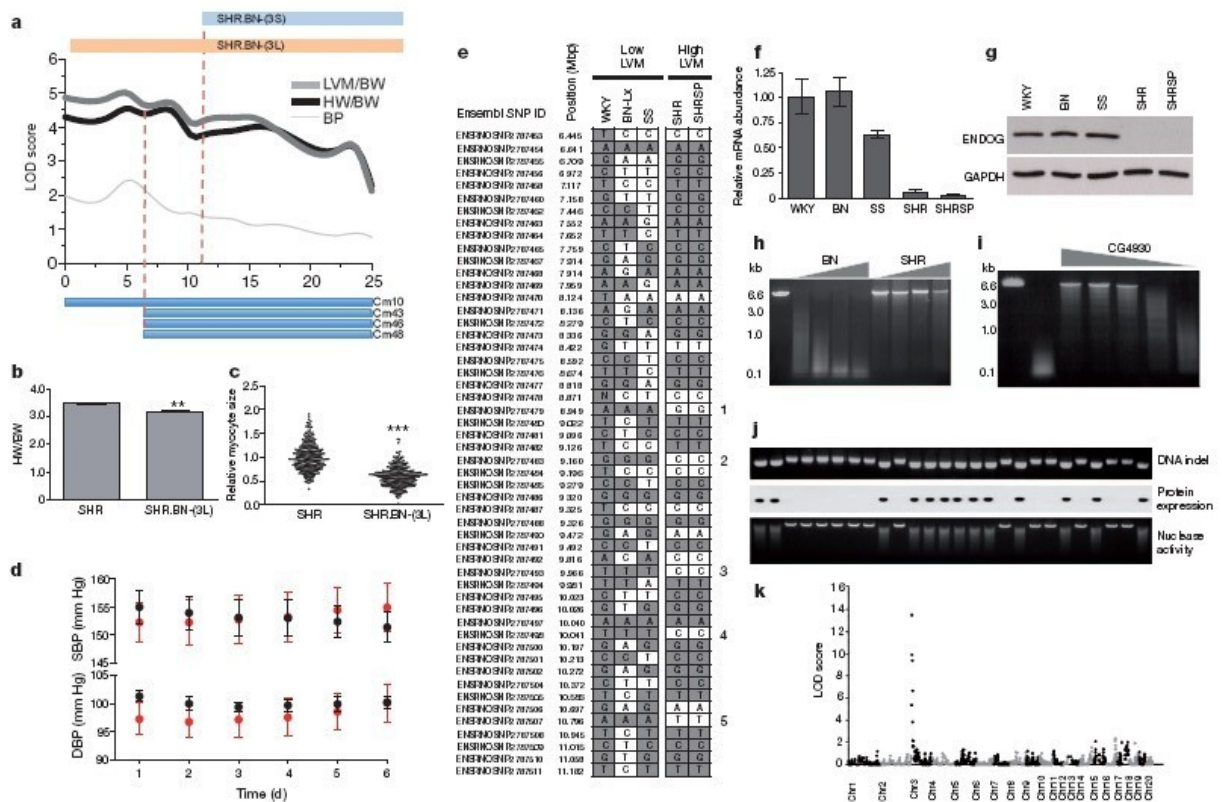


Figure 1 | Positional cloning of *Endog* as the gene underlying the rat chromosome 3p cardiac mass QTL. **a**, Mapping of heart weight (HW) and LVM corrected for body weight (BW) to chromosome 3p in the BN \times SHR F₂ population. The telomeric limits of the congenic strains (SHR.BN-(3L) and SHR.BN-(3S)) and the previously mapped cardiac mass (Cm) QTLs^{13,14} are shown. The x axis indicates the physical position in Mbp, and the dashed lines show the limits of the refined QTL. BP, blood pressure. **b**, HW indexed to BW in the SHR ($n = 4$) and the SHR.BN-(3L) congenic strains ($n = 5$). **c**, Relative cardiomyocyte cross-sectional area in SHR and SHR.BN-(3L) congenic strains. **d**, *In vivo* telemetric systolic blood pressure (SBP) and diastolic blood pressure (DBP) measurements in the SHR (red) and SHR.BN-(3L) (black) strains ($n = 8$ per genotype). **d**, days. **e**, Haplotype analysis of the refined QTL region. Single nucleotide polymorphisms (SNPs) are depicted with reference to WKY alleles (grey, identical; and white, dissimilar) with numbers (1–5) denoting the regions that are polymorphic between strains with high LVM and low LVM. BN-Lx, Brown Norway-Lx; N, unidentified nucleotide. **f**, **g**, Quantitative PCR of *Endog*

messenger RNA expression (**f**) and immunoblotting analysis of ENDOG protein expression (**g**) in strains with low or high cardiac mass at the chromosome 3p locus. GAPDH is a loading control. **h**, Nuclease activity in BN and SHR heart extracts over a range of cardiac protein extract amounts (grey wedge) (see Supplementary Methods). The first lane shows linearized plasmid. **i**, Reversal of nuclease activity in BN-Lx cardiac lysates by addition of a *Drosophila*-derived inhibitor of ENDOG¹⁸, CG4930 (range 1,500–1.5 nM, grey wedge). The first lane shows linearized plasmid, and the second lane shows cardiac lysate in the absence of inhibitor. **j**, Association of the *Endog* indel (insertion and/or deletion) with loss of ENDOG protein expression and diminished nuclease activity in the recombinant inbred strains. Top, centre and bottom panels show the DNA indel, protein expression and nuclease activity, respectively. **k**, Linkage mapping of nuclease activity in the recombinant inbred strains using a quantitative fluorescence-based assay (see Supplementary Methods). Chr, chromosome. All data are represented as mean \pm s.e.m. *, $P < 0.05$; **, $P < 0.01$; ***, $P < 0.001$.

a proposed but disputed function in apoptosis^{8,15–17} and no known effect on cardiac mass or function. We observed reduced expression of *Endog* transcripts and lack of ENDOG protein in all strains that had increased cardiac mass (Fig. 1f, g). Sequencing of *Endog* revealed promoter and coding sequence variation, and we identified an SHR-specific, frame-shift-causing insertion in exon 1 of *Endog* that was associated with increased heart weight and LVM (Supplementary Fig. 2). There was a marked reduction in cardiac nuclease activity, which was ENDOG dependent¹⁸, in the SHR heart compared with the BN heart (Fig. 1h, i). In recombinant inbred strains derived from the SHR and BN strains⁶⁷, we confirmed the direct relationship between the insertion in SHR and the lack of nuclease activity (Fig. 1j), and we mapped *Endog*-dependent nuclease activity to a single locus that encodes *Endog* (Fig. 1k). These data identify *Endog* as the candidate gene at the QTL and implicate *Endog* loss of function as the mechanism for increased cardiac mass and impaired heart function.

We performed immunoblotting across rat and mouse tissues and determined that ENDOG was most highly expressed in the heart, where it was localized to cardiomyocytes (Fig. 2a, b) and co-localized with mitochondria (Supplementary Fig. 3). Using a short hairpin RNA (shRNA) knockdown of *Endog* (sh*Endog*)¹⁹, we tested the effect of *Endog* loss of function in cardiomyocytes and observed an increase in hypertrophic biomarkers and cell size in the absence of pro-hypertrophic stimulation (Fig. 2c, d). Conventional blood-pressure-dependent hypertrophic signalling pathways¹² were not activated in sh*Endog*-treated cells, but AMP-activated protein kinase (AMPK) was activated (Supplementary Fig. 4), which can induce cardiac hypertrophy²⁰. We also observed increased amounts of reactive oxygen species (ROS), which are also pro-hypertrophic stimuli²¹ that act through multiple downstream effectors (Supplementary Fig. 4). These data show that *Endog* loss of function directly induces cardiomyocyte hypertrophy *in vitro* and that this hypertrophy is associated with the activation of two

RESEARCH LETTER

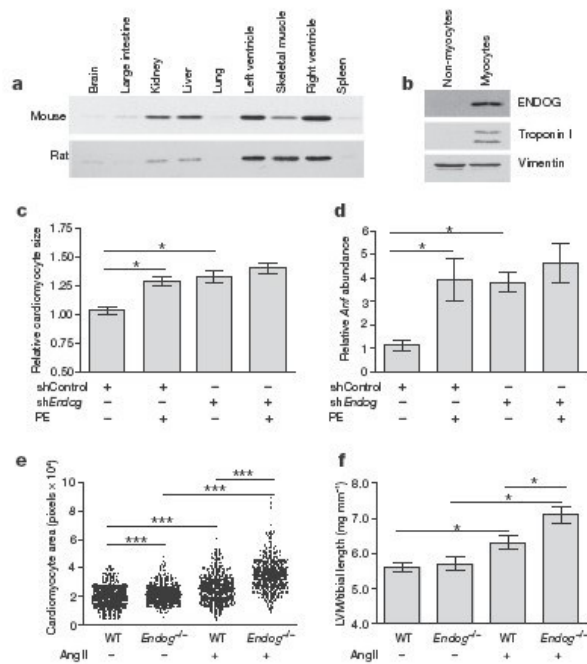


Figure 2 | *Endog* regulates cardiac hypertrophy. **a**, Immunoblotting analysis of ENDOG expression in mouse and rat tissues (ENDOG, ~30 kDa). **b**, Immunoblotting analysis of ENDOG expression in cardiomyocyte and non-cardiomyocyte populations isolated from neonatal rat hearts. **c**, The size of cardiomyocytes ($n \geq 100$ cells, $n = 3$ independent experiments) treated with shRNA against *Endog* (sh*Endog*) or control shRNA (shControl) in the presence or absence of the hypertrophic stimulant phenylephrine (PE, 100 μ M, 24 h). **d**, Expression of the hypertrophic biomarker *Anf* (which encodes atrial natriuretic factor) in sh*Endog*- or shControl-treated cardiomyocytes. **e**, Cardiomyocyte size (see also Supplementary Fig. 5) in *Endog*^{-/-} and wild-type (WT) mice at baseline and after angiotensin II (AngII)-induced cardiac hypertrophy. **f**, LVM to tibial length ratio in *Endog*^{-/-} and WT mice at baseline and after stimulation with AngII. **c–f**, Data are presented as mean \pm s.e.m. *, $P < 0.05$; ***, $P < 0.001$.

pro-hypertrophic pathways, both of which have previously been linked to mitochondrial dysfunction^{20–22}.

We then examined the effects of *Endog* loss of function *in vivo* in the *Endog*-deleted (*Endog*^{-/-}) mouse¹⁷, which shows no detectable difference in apoptotic phenotypes compared with wild-type mice, an observation that was confirmed in an independent *Endog*-deleted strain¹⁶. Compared with controls, *Endog*^{-/-} mice had larger cardiomyocytes at baseline (Fig. 2e) in the absence of stimulation, in keeping with our observations in the SHR.BN-(3L) rat (Fig. 1c) and *in vitro* (Fig. 2c). Following angiotensin-II-mediated stimulation of hypertrophy, which is largely ROS dependent²³, we observed an increase in cardiomyocyte size, hypertrophic biomarker expression and LVM in *Endog*^{-/-} mice (Fig. 2e, f and Supplementary Fig. 5). *Endog*^{-/-} mice had blood pressures that were equivalent to those of control mice at baseline ($P = 0.49$) and after stimulation with angiotensin II ($P = 0.51$) (data not shown). Together, our *in vitro* and *in vivo* data confirm a role for *Endog* in cardiomyocyte hypertrophy and identify ROS as conserved pro-hypertrophic stimuli in both systems.

Endog has been proposed to be important for apoptotic cell death⁸; however, this was subsequently disputed^{16,17}, and it was unclear how *Endog* loss of function was associated with cardiac hypertrophy and dysfunction. To infer the function of *ENDOG* in the human heart, we carried out genome-wide co-expression network analysis²³ in a large human cardiac expression data set ($n = 210$) (see Supplementary Methods). *ENDOG* was identified in a network that was highly

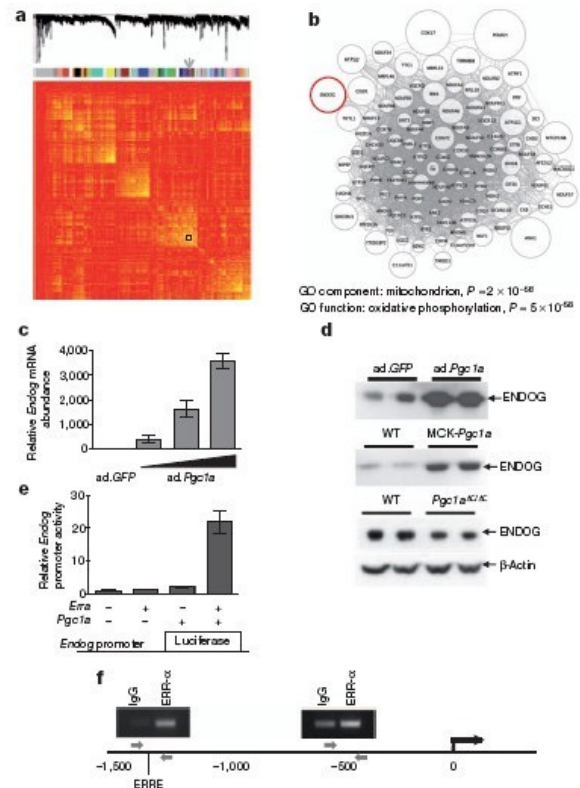


Figure 3 | *ENDOG* is co-expressed with a mitochondria-specific gene network and is regulated by *PGC1 α* and *ERR- α* . **a**, The genes (8,490 from 210 data sets) were clustered and plotted based on the dissimilarity metric between their expression profiles (see Supplementary Methods). Low-hanging branches in the dendrogram (top) represent groups of genes (modules) that have a high similarity metric. Modules are shown beneath the dendrogram (centre) and are colour coded. The arrow indicates the module (also boxed) that contains *ENDOG*. In the heat map of the correlations between expression profiles (bottom), high and low similarities are coloured yellow and red, respectively. **b**, Weighted gene co-expression network analysis (WGCNA)²³ for the module that contains *ENDOG*, providing functional annotation through cellular localization by Gene Ontology (GO) classification (Supplementary Tables 2 and 3). Nodes represent genes, and edges represent significant co-expression between genes. The node size is proportional to the relative degree of interconnectivity of each gene within the module. **c**, Quantitative PCR analysis of *Endog* expression in cultured cardiomyocytes after infection with adenovirus (ad) expressing green fluorescent protein (GFP) (ad*GFP*) or increasing amounts of adenovirus expressing *Pgc1a* (ad*Pgc1a*) (wedge). **d**, Immunoblotting analysis of *Endog* expression in ad*Pgc1a*-infected cardiomyocytes (top), skeletal muscle of WT mice and transgenic mice expressing *Pgc1a* under the control of muscle creatine kinase (MCK-*Pgc1a*) (centre), and hearts of WT and cardiac-specific *Pgc1a*-deleted mice (*Pgc1a*^{AC/AC}) (bottom). **e**, *Endog* promoter activity, measured using a luciferase reporter, in HEK293 cells infected with ad*Pgc1a* and/or ad*Erra*. **f**, *ERR- α* ChIP-PCR of two regions of the *ENDOG* promoter. Red arrows denote primers, and ERRE specifies the location of a consensus ERR response element (1,304 bases upstream of the transcription start site). The experiment was repeated three times with similar results, and PCR products were quantified by quantitative PCR.

enriched for mitochondrial genes ($P = 2 \times 10^{-58}$) and oxidative metabolism processes ($P = 5 \times 10^{-38}$) (Fig. 3 and Supplementary Tables 2 and 3). Taken together, the high levels of *Endog* expression in metabolically active organs (Fig. 2a) and in brown fat (Supplementary Fig. 6), the unique co-expression of *ENDOG* with oxidative metabolism genes, and the link to AMPK signalling and ROS production

pointed to an unappreciated effect of *Endog* in physiological mitochondrial processes.

Peroxisome proliferator activated receptor- γ co-activator 1 α (PGC1 α) is widely recognized as a master regulator of mitochondrial function²⁴ and activates many target genes that are components of the *ENDOG*-associated network (Fig. 3b) through interaction with oestrogen-related receptor- α (ERR- α)⁹. Therefore, we tested whether PGC1 α also regulates *Endog*, and we observed robust PGC1 α -induced *Endog* transcript and *ENDOG* protein expression in cardiomyocytes *in vitro* (Fig. 3c, d). We confirmed the effects of varying *Pgc1a* expression on *ENDOG* protein expression *in vivo* using mice that overexpressed *Pgc1a* under the control of muscle creatine kinase (*MCK-Pgc1a*) and in mice in which *Pgc1a* had been deleted specifically in cardiomyocytes (*Pgc1a*^{AC/ΔC}) (Fig. 3d and Supplementary Methods). Luciferase studies revealed strong activation of the *Endog* promoter by PGC1 α and ERR- α together (Fig. 3e), and we confirmed direct binding of ERR- α to the *ENDOG* promoter by chromatin immunoprecipitation and PCR (ChIP-PCR) in a region containing an *ERRA* response element ($P < 0.001$) (Fig. 3f). These data show that *Endog* is a direct target of ERR- α and PGC1 α , master regulators of mitochondrial and heart function, further implicating *Endog* in mitochondrial and cardiac biology.

It was apparent that the effects of *Endog* loss of function on cardiac hypertrophy might be mediated through perturbations of mitochondrial physiology, which we therefore examined. Electron microscopy revealed lipid-like droplets associated with the mitochondria of *Endog*^{-/-} mice, and these droplets were more numerous and larger than those seen in control mice (Fig. 4a, b). Molecular studies revealed

a marked elevation of triglyceride levels in the hearts of *Endog*^{-/-} mice (Fig. 4c) that manifested as cardiomyocyte steatosis (Fig. 4a and Supplementary Fig. 7) but was not associated with variation in the expression levels of fatty acid metabolism or mitochondrial biogenesis genes (Supplementary Figs 8 and 9). Compared with their wild-type littermates, *Endog*^{-/-} mice had impaired mitochondrial respiration and increased ROS production (Fig. 4f, g).

To assess for mitochondrial depletion, we examined the ratio of mitochondrial DNA (mtDNA) to genomic DNA and the mitochondrial protein to tissue weight ratios, which were both diminished in the hearts of *Endog*^{-/-} mice (Fig. 4d, e) in the absence of mtDNA structural variation (Supplementary Fig. 10). This was an intriguing finding given the previously proposed roles for *Endog* in mtDNA synthesis, processing of polycistronic mtRNA and mitochondrial biogenesis^{25,26}, which had subsequently been discarded based primarily on experiments in *Endog*-deleted mice^{16,17}. We re-examined a role for *ENDOG* in mitochondrial biogenesis and demonstrated an increase in mitochondrial mass with chronic *ENDOG* expression in HEK293 cells ($P < 0.01$) and with acute *Endog* overexpression in a cardiomyocyte-derived cell line ($P < 0.001$) (Fig. 4h–k) in the absence of an effect on apoptotic or necrotic cell death (Supplementary Fig. 11). A role for *ENDOG* in mtDNA biology^{25,26} was supported further by ChIP-PCR experiments that showed direct binding of *ENDOG* throughout the mtDNA molecule (Fig. 4l), as previously demonstrated for mitochondrial transcription factor A (TFAM)²⁷, which is a crucial determinant of mtDNA synthesis and repair that when deleted causes eccentric cardiac hypertrophy and heart failure²⁸.

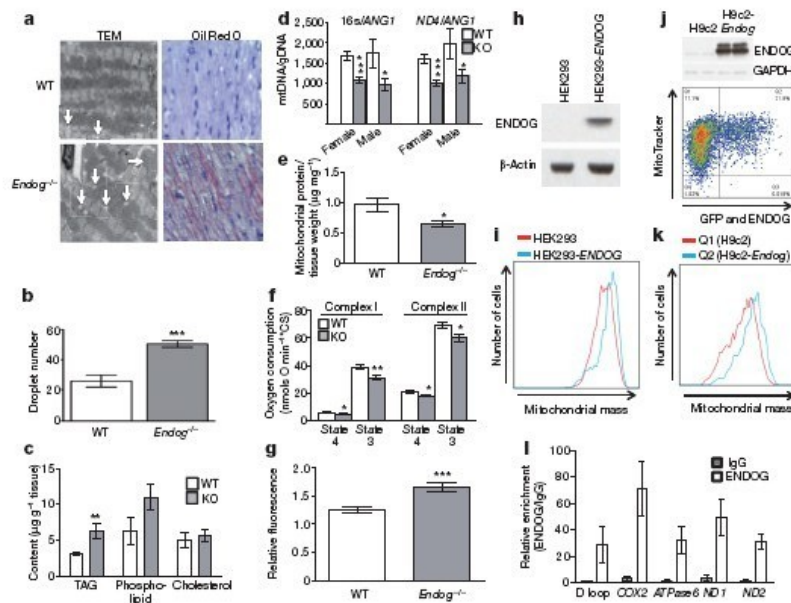


Figure 4 *Endog* regulates mitochondrial function and cardiac lipid metabolism. **a**, Transmission electron micrographs (TEM) and oil red O stained micrographs (high resolution in Supplementary Fig. 7) of left ventricular sections from WT and *Endog*^{-/-} mice. Vertical arrows indicate lipid droplets, and the horizontal arrow indicates a mitochondrion. **b**, Quantification of the number of mitochondria-associated droplets in WT and *Endog*^{-/-} mice. **c**, Quantification of cardiac triglyceride (TAG), phospholipid and cholesterol content in the hearts of WT and *Endog*^{-/-} (KO) mice ($n = 5$). **d**, Ratio of mtDNA to genomic DNA (gDNA) in the hearts of WT and *Endog*^{-/-} (KO) mice. **e**, Quantification of mitochondrial protein content in WT and *Endog*^{-/-} mice ($n = 5$). **f**, State 3 and state 4 oxygen consumption in the presence of substrates for complex I or complex II of the electron transport chain in cardiac mitochondria isolated from WT ($n = 6$) or *Endog*^{-/-} (KO) ($n = 5$) mice. *CS, corrected for citrate synthase activity. **g**, Relative

fluorescence-based measurement of ROS production by mitochondria isolated from WT ($n = 6$) or *Endog*^{-/-} ($n = 5$) mice. **h–k**, Representative flow cytometric analysis of mitochondrial mass in HEK293 and H9c2 cells overexpressing human or rat *ENDOG*, respectively ($n = 4$). **h**, Stable expression of *ENDOG* in HEK293 cells (HEK293-*ENDOG*). **i**, Flow cytometric analysis of HEK293 and HEK293-*ENDOG* cells stained with MitoTracker. **j**, Adenovirus (ad)-mediated expression of GFP and rat *ENDOG* in cardiomyocytes (top), and flow cytometric analysis of ad-*Endog*-infected cells (Q2) and uninfected control cells (Q1). Colours denote the event density: from highest to lowest density, red, orange, green then blue. **k**, Number of events plotted against mitochondrial mass for ad-*Endog*-infected cells (Q2) and uninfected control cells (Q1). **l**, Quantitative PCR of mtDNA–protein complexes after ChIP of mitochondrial chromatin using anti-*ENDOG* antibody or IgG. All data are presented as mean \pm s.e.m. * $P < 0.05$; ** $P < 0.01$; *** $P < 0.001$.

RESEARCH LETTER

Mitochondria are essential for oxidative metabolism, and mitochondrial dysfunction and/or depletion in the heart causes maladaptive cardiac hypertrophy and cardiac dysfunction associated with increased amounts of ROS and lipotoxicity^{4,5,28,29}. Here we identified *Endog* loss of function as a primary determinant of maladaptive cardiac hypertrophy that is associated with mitochondrial dysfunction and depletion and with marked cardiomyocyte steatosis. The mechanism underlying cardiac hypertrophy that results from impaired mitochondrial function is not limited to a single pathway, but we demonstrated a conserved increase in ROS, which are established hypertrophic stimuli^{21,22}, in *Endog* loss-of-function models. Our studies resolve some of the uncertainty about the non-apoptotic function of *Endog*^{15–17} and reveal its importance in mitochondrial biology, which has intriguing parallels with the dual roles of apoptosis-inducing factor³⁰. We propose that END OG, which we show binds to mtDNA, modulates mtDNA synthesis, maintenance and/or transcription, which is consistent with previous hypotheses^{25,26}. Therapeutic targeting of the *PGC1A-ERRA* axis has been proposed to improve mitochondrial function in cardiac failure¹¹, and our studies suggest that regulation of *Endog* is an important component of this process. We conclude that *Endog* is a novel determinant of maladaptive cardiac hypertrophy with previously unappreciated mitochondrial functions.

METHODS SUMMARY

Linkage mapping was carried out using microsatellite genotypes in the BN × SHR F₂ population. *Ex vivo* heart weight analysis was performed in the congenic rat strains, which were characterized using *in vivo* blood pressure telemetry. Comparative haplotype analysis was performed using single nucleotide polymorphism data (Rat Genome Database; <http://rgd.mcw.edu/>) for all strains used in the QTL mapping studies. Microarray-based expression analysis was conducted as described previously⁶⁷. Cell size and hypertrophy biomarker expression were measured in cardiomyocytes after lentivirus-mediated *Endog* knockdown. Heart weight, hypertrophy biomarker expression and cardiomyocyte size were measured in *Endog*^{-/-} mice at baseline and after angiotensin-II-induced hypertrophy. Triglyceride abundance, mitochondrial mass and respiratory activity were measured in *Endog*^{-/-} mice as described in the Supplementary Information. Weighted gene co-expression network analysis (WGCNA)²³ was applied to the largest publicly available human heart transcriptome data set. Regulation of *Endog* by *PGC1α* was investigated in neonatal cardiomyocytes infected with adenovirus expressing *Pgc1α*, in MCK-*Pgc1α* skeletal muscle and in *Pgc1α*^{ΔC/ΔC} heart samples. The association of *ERR-α* with the *ENDOG* promoter and the *ENDOG*-mtDNA interaction were determined using ChIP. The histological analysis and electron microscopy of *Endog*^{-/-} hearts was carried out to study mitochondrial structure and abundance, as well as lipid deposition. Genomic DNA and mtDNA copy number were assessed by quantitative PCR. The mitochondrial abundance in cells was studied by flow cytometry. Full methods are provided in the Supplementary Methods.

Received 6 March; accepted 17 August 2011.

- Post, W. S., Larson, M. G., Myers, R. H., Galderisi, M. & Levy, D. Heritability of left ventricular mass: the Framingham Heart Study. *Hypertension* **30**, 1025–1028 (1997).
- Lorell, B. H. & Carabello, B. A. Left ventricular hypertrophy: pathogenesis, detection, and prognosis. *Circulation* **102**, 470–479 (2000).
- Vasan, R. S. *et al.* Genetic variants associated with cardiac structure and function: a meta-analysis and replication of genome-wide association data. *J. Am. Med. Assoc.* **302**, 168–178 (2009).
- McGavock, J. M., Victor, R. G., Unger, R. H. & Szczepaniak, L. S. Adiposity of the heart, revisited. *Ann. Intern. Med.* **144**, 517–524 (2006).
- Wong, C. & Marwick, T. H. Obesity cardiomyopathy: pathogenesis and pathophysiology. *Nature Clin. Pract. Cardiovasc. Med.* **4**, 436–443 (2007).
- Heinig, M. *et al.* A trans-acting locus regulates an anti-viral expression network and type 1 diabetes risk. *Nature* **467**, 460–464 (2010).
- Petretto, E. *et al.* Integrated genomic approaches implicate osteoglycin (*Ogn*) in the regulation of left ventricular mass. *Nature Genet.* **40**, 546–552 (2008).
- Li, L. Y., Luo, X. & Wang, X. Endonuclease G is an apoptotic DNase when released from mitochondria. *Nature* **412**, 95–99 (2001).
- Dufour, C. R. *et al.* Genome-wide orchestration of cardiac functions by the orphan nuclear receptors *ERRα* and *γ*. *Cell Metab.* **5**, 345–356 (2007).
- Wu, Z. *et al.* Mechanisms controlling mitochondrial biogenesis and respiration through the thermogenic coactivator PGC-1. *Cell* **98**, 115–124 (1999).
- Finck, B. N. & Kelly, D. P. PGC-1 coactivators: inducible regulators of energy metabolism in health and disease. *J. Clin. Invest.* **116**, 615–622 (2006).
- Hill, J. A. & Olson, E. N. Cardiac plasticity. *N. Engl. J. Med.* **358**, 1370–1380 (2008).
- Inomata, H. *et al.* Identification of quantitative trait loci for cardiac hypertrophy in two different strains of the spontaneously hypertensive rat. *Hypertens. Res.* **28**, 273–281 (2005).
- Siegel, A. K. *et al.* Genetic loci contribute to the progression of vascular and cardiac hypertrophy in salt-sensitive spontaneous hypertension. *Arterioscler. Thromb. Vasc. Biol.* **23**, 1211–1217 (2003).
- Büttner, S. *et al.* Endonuclease G regulates budding yeast life and death. *Mol. Cell* **25**, 233–246 (2007).
- David, K. K., Sasaki, M., Yu, S. W., Dawson, T. M. & Dawson, V. L. EndoG is dispensable in embryogenesis and apoptosis. *Cell Death Differ.* **13**, 1147–1155 (2006).
- Irvine, R. A. *et al.* Generation and characterization of endonuclease G null mice. *Mol. Cell. Biol.* **25**, 294–302 (2005).
- Temme, C. *et al.* The *Drosophila melanogaster* gene *cg4930* encodes a high affinity inhibitor for endonuclease G. *J. Biol. Chem.* **284**, 8337–8348 (2009).
- Bahi, N. *et al.* Switch from caspase-dependent to caspase-independent death during heart development: essential role of endonuclease G in ischemia-induced DNA processing of differentiated cardiomyocytes. *J. Biol. Chem.* **281**, 22943–22952 (2006).
- Arad, M. *et al.* Constitutively active AMP kinase mutations cause glycogen storage disease mimicking hypertrophic cardiomyopathy. *J. Clin. Invest.* **109**, 357–362 (2002).
- Dai, D. F. *et al.* Mitochondrial oxidative stress mediates angiotensin II-induced cardiac hypertrophy and Gαq overexpression-induced heart failure. *Circ. Res.* **108**, 837–846 (2011).
- Seddon, M., Looi, Y. H. & Shah, A. M. Oxidative stress and redox signalling in cardiac hypertrophy and heart failure. *Heart* **93**, 903–907 (2007).
- Zhang, B. & Horvath, S. A general framework for weighted gene co-expression network analysis. *Stat. Appl. Genet. Mol. Biol.* **4**, 17 (2005).
- Spiegelman, B. M. Transcriptional control of mitochondrial energy metabolism through the PGC1 coactivators. *Novartis Found. Symp.* **287**, 60–69 (2007).
- Cote, J. & Ruiz-Carrillo, A. Primers for mitochondrial DNA replication generated by endonuclease G. *Science* **261**, 765–769 (1993).
- Tiranti, V. *et al.* Chromosomal localization of mitochondrial transcription factor A (TFAM), single-stranded DNA-binding protein (SSBP), and endonuclease G (ENDOG), three human housekeeping genes involved in mitochondrial biogenesis. *Genomics* **25**, 559–564 (1995).
- Rothfuss, O. *et al.* Parkin protects mitochondrial genome integrity and supports mitochondrial DNA repair. *Hum. Mol. Genet.* **18**, 3832–3850 (2009).
- Wang, J. *et al.* Dilated cardiomyopathy and atrioventricular conduction blocks induced by heart-specific inactivation of mitochondrial DNA gene expression. *Nature Genet.* **21**, 133–137 (1999).
- Lewis, W. *et al.* Decreased mtDNA, oxidative stress, cardiomyopathy, and death from transgenic cardiac targeted human mutant polymerase *γ*. *Lab. Invest.* **87**, 326–335 (2007).
- Vahsen, N. *et al.* AIF deficiency compromises oxidative phosphorylation. *EMBO J.* **23**, 4679–4689 (2004).

Supplementary Information is linked to the online version of the paper at www.nature.com/nature.

Acknowledgements We acknowledge funding from the Medical Research Council (UK), the National Institute for Health Research (UK), the Royal Brompton and Harefield Cardiovascular Biomedical Research Unit, the Imperial College Healthcare Biomedical Research Centre, the British Heart Foundation, Fondation Leducq, the Wellcome Trust, the Grant Agency of the Czech Republic (301/08/0166), the Ministry of Education of the Czech Republic (1M0520), the Ministerio de Ciencia e Innovación (Spain; PTQ-08-03-07880, SAF2008-02271, SAF2008-03067 and SAF2010-19125), the Agencia de Gestió d'Ajuts Universitaris i Recerca (Spain; 2009-SGR-346), the Fondo de Investigaciones Sanitarias (Spain; PS09/O2034, PS09/O1602 and PS09/O1591), the European Community's Seventh Framework Programme (FP7/2007-2013) under grant agreement no. HEALTH-F4-2010-241504 (EURATRANS), and the German National Genome Research Network (NGFN-Plus) Heart Failure. We thank M. R. Lieber for providing the *Endog* deleted mice and E. Wahle for providing the CG4930 expression plasmid. We thank the National BioResource Project for the Rat (<http://www.anim.med.kyoto-u.ac.jp/NBR/>) for providing rat strains.

Author Contributions C.M.-R., J.Y., X.-M.S., A.S., J.Z., A.B., R.B., D.H., H.L., G.C.R., R.M. and E.G.-A. performed the laboratory-based experiments. R.A., P.M., M.M., V.Z., F.P., M.C., M.R.-M. and F.K. performed the physiology experiments. N.H., H.J., L.E.F., P.J.R.B. and T.S. provided gene expression and physiology data. J.W., L.B. and E.P. performed genetic mapping and network studies. X.C., J.X.C., Z.A., M.P. and D.C.-D. supervised the data analysis and contributed to the experimental design. S.A.C. and D.S. planned the experiments. S.A.C. wrote the manuscript with input and discussion from all of the co-authors.

Author Information Reprints and permissions information is available at www.nature.com/reprints. The authors declare no competing financial interests. Readers are welcome to comment on the online version of this article at www.nature.com/nature. Correspondence and requests for materials should be addressed to S.A.C. (stuart.cook@imperial.ac.uk) or D.S. (daniel.sanchis@cmb.ucl.ac.uk).

Annex 2. Translation of MEF2 is induced by hypertrophic stimuli in cardiomyocytes through a Calcineurin-dependent pathway



Original article

Translation of Myocyte Enhancer Factor-2 is induced by hypertrophic stimuli in cardiomyocytes through a Calcineurin-dependent pathway

Junmei Ye ^a, Maria Cardona ^a, Marta Llovera ^a, Joan X. Comella ^b, Daniel Sanchis ^{a,*}^a Institut de Recerca Biomèdica de Lleida (IRBLLEIDA) – Universitat de Lleida, Edifici Biomedicina-I. Av. Rovira Roure, 80. 25198 Lleida, Spain^b Cibernet, Institut de Neurociències, Hospital Vall d'Hebron, UAB, Vall d'Hebron Institut de Recerca. Av. Vall d'Hebron, 119-129. 08035 Barcelona, Spain

ARTICLE INFO

Article history:

Received 20 June 2012

Received in revised form 18 July 2012

Accepted 19 July 2012

Available online 28 July 2012

Keywords:

Cardiomyocyte

Hypertrophy

Myocyte Enhancer Factor-2

Protein translation

ABSTRACT

The Myocyte Enhancer Factor-2 (MEF2) family of transcription factors regulates gene expression during cardiomyocyte differentiation and adaptation of the myocardium to stress. MEF2 activity is enhanced by increasing its transcription and by MAPK-dependent phosphorylation, and is reduced by binding to class-II Histone Deacetylases and by miR-1-mediated degradation of its transcript. Here we show that MEF2 protein abundance is regulated at the translational level, determining myocyte size, during hypertrophy. In order to reduce MEF2 protein expression, its silencing through RNA interference required serum deprivation and, even in this condition, MEF2 protein abundance recovered to basal levels in presence of phenylephrine. Hypertrophic agonist stimulation of neonatal ventricular cardiomyocytes increased Mef2 expression by enhancing its translation, without changing its transcription or blocking degradation of the protein. MEF2 abundance was increased by Calcineurin overexpression *in vivo* and was reduced by Calcineurin inhibition *in vitro*, without affecting Mef2 mRNA levels. Calcineurin activity influenced expression of Polypyrimidine Tract Protein (PTB), contributing to MEF2 translation. Thus, our results show a previously unrecognized but relevant level of MEF2 activity regulation through the control of its translation that involves Calcineurin and PTB.

© 2012 Elsevier Ltd. All rights reserved.

1. Introduction

The myocyte enhancer factor-2 family of transcription factors (MEF2) controls transcription of genes required for myocyte differentiation and growth [1]. MEF2C is expressed in heart precursor cells and controls gene expression during heart development and its deletion blocks heart tube looping and formation of the right ventricle [2]. However, late conditional Mef2c targeting in the myocardium and in skeletal muscle showed that MEF2C is not essential for postnatal growth and function of striated muscle [3]. On the contrary, MEF2A and MEF2D are important for the postnatal biology of the heart. MEF2A-deficient mice show disorganization of mitochondria, myofibrillar fragmentation, dilation of the right ventricle and die soon after birth [4], while MEF2D is involved in the response of the adult myocardium to stress, without any evident contribution to embryonic cardiac development [5].

Full knowledge of the regulation of MEF2 activity has important consequences for the understanding of cardiac biology and adaptation of

the myocardium to stress. Early after its discovery, it was found that MEF2 activity was regulated by transcription and by posttranslational modification. Mef2 transcription is regulated during embryonic development [6] and recent findings show that MEF2A can regulate its own transcription [7]. Posttranslational modifications allow rapid changes of MEF2-dependent transcription by growth and stress signals. MAPK-dependent phosphorylation enhances MEF2 transcriptional activity [8–11]. Transcription of MEF2-dependent genes is also stimulated by Calcium/Calmodulin signaling through activation of the Calcineurin phosphatase [12]. Calcineurin directly dephosphorylates different residues of MEF2, enhancing its activity [13,14] and also dephosphorylates cytosolic nuclear factor of activated T cells (NFAT), triggering its nuclear import [15] where it interacts with MEF2, potentiating its activity [16]. More recently, MEF2 activity has been shown to be enhanced by interaction with Myocardin [17]. On the opposite, MEF2 transcriptional activity is blocked by its binding to Class II Histone Deacetylases HDAC4 and 5 [11,18]. This inhibitory mechanism can be reverted by CaMK-dependent phosphorylation of Class II HDAC, which triggers their nuclear export, freeing MEF2-dependent transcription as reviewed in [19]. Finally, posttranscriptional regulation of MEF2 protein abundance has been described. The 3'UTR of MEF2A can inhibit translation of the transcript *in vitro* and in muscle cell lines [20] and the cardiac-specific micro-RNA miR-1, which modulates the effects of cardiogenic transcription factors and targets MEF2A [21,22], destabilizes Mef2a mRNA inducing its degradation [23].

Abbreviations: CnA, Calcineurin A; CaMK, Calcium/Calmodulin-dependent kinase; eIF2, eukaryotic Initiator Factor-2; 4E-BP, eIF4E-binding protein; MEF2, myocyte enhancer factor-2; PTB, Polypyrimidine Tract Binding Protein; RNAi, RNA interference; shRNA, small hairpin RNA; nppa, natriuretic precursor peptide; acta1, alpha-actin skeletal muscle isoform; UTR, untranslated region.

* Corresponding author. Tel.: +34 973702949.

E-mail address: daniel.sanchis@cmb.udl.cat (D. Sanchis).

However, the potential activation of MEF2 translation in response to stress is not well known. We only found one article showing MEF2A translation enhancement by serum in vascular smooth muscle cells [24] and no data was found dealing with the regulation of Mef2a translation in cardiomyocytes. Our discovery that MEF2 protein abundance and transcript levels did not change consistently during myocyte response to hypertrophic stimuli prompted us to investigate this fact, leading us to find that during hypertrophy in vivo and in vitro, translation of MEF2A and MEF2D is enhanced by a Calcineurin-dependent pathway involving PTB in cardiomyocytes.

2. Materials and methods

2.1. Cardiomyocyte culture and tissue samples

The investigation with experimental animals conforms to the Guide for the Care and Use of Laboratory Animals published by the US National Institutes of Health (NIH Publication No. 85–23, revised 1996) and the National Guidelines for the regulation of the use of experimental laboratory animals from the Generalitat de Catalunya and the Government of Spain (article 33.a 214/1997) and was evaluated and approved by the Experimental Animal Ethic Committee of the University of Lleida (CEEAA) (Permit numbers for dissection of adult rat tissues: CEEA 04–03/08 and for the sacrifice of zero to five-day-old (P0–P5) neonatal rats to obtain tissues and primary cell culture of cardiomyocytes: CEEA 06–03/08). The hearts of 5-month-old MHC-Calcineurin transgenic mice and wild type littermates [15] were a gift by Eric N Olson (UT Southwestern Medical Center, Dallas, USA). Adult 2-month-old male Sprague Dawley rats were sacrificed by exposure to carbon dioxide and tissues were dissected as previously described [25]. P2–P4 Sprague–Dawley rat neonates were sacrificed, following the above Guide approved by the CEEAA, by decapitation and cardiomyocytes were obtained from the hearts as described elsewhere [26]. Purity of cardiomyocyte cultures was routinely checked by immunocytochemistry with a cardiac sarcomeric α -actinin antibody (clone EA-53, SIGMA, Saint Louis, MO, USA) and was found to be higher than 90% after 24–48 h in vitro.

2.2. Drugs

Actinomycin D (Sigma-Aldrich, A9415, 1, 2, 5 μ g/ml); Angiotensin II (Sigma-Aldrich, A9525, 100 nM); Cycloheximide (Sigma-Aldrich, c7698, 10, 20, 50 μ g/ml); Calcineurin Inhibitor VIII (Calbiochem, 207003, 2 μ M); Endothelin-1 (Sigma-Aldrich, E7764, 0.1 μ M); Lactacystin (clasto-lactacystin β -Lactone, Calbiochem, 426102, 2 μ M); Phenylephrine ((R)-(-)-Phenylephrine hydrochloride, Sigma-Aldrich, P6126, 100 μ M); Proteasome inhibitor MG-132 (Calbiochem, 474790, 5 μ M).

2.3. MEF2 knockdown

Validated MISSIONR clone NM_005587.1-709s1c1 for lentiviral-driven shRNA (SIGMA) was used for knockdown of Mef2a. Lentiviruses were prepared in the HEK293T packing cell line and titered as described previously [27]. Cardiomyocytes were treated with shRNA or scrambled lentiviruses 3 h after seeding and let stand overnight in DMEM medium supplemented with 5% fetal calf serum (FCS), 10% horse serum (HS), glutamine and antibiotics. The medium was replaced 12 h later with a medium containing 5% horse serum and cells were cultured for two days in this condition before any further treatment was performed (e.g. 24 or 38 h in the presence of agonists, completely depriving from serum).

2.4. RNA extraction, conventional RT-PCR and Real Time quantitative RT-PCR

Total RNA was obtained from frozen tissues or cell pellets with the RNeasy Mini Kit (Qiagen). RNA concentration measurements and

reverse transcription were done as described [25,27]. Conventional semi-quantitative PCR was performed as previously described [27] using the primers forward: GGAATGAACAGTCGGAAACC and reverse: CAAGCTTGGAGTTGTCACAG(Rn); for mef2a, forward: AGGGAGGCAA AGGGTTAATG and reverse: AGTGGCATGGAGAGAAG for mef2d and forward: ATCATCTGACCGGAGGACTG and reverse: TGAACGTTCC CTTCCATC for unr (loading control [25,27]). Quantitative Real Time PCR was performed in an iCycler iQ PCR detection system and iQ v.3 and iQ v.5 software (BioRad), using the TaqMan Gene Expression Master Mix (Cat.N. 4369016) and the Gene Expression Assays Rn01478096_m1, Rn01455530_g 1 and Rn00561661_m1, Rn01641150_m 1 to amplify mef2a, mef2d, nppa (natriuretic peptide precursor) and, acta1 (α -actin), with parallel amplification of Gapdh (Rn01462662_g1) as loading control (all from Applied Biosystems).

2.5. Western blot and immunofluorescence

For Western blot, whole cell lysates were obtained and processed as described [27]. Equal amounts of protein were electrophoresed by SDS-PAGE, transferred to PVDF membranes (Amersham), and probed with specific antibodies. Antibodies used were against MEF2A (Cell Signaling, #9736), MEF2D (Abcam, ab60717), PTB C-terminus (ZYMED, #324800), eIF2S1 (Abcam, ab26197), eIF2S1 (phosphor-Ser51) (Abcam, ab32157), eIF4E-BP1 (4E-BP, ab2606), Prohibitin (NeoMarkers, 292P501F), and all secondary antibodies were from Invitrogen. Immunofluorescence was performed in cultures grown in Nunclon M4 multi-well plates (Nunc), after fixing cells with 4% paraformaldehyde (PFA) for 30 min as previously described, with an anti- α -actinin antibody (clone EA-53, SIGMA) [26].

2.6. Cell area

Cardiomyocyte areas were measured in cultures treated as described in the legend of Fig. 1 after fixation and immunofluorescence staining of α -actinin, using the Image J software (freely available at <http://rsbweb.nih.gov/ij/>). Values (arbitrary units, A.U.) were calculated from 100 cells analyzed in two replicate wells from 4 independent experiments.

2.7. In vivo ³⁵S-protein labeling and MEF2 immunoprecipitation

Cardiomyocytes were cultured in standard medium and serum for 24 h after seeding. The medium was discarded, cells were washed with PBS and were cultured 24 h in fresh medium without serum. Then, the standard medium was replaced by Methionine/Cysteine-free medium (GIBCO Cat. No. 21013-024) and 120 μ Ci of ³⁵S labeled Cysteine and Methionine cocktail (EasyTag EXPRESS³⁵S Protein Labelling Mix 74 MBq (2 mCi), Cat. No. NEG772002MC, Perkin Elmer). Duplicate plates were cultured in these conditions in the presence or absence of 100 μ M Phenylephrine or 2 μ M proteasome inhibitor Lactacystin. Thirty six hours later, cells were rinsed with cold PBS and MEF2 immunoprecipitation was performed with a specific antibody (Santa Cruz, H-300: sc-10794, 1 μ g Ab/100 μ g cell lysate) using equivalent amounts of protein on an orbital shaker at 4°C for 2 h. Afterwards 40 μ l protein A-Sepharose beads suspension (50% of A-Sepharose) was added to each sample and incubated overnight. Then, sepharose beads were washed three times with washing buffer (50 mM Tris pH 7.4, 150 mM NaCl, 5 mM EDTA, 1% Nonidet P-40, 0.1% sodium deoxycholate and 0.1% SDS), 20 μ l loading buffer 2 \times was added to each sample and SDS-PAGE was performed. Finally the gel was dried up and was exposed for 16 h in a cassette at –80°C. 10 μ g total cell lysate of each sample was used as loading control. The experiment was performed three times.

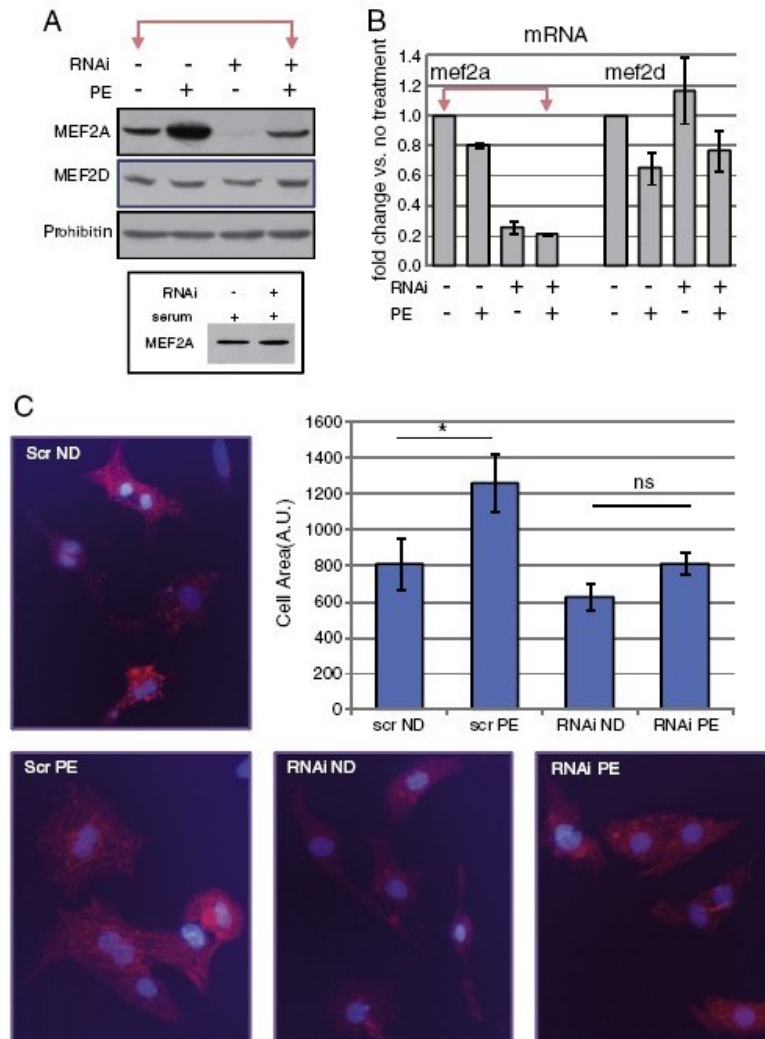


Fig. 1. MEF2A protein abundance and function are unrelated to its transcript level during agonist stimulation in neonatal rat ventricular cardiomyocytes. (A) MEF2 protein expression was analyzed in serum-deprived cardiomyocytes transfected with a Mef2a-specific shRNA or a scrambled vector, as described in the Materials and methods section, in the presence or absence of 100 μ M phenylephrine (PE) during 24 h. Inset: same treatments as in (A) but in the presence of serum (5% FCS, 10% HS) in the culture medium. Representative Western Blots are shown from $n = 5$. (B) Mef2a and Mef2d mRNA abundance in the same cultures, measured by TaqMan quantitative PCR from total RNA extracts of cultures treated as in (A), $n = 5$. Arrows highlight comparison between serum deprived myocytes and myocytes treated with PE and RNAi to point at the similar abundance of protein despite very different amounts of mRNA. (C) Cardiomyocyte areas were measured in cultures of neonatal cardiomyocytes treated as in (A). Values (arbitrary units, A.U.) were calculated as described in the Materials and methods section, from 100 cells analyzed in two replicate wells from 4 independent experiments. The bar graph represents means of 4 independent experiments \pm SEM. * $p < 0.05$. ns: not significant. Representative fluorescence microscopy images of cardiomyocyte cultures are shown after staining for α -actinin (red) and nuclei (blue). Scr ND, scrambled no drug; Scr PE, scrambled phenylephrine (24 h, 100 μ M); RNAi ND, MEF2a-specific RNA interference-driven silencing with no drug; RNAi PE, MEF2a-specific RNA interference-driven silencing plus phenylephrine (24 h, 100 μ M).

2.8. PTB overexpression and knockdown

The human PTB 1 cDNA (gift from Chris W Smith, Cambridge, UK) was cloned into pEIGW vector (from Didier Trono, Geneva, Switzerland) using the SmaI and NdeI sites. Ptb nucleotide sequence GCACAGTC CTGAAGATCAT was chosen for PTB-specific expression silencing using free RNAi design interfaces and has been validated previously [28]. Primers for small hairpin RNA interference (shRNA) were subcloned into the pLVTHM plasmid as described before [28]. pEIGW or pLVTHM constructs were transfected into HEK293T packing cell line and tittered as described previously [28]. Cardiomyocytes were seeded and in 3 h later they were treated with shRNA/scrambled/overexpression/empty vector-carrying lentiviruses for Polypirimidine

Binding Protein (PTB). Cultures were let stand overnight in cardiomyocyte medium. After 12 h, the medium was replaced with standard medium and cells were cultured for three more days. On the fourth day cells were serum deprived, and 24 h later, the medium was replaced with complete medium without-serum. Twenty four hours later, cells were processed for analysis.

2.9. Statistics

Results are presented as mean \pm SEM. Comparisons between values (e.g. control vs. agonist-treated) were made using a Student's *t*-test.

3. Results

3.1. Pro-hypertrophic agonists induce an increase in myocyte size that depends on increased MEF2 protein abundance without changes in its transcript

MEF2A protein abundance was unaffected in neonatal ventricular cardiomyocyte cultures transfected with lentivirus carrying a small hairpin RNA (shRNA)-based RNA interference (RNAi) vector, in the presence of the standard serum concentrations (5% FCS and 10% HS) in the culture medium (Fig. 1A, inset). However, a reduction of 80% Mef2a transcript abundance in RNAi-treated cells was detected by Real Time RT-PCR using validated gene-specific assays. Because serum is pro-hypertrophic [29] and could stimulate MEF2 expression, we deprived cells from serum after viral transduction. In these conditions, MEF2A protein abundance was reduced to almost undetectable amounts by shRNA-driven RNAi (Fig. 1A) coinciding with efficient gene silencing to 20% of the basal mRNA levels (Fig. 1B). Upon addition of Phenylephrine (PE), MEF2A protein abundance increased three-fold in shRNA-treated cardiomyocytes (Fig. 1A) despite no changes in the RNAi-induced low mRNA level (Fig. 1B). The changes in MEF2A protein abundance by RNAi and PE treatment affected cell size, showing that MEF2A abundance determines cell size in neonatal myocytes (Fig. 1C), in addition to the well known effects on cell growth due to MEF2A posttranslational modification [1]. These results suggested strong posttranscriptional regulation of MEF2A expression in the presence of hypertrophic agonists, influencing cell size, which was different to the one controlled by miR-1 [23] in that the later has been shown to reduce Mef2 transcript levels.

Given the relevance of MEF2A and MEF2D in the postnatal heart response to stress [4,5], we decided to investigate the mechanisms underlying the observed control of MEF2 abundance during agonist stimulation. Treatment of cardiomyocytes with different pro-hypertrophic drugs, in the absence of serum, induced a rapid increase of MEF2A protein abundance, detectable at 15 h (data not shown) and steadily progressing at 24 h and 48 h, and a slower increase of MEF2D expression, detectable at 24 h or 48 h, depending on the stimulus (Fig. 2A). Mef2a and Mef2d transcript levels did not show any significant changes during these treatments, as analyzed by conventional RT-PCR (data not shown) and Real Time Quantitative PCR (Fig. 2B), while the hypertrophy markers atrial natriuretic precursor peptide (nppa) and skeletal α -actin (acta1) isoform were strongly induced as expected [30,31]. In addition to the well established pathways of posttranslational regulation [1], and the miR1-dependent pathway, which affects the transcript levels [23], our results suggested a previously undetected level in MEF2 regulation during cardiomyocyte growth.

3.2. Agonist-induced increase of MEF2 protein abundance is due to its increased translation

The role of transcription in the control of MEF2 expression in pro-hypertrophic culture medium was analyzed. Inhibition of transcription with Actinomycin D (ActD) induced a decrease of MEF2A and MEF2D protein abundance in cardiomyocytes treated with PE (Fig. 3A), correlating with an important decrease in the corresponding mRNA levels due to ActD (Fig. 3C). Addition of the translational inhibitor Cycloheximide (CHX) also rapidly hampered the increase of MEF2 levels observed during PE treatment (Fig. 3B) that did not correlate with

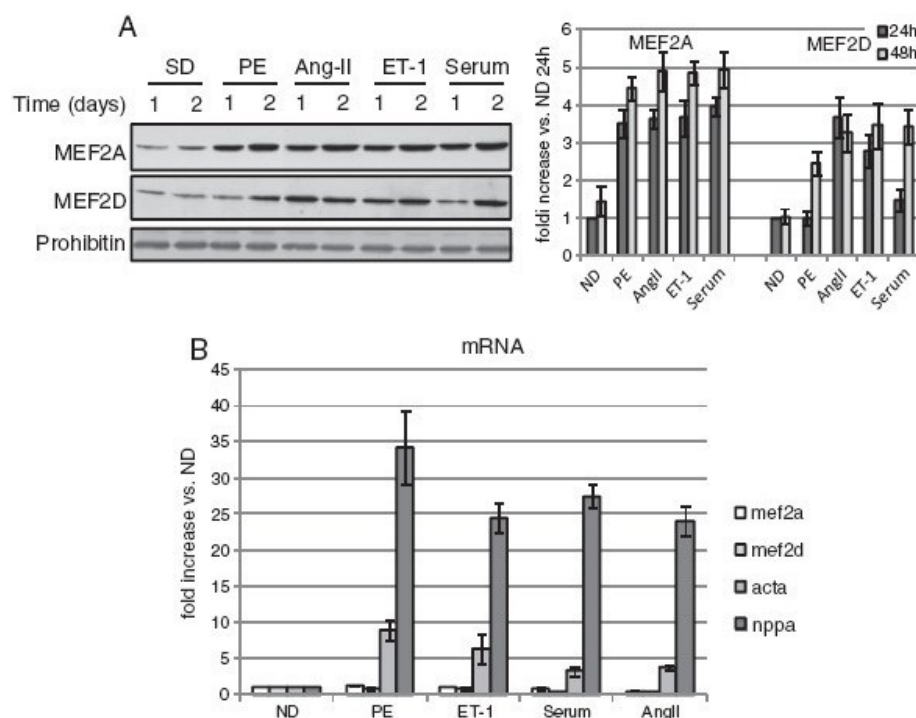


Fig. 2. Pro-hypertrophic stimuli enhance MEF2 protein expression posttranscriptionally in primary cardiomyocytes. (A) MEF2 protein expression in serum-deprived cardiomyocytes treated as described in the Materials and methods section during 1 or 2 days with different agonists: ND, serum-deprived no drug; PE, 100 μ M phenylephrine; Ang-II, 100 nM Angiotensin II; ET1, 0.1 μ M Endothelin-1, or serum, 10% HS plus 5% FCS, as described in the Materials and methods section. Representative images are shown from 5 independent experiments. Densitometry of Western blot bands was performed with the Image J software. Bars are means of 5 independent experiments \pm SEM. (B) Mef2 mRNA abundance in cultures treated as in (A) was quantified by TaqMan quantitative PCR from total RNA extracts, $n = 5$. Nppa (atrial natriuretic peptide precursor) and acta1 (alpha-actin) transcript abundance were also monitored to confirm induction of hypertrophic signaling. Bars are means of 5 independent experiments \pm SEM. No treatment induced statistically significant changes in Mef2 transcript abundance.

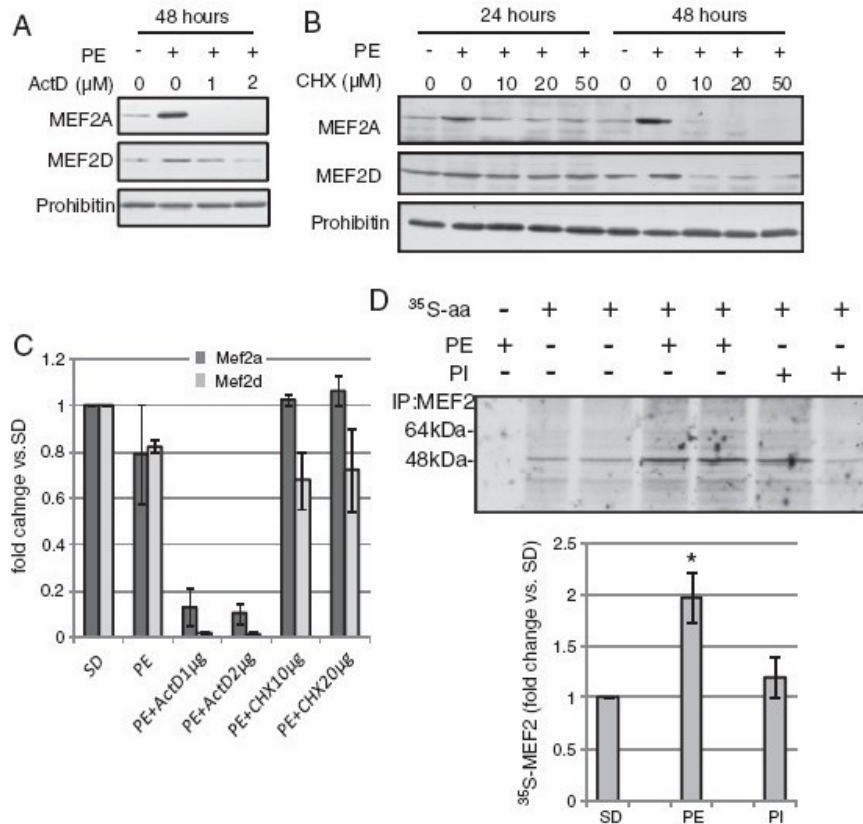


Fig. 3. MEF2A and MEF2D proteins have a short life requiring continuous translation sustained by agonist stimulation in cardiomyocytes. (A) MEF2 protein expression in cardiomyocytes treated with phenylephrine (PE) in the presence or absence of the transcription inhibitor Actinomycin D (ActD) or (B) in the presence or absence of the translational inhibitor cycloheximide (CHX). Representative Western blots are shown from 4 independent sets of samples. (C) Mef2 mRNA levels were measured by TaqMan quantitative PCR of retro-transcribed total RNA extracts from replicate cultures of cardiomyocytes used in (A) and (B). Bars are means \pm SEM, $n=5$. (D) *De novo* MEF2 translation was assessed by analyzing ³⁵S-Cysteine and ³⁵S-Methionine incorporation into MEF2 during 24 h in serum deprived cardiomyocytes treated with 100 μ M phenylephrine (PE) or 2 μ M of the proteasome inhibitor Lactacystin (PI). Bars are means \pm SEM, $n=3$. * $p<0.05$ vs. untreated, serum-deprived cells (SD).

changes in the respective mRNA levels (Fig. 3C), demonstrating the requirement of continuous translation and showing that MEF2 degradation was not arrested by PE treatment, otherwise CHX-treated cells would have kept high levels of MEF2. These results demonstrated a short life of MEF2 proteins compared, for example, with the mitochondrial protein prohibitin, used as loading control because of its steady expression both during cardiomyocyte differentiation and their response to stress [25,32]. To directly assess induction of MEF2 by hypertrophic agonists, cardiomyocytes were deprived from serum to reach basal levels of MEF2 expression and then, the incorporation of ³⁵S-labeled amino acids to MEF2 was analyzed in cultures treated with PE or the proteasome inhibitor Lactacystin. A twofold increase in ³⁵S-Cysteine and ³⁵S-Methionine incorporation to MEF2 was observed in serum and PE-treated myocytes compared to controls, but not in proteasome-treated cells, demonstrating that agonists were inducing *de novo* MEF2 translation (Fig. 3D). Inhibition of the proteasome only induced a small increase in newly synthesized protein. Comparison of MEF2 protein abundance in freshly isolated myocytes and serum-deprived myocyte cultures treated or not with PE, showed a progressive loss of MEF2 in the absence of serum, in agreement with its short life suggested by the previous experiments, and an increase in MEF2 abundance upon PE addition starting from levels below the initial abundance (24 h i.v.) (Fig. 4A), unrelated to changes in Mef2 transcript abundance (Fig. 4B). Then, the potential contribution of changes in protein degradation to increased MEF2 abundance was assessed by comparing MEF2 expression

in cardiomyocytes treated with PE or with two different proteasome inhibitors (M132 and Lactacystin) after serum deprivation. Only PE induced a significant increase in MEF2 abundance (Fig. 4C). These results discarded an eventual reduction of MEF2 degradation contributing to the high abundance of MEF2 in agonist-treated cells. Taken together, these data demonstrated a) that Mef2 transcripts and proteins are short lived, depending on continuous transcription and undergoing rapid proteasome-dependent degradation, respectively, b) that lack of serum neither decreased transcription nor protein degradation but reduced translation, and c) that PE addition in these conditions induced MEF2 expression through enhancing translation.

3.3. Calcineurin mediates the posttranscriptional enhancement of MEF2 expression *in vivo* and *in vitro*

Calcium/Calmodulin-dependent phosphatase Calcineurin has been shown to be involved in MEF2 dephosphorylation [13,14] potentiating MEF2 activity and is activated during agonist stimulation [33]. We assessed MEF2 expression in the ventricles of adult mice overexpressing Calcineurin in the myocardium, which present hypertrophy [15] and observed that despite unchanged Mef2 transcript levels, MEF2A and MEF2D proteins were more abundant than in the heart of their wild type littermates (Figs. 5A,B). To discard that increased MEF2 abundance was indirectly induced by hemodynamic changes due to the hypertrophied heart in Calcineurin-transgenic mice, we treated cultured neonatal rat

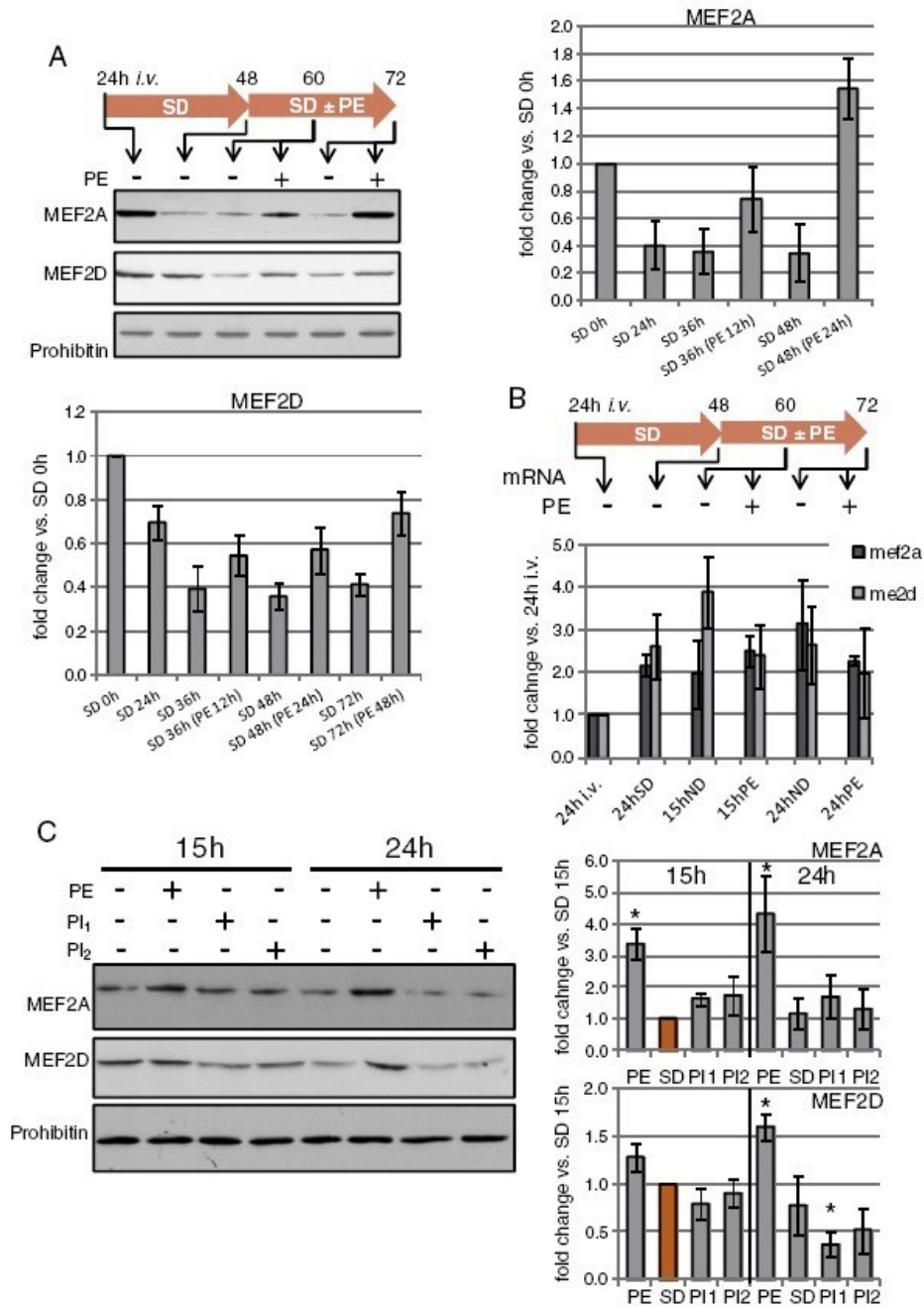


Fig. 4. Regulation of protein degradation does not contribute to sustain high levels of MEF2 during agonist stimulation in cardiomyocytes. (A) Time course of MEF2 protein expression during serum deprivation (SD) started 24 h after seeding (24 h i.v. = 24 h in vitro), and \pm 100 μ M phenylephrine (PE) addition in cultured cardiomyocytes. Numbers above arrows are hours in vitro (after seeding). Bar graph shows the Western blot densitometric analysis of 4 independent experiments presented as means \pm SEM (hours in parenthesis is time in the presence of PE). (B) Mef2 transcript abundance was measured by TaqMan quantitative PCR of retro-transcribed total RNA extracts from replicate cultures as in (A), bars are means \pm SEM, $n=4$. (C) Comparison of the time-related changes in MEF2 abundance in serum deprived cardiomyocytes (SD) and cardiomyocytes treated with phenylephrine (100 μ M, PE), or the proteasome inhibitors MG-132 (5 μ M, PI₁) or lactacystin (2 μ M, PI₂). Bars are means \pm SEM, $n=3$. * $p<0.05$ vs. SD at 15 h.

ventricular cardiomyocytes with the Calcineurin inhibitor CN585, which has been described recently to be specific for Calcineurin ($K_i=3.8 \mu$ M) without affecting other Ser/Thr protein phosphatases or peptidyl prolyl cis/trans isomerases [34]. A low dose of CN585 (2 μ M, far below its K_i) efficiently blunted the PE-dependent increase of MEF2 abundance (Fig. 5C),

without affecting Mef2 transcript levels (Fig. 5D). This demonstrated a direct effect of Calcineurin signaling on Mef2 translation in myocytes in the absence of any hemodynamic input. These results show that Calcineurin is involved in agonist-induced translation of MEF2, adding a novel level of MEF2 activity regulation by this phosphatase.

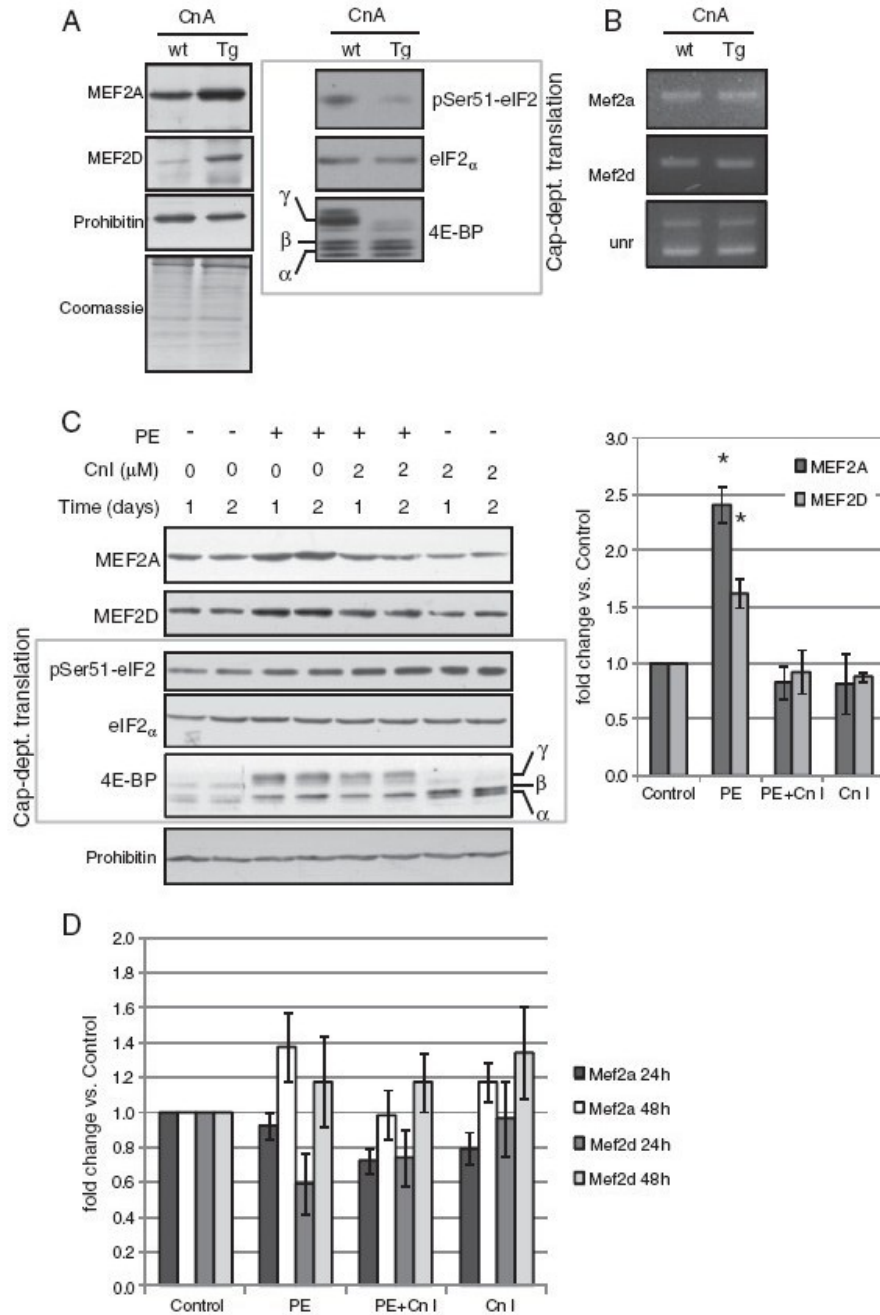


Fig. 5. Calcineurin mediates translation of MEF2 in vivo and in vitro during hypertrophy. (A) MEF2, eIF2 α , phosphoSer51-eIF2 and 4E-BP1 expression in total protein extracts of the hearts of hypertrophied 5-months-old Calcineurin A (CnA)-transgenic mice and wild type controls were analyzed by Western blot. A representative image is shown from the analysis of 4 independent hearts per genotype (Wt: wild type; Tg: CnA-transgenic). (B) Representative image of an agarose gel showing RT-PCR reactions of Mef2 mRNA transcript expression in the same hearts. Amplification of a fragment of unr (upstream of n-ras) mRNA including two exons, which in addition detects two co-expressed unr isoforms is used as a well established loading control [25,27]. (C) Effect of the addition of the Calcineurin Inhibitor VIII also known as CN585 (Cn I; Calbiochem, 207003, 2 μ M) in MEF2, eIF2 α , phosphoSer51-eIF2 and 4E-BP1 protein expression during phenylephrine (100 μ M, PE) treatment in cultured cardiomyocytes. Bar graph shows the Western blot densitometric analysis of 5 independent experiments presented as means \pm SEM. * p <0.05 vs. control values. (D) Mef2 transcript abundance was measured by TaqMan quantitative PCR of retro-transcribed total RNA extracts from replicate cultures as in (C) and bars are means \pm SEM. α , β and γ indicate increasingly phosphorylated forms of 4E-BP1.

3.4. Calcineurin-mediated increase of MEF2A expression involves Polypyrimidine Tract Binding Protein

The above results showed that hypertrophic agonist stimulation induced increased MEF2 translation, that this increase was dependent

on Calcineurin activity in cultured myocytes and that Calcineurin overexpression in vivo also triggered higher MEF2 abundance. To gain insight about the mechanisms connecting Calcineurin and MEF2 translation, we checked phosphorylation of key regulators of Cap-dependent translation in cardiomyocytes stimulated with PE in

the presence or absence of Calcineurin inhibitors and in the Calcineurin transgenic hearts. Initiation of Cap-dependent translation involves eukaryotic Initiator Factor-2 (eIF2), which mediates binding of tRNA^{met} to the 40S ribosomal subunit [35] and phosphorylation of eIF4E-binding protein (4E-BP1) inducing its detachment from eIF4E [36], which then mediates the binding of the cap structure of mRNAs to the ribosome. The phosphorylation status of eIF2 and 4E-BP1 was different in PE-treated myocytes and Calcineurin transgenic hearts (Figs. 5A,C), both showing high levels of MEF2A (Figs. 5A,C). This suggested that Calcineurin-dependent control of phosphorylation of the cap-dependent translation complex was not determining MEF2 translation.

Polypyrimidine Tract Binding Protein (PTB) is a RNA-interacting protein that contributes to cap-independent protein translation [37], in addition to be involved in RNA maturation. Our previous work identified PTB as a key regulator of apoptotic gene translation in differentiating cardiomyocytes [28]. We also showed that PTB expression decreases during heart development [28]. Calcineurin overexpression induced an important increase in PTB abundance in the adult heart (Fig. 6A), and agonist stimulation of cardiomyocytes in vitro also induced higher PTB expression (Fig. 6B). Interestingly, Calcineurin inhibition prevented PE-triggered expression of PTB. Thus, PTB abundance correlated with MEF2 expression in PE-treated myocytes and in the Calcineurin-overexpressing heart, suggesting a

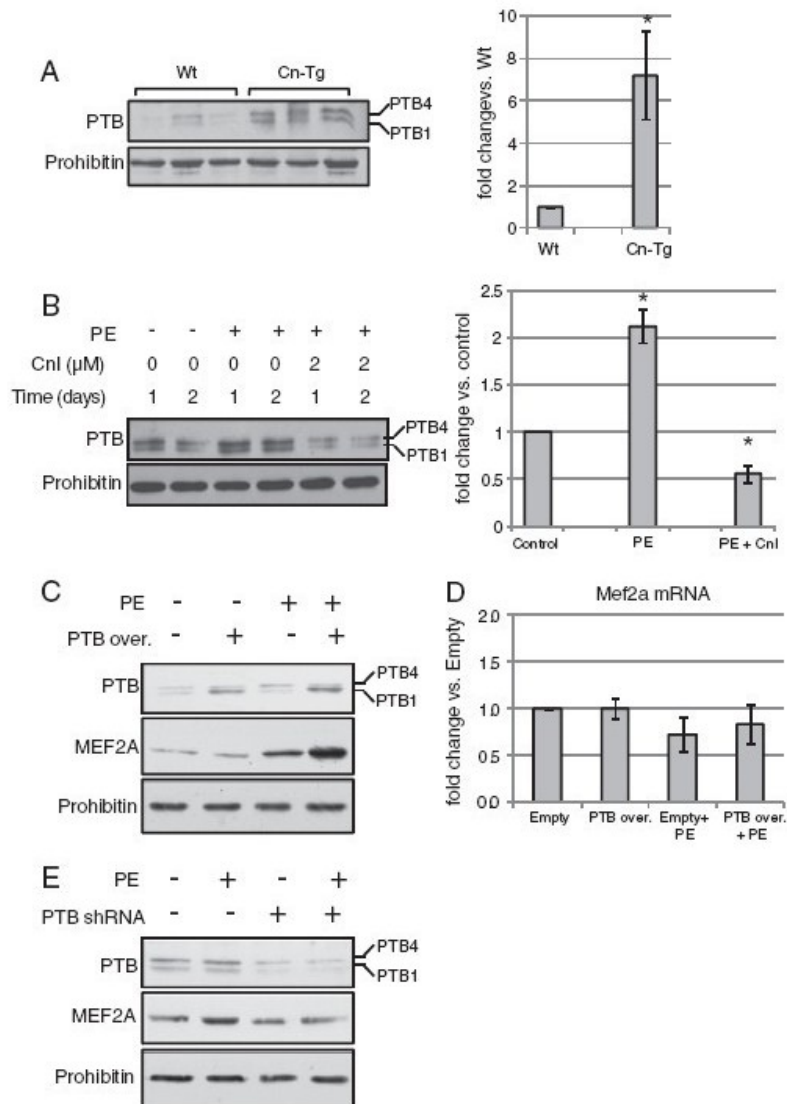


Fig. 6. Calcineurin-dependent control of PTB expression determines MEF2A protein abundance in cardiomyocytes. (A) PTB protein expression in total protein extracts of the hearts of hypertrophied 5-month-old Calcineurin (Cn-Tg) mice and wild type (Wt) controls were analyzed by Western blot. Right panel shows densitometric analysis of PTB expression in Cn-Tg hearts compared to paired wild type hearts in four independent sets of Western blots of 1 Wt heart and 1 Tg heart protein samples extracted, processed and analyzed together. * $p < 0.05$ vs. Wt. (B) PTB protein abundance in cultured cardiomyocytes during phenylephrine (100 μM, PE) treatment for 1 or 2 days and effect of adding the Calcineurin Inhibitor VIII also known as CN585 (Cn I; Calbiochem, 207003). Right panel shows densitometric analysis of PTB expression in the same samples at 1 day of treatment. Bars are means \pm SEM, $n = 3$. * $p < 0.05$ vs. controls (cells cultured without neither serum nor PE). (C) PTB and MEF2A expression in cardiomyocytes transduced with lentiviruses carrying empty vector (empty) or a vector carrying the PTB1 human sequence (PTB over) as described in Materials and methods section and treated or not with PE for the last 24 h before protein extraction $n = 3$. (D) Quantitative RT-PCR analysis of MEF2A mRNA in cultures as in (C). Bars are means \pm SEM, $n = 3$. (E) PTB and MEF2A expression in cardiomyocytes transduced with lentiviruses containing a vector carrying a Ptb scrambled sequence or a vector carrying a sequence for Ptb expression silencing (shRNA) as described in Materials and methods section and treated or not with PE for the last 24 h before protein extraction $n = 3$.

functional link. Lentiviral-driven PTB overexpression induced an increase of MEF2A protein abundance only in the presence of PE (Fig. 6C) without affecting its transcript (Fig. 6D), and lentiviral-driven silencing of Ptb expression hampered PE-induced MEF2A translation (Fig. 6E). Altogether, these results showed that Calcineurin-dependent regulation of MEF2 translation in the heart involved PTB.

4. Discussion

The principal finding of this paper is that abundance of the transcription factors MEF2A and MEF2D in differentiated cardiomyocytes is increased at the translational level during hypertrophic agonist stimulation through a pathway involving Calcineurin and PTB, determining cardiomyocyte cell growth.

Because of the early discovery that MEF2 activity is regulated by transcription during embryogenesis [6,38] and then by posttranslational modification [8] combined with association to enhancers such as NFAT [16] or inhibitors such as Class II HDACs [18,39], the vast majority of information available on MEF2 activity regulation focus on MEF2 transcription in the embryo, reviewed in [40] and on its post-translational regulation, reviewed in [41]. This could lead to the impression that MEF2 abundance is not a relevant point of regulation during adaptation to stress in the postnatal heart and that relative MEF2 abundance influences only marginally cardiac growth. Reports simultaneously comparing expression of Mef2 both at the transcript and protein levels during agonist stimulation are scarce [23,24] and there was no such data available for cardiac development. Here, by comparing the response to the hypertrophic agonist phenylephrine of cardiomyocytes expressing different levels of MEF2A, we show that its abundance does influence agonist-induced growth of differentiated cardiomyocytes *in vitro*. These results are in agreement with the partial blockade of Calcineurin-induced hypertrophy *in vivo* by overexpression of a dominant negative Mef2a [42] and with ventricular hypertrophy observed in Mef2a transgenic mice [43], but here we used a direct approach by changing the endogenous levels of Mef2a instead of adding a negative competitor or enhancing its expression. In addition, our observation that Calcineurin-overexpressing mice express high levels of MEF2A and that Calcineurin inhibition *in vitro* blocks MEF2A expression during phenylephrine treatment establishes a link between Calcineurin and MEF2 expression that helps clarify the previous suggestion that MEF2 could function independently of Calcineurin-directed hypertrophy [43]. Our results also show that MEF2A and MEF2D abundance increase during agonist stimulation by enhancing their translation and demonstrate that MEF2 proteins, not their transcripts, are more abundant in a model of hypertrophied heart *in vivo*. Given that our results also show, for the first time to our knowledge, that MEF2D expression decreases during aging (Suppl. Fig. 1), our data showing that MEF2D protein abundance is upregulated in the hypertrophied Calcineurin-overexpressing heart, contributes to the understanding of its essential role during stress-induced cardiac hypertrophy [5].

Previous knowledge about posttranscriptional regulation of MEF2 abundance was limited to the autoinhibitory role of Mef2a transcript's 3'UTR [20] and the miR1-dependent Mef2a mRNA degradation [23]. Ikeda and co-workers found that miR-1 binds to Mef2a 3'UTR and induces degradation of the transcript and that Calcium signaling induces reduction of miR-1 expression [23]. Interestingly, these authors found increased MEF2A protein expression in the Calcineurin-overexpressing heart; the same *in vivo* model used by us, but suggested it was due to Calcium-dependent miR-1 downregulation [23]. This would have lead to increased Mef2a mRNA levels. However, cardiac Mef2a mRNA levels, which should be higher in the transgenic heart if miR-1 played a relevant role in MEF2 regulation in this model, were not measured. Thus, our results showing that Mef2a and Mef2d transcripts are actually unaffected in the heart of Calcineurin transgenic mice are not in contradiction with Ikeda's group results, but rather

complete them, opening the possibility that regulation of MEF2A protein abundance in the hypertrophied heart *in vivo* involves other mechanisms than miR-1-dependent signaling, including Mef2 enhanced translation. Calcineurin has been shown to promote cap-dependent protein translation in the pancreas [44]. However, our results suggest that cap-dependent translation is not involved in MEF2 translation in the myocardium during hypertrophy because Calcineurin overexpression reduced the phosphorylation status of eIF2 and the abundance of the hyperphosphorylated form of 4E-BP1, yet induced MEF2 translation. Finally, our results demonstrate that PTB, which has been shown previously by many groups to be involved in cap-independent translation [e.g. 28,37] is a novel downstream target of Calcineurin activity and modulates MEF2A translation in cardiomyocytes.

In conclusion, our results a) support induction of translation as a previously unrecognized level modulating MEF2 activity, b) add information about the regulation of MEF2A, a master coordinator of gene expression during cell differentiation and organogenesis, c) contribute to understand the function of MEF2D, whose expression is shown here to decay during postnatal heart growth to almost undetectable levels, yet is known to be required for cardiac hypertrophy in the adult, and d) show a novel pathway, translation, by which Calcineurin signaling regulates MEF2 activity, involving the control of PTB expression.

Supplementary data to this article can be found online at <http://dx.doi.org/10.1016/j.jmcc.2012.07.013>.

Sources of funding

This work was supported by grant SAF2010_19125 from the Ministerio de Innovación y Ciencia de Spain (MICINN, now Ministerio de Economía y Competitividad) to DS and by the Agencia de Gestió d'Ajuts a Grups de Recerca (AGAUR) from the Generalitat de Catalunya 2009SGR-346 to DS and JXC. JY is a recipient of a fellowship from the Universitat de Lleida (Spain) and MC has a FPU (Formación de profesorado universitario) fellowship from MICINN.

Disclosure statement

None declared.

Acknowledgments

We want to thank the efficient technical support of Carme Guerris and Cristina Girón at the lab and Jessica Pairada at the Animal Service (Estabulari de la Universitat de Lleida). We are grateful to Eric N Olson for the gift of the Calcineurin transgenic hearts.

References

- [1] Potthoff MJ, Olson EN. MEF2: a central regulator of diverse developmental programs. *Development* 2007;134(23):4131–40.
- [2] Lin Q, Schwarz J, Bucana C, Olson EN. Control of mouse cardiac morphogenesis and myogenesis by transcription factor MEF2C. *Science* 1997;276(5317):1404–7.
- [3] Vong LH, Ragusa MJ, Schwarz JJ. Generation of conditional Mef2cloxP/loxP mice for temporal- and tissue-specific analyses. *Genesis* 2005;43(1):43–8.
- [4] Naya FJ, Black BL, Wu H, Bassel-Duby R, Richardson JA, Hill JA, et al. Mitochondrial deficiency and cardiac sudden death in mice lacking the MEF2A transcription factor. *Nat Med* 2002;8(11):1303–9.
- [5] Kim Y, Phan D, van Rooij E, Wang DZ, McAnally J, Qi X, et al. The MEF2D transcription factor mediates stress-dependent cardiac remodeling in mice. *J Clin Invest* 2008;118(1):124–32.
- [6] Edmondson DG, Lyons GE, Martin JF, Olson EN. Mef2 gene expression marks the cardiac and skeletal muscle lineages during mouse embryogenesis. *Development* 1994;120(5):1251–63.
- [7] Ramachandran B, Yu G, Li S, Zhu B, Gulick T. Myocyte enhancer factor 2A is transcriptionally autoregulated. *J Biol Chem* 2008;283(16):10318–29.
- [8] Molkenin JD, Li L, Olson EN. Phosphorylation of the MADS-Box transcription factor MEF2C enhances its DNA binding activity. *J Biol Chem* 1996;271(29):17199–204.

- [9] Ornatsky OI, Cox DM, Tangirala P, Andreucci JJ, Quinn ZA, Wrana JL, et al. Post-translational control of the MEF2A transcriptional regulatory protein. *Nucleic Acids Res* 1999;27(13):2646–54.
- [10] Zhao M, New I, Kravchenko VV, Kato Y, Gram H, di Padova F, et al. Regulation of the MEF2 family of transcription factors by p38. *Mol Cell Biol* 1999;19(1):21–30.
- [11] Lu J, McKinsey TA, Zhang CL, Olson EN. Regulation of skeletal myogenesis by association of the MEF2 transcription factor with class II histone deacetylases. *Mol Cell* 2000;6(2):233–44.
- [12] Stewart AA, Ingebritsen TS, Manalan A, Klee CB, Cohen P. Discovery of a Ca²⁺ and calmodulin-dependent protein phosphatase: probable identity with calcineurin (CaM-BP80). *FEBS Lett* 1982;137(1):80–4.
- [13] Wu H, Naya FJ, McKinsey TA, Mercer B, Shelton JM, Chin ER, et al. MEF2 responds to multiple calcium-regulated signals in the control of skeletal muscle fiber type. *EMBO J* 2000;19(9):1963–73.
- [14] Wu H, Rothermel B, Kanatous S, Rosenberg P, Naya FJ, Shelton JM, et al. Activation of MEF2 by muscle activity is mediated through a calcineurin-dependent pathway. *EMBO J* 2001;20(22):6414–23.
- [15] Molkenin JD, Lu JR, Antos CL, Markham B, Richardson J, Robbins J, et al. A calcineurin-dependent transcriptional pathway for cardiac hypertrophy. *Cell* 1998;93(2):215–28.
- [16] Chin ER, Olson EN, Richardson JA, Yang Q, Humphries C, Shelton JM, et al. A calcineurin-dependent transcriptional pathway controls skeletal muscle fiber type. *Genes Dev* 1998;12(16):2499–509.
- [17] Creemers EE, Sutherland LB, Oh J, Barbosa AC, Olson EN. Coactivation of MEF2 by the SAP domain proteins myocardin and MASTR. *Mol Cell* 2006;23(1):83–96.
- [18] Miska EA, Karlsson C, Langley E, Nielsen SJ, Pines J, Kouzarides T. HDAC4 deacetylase associates with and represses the MEF2 transcription factor. *EMBO J* 1999;18(18):5099–107.
- [19] McKinsey TA, Olson EN. Toward transcriptional therapies for the failing heart: chemical screens to modulate genes. *J Clin Invest* 2005;115(3):538–46.
- [20] Black BL, Lu J, Olson EN. The MEF2A 3' untranslated region functions as a cis-acting translational repressor. *Mol Cell Biol* 1997;17(5):2756–63.
- [21] Zhao Y, Samal E, Srivastava D. Serum response factor regulates a muscle-specific microRNA that targets Hand2 during cardiogenesis. *Nature* 2005;436(7048):214–20.
- [22] Liu N, Williams AH, Kim Y, McAnally J, Bezprozvannaya S, Sutherland LB, et al. An intragenic MEF2-dependent enhancer directs muscle-specific expression of microRNAs 1 and 133. *Proc Natl Acad Sci U S A* 2007;104(52):20844–9.
- [23] Ikeda S, He A, Kong SW, Lu J, Bejar R, Bodyak N, et al. MicroRNA-1 negatively regulates expression of the hypertrophy-associated calmodulin and Mef2a genes. *Mol Cell Biol* 2009;29(8):2193–204.
- [24] Suzuki E, Guo K, Kolman M, Yu YT, Walsh K. Serum induction of MEF2/RSRF expression in vascular myocytes is mediated at the level of translation. *Mol Cell Biol* 1995;15(6):3415–23.
- [25] Zhang J, Bahi N, Zubiaga AM, Comella JX, Llovera M, Sanchis D. Developmental silencing and independency from E2F of apoptotic gene expression in postmitotic tissues. *FEBS Lett* 2007;581(30):5781–6.
- [26] Sanchis D, Mayorga M, Ballester M, Comella JX. Lack of Apaf-1 expression confers resistance to cytochrome c-driven apoptosis in cardiomyocytes. *Cell Death Differ* 2003;10(9):977–86.
- [27] Bahi N, Zhang J, Llovera M, Ballester M, Comella JX, Sanchis D. Switch from caspase-dependent to caspase-independent death during heart development: essential role of endonuclease G in ischemia-induced DNA processing of differentiated cardiomyocytes. *J Biol Chem* 2006;281(32):22943–52.
- [28] Zhang J, Bahi N, Llovera M, Comella JX, Sanchis D. Polypyrimidine tract binding proteins (PTB) regulate the expression of apoptotic genes and susceptibility to caspase-dependent apoptosis in differentiating cardiomyocytes. *Cell Death Differ* 2009;16(11):1460–8.
- [29] Simpson P, McGrath A, Savion S. Myocyte hypertrophy in neonatal rat heart cultures and its regulation by serum and by catecholamines. *Circ Res* 1982;51(6):787–801.
- [30] Day ML, Schwartz D, Wiegand RC, Stockman PT, Brunnert SR, Tolunay HE, et al. Ventricular atriopeptin. Unmasking of messenger RNA and peptide synthesis by hypertrophy or dexamethasone. *Hypertension* 1987;9(5):485–91.
- [31] Bishopric NH, Simpson PC, Ordahl CP. Induction of the skeletal alpha-actin gene in alpha 1-adrenoceptor-mediated hypertrophy of rat cardiac myocytes. *J Clin Invest* 1987;80(4):1194–9.
- [32] Zhang J, Ye J, Altafaj A, Cardona M, Bahi N, Llovera M, et al. EndoG links Bnip3-induced mitochondrial damage and caspase-independent DNA fragmentation in ischemic cardiomyocytes. *PLoS One* 2011;6(3):e17998.
- [33] Taigen T, De Windt IJ, Lim HW, Molkenin JD. Targeted inhibition of calcineurin prevents agonist-induced cardiomyocyte hypertrophy. *Proc Natl Acad Sci U S A* 2000;97(3):1196–201 [1].
- [34] Erdmann F, Weiwad M, Kilka S, Karanik M, Pätzl M, Baumgrass R, et al. The novel calcineurin inhibitor CN585 has potent immunosuppressive properties in stimulated human T cells. *J Biol Chem* 2010;285(3):1888–98.
- [35] Siekierka J, Mauser L, Ochoa S. Mechanism of polypeptide chain initiation in eukaryotes and its control by phosphorylation of the alpha subunit of initiation factor 2. *Proc Natl Acad Sci U S A* 1982;79(8):2537–40.
- [36] Pause A, Belsham GJ, Gingras A-C, Donze O, Lin T-A, Lawrence JC, et al. Insulin-dependent stimulation of protein synthesis by phosphorylation of a regulator of 5'-cap function. *Nature* 1994;371:762–7.
- [37] Mitchell SA, Brown EC, Coldwell MJ, Jackson RJ, Willis AE. Protein factor requirements of the Apaf-1 internal ribosome entry segment: roles of polypyrimidine tract binding protein and upstream of N-ras. *Mol Cell Biol* 2001;21:3364–74.
- [38] Naya FJ, Wu C, Richardson JA, Overbeek P, Olson EN. Transcriptional activity of MEF2 during mouse embryogenesis monitored with a MEF2-dependent transgene. *Development* 1999;126(10):2045–52.
- [39] Lu J, McKinsey TA, Nicol RL, Olson EN. Signal-dependent activation of the MEF2 transcription factor by dissociation from histone deacetylases. *Proc Natl Acad Sci U S A* 2000;97(8):4070–5.
- [40] Molkenin JD, Olson EN. Combinatorial control of muscle development by basic helix-loop-helix and MADS-box transcription factors. *Proc Natl Acad Sci U S A* 1996;93(18):9366–73.
- [41] McKinsey TA, Zhang CL, Olson EN. MEF2: a calcium-dependent regulator of cell division, differentiation and death. *Trends Biochem Sci* 2002;27(1):40–7.
- [42] van Oort RJ, van Rooij E, Bourajaj M, Schimmel J, Jansen MA, van der Nagel R, et al. MEF2 activates a genetic program promoting chamber dilation and contractile dysfunction in calcineurin-induced heart failure. *Circulation* 2006;114(4):298–308.
- [43] Xu J, Gong NL, Bodi I, Aronow BJ, Backx PH, Molkenin JD. Myocyte enhancer factors 2A and 2C induce dilated cardiomyopathy in transgenic mice. *J Biol Chem* 2006;281(14):9152–62.
- [44] Sans MD, Williams JA. Calcineurin is required for translational control of protein synthesis in rat pancreatic acini. *Am J Physiol Cell Physiol* 2004;287(2):C310–9.

Annex 3. A pathway involving HDAC5, cFLIP and caspases regulates PTB expression influencing Mef2 alternative splicing in the heart

A pathway involving HDAC5, cFLIP and caspases regulates expression of the splicing regulator Polypyrimidine Tract Binding Protein expression in the heart

Junmei Ye^{1*}, Miriam Llorian^{2*}, Maria Cardona¹, Anthony Rongvaux³, Rana Moubarak⁴, Joan X Comella⁴, Rhonda Bassel-Duby⁵, Richard A. Flavell³, Eric N Olson⁵, Christopher W. J. Smith², Daniel Sanchis¹.

- 4) Departament Ciències Mèdiques Bàsiques, Universitat de Lleida – IRBLLEIDA, Av Rovira Roure, 80, Lleida, 25198 Spain.
- 5) Department of Biochemistry, University of Cambridge, Building O, Downing site, Cambridge, CB2 1QW, UK.
- 6) Department of Immunobiology, and f. Howard Hughes Medical Institute, Yale University School of Medicine, New Haven, CT 06520, USA.
- 7) Cibernet, Institut de Recerca Hospital Universitari Vall d'Hebró- UAB, Barcelona, 08035, Spain.
- 8) Department of Molecular Biology, University of Texas Southwestern Medical Center, 6000 Harry Hines Boulevard, Dallas, Texas 75390-9148, USA.

Running title: *HDAC-dependent control of Mef2 splicing*

* These authors contributed equally to this work

Word count (Materials and Methods):

Word count (Introduction, Results and Discussion):

Corresponding author: Daniel Sanchis. Departament Ciències Mèdiques Bàsiques, Universitat de Lleida – IRBLLEIDA, Av Rovira Roure, 80, Lleida, 25198 Spain Tel: +34 973702215 Fax: +34 973702213. Email: daniel.sanchis@cmb.udl.cat

ABSTRACT

Polypyrimidine Tract Binding Protein (PTB) regulates pre-mRNA splicing, having special relevance for determining gene expression in the differentiating muscle. We have previously shown that PTB protein abundance is progressively reduced during heart development without reduction of its own transcript. Simultaneous reduction of Histone Deacetylase (HDAC) expression and changes in Myocyte Enhancer Factor-2 splicing pattern prompted us to investigate the potential link between these events. HDAC5-deficient mice have reduced cardiac PTB protein abundance, and HDAC inhibition in myocytes causes caspase-dependent cleavage of PTB and a reduction in endogenous expression of cFLIP. In agreement with this, cardiac PTB expression is abnormally high in mice with cardiac-specific executioner caspase deficiency and cFLIP overexpression prevents PTB cleavage *in vitro*. Caspase-dependent cleavage triggers further fragmentation of PTB and these fragments accumulate in the presence of proteasome inhibitors. Experimental modification of the above processes *in vivo* and *in vitro* resulted in coherent changes in the splicing of Myocyte Enhancer Factor-2 (Mef2) exon β . Thus, we report a pathway connecting HDAC, cFLIP and caspases regulating the progressive disappearance of PTB, which enables the expression of the adult variants of Mef2 during heart development.

INTRODUCTION

Polypyrimidine Tract Binding Protein (PTB) is an RNA-binding protein well known for its role in the regulation of alternative splicing of many transcripts (13), including those coding for sarcomeric proteins β -tropomyosin, α -tropomyosin, α -actinin and troponin-T (8,25,28,33). Global profiling of PTB targets in HeLa cells confirmed that PTB represses many neuronal and striated muscle specific exons in genes encoding cytoskeletal and signaling proteins (19,34). PTB is also involved in cap-independent protein translation (23,32) and our previous results showed that PTB supports apoptotic protein translation in differentiating cardiomyocytes (36). All these results suggest an important contribution of PTB in the post-transcriptional control of gene expression during muscle differentiation. However, regulation of PTB expression has been only partially elucidated. PTB limits its own expression by inhibiting inclusion of exon 11 in its own mRNA inducing its degradation by nonsense-mediated decay (NMD) in HeLa cells (36). Down-regulation of PTB expression is important for orchestrating regulated splicing programs during neurogenesis (6). Neuron-specific microRNA miR-124 targets the PTB mRNA reducing PTB levels in differentiating neurons (21). Likewise, in differentiating C2C12 myoblasts nPTB expression is downregulated by miR-133 (5). Thus, it seems that targeting PTB mRNA is important for the control of PTB activity in cell lines and during neuronal development. However, there has been little information regarding the regulation of PTB levels in cardiac muscle. Here, we show that PTB levels in the developing heart are reduced post-translationally by a pathway involving histone deacetylases (HDAC) and the direct cleavage of PTB by caspases.

Class IIa histone deacetylases (HDAC) are involved in the control of gene expression in striated muscle (11). In particular, HDAC4 and 5 bind MEF2 transcription factor, inhibiting its transcriptional activity (20). Double deletion of HDAC5 and 9 is embryonic lethal in mice accompanied by defects in the cardiac structure (7). It was suggested that this phenotype could ensue from precocious differentiation due to premature derepression of MEF2 activity (7), but the hypothesis remains unexplored.

The caspase-dependent signaling machinery is expressed in the embryonic myocardium but is repressed during heart differentiation (2,41). Deficiency in Caspase-8 (35), Fas-associated Death Domain protein (FADD) (39) or cellular FLICE-like Inhibitory Protein (cFLIP) (38), which regulates the death receptor-dependent pathway, as well as the double deletion of executioner caspases 3 and 7 (15) induced embryonic lethality with alteration of the cardiac ventricular structure. Cardiac defects of caspase-8 deficient mice including abnormal myocyte death were rescued by ex vivo embryo culture and pointed to a role of Caspase-8 in the control of cell death during development (31). Strikingly, the rate of apoptosis in the FADD and cFLIP mutant hearts was low and similar to wild type tissue but the differentiation process of the ventricles was altered suggesting that these factors have functions unrelated to cell death during heart development (38,39). Despite the relevant contribution of the caspase-dependent signaling to cardiac morphogenesis, its precise function in the heart remains unknown. Caspases have been shown to directly target PTB in cell lines treated with toxic drugs (1), but there has been no previous indication of a role for such processing in a normal physiological setting.

The myocyte enhancer factor 2 (MEF2) family of transcription factors, comprised of four members termed MEF2A-D, is involved in the transcription of genes required for skeletal and heart muscle development as well as for muscle adaptation to stress (30). MEF2A is the most abundant MEF2 variant in the adult heart (38) and its deletion in mice induces death during the first week of life with alterations in cardiomyocyte ultrastructure (27). Deletion of MEF2C induces profound morphological defects in the heart (17). Finally, deletion of MEF2D hampers cardiac hypertrophy in the adult (14). Therefore, MEF2 activity is essential for heart development and cardiac adaptation to stress. An alternative splicing event in Mef2 transcripts involving the inclusion of a short exon (exon β) occurs in striated muscle and brain, two tissues with MEF2-regulated gene transcription (40). Inclusion of exon β increases during C2C12 myoblast differentiation *in vitro* (40,42), resulting in translation of a MEF2 variant with stronger transcriptional activity (48). *In vitro* experiments in HeLa cells showed that PTB induces exon β skipping in Mef2d (18) and in cultured C2C12 myoblasts exon β

inclusion in Mef2c seems to require PTB (16). In addition, exon β inclusion was detected in RNA extracts of adult heart yet the timing and mechanisms regulating the splicing of exon β in the heart have not yet been characterized. (40,42).

In this study, we present *in vivo* and *in vitro* data showing that expression of the splicing repressor PTB in the developing myocardium is reduced through its caspase-dependent cleavage. Upstream control of the caspase activity is influenced by HDAC activity, while one of the downstream consequences of reduced PTB levels is the inclusion of exon β in the Mef2 transcripts to express the adult variants. These findings reveal a new pathway of regulation of the splicing repressor PTB during heart development.

MATERIALS AND METHODS

Animal, tissues and cell cultures. The investigation with experimental animals conforms to the Guide for the Care and Use of Laboratory Animals published by the US National Institutes of Health (NIH Publication No. 85-23, revised 1996) and was approved by our Experimental Animal Ethic Committee. For analysis of protein expression we used hearts from Sprague–Dawley rats (Charles-River) housed in our Experimental Animal Facility at the University of Lleida. Full Caspase-7 deficient, cardiac-specific caspase-3 deficient mouse strain was generated by sequential crossing of Casapase-7 null mice (15) with Caspase-3 floxed mice (gift from Richard Flavell) and then with the Nkx2.5-Cre mouse strain (gift from Eric Olson). Genotypes were analyzed by PCR.. HDAC5 and HDAC9 strains (7) and HDAC1and 2 double mutant strain (24) were housed in their laboratories of origin. Hearts were dissected minced into small cubes, rinsed with cold phosphate buffered saline and snap-frozen into liquid nitrogen. Rat neonatal cardiomyocytes were obtained from the ventricles of 2 to 4-day-old pups as described elsewhere (2). Human Embryonic Kidney 293 cells (HEK293) were cultured and used both for experiments and for virus production as reported previously (2).

Pharmacological treatments, lentivirus production and cell transduction. HDAC inhibitors Sodium Butyrate (Na-But, Cat.N. B5887) and Trichostatin-A (TSA, Cat. N. T8552) were purchased from SIGMA. Caspase inhibitors z-VAD-fmk (Cat. N. 550377) and z-IETD-fmk (Cat. N. 550380) were from BD Pharmingen. Proteasome inhibitor Lactacystin (L6785) was from SIGMA. Lentiviral particles empty or for inducing overexpression of human PTB1 and PTB4 (41) and mouse c-FLIP-L were prepared as previously reported (41) and cardiomyocytes were treated after 3 days of transduction as described elsewhere (2).

RNA extraction, Real Time and quantitative RT-PCR. For heart and cardiomyocytes, total RNA was obtained from frozen tissues or cell pellets with the RNeasy Mini Kit (Qiagen). RNA concentration measurements and reverse transcription were done as described (2, 41).

Quantitative Real Time PCR was performed in a iCycler iQ PCR detection system and iQ v.3 and iQ v.5 software (BioRad), using the Taq Man Gene Expression Master Mix (Cat.N. 4369016) and the Gene Expression Assays Mm00943334_m1 and Rn00821112_m1 to amplify mouse and rat Ptb, respectively and Rn00589205_m1 to amplify rat cFlip, with simultaneous amplification of Gapdh as loading control (Applied Biosystems). For radioactive quantitative PCR, reverse transcriptase reactions were carried out using 1µg of total RNA, oligo dT and Superscript II (Invitrogen) following manufacturer's instructions. PCR reactions were carried out with 10 pmol of forward primer and 4 pmol of ³²P-labeled reverse primer (Supplemental Table S1) and 1U/µl of Taq polymerase, under the following conditions: 94°C for 30s, 55°C for 30s and 72°C for 30 s, 25 or 30 cycles. 1/20 of the PCR was separated on 8% polyacrylamide urea gel. Gels were dried and expose in phosphorimager cassettes. PCR band ratios were determined using Molecular Dynamics PhosphorImager and shown as fraction of the total. Data shown is mean ± SD, n=3.

Protein extraction, SDS-PAGE and Western Blot. Protein expression was analyzed in protein extracts diluted in Tris-buffered 2% SDS solution at pH 6.8 and SDS-PAGE was performed as described (2). Antibody specifications are described in Supplemental Table S2. Western blots were performed as reported (2).

RESULTS

PTB expression is silenced perinatally during heart development through postranscriptional mechanisms blocked by HDAC5. We examined the expression pattern of PTB in the rat heart at different development stages. PTB protein levels were reduced rapidly after birth (Fig. 1A), and by day 90, PTB was undetectable. Interestingly, we did not detect significant changes in the *Ptb* mRNA level during the perinatal period of development. In the adult, *Ptb* levels had decreased by only 40% while PTB protein had already disappeared (Fig. 1B), suggesting postranscriptional regulation.

HDAC proteins are regulators of gene expression in many tissues and, in particular, they have an essential function during heart development (7,24). Mice deficient for Class II HDAC 5 and 9 or Class I HDAC 1 and 2 show propensity to lethal cardiac defects (7,24). Therefore, we measured the expression of HDAC proteins in the heart and observed that HDAC 1, 2 and 5 were abundant in the embryonic myocardium and there is a positive correlation in their temporal expression pattern to that of PTB (Fig. 1A). Consistent with a causal relationship between the decrease in expression of HDACs and PTB, we also observed lower amounts of PTB in the hearts of neonatal mice deficient for HDAC5 expression (Fig. 1C), although *Ptb* transcript levels were similar to wild type age-matched littermates (Fig. 1D). This effect was specific for HDAC5 because neither lack of HDAC9 nor the double deletion of Class I HDAC1 and 2 modified PTB expression significantly *in vivo* (Fig. 1C). These results suggest that HDAC5 influences the post-transcriptional regulation of *Ptb* in the heart *in vivo*. However, given its molecular function as a histone deacetylase it is unlikely that it acts directly as a positive effector of PTB expression.

HDAC sustains PTB expression in cardiomyocytes through inhibition of caspase-dependent PTB cleavage. To further explore the relationship between HDAC activity and PTB expression, we investigated the effects of treating postnatal rat cardiomyocytes with the HDAC inhibitors, sodium-butyrate (NaB) or Trichostatin-A (TSA) (Fig. 2A,B). Both

treatments led to a reduction of full length PTB protein abundance, with no effects upon Ptb mRNA levels (Fig. 2A,B). However, the reduction in full length PTB was accompanied by the appearance of faster migrating doublet, (Fig. 2A, left panel) as detected with an antibody obtained against the C-terminal region of PTB. The size of the faster migrating PTB doublet (~40 kDa) observed in cardiomyocytes treated with HDAC inhibitors is consistent with cleavage by caspases between the RRM1 and RRM2 domains of PTB (1). This effect was not observed in HEK293 cells (Fig. 2A, right panel), which express high levels of Class I HDAC but lack detectable expression of HDAC5. Consistent with PTB cleavage by caspases in cardiomyocytes treated with HDAC inhibitors, the pan-caspase inhibitor z-VAD-fmk abolished appearance of the smaller PTB fragments, preserving the abundance of the full length form (Fig. 2A). Caspase-dependent PTB cleavage induced by HDAC inhibition was not associated with a significant increase in cell death (Fig. 2B). If caspases play a physiological role in PTB cleavage *in vivo*, caspase deficiency should lead to increased abundance of PTB in the developing heart. Consistent with this prediction, PTB was more abundant in the neonatal heart of cardiac-specific Caspase-3 and 7 deficient mice than in their wild type age-matched controls (Fig. 2C), while the abundance of the Ptb transcript was unchanged (Fig. 2D).

The preceding data indicate that caspases are responsible for the reduction in PTB levels during cardiac development. However, it is not clear how the activity of caspases upon PTB is regulated. Given that disruption of cFLIP, a natural inhibitor of caspase activity, interferes with heart development (38), we next aimed to assess the contribution of cFLIP to HDAC inhibitor-induced PTB cleavage *in vitro*. cFLIP mRNA (Fig. 3A) and protein (Fig. 3C) expression was reduced in cardiomyocytes treated with HDAC inhibitors and cFLIP-L overexpression or treatment with the Caspase-8 inhibitor z-IETD-fmk prevented HDAC inhibitor-induced PTB cleavage (Fig. 3B). cFLIP overexpression also prevented fragmentation of PTB into a smaller fragment of approximately 25 kDa (Fig. 3C). Taken together, our results demonstrated a role of the extrinsic pathway of apoptosis, unrelated to cell death and regulated by HDAC, in the control of PTB expression in the myocardium.

Caspase-dependent cleavage of PTB triggers its proteasome-dependent degradation

Upon performing a time course of PTB degradation in cardiomyocytes treated with HDAC inhibitors, a small fragment of ~25kDa was observable at later time points (Fig. 4A). This suggests that the caspase-dependent fragments of PTB previously observed (Fig. 3) are being further processed. It has been reported that caspase-dependent fragmentation could trigger the proteasome-dependent degradation of the targeted protein (9,29). Therefore, we assessed if PTB was degraded by the proteasome. In the presence of the proteasome inhibitor Lactacystin we observed an accumulation of the smallest PTB fragments produced during Sodium Butyrate treatment (Fig. 4B), suggesting that PTB fragments generated by caspase activity were further degraded by the proteasome.

Abundance of PTB determines inclusion of exon β in Mef2 transcripts during cardiac muscle differentiation.

The reduction in PTB levels during cardiac development is likely to be responsible for numerous changes in alternative splicing (18). We were interested in exploring the possibility that the MEF2 transcription factors may constitute important targets of regulation by altered PTB levels. MEF2 proteins are expressed abundantly in the developing heart, with MEF2A being most highly expressed at later stages of development (Fig. 5A). In muscle, brain and in differentiated C2C12 cells, Mef2 transcripts may contain an alternatively spliced exon (β) encoding a short glutamic acid-rich sequence (e.g. SEEEELEL in MEF2A) that gives rise to MEF2 proteins with stronger transcriptional activity (40,42 Fig. 5B and see Fig. S1 in the supplemental material). Previous reports have shown that PTB can regulate different members of the Mef2 family in HeLa, C2C12 and N2A cells (6,16,18). Our results showed that during heart development, exon β was progressively included in Mef2a and Mef2d transcripts at the same time as PTB protein levels decrease in the myocardium to form the transcript variants most abundant in the adult heart (the rat sequence has been deposited in GenBank with Acc. No. GU646868), while the most abundant Mef2c variant lacked this exon during the time scale of the experiment (Fig. 5B). PTB regulates alternative splicing of genes relevant for muscular function (8,25,28,33) and we showed that its expression was reduced in the heart after birth (41, Fig. 1A, Fig. 5A).

Overexpression of either PTB1 or PTB4 in neonatal cardiomyocytes, which express low levels of these proteins, induced exon β skipping in Mef2a and Mef2d, but not in Mef2c (Fig. 5C). In addition, UV-crosslinking experiments in HeLa nuclear extracts, where PTB is abundantly expressed and influenced exon β splicing (see Fig. S2A in the supplemental material), showed that PTB can bind to human Mef2a and Mef2d RNAs fragments containing exon β and their respective intronic flanking regions (see Fig. S2B in the supplemental material), suggesting that PTB might regulate Mef2 alternative splicing by binding to their RNAs. Moreover, deficiency of HDAC5, which induced premature reduction in PTB abundance, caused increased exon β inclusion in Mef2 (Fig. 5D), whereas cardiomyocyte-specific deficiency of executioner caspases 3 and 7, which induced abnormal abundance of PTB (Fig. 2C), caused reduced exon β inclusion in Mef2 (Fig. 5E). Taken together, these results showed that PTB expression, controlled by HDAC and caspases, determined inclusion of exon β in Mef2a and Mef2d transcripts in differentiating myocytes.

DISCUSSION

This study reveals a novel signaling network that regulates the progressive disappearance of the splicing repressor PTB during cardiac muscle differentiation involving the action of caspases, which influences alternative splicing of muscle-enriched transcription factors MEF2A and MEF2D. The results presented here show that HDAC regulate the caspase-dependent cleavage of PTB inducing its degradation by the proteasome. PTB degradation allows inclusion of the alternatively spliced exon β in Mef2 transcripts (Fig. 6).

Though the importance of PTB in the regulation of relevant splicing events influencing the expression and function of many genes, including some coding for structural proteins relevant for muscle cells, is well established (8,25,28,33), knowledge about the signaling pathways that control PTB expression in muscle cells is more limited, and is mainly derived from studies in the C2C12 myoblast cell line (5,16). In differentiating neurons a switch between expression of PTB and the neuronal paralog nPTB is driven by the neuronal micro-RNA miR-124, which down-regulates PTB expression leading to a series of neuronal specific alternative splicing events (21,6). In C2C12 cells, the protein RBM4 promotes skipping of PTB exon 11 and nPTB exon 10, leading to Nonsense Mediated mRNA Decay (NMD) and reduced PTB and nPTB levels (16). In addition, miR-133 reduces nPTB expression (5).

Here, we demonstrate a novel mechanism for the control of PTB expression in primary cardiomyocytes and in the rodent heart *in vivo*. Caspase-dependent cleavage of PTB is demonstrated *in vitro* in neonatal cardiomyocytes (Fig. 2A) and is suggested to regulate PTB abundance in the heart *in vivo*, because cardiac-specific caspase-3 and 7 null mice express more PTB than wild type mice (Fig. 2B). Caspases were previously shown to cleave PTB in cell lines treated with toxic drugs (1), but here we show that this cleavage occurs as part of a normal developmental program. By reducing PTB abundance, caspase activity could contribute to the control of many PTB-dependent splicing events in the perinatal period of heart development. This could be involved in the deleterious effects caused by *in vivo*

deletion of key regulators of the extrinsic apoptotic signaling, which obstruct heart development without affecting the rate of cardiac cell death (38,39). PTB cleavage induced by HDAC inhibitors in cardiomyocytes was blocked by overexpressing cFLIP-L or by adding a Caspase-8 inhibitor, in agreement with the contribution of the extrinsic pathway to PTB degradation. These results together with previous reports showing that Caspase-3 and caspase-9 regulate differentiation of C2C12 myoblasts *in vitro* (10,26) support a role of the caspase-dependent cell signaling during muscle differentiation (2,41). Although PTB cleavage induced by HDAC inhibition produced C-terminal fragments of ~40 kDa, we did not detect the presence of these fragments *in vivo* in correlation to the reduction of full length PTB in the developing heart. However, the increased abundance of PTB proteins in the heart of cardiac-specific caspase-3 and 7 double knockout strongly support a role of caspases in the control of PTB expression *in vivo*. The results presented here also suggest that the initial cleavage of PTB by caspases triggers further PTB degradation by the proteasome. Caspase-dependent processing inducing further degradation of the target has been demonstrated for other proteins (9,29).

The regulated programs of alternative splicing in developing heart involve numerous factors in addition to PTB; bioinformatic analysis of exons that are co-regulated during cardiac development indicated enrichment of binding sites for CELF, MBNL and FOX proteins in addition to PTB (12). Indeed, all of these proteins were also implicated in the computationally assembled muscle “splicing code” (4. Also review: 19). Curiously, while the preceding report demonstrated changes in the levels of CELF, MBNL and FOX proteins, no changes in levels of PTB expression were observed during post-natal heart development in mouse (12). The reasons for this discrepancy between our observations and those of Kalsotra *et al.* (12) are unclear. Nevertheless, we reproducibly observed a rapid decrease in PTB protein abundance in both mouse and rat hearts after birth, using two independent PTB-specific antibodies against two different regions of the protein, whose specificity has been previously confirmed (Fig. 2A and (41)).

In addition, our findings expand the current knowledge about the relevance of PTB in the biology of striated muscle by showing its role in Mef2 alternative splicing in the developing heart. Thus, although it is known that PTB regulates splicing of many genes involved in muscle contraction, our data reveal that PTB is also involved in the splicing of the transcription factor Mef2a and Mef2d, which are important for the control of gene expression during cardiac muscle differentiation (25) and for the adaptation of the cardiac muscle to stress (14).

MEF2 and HDAC are mutually regulated factors involved in the control of gene expression during heart development (22,30). Deficiency in either MEF2A or MEF2C induces profound alterations in heart morphology, and MEF2D deficiency hampers the normal response of the heart to stress in the adult (14,17,27). Inclusion of exon β in Mef2 transcripts generates mRNAs coding for MEF2 variants bearing an acidic peptide in the transcription activation domain (ref. 40; see also Supplementary Fig. 1) that enhances transcriptional activity of MEF2 (42). On the other hand, mice deficient for Class II HDAC 5 and 9 or Class I HDAC 1 and 2 show propensity to lethal cardiac defects (7,24). Class II HDACs directly bind to MEF2 and inhibit MEF2-dependent gene transcription contributing to the regulation of muscle-specific gene expression (20). Given the essential role of MEF2 in heart development, it seems that adjusting MEF2 activity through regulation of exon β splicing can be relevant for the correct contribution of MEF2-dependent transcription, regulated by Class II HDAC, during heart organogenesis. Our results showed that exon β inclusion in *Mef2a* and *Mef2d* occurs progressively during heart development. We also observed an inverse relationship between β inclusion and PTB expression and show reduced PTB expression perinatally in the hearts of rats and mice. Furthermore, we show that PTB expression is sustained by HDAC5, thus linking HDAC5 with the regulation of MEF2A and MEF2D activity through the control of mRNA splicing. These results unveil an additional new pathway by which HDAC can influence MEF2 activity without direct interaction.

The reason for exon β inclusion in the transcript of Mef2a and Mef2d but not in Mef2c in the

heart is unknown but our results show that exon β inclusion in Mef2a and Mef2d is regulated by PTB. MEF2C is essential for the heart only during early development (17), and our results show that PTB is abundant during that period. On the contrary, MEF2A plays a key role during the late phase of myocardial differentiation (27), precisely coinciding with the reduction of PTB expression and exon β inclusion, as we show here. Exon β inclusion in MEF2A seems correlated to its trans-activating activity (40) suggesting that it could be essential for the correct function of MEF2A *in vivo*. Furthermore, we showed that a significant fraction of the transcript for MEF2D, which plays a relevant role in stress-induced gene expression in the adult (14), includes exon β in a PTB-inhibitable manner progressively after birth. Interestingly, we have recently found increased expression of MEF2A and MEF2D in myocytes treated with hypertrophic agonists and the hypertrophied adult heart (37). It can be hypothesized that, in the heart, exon β inclusion is important to define the activity of MEF2A and MEF2D when they are essential, but not in MEF2C, and that this splicing event is regulated by different mechanisms depending on the gene, with PTB being a relevant regulator of exon β splicing in Mef2a and Mef2d transcripts.

In conclusion, our data show that abundance of PTB is dependent on HDAC5 through the regulation of its FLIP-inhibitable, caspase-dependent cleavage and that progressive reduction of PTB expression permits the inclusion of exon β in Mef2a and Mef2d mRNAs in the heart during cardiac muscle differentiation. These findings contribute to the understanding of the role of caspases in myocyte differentiation, revealing the involvement of HDAC5 in its regulation and suggesting a previously unknown pathway for the control of MEF2 activity by HDAC without direct interaction, involving the splicing repressor PTB.

ACKNOWLEDGEMENTS

This work was partially supported by Grant SAF2010_19125 from Ministerio de Ciencia e Innovación (MICINN) and “Ramón y Cajal” Program from (MICINN) to D.S., Grant 2009SGR-346 from the Agència de Gestió d’Ajuts Universitaris i de Recerca (AGAUR) to J.X.C. and D.S., and by a Wellcome Trust Programme grant (092900) to C.W.J.S. R.A.F. is an investigator of the Howard Hughes Medical Institute. Work done in the laboratory of E.N.O. was supported by grants from NIH, the Donald W. Reynolds Center for Clinical Cardiovascular Research, the Leducq Foundation and the Robert A. Welch Foundation.

REFERENCES

1. **Back, S.H., Shin, S., and S.K. Jang.** 2002. Polypyrimidine Tract Binding Proteins are cleaved by caspase-3 during apoptosis. *J. Biol. Chem.* **277**:27200-27209.
2. **Bahi, N., Zhang, J., Llovera, M., Ballester, M., Comella, J.X., and D. Sanchis.** 2006. Switch from caspase-dependent to caspase-independent death during heart development: essential role of endonuclease G in ischemia-induced DNA processing of differentiated cardiomyocytes. *J. Biol. Chem.* **281**:22943-22952.
3. **Bangert, A., Cristofanon, S., Eckhardt, I., Abhari, B.A., Kolodziej, S., Häcker, S., Vellanki, S.H., Lausen, J., Debatin, K.M., and S. Fulda.** 2012. Histone deacetylase inhibitors sensitize glioblastoma cells to TRAIL-induced apoptosis by c-myc-mediated downregulation of cFLIP. *Oncogene.* doi: 10.1038/onc.2011.614.
4. **Barash Y., Calarco J.A., Gao W., Pan Q., Wang X., Shai O., Blencowe B.J., and B.J. Frey.** 2010. Deciphering the splicing code. *Nature.* **465**:53-59.
5. **Boutz, P.L., Chawla, G., Stoilov, P., and D.L. Black.** 2007. MicroRNAs regulate the expression of the alternative splicing factor nPTB during muscle development. *Genes Dev.* **21**:71-84.
6. **Boutz, P.L., Stoilov, P., Li, Q., Lin, C.H., Chawla, G., Ostrow, K., Shiue, L., Ares, M. Jr., and D.L. Black.** 2007. A post-transcriptional regulatory switch in polypyrimidine tract-binding proteins reprograms alternative splicing in developing neurons. *Genes Dev.* **21**:1636-1652.
7. **Chang, S., McKinsey, T.A., Zhang, C.L., Richardson, J.A., Hill, J.A., and E.N. Olson.** 2004. Histone deacetylases 5 and 9 govern responsiveness of the heart to a subset of stress signals and play redundant roles in heart development. *Mol. Cell. Biol.* **24**:8467-8476.
8. **Charlet-B. N., Logan, P., Singh, G., and T.A. Cooper.** 2002. Dynamic antagonism between ETR-3 and PTB regulates cell type-specific alternative splicing. *Mol. Cell* **9**:649-658.

9. **Demontis, S., Rigo, C., Piccinin, S., Mizzau, M., Sonogo, M., Fabris, M., Brancolini, C., and R. Maestro.** 2006. Twist is substrate for caspase cleavage and proteasome-mediated degradation. *Cell Death Differ.* **13**:335-345.
10. **Fernando, P., Kelly, J.F., Balazsi, K., Slack, R.S., and L.A. Megeney.** 2002. Caspase 3 activity is required for skeletal muscle differentiation. *Proc. Natl. Acad. Sci. U. S. A.* **99**:11025-11030.
11. **Haberland, M., Montgomery, R.L., and E.N. Olson.** 2009. The many roles of histone deacetylases in development and physiology: implications for disease and therapy. *Nat. Rev. Genet.* **10**:32-42.
12. **Kalsotra, A., Xiao, X., Ward, A.J., Castle, J.C., Johnson, J.M., Burge, C.B., and T.A. Cooper.** 2008. A postnatal switch of CELF and MBNL proteins reprograms alternative splicing in the developing heart. *Proc. Natl. Acad. Sci. U. S. A.* **105**:20333-20338.
13. **Keppetipola N., Sharma S., Li Q., and D.L. Black.** 2012. Neuronal regulation of pre-mRNA splicing by polypyrimidine tract binding proteins, PTBP1 and PTBP2. *Crit. Rev. Biochem. Mol. Biol.* **47**:360-378.
14. **Kim, Y., Phan, D., van Rooij, E., Wang, D.Z., McAnally, J., Qi, X., Richardson, J.A., Hill, J.A., Bassel-Duby, R., and E.N. Olson.** 2008. The MEF2D transcription factor mediates stress-dependent cardiac remodeling in mice. *J. Clin. Invest.* **118**:124-132.
15. **Lakhani, S.A., Masud, A., Kuida, K., Porter, G.A. Jr., Booth, C.J., Mehal, W.Z., Inayat, I., and R.A. Flavell.** 2006. Caspases 3 and 7: key mediators of mitochondrial events of apoptosis. *Science* **311**:847-851.
16. **Lin, J.C., and W.Y. Tarn.** 2011. RBM4 down-regulates PTB and antagonizes its activity in muscle cell-specific alternative splicing. *J Cell Biol.* **193**:509-520.
17. **Lin, Q., Schwarz, J., Bucana, C., and E.N. Olson.** 1997. Control of mouse cardiac morphogenesis and myogenesis by transcription factor MEF2C. *Science* **276**:1404-1407.

18. **Llorian, M., Schwartz, S., Clark, T.A., Hollander, D., Tan, L.Y., Spellman, R., Gordon, A., Schweitzer, A.C., de la Grange, P., Ast, G., and C.W. Smith.** 2010. Position-dependent alternative splicing activity revealed by global profiling of alternative splicing events regulated by PTB. *Nat. Struct. Mol. Biol.* **17**:1114-1123.
19. **Llorian, M., and C.W. Smith.** 2011. Decoding muscle alternative splicing. *Curr. Opin. Genet. Dev.* **21**:380-37.
20. **Lu, J., McKinsey, T.A., Nicol, R.L., and E.N. Olson.** 2000. Signal-dependent activation of the MEF2 transcription factor by dissociation from histone deacetylases. *Proc. Natl. Acad. Sci. U. S. A.* **97**:4070-4075.
21. **Makeyev, E.V., Zhang, J., Carrasco, M.A., and T. Maniatis.** 2007. The MicroRNA miR-124 promotes neuronal differentiation by triggering brain-specific alternative pre-mRNA splicing. *Mol Cell.* **27**:435-448.
22. **McKinsey, T.A., and E.N. Olson.** 2005. Toward transcriptional therapies for the failing heart: chemical screens to modulate genes. *J. Clin. Invest.* **115**:538-546.
23. **Mitchell, S.A., Brown, E.C., Coldwell, M.J., Jackson, R.J., and A.E. Willis.** 2001. Protein factor requirements of the Apaf-1 internal ribosome entry segment: roles of polypyrimidine tract binding protein and upstream of N-ras. *Mol Cell Biol.* **21**:3364-3374.
24. **Montgomery, R.L., Hsieh, J., Barbosa, A.C., Richardson, J.A., and E.N. Olson.** 2007. Histone deacetylases 1 and 2 redundantly regulate cardiac morphogenesis, growth, and contractility. *Genes Dev.* **21**:1790-1802.
25. **Mulligan, G.J., Guo, W., Wormsley, S., and D.M. Helfman.** 1992. Polypyrimidine tract binding protein interacts with sequences involved in alternative splicing of beta-tropomyosin pre-mRNA. *J. Biol. Chem.* **267**:25480-25487.
26. **Murray, T.V., McMahon, J.M., Howley, B.A., Stanley, A., Ritter, T., Mohr, A., Zwacka, R., and H.O. Fearnhead.** 2008. A non-apoptotic role for caspase-9 in muscle differentiation. *J. Cell Sci.* **121**:3786-3793.

27. **Naya, F.J., Black, B.L., Wu, H., Bassel-Duby, R., Richardson, J.A., Hill, J.A., and E.N. Olson.** 2002. Mitochondrial deficiency and cardiac sudden death in mice lacking the MEF2A transcription factor. *Nat. Med.* **8**:1303-1309.
28. **Pérez, I., Lin, C.H., McAfee, J.G., and J.G. Patton.** 1997. Mutation of PTB binding sites causes misregulation of alternative 3' splice site selection *in vivo*. *RNA* **3**:764-778.
29. **Plesca, D., Mazumder, S., Gama, V., Matsuyama, S., and A. Almasan.** 2008. A C-terminal fragment of Cyclin E, generated by caspase-mediated cleavage, is degraded in the absence of a recognizable phosphodegron. *J. Biol. Chem.* **283**:30796-30803.
30. **Potthoff, M.J., and E.N. Olson.** 2007. MEF2: a central regulator of diverse developmental programs. *Development.* **134**:4131-4140.
31. **Sakamaki, K., Inoue, T., Asano, M., Sudo, K., Kazama, H., Sakagami, J., Sakata, S., Ozaki, M., Nakamura, S., Toyokuni, S., Osumi, N., Iwakura, Y., and S. Yonehara.** 2002. Ex vivo whole-embryo culture of caspase-8-deficient embryos normalize their aberrant phenotypes in the developing neural tube and heart. *Cell Death Differ.* **9**:1196-1206.
32. **Sawicka K., Bushell M., Spriggs K.A., and A.E. Willis.** 2008. Polypyrimidine-tract-binding protein: a multifunctional RNA-binding protein. *Biochem. Soc. Trans.* **36**:641-647.
33. **Southby, J., Gooding, C., and C.W. Smith.** 1999. Polypyrimidine tract binding protein functions as a repressor to regulate alternative splicing of alpha-actinin mutually exclusive exons. *Mol. Cell. Biol.* **19**:2699-2711.
34. **Spellman, R., Llorian, M., and C.W. Smith.** 2007. Crossregulation and functional redundancy between the splicing regulator PTB and its paralogs nPTB and ROD1. *Mol. Cell* **27**:420-434.
35. **Varfolomeev, E.E., Schuchmann, M., Luria, V., Chiannikulchai, N., Beckmann, J.S., Mett, I.L., Rebrikov, D., Brodianski, V.M., Kemper, O.C., Kollet, O., Lapidot, T., Soffer, D., Sobe, T., Avraham, K.B., Goncharov, T., Holtmann, H., Lonai, P., and D. Wallach.** 1998. Targeted disruption of the mouse caspase 8 gene

- ablates cell death in duodenum by the TNF receptors, Fas/Apo1, and DR3 and is lethal perinatally. *Immunity* **9**:267-276.
- 36 **Collerton, M.C., Gooding, C., Wagner, E.J., Garcia-Blanco, M.A., and C.W. Smith.** 2004. Autoregulation of polypyrimidine tract binding protein by alternative splicing leading to nonsense-mediated decay. *Mol Cell*. **13**:91-100.
- 37 **Ye, J., Cardona, M., Llovera, M., Comella, J.X., Sanchis, D.** 2012. Translation of Myocyte Enhancer Factor-2 is induced by hypertrophic stimuli in cardiomyocytes through a Calcineurin-dependent pathway. Doi 10.1016/j.yjmcc.2012.07.013.
- 38 **Yeh, W.C., Itie, A., Elia, A.J., Ng, M., Shu, H.B., Wakeham, A., Mirtsos, C., Suzuki, N., Bonnard, M., Goeddel, D.V., and T.W. Mark.** 2000. Requirement for Casper (c-FLIP) in regulation of death receptor-induced apoptosis and embryonic development. *Immunity* **12**:633-642.
- 39 **Yeh, W.C., Pompa, J.L., McCurrach, M.E., Shu, H.B., Elia, A.J., Shahinian, A., Ng, M., Wakeham, A., Khoo, W., Mitchell, K., El-Deiry, W.S., Lowe, S.W., Goeddel, D.V., and T.W. Mak.** 1998. FADD: essential for embryo development and signaling from some, but not all, inducers of apoptosis. *Science* **279**:1954-1958.
- 40 **Yu, Y.T., Breitbart, R.E., Smoot, L.B., Lee, Y., Mahdavi, V., and B. Nadal-Ginard.** 1992. Human myocyte-specific enhancer factor 2 comprises a group of tissue-restricted MADS box transcription factors. *Genes Dev*. **6**:1783-1798.
- 41 **Zhang, J., Bahi, N., Llovera, M., Comella, J.X., and D. Sanchis.** 2009. Polypyrimidine tract binding proteins (PTB) regulate the expression of apoptotic genes and susceptibility to caspase-dependent apoptosis in differentiating cardiomyocytes. *Cell Death Differ*. **16**:1460-1468.
- 42 **Zhu, B., Ramachandran, B., and T. Gulick.** 2005. Alternative premRNA splicing governs expression of conserved acidic transactivation domain in myocyte enhancer factor 2 factors in striated muscle and brain. *J. Biol. Chem.* **280**:28749-28760.

FIGURE LEGENDS**Figure 1. PTB expression during cardiomyocyte differentiation is regulated postranscriptionally by HDAC5.**

A) Expression of PTB and HDAC proteins in heart protein extracts from rats of different ages ranging from embryos (E18) to 3-month-old adults. PTB was analyzed with antibodies against the N-terminal region and C-terminal region. Two alternatively spliced variants of PTB were detected (lower band, PTB1 and upper band, PTB4 translated from a transcript including exon 9). B) Ptb transcript abundance was quantified in quadruplicates by Real Time qRT-PCR in total RNA extracts of the same hearts as in A and referred to the value of the house keeping gene Gapdh amplified in the same reaction. Error bars are s.e.m. from three independent experiments. Asterisk: $p < 0.05$ vs. embryo. C) PTB abundance in protein extracts from hearts of wild type newborns, young and young adults and HDAC5-deficient and HDAC9-deficient littermates as well as wild type and HDAC1 and 2-double deficient neonates. Similar results were obtained with two independent set of samples. D) Ptb total transcript abundance was quantified by Real Time PCR from the hearts of 1-day-old neonatal wild type and HDAC5-deficient mice. Error bars: s.e.m. from 3 independent experiments.

Figure 2. HDAC inhibition induces the caspase-dependent cleavage of PTB.

A) Rat neonatal ventricular cardiomyocytes were treated with HDAC inhibitors NaB (5 mM) or TSA (100 nM) for 48 or 72 hours in the presence or absence of the pan-caspase inhibitor z-VAD-fmk (50 μ M). PTB abundance was detected with an antibody against the C-terminal region. Small panel: Human Embryonic Kidney 293 cells were treated for 3 days with TSA and PTB was detected in total protein amounts with the same antibody. The experiments were repeated four times with comparable results. Prohib.: prohibitin was used as loading control. B) Cell survival was counted by the Trypan Blue exclusion assay in cardiomyocyte cultures treated for 3 days with either TSA or NaB at the doses reported above or cultured without drugs (Contr.). Values are expressed as percentage of cell survival versus control plates processed before addition of the drugs. Each experiment was made in triplicates. N=3, error bars are

s.e.m. Ns: not significant changes vs. controls (paired Student's *t* test). C) PTB abundance was analyzed in total protein extracts of hearts from young wild type (WT) and cardiac-specific Caspase-3 and 7 deficient mice (DKO). Lower panel: Western Blot densitometric analysis (AU: Arbitrary units). Asterisk: $p < 0.05$ vs. WT. D) Quantitative Real Time PCR of Ptb transcript in the same hearts as in C. N=3, Error bars: s.e.m. Ns: not significant changes vs. WT (paired Student's *t* test).

Figure 3. HDACs block caspase-dependent cleavage of PTB in cardiomyocytes by supporting expression of the endogenous caspase inhibitor cFLIP. A) Rat neonatal ventricular cardiomyocytes were treated with the HDAC inhibitor NaB (5 mM) for 24h and cFLIP transcript abundance was analyzed by quantitative Real Time PCR. N=3, Error bars: s.e.m. Asterisk: $p < 0.05$ vs. control (paired Student's *t* test). B) PTB protein abundance was assessed with an antibody against the C-terminal region of PTB in protein extracts from cardiomyocytes transduced with empty viruses or viruses inducing cFLIP-L overexpression (FLIP) treated or not with the HDAC inhibitor NaB (5 mM) during 24 h in the presence or absence of the Caspase-8 inhibitor z-IETD-fmk (20 μ M). C) Cardiomyocytes were transduced with empty viruses or viruses inducing cFLIP-L overexpression and were treated or not with the HDAC inhibitor NaB (5 mM) during the last 24 h. Expression of cFLIP (white arrow shows overexpressed FLAG-cFLIP and black arrow shows endogenous cFLIP) and PTB was analyzed in total protein extracts. The bar graph shows the densitometric analysis of PTB protein abundance from experiments shown in C. Error bars: s.e.m of n=4 experiments (upper band: full length PTB; middle band: ~40 kDa fragment; bottom band: ~25 kDa fragment).

Figure 4. Caspase-dependent cleavage of PTB triggers its proteasome-dependent degradation. A) Time-course of PTB processing in rat neonatal cardiomyocytes treated with the HDAC inhibitor NaB (5 mM). The bar graph shows the densitometric analysis of PTB protein abundance. Error bars: s.e.m of n=3 experiments (upper band: full length PTB; middle band: ~40 kDa fragment; bottom band: ~25 kDa fragment). B) Effect of the addition of the proteasome inhibitor Lactacystin (2 μ M) on PTB processing during HDAC inhibitor

NaB (5mM) treatment for 72 h. Right panels: Densitometric analysis of PTB protein abundance. b₁: full length PTB, b₂: ~40 kDa band, b₃: ~25 kDa band. Error bars: s.e.m of n=4 experiments made in duplicates. Asterisk: p<0.05 vs. control. ns: not significant.

Figure 5. PTB expression determines skipping of exon β in *Mef2a* and *Mef2d* transcripts

in cardiomyocytes. A) Expression of PTB and MEF2 (A, C and D) in cardiac protein extracts of rat embryos (E18), 2-day-old neonates and 2-month-old adults, with an antibody raised against the N-terminal region of PTB. Similar results were obtained in two analysis using independent samples. Prohibitin was used as loading control. B) *Mef2* alternative splicing event occurring during heart development (see more detailed explanation in Supplementary Figure 1). Exon β inclusion in *Mef2a*, *Mef2c* and *Mef2d* transcripts was analyzed by radioactive qRT-PCR with primers flanking the alternatively spliced exon in total mRNA samples from hearts of rat embryos (E18), 2-day-old neonates and 2-month-old adults. +/- β indicates inclusion or exclusion of exon β , respectively. Bar graph: Quantification of radioactive products obtained by qRT-PCR. Nd: not detected. Error bars are s.e.m. from three independent samples. Asterisk: $p \leq 0.05$ vs. E18. C) Effects of PTB overexpression in cardiomyocytes on *Mef2* exon β splicing. Upper panels: Time-course of PTB1 and PTB4 overexpression in P4 cardiomyocytes. Neonatal cardiomyocytes were transduced with empty lentiviruses (\emptyset) or lentiviruses inducing overexpression of PTB, and PTB abundance was monitored by Western blot. Lower panels: *Mef2* exon β splicing. Total RNA was extracted at day four post-transduction and exon β inclusion in *Mef2a*, *Mef2c* and *Mef2d* transcripts was analyzed by radioactive qRT-PCR. Two independent experiments were performed with similar results. D) Analysis of exon β inclusion ($-\beta$, not included; $+\beta$, included) in *Mef2* transcripts was assessed in total RNA extracts from hearts of 2-day-old wild type (WT) and HDAC5-deficient mice (HDAC5 KO) and is expressed as fold change compared to WT. E) Analysis of exon β inclusion ($-\beta$, not included; $+\beta$, included) in *Mef2* transcripts was assessed in total RNA extracts from hearts of 1-month-old wild type (WT) and cardiac-specific caspase 3 and 7-deficient mice (Caspase KO) and is expressed as fold change compared to WT. Error bars in D and E are s.e.m. of data from three hearts per

genotype. Asterisk: $p < 0.05$ vs. WT.

Figure 6. Model of the regulation of Mef2 alternative splicing by HDAC and caspases through the control of PTB abundance during heart development. The expression of HDAC decreases during perinatal cardiomyocyte differentiation. In addition to regulate MEF2-dependent transcription by directly binding to this transcription factor, developmental downregulation of HDAC induce the reduction of cFLIP expression allowing caspases to cleave the splicing repressor PTB. Caspase-dependent PTB cleavage triggers its degradation by the proteasome. Low levels of PTB in the postnatal heart permits inclusion of exon β in the Mef2a and Mef2d transcripts, which code for variants with more robust transcriptional activity (42).

Fig.1

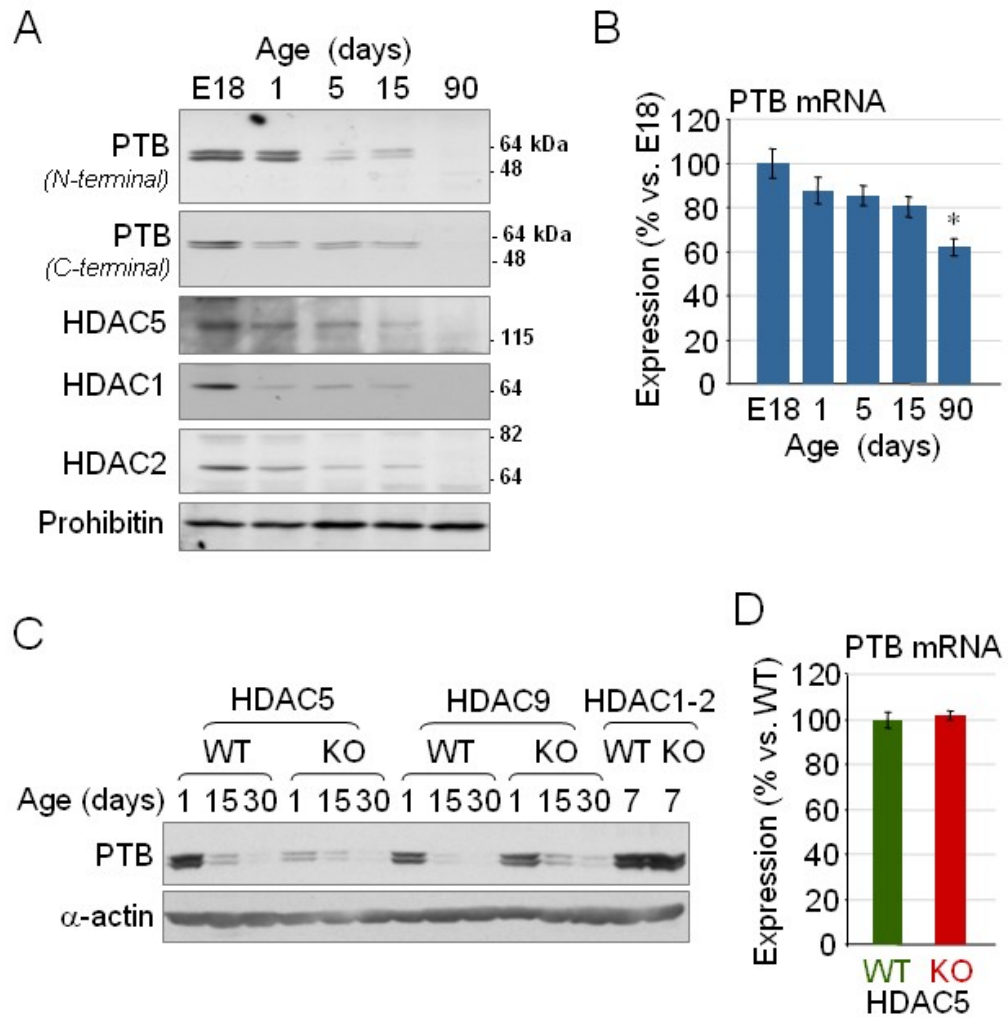


Fig.2

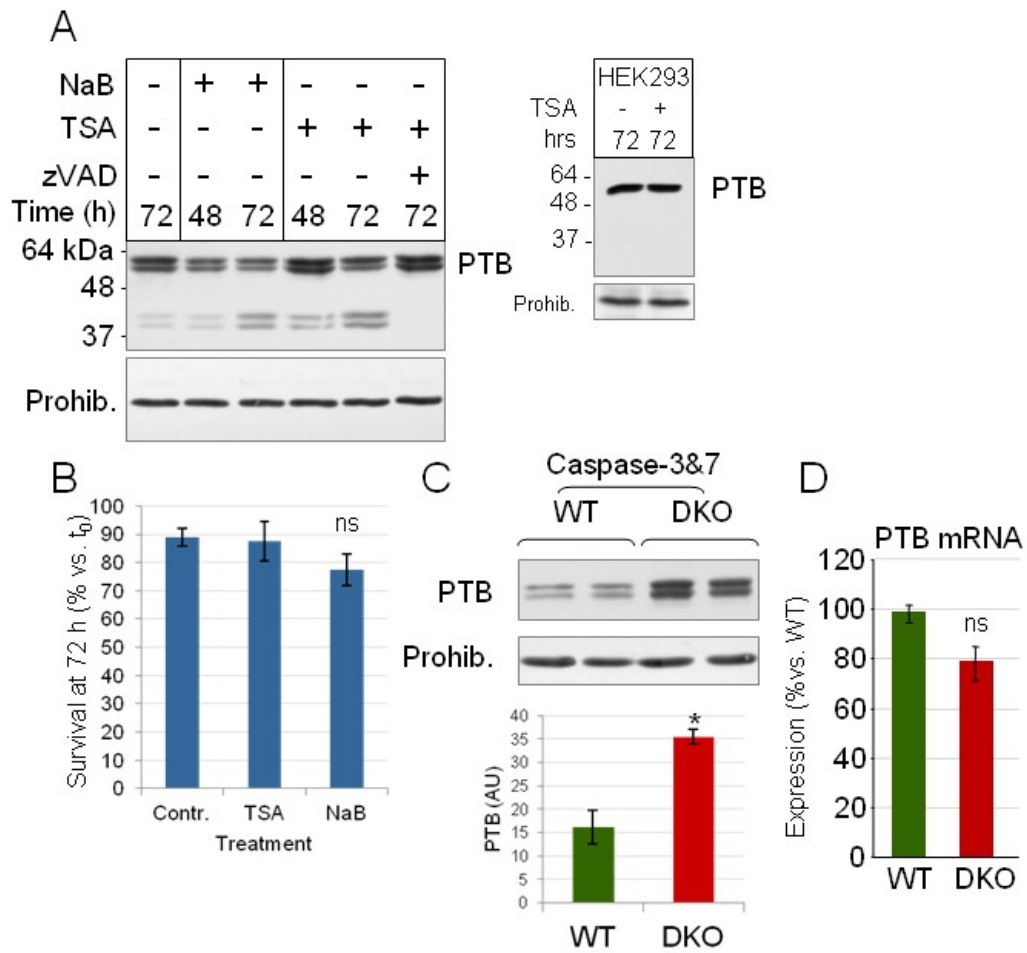


Fig.3

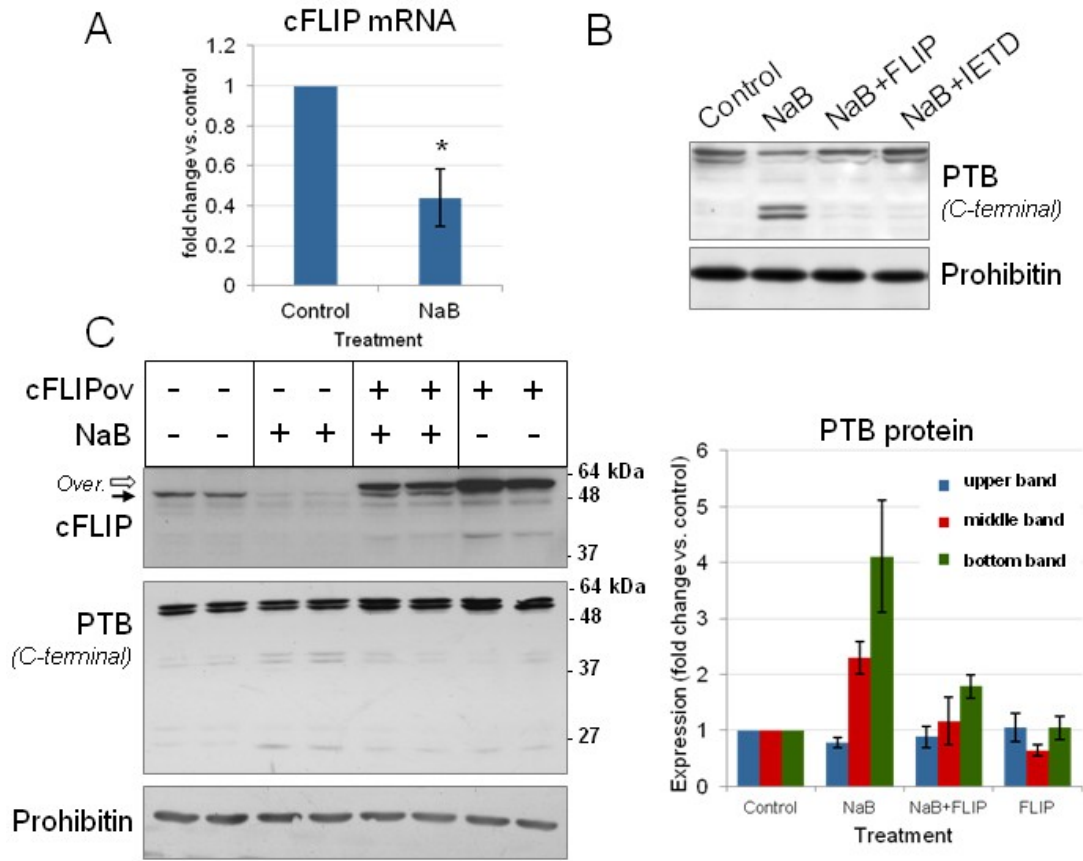


Fig.4

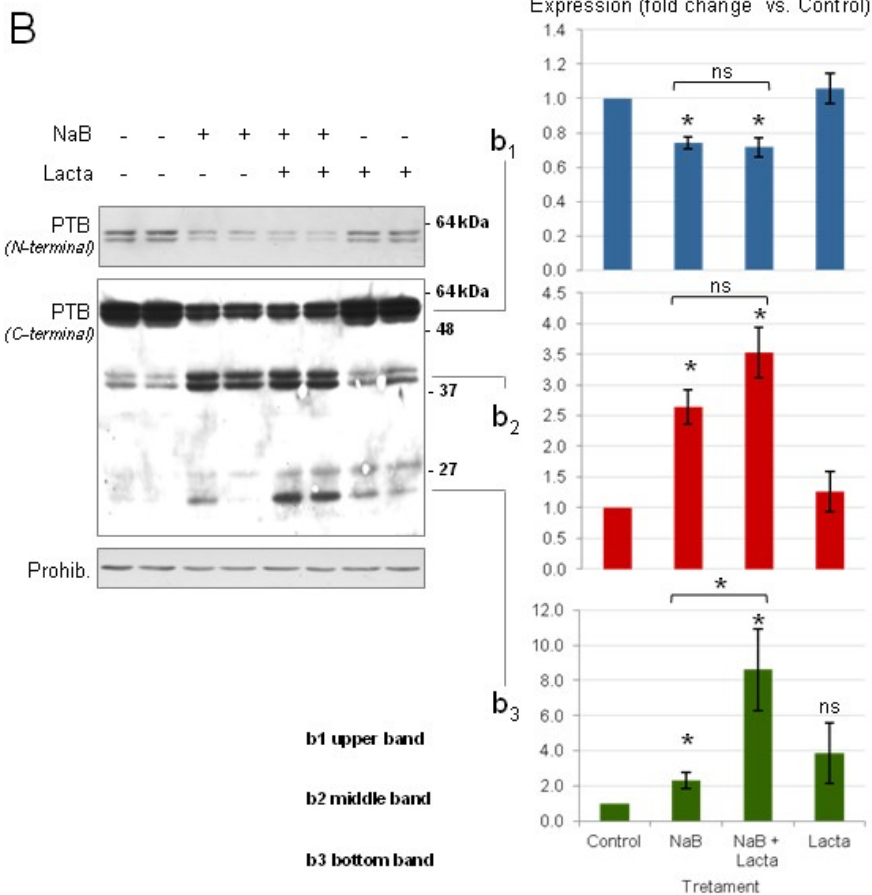
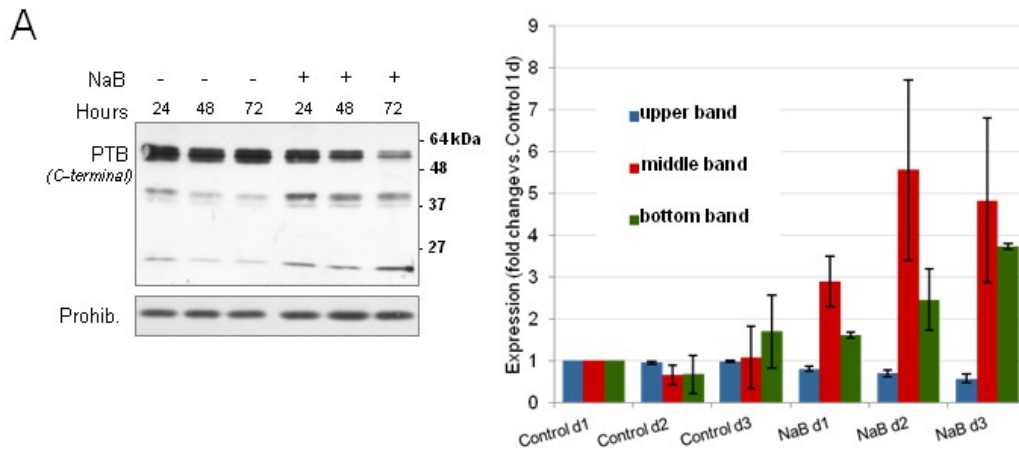


Fig.5

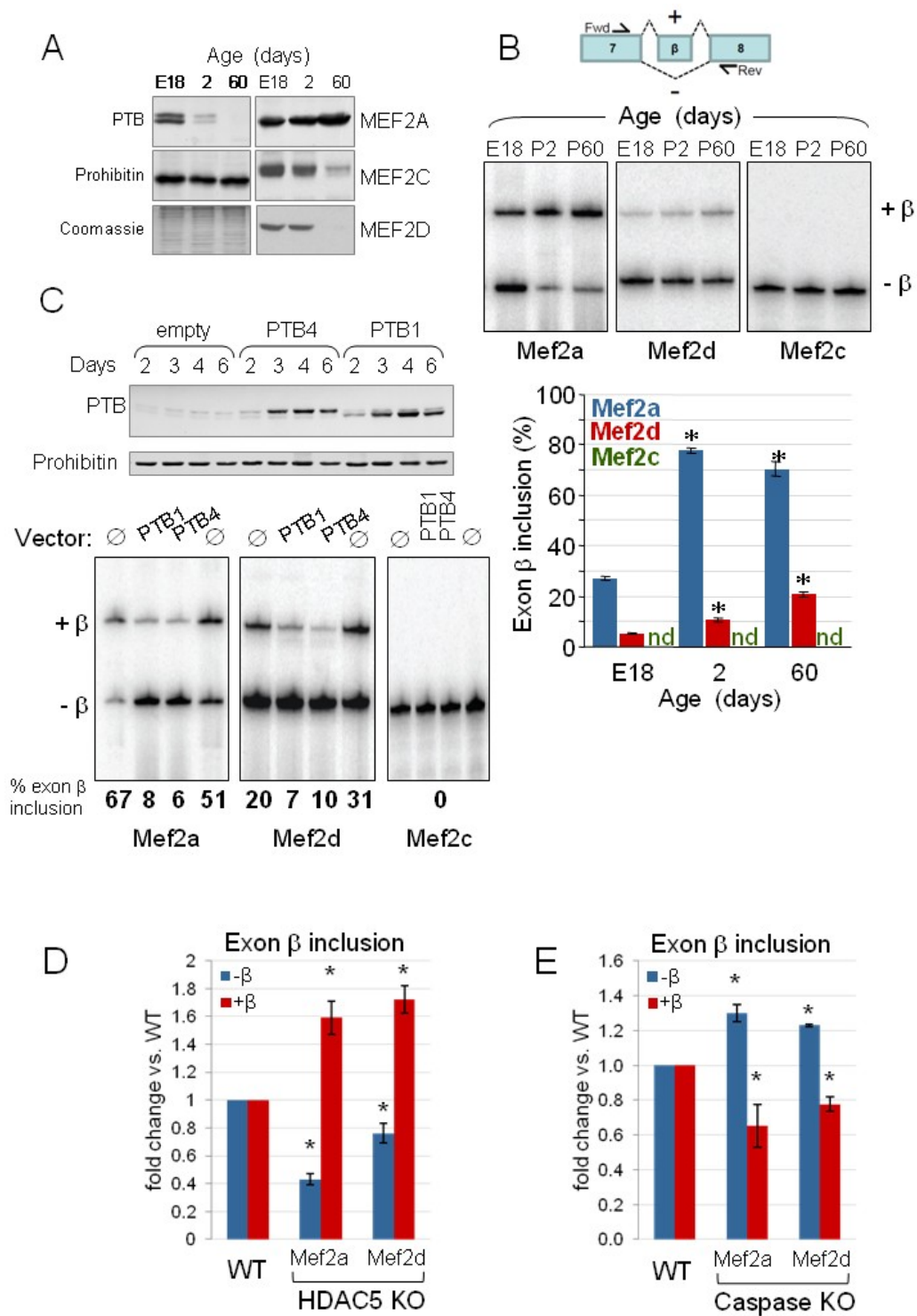


Fig.6

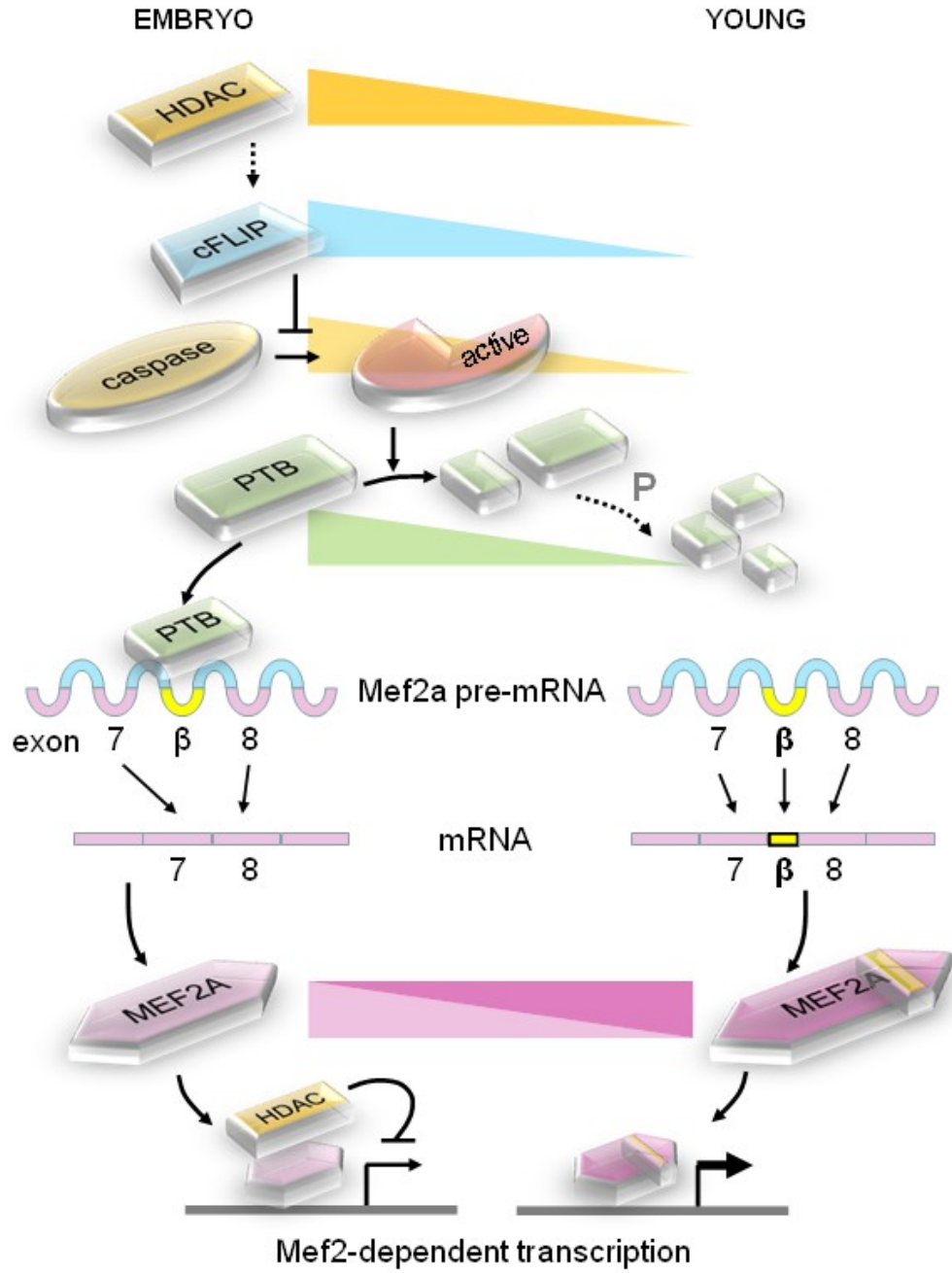


Figure S1. Structure of the *Mef2a* gene, transcript and protein. **A)** *Mef2a* human gene region around the alternatively spliced exon β , top row: gene structure (based on Yu et al., 1992); middle row: transcript sequence surrounding exon β in the rat *Mef2a* transcript obtained from adult cardiac ventricle retrotranscribed by random priming, PCR-amplified and sequenced using primers Forward: ggaatgaacagtggaaacc and Reverse: gaggcaagcttggagttgtc. Location of the putative peptide in the protein sequence (from Olson EN, Perry M and Schulz RA Dev Biol 172: 2-14; 1995). Sequencing the region including the mutually exclusive exons coding for the peptides “MEF2” and “aMEF2” (\uparrow) with primers Forward: atgagaggaaccgacaggtg and Reverse: cgagtgaactcctctgggta showed that the most abundant *Mef2a* variant expressed in the rat heart includes “MEF2” exon (orange) and not “aMEF2”. **B)** GenBank accession numbers of sequences for *Mef2a* transcript variants lacking (skipped) or containing (included) exon β . * We have contributed the sequence of the rat (Rn) *Mef2a* isoform containing exon β expressed in the heart (GU646868).

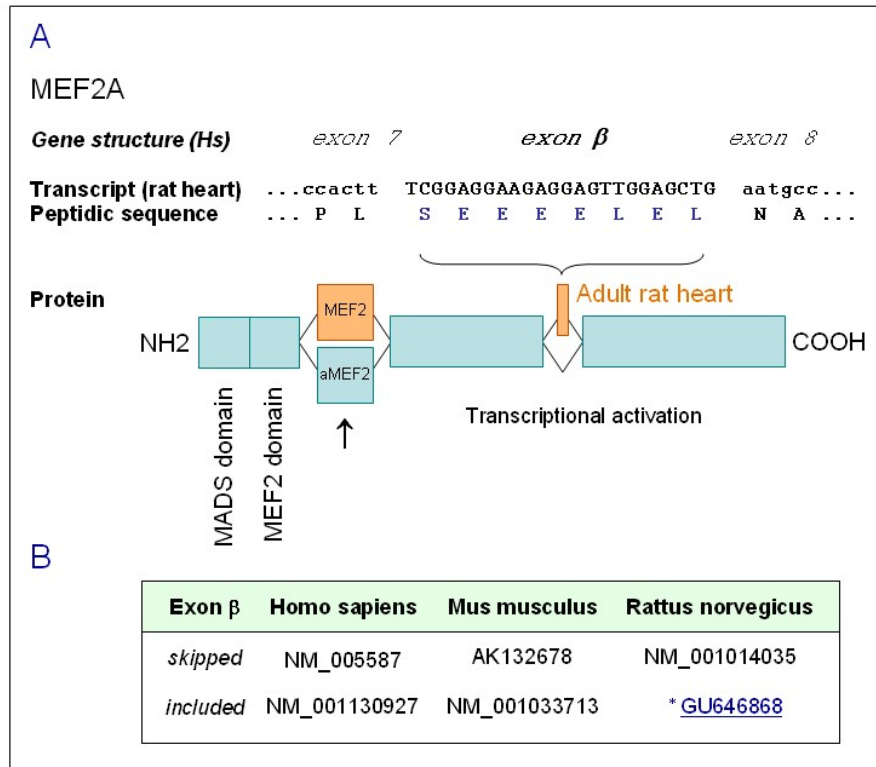


Figure S2. PTB associates with Mef2A and Mef2D transcripts. A) HeLa cells were transfected with siRNAs against PTB and nPTB or control siRNAs (upper panel). Effect of PTB knockdown on endogenous Mef2D exon β inclusion was assessed by RT-PCR (left panel). Amplicon size: 135 bp for inclusion and 114 bp for skipping. Mouse Mef2D minigene was cotransfected with siRNAs against PTB and nPTB or control siRNAs in HeLa cells. RT-PCR was then carried out with minigene specific primers (right panel). Amplicon size: 340 bp for inclusion and 319 for skipping. Percentage of exon β inclusion is shown at the bottom (mean \pm SD, n=3). Gels shown are representative of three independent transfections.

B) UV-crosslinking and immunoprecipitation of human Mef2A and Mef2D exon β containing RNAs, in HeLa nuclear extracts. Probes for the human MefA and Mef2D RNAs contain exon β and around 200nt of the flanking intronic sequence. Body-labeled RNA probes were incubated with buffer E (Lanes 1, 5) or 2ml of HeLa nuclear extract (lanes 2, 6). After UV-crosslinking samples were immunoprecipitated with pre-immune serum (lanes 3, 7) or anti:PTB antibody (lanes 4, 8). Molecular markers are shown to the left and the position of the PTB crosslinked doublet is shown as an arrow to the right of the gel. Gels shown are representative of three independent experiments. (see Suppl. Materials and Methods)

